



# HEPATOLOGY

---

# FORUM

## Methylation-Based Fibrosis Staging in MASLD



Gut Microbiota in MASLD

GALAD Score in  
HCV-Related HCC

AI and Fibrosis  
Patterns in SLD

SPSS Embolization for Refractory HE

**Editorial Board****Editor-in-Chief****Ulus Salih Akarca**

ulus.salih.akarca@ege.edu.tr

**Associate Editors (Alphabetically)****Ali Riza Caliskan**

Department of Gastroenterology, Adiyaman Training and  
Research Hospital, Adiyaman, Turkiye  
komamir02@hotmail.com

**Berna Savas**

Department of Pathology, Ankara University School of  
Medicine, Ankara, Turkiye  
bernasavas@gmail.com

**Cem Simsek**

Department of Gastroenterology, Hacettepe University School  
of Medicine, Istanbul, Turkiye  
cemsimsek90@gmail.com

**Cemal Nuri Ercin**

Department of Gastroenterology, Saglik Bilimleri University  
Gulhane School of Medicine, Ankara, Turkiye  
ncercin@hotmail.com

**Coskun Ozer Demirtas**

Department of Gastroenterology, Marmara University School  
of Medicine, Istanbul, Turkiye  
coskun\_demirtas10@hotmail.com

**Cumali Efe**

Sanliurfa Harran University, Faculty of Medicine, Sanliurfa, Turkiye  
scumaliefe@gmail.com

**Dilara Turan Gokce**

Department of Gastroenterology, Ankara University School of  
Medicine, Ankara, Turkiye  
dilaraturan89@yahoo.com

**Fatih Guzelbulut**

Department of Gastroenterology, Haydarpaşa Numune Training  
and Research Hospital, Istanbul, Turkiye  
fguzelbulut@hotmail.com

**Gokhan Kabacam**

Department of Gastroenterology, Guven Hospital, Ankara, Turkiye  
gokhankabacam@yahoo.com

**Gupse Adali**

Department of Gastroenterology, University of Health Sciences  
Istanbul Umraniye Training and Research Hospital, Istanbul, Turkiye  
gupseadali@gmail.com

**Hale Gokcan**

Department of Gastroenterology, Ankara University, Ankara,  
Turkiye  
halesumer@yahoo.com

**Ilker Turan**

Department of Gastroenterology, Ege University School of  
Medicine, Izmir, Turkiye  
ilkerturan@gmail.com

**Mujdat Zeybel**

Department of Gastroenterology, Koc University School of  
Medicine, Istanbul, Turkiye  
mzeybel@ku.edu.tr

**Nuray Yazihan**

Department of Pathophysiology, and Internal Medicine Ankara  
University School of Medicine, Ankara, Turkiye  
Ankara University, Institute of Health Sciences,  
Interdisciplinary Food, Metabolism and Clinical Nutrition  
Department, Ankara, Turkiye  
nurayyazihan@yahoo.com

**Serkan Yaras**

Department of Gastroenterology, Mersin University School of  
Medicine, Mersin, Turkiye  
drserkan1975@hotmail.com

**Suna Yapali**

Department of Gastroenterology, Acibadem Mehmet Ali  
Aydinlar University School of Medicine, Istanbul, Turkiye  
sunayapali@yahoo.com

**Yasemin Balaban**

Department of Gastroenterology, Hacettepe University School  
of Medicine, Ankara, Turkiye  
ybalaban@hacettepe.edu.tr

**Yusuf Yilmaz**

Department of Gastroenterology, Recep Tayyip Erdogan  
University, School of Medicine, Rize, Turkiye  
dryusufyilmaz@gmail.com

---

**Zarife Kuloglu**

Department of Pediatrics, Ankara University School of  
Medicine, Ankara, Turkiye  
zarifekuloglu@yahoo.com

**International Associate Editors (Alphabetically)**

**Ahmet Gurakar, USA**

Department of Gastroenterology and Hepatology, Johns  
Hopkins University School of Medicine, Baltimore, USA  
aguraka1@jhmi.edu

**Alexandre Louvet, France**

University Hospital of Lille, France  
alexandre.louvet@chru-lille.fr

**Ali Canbay, Germany**

Department of Gastroenterology, Hepatology, and Infectious  
Diseases, Magdeburg University Hospital, Magdeburg,  
Germany  
ali.canbay@med.ovgu.de

**Ashok Kumar Choudhury, India**

Associate Professor of Hepatology and Liver Transplant  
Institute of Liver & Biliary Sciences D-1 Vasant Kunj New  
Delhi, India  
Ashokkumar123@gmail.com

**Azra Husic-Selimovic, Bosnia and Herzegovina**

General Hospital Abdulah Nakas  
husic\_azra@yahoo.com

**Eda Kaya, Germany**

Department of Medicine Universitätsklinikum  
Knappschafts Krankenhaus Bochum, Germany  
edakaya93@gmail.com

**Georgios Papatheodoridis, Greece**

Department of Gastroenterology and Hepatology, National and  
Kapodistrian University of Athens Medical School, Athens,  
Greece  
gepapath@med.uoa.gr

**Jasmohan Bajaj, USA**

Division of Gastroenterology, Hepatology and Nutrition,  
Virginia Commonwealth University, Virginia, USA  
jasmohan.bajaj@vcuhealth.org

**Jordan Feld, Canada**

Department of Gastroenterology and Center for Liver Diseases,  
University of Toronto, Toronto, Canada  
jordan.feld@uhn.ca

**Ming-Hua Zheng, China**

NAFLD Research Center, Department of Hepatology, the First  
Affiliated Hospital of Wenzhou Medical University, China  
zhengmh@wmu.edu.cn

**Patrick Kamath, USA**

Department of Gastroenterology and Hepatology, Mayo Clinic  
College of Medicine, Rochester, MN, USA  
kamath.patrick@mayo.edu

**Paul Kwo, USA**

Department of Gastroenterology and Hepatology, Stanford  
University Medical Center, CA, USA  
pkwo@stanford.edu

**Senem Ceren Karatay, Germany**

Department of Medicine II, Saarland University Medical  
Center, Saarland University, Homburg, Germany  
senem.ozen-karatayli@uks.eu

**Sevda Agayeva, Azerbaijan**

Department of Gastroenterology, Baku Medical Plaza Hospital,  
Baku, Azerbaijan  
seva\_agayeva@yahoo.com

**Sukru Emre, USA**

Transplant and Immunology Center Yale School of Medicine,  
New Haven, CT, USA  
sukru.emre@yale.edu

**Timucin Taner, USA**

Department of Surgery, Mayo Clinic College of Medicine,  
Rochester, MN, USA  
taner.timucin@mayo.edu

**Managing Editor**

**Cumali Efe**

Department of Gastroenterology, Diyarbakir Training and  
Research Hospital, Diyarbakir, Turkiye  
drcumi21@hotmail.com

---

### Consulting Biostatistician

#### Beyza Doganay

Department of Biostatistics, Ankara University School of  
Medicine, Ankara, Turkiye  
bdoganay@medicine.ankara.edu.tr

### Editors Emeriti

#### Nurdan Tozun, Founding Editor

Department of Gastroenterology, Acibadem Mehmet Ali  
Aydinlar University School of Medicine, Istanbul, Turkiye  
nurdantozun@hotmail.com

#### Bulent Degertekin

Department of Gastroenterology, Acibadem Mehmet Ali  
Aydinlar University School of Medicine, Istanbul, Turkiye  
degertekinb@hotmail.com

### TASL Governing Board 2025–2027

#### Bulent Degertekin

Department of Gastroenterology, Acibadem Mehmet Ali  
Aydinlar University, School of Medicine, Istanbul, Turkiye  
degertekinb@hotmail.com

#### Gupse Adali

Department of Gastroenterology, Istanbul University of Health  
Sciences, Istanbul, Turkiye  
gupseadali@gmail.com

#### Suna Yapali

Department of Gastroenterology, Acibadem Mehmet Ali  
Aydinlar University, School of Medicine, Istanbul, Turkiye  
sunayapali@yahoo.com

#### Remzi Adnan Akdogan

Department of Gastroenterology, Recep Tayyip Erdogan  
University, School of Medicine, Rize, Turkiye  
remzi.akdogan@erdogan.edu.tr

#### Cumali Efe

Department of Gastroenterology, Diyarbakir Training and  
Research Hospital, Diyarbakir, Turkiye  
drcumi21@hotmail.com

#### Onur Keskin

Department of Gastroenterology, Hacettepe University School  
of Medicine, Ankara, Turkiye  
onurkeskin81@gmail.com

#### Ramazan Idilman

Department of Gastroenterology, Ankara University School of  
Medicine, Ankara, Turkiye  
ramazan.idilman@medicine.ankara.edu.tr

---

## Information for Authors

Hepatology Forum welcomes original articles, reviews, case reports, clinical images, and letters. All manuscripts must be submitted via the online submission system at [www.hepatologyforum.org](http://www.hepatologyforum.org). Please consult the website for the most current instructions, formatting guidelines, and ethical policies.

## Abstracting and Indexing

Hepatology Forum is indexed in **PubMed**, **PubMed Central**, **Web of Science (ESCI)**, **EBSCO**, **ProQuest**, **Open Ukrainian Citation Index**, **CAS**, **MIAR (2024)**, **TUBITAK TR Index (2022)** and **Turkiye Citation Index**.

---

## Contact

**Editor in Chief:** Prof. Ulus Salih Akarca  
**Address:** EKD, 184 S, 1/4, 35100, Bornova, Izmir  
**E-mail:** ulus.salih.akarca@ege.edu.tr

### Turkish Association for the Study of the Liver

**Address:** Inonu mah. Cumhuriyet cad. No: 131 Mutlu apt. Kat: 4  
D: 5 Harbiye, Istanbul/Turkiye  
**Phone:** +90 212 244 30 71  
**Fax:** +90 212 234 19 60  
**Web:** [www.tasl.org.tr](http://www.tasl.org.tr)  
**E-mail:** [tasl@tasl.org.tr](mailto:tasl@tasl.org.tr)

**Publisher:** Kare Media  
**Address:** Goztepe Mahallesi, Fahrettin Kerim Gokay Caddesi,  
No: 200, Daire: 2, Kadikoy, Istanbul/Turkiye  
**Phone:** +90 216 550 61 11  
**Fax:** +90 216 550 61 12  
**Web:** [www.karepb.com](http://www.karepb.com)  
**E-mail:** [kare@karepb.com](mailto:kare@karepb.com)

## Content

### Editorial

- From dysbiosis to MASLD: The central role of the gut microbiota .....85  
*Khalenkow M, Kaya E, Canbay A*

### Invited Editorial

- AI redefines fibrosis patterns in steatotic liver disease: Opportunities and challenges .....88  
*Zhou X-D, Yilmaz Y, Zheng M-H*

### Systematic Review

- Embolization of spontaneous portosystemic shunts for refractory hepatic encephalopathy in cirrhosis patients: A meta-analysis .....91  
*Patel P, Ebrahim M, Zaher E, Khataniar H, Loganathan P, Adler DG*

### Original Articles

- Assessment of GALAD score as a diagnostic and prognostic factor of *de novo* hepatitis C–related hepatocellular carcinoma post treatment with direct-acting antivirals.....101  
*Ramadan A, Abdelaziz AO, Nabeel MM, Atef M, Kamel MH, Elbaz TM, Hatem A, Medhat E, Abdelmaksoud AH, Lithy R, Maher R, Mohamed SAA, Kamel AH, Shousha HI*

- High expression of USP15 affects tumor progression and immune infiltration in hepatocellular carcinoma.....108  
*Wu S-P, Zhang X-Y, Chen H-D, Jin F-Z, Jiang N, Zhang J-X, Liang Z-L*

- The usefulness of a simultaneous immunoassay for hepatitis C virus antigen-antibody using the ELECSYS HCV Duo assay..... 118  
*Amano K, Sano T, Ide T, Nakano D, Bekki S, Arinaga-Hino T, Kawaguchi T*

- Plasma *PDGFRβ* and *PSD4* methylation levels for non-invasive staging of liver fibrosis .....125  
*Ulukan B, Yang H, Uludag H, Zhang C, Mutlu A, Dayangac M, Akyildiz M, Yigit B, Soleimani S, Kirimlioglu H, Saka B, Ataizi Celikel C, Eren F, Mardinoglu A, Yilmaz Y, Zeybel M*

- Evaluation of percutaneous endobiliary punch biopsy in suspected malignant biliary strictures: Five-year experience from a tertiary center .....133  
*Avcioğlu U, Demiroz H, Soylu AI, Uzunkaya F, Akkaya H, Goren I, Ayyıldız T, Ustaoglu Dede M, Bektas A*

- Empagliflozin versus dapagliflozin in patients with liver cirrhosis: A comparative real-world study on hepatic decompensation.....139  
*Ahmed H, Razzak IA, Abdulrazzak E, Goma S, Lauchner J*

### Reviews

- Occult hepatitis B infection .....146  
*Wati ME, Yusra*

- A traditional herbal remedy in liver diseases: *Momordica charantia* L. (kudret narı/bitter melon).....154  
*Altintas Gunduz D, Balaban Y, Koca Caliskan U*

### Case Reports

- Methylprednisolone for *Swietenia macrophylla* seeds-induced liver injury: A report of two cases.....163  
*Huang Z-Y, Zhang X-J, Tong X-C, Xue Y*

- Peritonitis due to brucellosis in a patient newly diagnosed with liver cirrhosis complicated by ascites: A case report and literature review .....167  
*Ekici R, Filiz M, Onus S, Akcay AG, Bakir T, Buyukturan G, Aydin EG, Ekici M, Aydinli M, Ercin CN*

- Chanarin-Dorfman Syndrome: Two siblings with steatohepatitis, cirrhosis, and a novel mutation.....171  
*Mutlu Bilgic N, Adali G, Ozturkeri B, Canbek S, Surmeli R*

## EDITORIAL

# From dysbiosis to MASLD: The central role of the gut microbiota

 Maxim Khalenkow<sup>1</sup>,  Eda Kaya<sup>2,3</sup>,  Ali Canbay<sup>2</sup>

1: Ghent University Hospital, Corneel Heymanslaan 10, 9000 Ghent, Belgium

2: Department of Medicine, Universitätsklinikum Knappschafts Krankenhaus Bochum, Ruhr University Bochum, Bochum, Germany

3: The Global NASH Council, Washington, DC, USA

Metabolic dysfunction–associated steatotic liver disease (MASLD) is the most prevalent chronic liver disease worldwide, yet treatment options remain limited.<sup>[1]</sup> Recent studies indicate that MASLD is associated with impaired pathophysiological mechanisms within the gut–liver axis, including increased intestinal permeability and consequent oxidative stress. These findings suggest that interventions targeting the gastrointestinal microbiota or restoring intestinal barrier integrity may attenuate downstream hepatic inflammation.<sup>[2]</sup>

In this context, we read with great interest the study by Celik et al.,<sup>[3]</sup> which investigated the effects of rifaximin—an intestinal decontaminant used in the management of hepatic encephalopathy—in an experimental model of fructose-induced MASLD. In fructose-fed mice, rifaximin exerted significant anti-inflammatory and antioxidant effects. The authors also discussed that these changes might be associated with improvements in the intestinal microflora and reductions in inflammatory parameters. Unfortunately, the authors did not include an analysis of the intestinal microbiota; therefore, it is difficult to determine whether rifaximin exerts its effects primarily through barrier-related or microbiome-mediated mechanisms, or via alternative or direct anti-inflammatory pathways. On the other hand, such an effect is plausible under rifaximin treatment. Previous mouse model studies have reported rifaximin-induced shifts in the gut microbiota, notably characterized by an increased abundance of *Lactobacillus*.<sup>[4]</sup> Moreover, Wan et al.<sup>[5]</sup> provided a mechanistic explanation for this variability by demonstrating that, in methionine–choline-deficient diet–induced MASH, rifaximin ameliorated steatosis, inflammation, and fibrosis, apparently through a specific microbiome–bile acid–host signaling axis.

Gut-microbiome–associated disturbances in bile acid metabolism have also been linked to abnormalities in lipid metabolism and the development of MASLD. Bile acids play a key regulatory role by activating the farnesoid X receptor (FXR), which in turn modulates pathways involved in lipid metabolic control.<sup>[6]</sup> In a mouse model, treatment with rifaximin appeared to reduce levels of the secondary bile acid deoxycholic acid rather than affecting primary bile acids, and this reduction was associated with alterations in the gut microbiome. Because deoxycholic acid directly activates FXR, mice receiving rifaximin showed improvements in MASH, suggesting that microbiome-mediated changes in bile acid composition may contribute to the therapeutic effect.<sup>[7]</sup>

**How to cite this article:** Khalenkow M, Kaya E, Canbay A. From dysbiosis to MASLD: The central role of the gut microbiota. *Hepatology Forum* 2026; 7(2):85–87.

**Received:** February 16, 2026; **Revised:** February 28, 2026; **Accepted:** March 09, 2026; **Available Online:** April 07, 2026

**Corresponding author:** Ali Canbay; Department of Medicine, Universitätsklinikum Knappschafts Krankenhaus Bochum, Ruhr University Bochum, Bochum, Germany;

**E-mail:** ali.canbay@rub.de



This work is licensed under a Creative Commons Attribution-NonCommercial 4.0 International License.

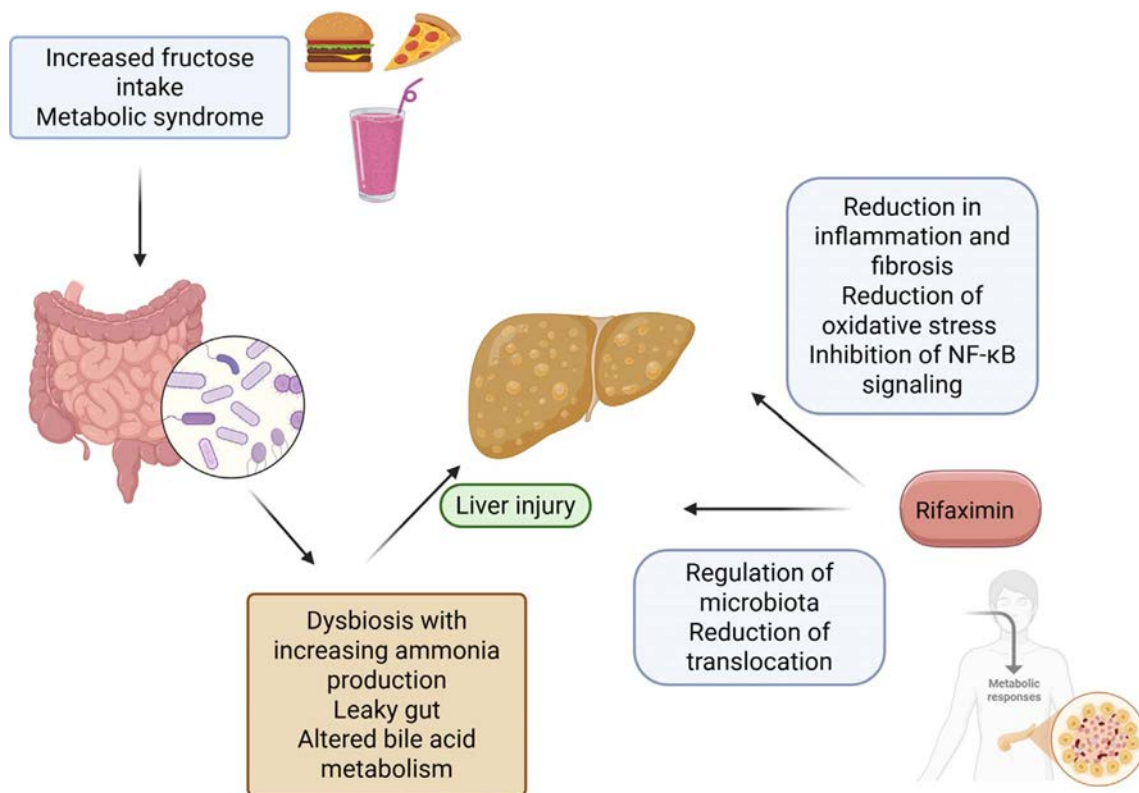


**Figure 1.** Effects of rifaximin on gut microbiota regulation and metabolic dysfunction–associated steatohepatitis (MASH).

The gut microbiota is implicated not only in MASH pathophysiology but also in the development of hepatocellular carcinoma (HCC). Comparative analyses have demonstrated a progressive reduction in the relative abundance of Bacteroidetes and, to a lesser extent, Actinobacteria across disease stages, from healthy controls to MASH and MASH-associated HCC.<sup>[8]</sup> Increasing evidence indicates stage-specific alterations in intestinal microbiota composition associated with liver disease severity, supporting the exploration of microbiota-targeted therapeutic strategies such as probiotics, antimicrobial agents, and fecal microbiota transplantation.<sup>[9]</sup> Clinical studies, however, demonstrate heterogeneous effects of rifaximin, with improvements in hepatic inflammation and fibrosis mainly observed in long-term rather than short-term interventions, suggesting that sustained modulation of the intestinal microbiota may be required to achieve meaningful benefits.<sup>[10,11]</sup> Taken together, the long-term effects of rifaximin on gut microbiota composition and liver health remain insufficiently understood, and the mechanisms mediating fibrotic and inflammatory activation require further investigation. The effects of rifaximin are summarized in Figure 1.

Over recent years, substantial progress has been made in the field of MASLD, beginning with the establishment of an updated disease classification,<sup>[12]</sup> followed by the conditional and full approval of the first pharmacological therapies for MASH, including resmetirom and semaglutide.<sup>[13]</sup> In this evolving therapeutic landscape, the gut microbiota and associated bile acid metabolism are expected to

assume an increasingly important role. As knowledge continues to expand, microbiota-targeted strategies may enable modification of disease trajectories and potentially allow prevention at early stages. In this regard, Celik et al.<sup>[3]</sup> demonstrated in a well-designed mouse model that rifaximin ameliorated steatohepatitis, with biochemical improvements translating into consistent histopathological findings, thereby contributing to the existing body of evidence. However, the effects of rifaximin on the human microbiota—particularly whether these changes occur on an individual or generalizable level—and its long-term impact on metabolic and liver health remain insufficiently understood and require further investigation. In particular, integrative studies bridging experimental models and clinical research, while comprehensively addressing the multifaceted effects of rifaximin, are still lacking and represent an important priority for future research.

**Conflict of Interest:** The authors have no conflict of interest to declare.

**Financial Disclosure:** The authors declared that this study has received no financial support.

**Use of AI for Writing Assistance:** We did not use any artificial intelligence-assisted technologies in the preparation of this manuscript.

**Author Contributions:** Concept: EK, AC; Supervision: AC; Funding: AC; Analysis and/or Interpretation: MK, EK; Literature Search: MK, EK, AC; Writing: MK, EK, AC; Critical Reviews: EK, AC.

**Peer-review:** Externally peer-reviewed.

## References

1. Younossi ZM, Kalligeros M, Henry L. Epidemiology of metabolic dysfunction-associated steatotic liver disease. *Clin Mol Hepatol* 2025;31(Suppl):S32-S50. [\[CrossRef\]](#)
2. Torre P, Motta BM, Sciorio R, Masarone M, Persico M. Inflammation and Fibrogenesis in MAFLD: Role of the Hepatic Immune System. *Front Med (Lausanne)* 2021;8:781567. [\[CrossRef\]](#)
3. Celik NC, Goc RY, Bahcecioglu IH, Ozercan IH, Tuzcu M, Ilhan N, et al. Effects of rifaximin in fructose-induced steatohepatitis in rats. *Hepatol Forum* 2025;6(4):160-165. [\[CrossRef\]](#)
4. Brol MJ, Alvarez-Silva C, Schierwagen R, Uschner FE, Klein S, Trebicka J, et al. WED-548 Rifaximin-alpha acts through increased abundance of *Lactobacillus* spp. in murine models of chronic liver disease. *J Hepatol* 2024;80:S283. [\[CrossRef\]](#)
5. Wan YP, Li S, Li D, Huang XM, Wu JH, Jian J. Study on the molecular mechanisms of rifaximin in the treatment of non alcoholic steatohepatitis based on the *Helicobacter* DCA Fxr Hnf1 $\alpha$  signalling pathway. *Mol Med Rep* 2025;31(2):42. [\[CrossRef\]](#)
6. Hu H, Lin A, Kong M, Yao X, Yin M, Xia H, et al. Intestinal microbiome and NAFLD: molecular insights and therapeutic perspectives. *J Gastroenterol* 2020;55(2):142-158. [\[CrossRef\]](#)
7. Jian J, Nie MT, Xiang B, Qian H, Yin C, Zhang X, et al. Rifaximin ameliorates non-alcoholic steatohepatitis in mice through regulating gut microbiome-related bile acids. *Front Pharmacol* 2022;13:841132. [\[CrossRef\]](#)
8. Sydor S, Best J, Messerschmidt I, Manka P, Vilchez-Vargas R, Brodesser S, et al. Altered microbiota diversity and bile acid signaling in cirrhotic and noncirrhotic NASH-HCC. *Clin Transl Gastroenterol* 2020;11(3):e00131. [\[CrossRef\]](#)
9. Lau HC-H, Zhang X, Yu J. Gut microbiome in metabolic dysfunction-associated steatotic liver disease and associated hepatocellular carcinoma. *Nat Rev Gastroenterol Hepatol* 2025;22(9):619-638. [\[CrossRef\]](#)
10. Abdel-Razik A, Mousa N, Shabana W, Refaey M, Elzehery R, Elhelaly R, et al. Rifaximin in nonalcoholic fatty liver disease: hit multiple targets with a single shot. *Eur J Gastroenterol Hepatol* 2018;30(10):1237-1246. [\[CrossRef\]](#)
11. Cobbold JFL, Atkinson S, Marchesi JR, Smith A, Wai SN, Stove J, et al. Rifaximin in non-alcoholic steatohepatitis: An open-label pilot study. *Hepatol Res* 2018;48(1):69-77. [\[CrossRef\]](#)
12. Yilmaz Y. The heated debate over NAFLD renaming: An ongoing saga. *Hepatol Forum* 2023;4(3):89-91. [\[CrossRef\]](#)
13. Kaya E, Yilmaz Y, Alkhouri N. Metabolic dysfunction-associated steatohepatitis treatment: spotlight on the latest hepatoprotective drugs. *Expert Opin Pharmacother* 2025;26(14-15):1589-1598. [\[CrossRef\]](#)

## INVITED EDITORIAL

# AI redefines fibrosis patterns in steatotic liver disease: Opportunities and challenges

 Xiao-Dong Zhou<sup>1,2</sup>,  Yusuf Yilmaz<sup>3</sup>,  Ming-Hua Zheng<sup>1,2</sup>

1: MAFLD Research Center, Department of Hepatology, the First Affiliated Hospital of Wenzhou Medical University, Wenzhou, China

2: Key Laboratory of Diagnosis and Treatment for the Development of Chronic Liver Disease in Zhejiang Province, Wenzhou, China

3: Department of Gastroenterology, School of Medicine, Recep Tayyip Erdogan University, Rize, Turkiye

## Introduction

Steatotic liver disease (SLD) has emerged as a major global health burden, with rapidly rising prevalence and substantial contributions to both liver-related and cardiometabolic morbidity and mortality.<sup>[1]</sup> It comprises a heterogeneous group of chronic liver disorders with diverse pathophysiological drivers and variable clinical outcomes, posing significant challenges for risk stratification and therapeutic development.<sup>[2]</sup> Across its major subtypes, including metabolic dysfunction-associated steatotic liver disease (MASLD), metabolic dysfunction-associated alcoholic liver disease (MetALD), and alcoholic liver disease (ALD), patients are exposed to differing constellations of metabolic stress, alcohol-related toxicity, and inflammatory signaling. These distinct pathogenic influences may translate into variable patterns of fibrotic remodeling and organ-specific complications. However, conventional histopathology, which relies largely on semiquantitative scoring systems and interobserver interpretation, often lacks the resolution to capture such spatial and mechanistic nuances, thereby limiting deeper insight into disease biology and individualized risk assessment.

AI-based digital pathology provides a transformative platform to overcome these limitations by enabling automated, quantitative, and spatially resolved tissue analysis.<sup>[3]</sup> This approach allows high-resolution mapping of collagen deposition, zonal fibrosis patterns, and microenvironmental remodeling, providing a framework to link histologic features with underlying mechanisms and clinically relevant outcomes. By moving beyond global fibrosis staging to “where and how” fibrosis develops, AI-based approaches can elucidate both disease biology and individualized patient risk.

The potential of AI-based digital pathology spans several interrelated areas. First, AI-based spatial analysis may help explain the heterogeneity of fibrosis across SLD subtypes. MASLD, MetALD, and ALD represent distinct constellations of metabolic stress and alcohol-related injury, which may give rise to different regional patterns of fibrotic remodeling. In a recent study employing AI-based quantitative fibrosis assessment with second harmonic generation imaging in 88 biopsy samples, investigators demonstrated that, despite comparable overall fibrosis stages, MetALD and ALD exhibited significantly greater collagen density in periportal and zone 2 regions than MASLD.<sup>[4]</sup>

**How to cite this article:** Zhou X-D, Yilmaz Y, Zheng M-H. AI redefines fibrosis patterns in steatotic liver disease: Opportunities and challenges. *Hepatology Forum* 2026; 7(2):88–90.

**Received:** March 05, 2026; **Accepted:** March 07, 2026; **Available Online:** April 07, 2026

**Corresponding author:** Ming-Hua Zheng; MAFLD Research Center, Department of Hepatology, the First Affiliated Hospital of Wenzhou Medical University, Wenzhou, China; Key Laboratory of Diagnosis and Treatment for the Development of Chronic Liver Disease in Zhejiang Province, Wenzhou, China; **E-mail:** zhengmh@wmu.edu.cn



This work is licensed under a Creative Commons Attribution-NonCommercial 4.0 International License.

Similarly, lean patients with MASLD may exhibit different zonal distributions and collagen architectures compared with non-lean patients, reflecting differences in metabolic pathways, lipid deposition, and local inflammatory responses. Mapping these spatial patterns could provide both diagnostic insight and a framework for understanding subtype-specific pathophysiology.

Second, digital pathology enables mechanistic studies of SLD by dissecting how spatially resolved microenvironmental factors drive fibrosis. Regional variations in hepatic microcirculation and blood flow along the hepatic vascular axis modulate exposure of hepatocytes and stellate cells to metabolic substrates, alcohol, and inflammatory mediators. Metabolic dysfunction, cardiometabolic risk factors, and alcohol toxicity may therefore exert spatially distinct effects, promoting localized stellate cell activation, chronic inflammation, and vascular remodeling, which shape collagen deposition and extracellular matrix architecture. Each of these risk factors can contribute to liver fibrosis progression, but the relative influence of different factors in specific hepatic zones requires further investigation.<sup>[5,6]</sup> High-resolution spatial mapping integrated with molecular profiling can clarify whether metabolic inflammation and alcohol-induced injury act via separate or overlapping pathways. This mechanistic insight may inform the development of targeted therapies by identifying zone-specific and microenvironment-dependent fibrogenic pathways, clarifying how interventions reshape spatial fibrosis architecture, and supporting rational combination strategies that address both hepatic and cardiometabolic drivers of disease.<sup>[7]</sup>

Third, AI-based spatial analysis supports precision classification and individualized management by linking fibrosis patterns to clinical outcomes.<sup>[8]</sup> Patients with MASLD show heterogeneous trajectories: some primarily develop liver-related events such as cirrhosis or hepatocellular carcinoma, while others are prone to cardiometabolic complications.<sup>[9]</sup> AI-derived spatial signatures can identify fibrosis patterns predictive of specific outcomes. For example, prior AI-derived spatial analyses have shown that fibrosis progression in central and pericentral regions correlates with subsequent renal function decline.<sup>[10]</sup> Additionally, spatial analysis can define a cardiovascular-risk predominant MASLD subtype, characterized by fibrosis patterns reflecting systemic metabolic stress and a higher risk of cardiovascular events. Recognizing this subtype enables clinicians to prioritize cardiovascular risk management, including lifestyle modification, blood pressure and lipid control, and cardiac monitoring, while simultaneously addressing liver-directed therapy. By integrating hepatic and systemic risk stratification, AI-based digital pathology provides a pathway toward precision hepatology and heart-liver co-management.<sup>[11]</sup>

Fourth, digital pathology may support region-specific monitoring and therapy by distinguishing areas of stable versus rapidly progressing fibrosis within the same liver.<sup>[12]</sup> Fibrosis is rarely uniform, and different regions may progress at different rates due to local variations in blood supply, inflammation, or stellate cell activation. Identifying rapidly progressing regions enables clinicians to prioritize surveillance and interventions in areas at

highest risk, while avoiding unnecessary procedures in more stable regions. Such targeted monitoring could inform decisions on biopsy sampling, imaging follow-up, or even region-specific therapeutic approaches in the future. Moreover, mapping fibrosis dynamics at high spatial resolution may help anticipate complications such as portal hypertension or segmental liver dysfunction by linking structural remodeling to functional consequences. By capturing the intrahepatic heterogeneity of disease progression, AI-based digital pathology provides a precise framework for individualized, risk-adapted patient management.

Fifth, AI-based digital pathology offers unique opportunities in clinical trials by providing objective, quantitative, and spatially resolved endpoints.<sup>[13]</sup> Traditional histologic scoring often lacks sensitivity to detect subtle changes or regional effects of interventions. By contrast, AI-derived measures such as qFibrosis can capture both progression and regression of fibrosis on a continuous scale across multiple liver regions. For instance, strengthened lifestyle intervention in MASLD patients produced pronounced fibrosis regression in the periportal region, as detected by qFibrosis, whereas conventional histology failed to capture these regional differences.<sup>[14]</sup> Importantly, different pharmacologic agents may act on distinct microenvironments or fibrosis patterns within the liver, and AI-based spatial analysis can reveal these region-specific effects. Such insights enable the rational design of combination therapies targeting complementary fibrogenic pathways or spatially distinct microenvironments, thereby addressing the multifactorial nature of SLD and potentially enhancing overall efficacy.<sup>[15]</sup> Spatially resolved, quantitative endpoints, therefore, facilitate earlier and more precise evaluation of treatment effects, improve differentiation between intervention groups and placebo responses, and may reduce sample size requirements or study duration. By integrating digital pathology into clinical trials, researchers can accelerate drug development, optimize patient selection, and better understand how interventions reshape liver architecture at a mechanistic level, ultimately supporting precision and combined therapeutic strategies.<sup>[13]</sup>

Despite its transformative potential, several challenges must be addressed before AI-based digital pathology can be widely implemented in clinical practice. First, standardization of image acquisition and algorithm training is critical, as variations in slide preparation, staining protocols, scanning resolution, and even tissue handling can introduce bias and affect the consistency of extracted features. Without rigorous standardization, results may not be comparable across laboratories or studies. Second, cross-center reproducibility remains a major hurdle. Algorithms trained in one center may perform differently in another due to differences in patient populations, equipment, or local histology practices, limiting generalizability. Third, cost considerations and infrastructure requirements may pose barriers, as high-resolution scanners, computational resources, and specialized personnel are necessary to implement AI-based workflows, potentially restricting access to larger or resource-limited centers. Fourth, validation in large and diverse cohorts is essential. Current studies are often limited by small sample sizes, homogenous populations, or single-center data,

raising concerns about the robustness and reliability of identified spatial patterns when applied to broader patient populations. Finally, linking spatial histologic phenotypes to clinically meaningful outcomes requires carefully designed prospective studies. Only by correlating AI-derived tissue signatures with both hepatic endpoints (e.g., cirrhosis progression, hepatocellular carcinoma) and systemic outcomes (e.g., cardiovascular events, renal function) can we determine whether these digital biomarkers truly guide individualized management strategies and therapeutic decision-making. Addressing these challenges is crucial for translating the promise of AI-based digital pathology into actionable clinical tools.

## Conclusion

In conclusion, AI-based digital pathology should be regarded not merely as an advanced diagnostic tool but as a platform for understanding the spatial logic of liver disease. By capturing heterogeneity, linking microenvironmental mechanisms to fibrosis architecture, and associating patterns with distinct clinical outcomes, digital pathology provides a roadmap for precision hepatology. In an era where metabolic liver disease and cardiovascular disease are increasingly intertwined, leveraging spatial tissue analytics to inform individualized, integrated management may represent one of the most impactful directions for both research and clinical care.

**Financial Disclosure:** Ming-Hua Zheng serves as a speaker for AstraZeneca, Hisky Medical Technologies, and Novo Nordisk; as a consultant for Boehringer Ingelheim and Eieling Technology; and has received consulting fees from Boehringer Ingelheim. Yusuf Yilmaz has received personal consultancy fees from Novo Nordisk and Zydus.

**Conflict of Interest:** The remaining authors declare no conflicts of interest.

**Use of Artificial Intelligence:** The authors used an AI-assisted language editing tool (ChatGPT, OpenAI) to improve the clarity and grammar of the manuscript. The authors reviewed and edited the output and take full responsibility for the content of the publication.

**Author Contributions:** Concept: X-DZ, M-HZ; Design: M-HZ; Supervision: M-HZ; Data Collection and/or Processing: X-DZ, M-HZ; Analysis and/or Interpretation: X-DZ, YY, M-HZ; Literature Review: M-HZ; Writing: X-DZ, YY, M-HZ; Critical Review: X-DZ, YY, M-HZ.







**Peer-review:** Externally peer-reviewed.

## References

1. Suenghataiphorn T, Boonpiraks K, Prasitsumrit V, Kulthamrongsri N, Danpanichkul P. Future burden of MASLD in the United States: A state-level forecasting study, 2022-2050. *Hepatol Forum* 2026;7(1):32-37. [\[CrossRef\]](#)
2. Byrne CD, Armandi A, Pellegrinelli V, Vidal-Puig A, Bugianesi E. Metabolic dysfunction-associated steatotic liver disease: a condition of heterogeneous metabolic risk factors, mechanisms and comorbidities requiring holistic treatment. *Nat Rev Gastroenterol Hepatol* 2025;22(5):314-328. [\[CrossRef\]](#)
3. Pulaski H, Harrison SA, Mehta SS, et al. Clinical validation of an AI-based pathology tool for scoring of metabolic dysfunction-associated steatohepatitis. *Nat Med* 2025;31(1):315-322. [\[CrossRef\]](#)
4. Kim GA, Jang H, Kim MY, Park JH, Park JG, Cho EY, et al. Multicenter prospective cohort study on clinical outcomes and fibrosis patterns in biopsy-proven steatotic liver disease subtypes. *Gastroenterology* 2026 Jan 29;S0016-5085(26)00030-2. doi: 10.1053/j.gastro.2026.01.007. [Epub ahead of print]. [\[CrossRef\]](#)
5. Zhou XD, Lian LY, Chen QF, Kim SU, Cheuk-Fung Yip T, Petta S, et al. Effect of hypertension on long-term adverse clinical outcomes and liver fibrosis progression in MASLD. *J Hepatol* 2026;84(2):254-265. [\[CrossRef\]](#)
6. Zhou XD, Chen QF, Kim SU, Cheuk-Fung Yip T, Petta S, Nakajima A, et al. Long-term glycemic control and the risk of liver stiffness progression and liver-related events in MASLD. *Clin Gastroenterol Hepatol* 2025 Nov 4;S1542-3565(25)00867-5. doi: 10.1016/j.cgh.2025.10.003. [Epub ahead of print]. [\[CrossRef\]](#)
7. Zhou XD, Lazarus JV, Krittanawong C, Targher G, Byrne CD, Younossi ZM, et al. Pharmacotherapy for metabolic dysfunction-associated steatohepatitis: heart-liver co-management. *Lancet Gastroenterol Hepatol*. 2026 Feb 13;S2468-1253(25)00323-1. doi: 10.1016/S2468-1253(25)00323-1. [Epub ahead of print]. [\[CrossRef\]](#)
8. Aggarwal A, Bharadwaj S, Corredor G, Pathak T, Badve S, Madabhushi A. Artificial intelligence in digital pathology - time for a reality check. *Nat Rev Clin Oncol* 2025;22(4):283-291. [\[CrossRef\]](#)
9. Zhou XD, Song SJ, Guo CY, Chen QF, Lai-Hung Wong G, et al. Validation of a data-driven clustering model for MASLD: Evidence from three large-scale Asian cohorts. *JHEP Rep* 2025;8(1):101645. [\[CrossRef\]](#)
10. Sun DQ, Shen JQ, Tong XF, Ren YY, Yuan HY, Li YY, et al. Liver fibrosis progression analyzed with AI predicts renal decline. *JHEP Rep* 2025;7(5):101358. [\[CrossRef\]](#)
11. Zhou XD, Zheng MH. Heart-liver co-management in MASLD: from concept to clinical practice. *Nat Rev Gastroenterol Hepatol* 2026;23(2):117-118. [\[CrossRef\]](#)
12. Naoumov NV, Brees D, Loeffler J, Chng E, Ren Y, Lopez P, et al. Digital pathology with artificial intelligence analyses provides greater insights into treatment-induced fibrosis regression in NASH. *J Hepatol* 2022;77(5):1399-1409. [\[CrossRef\]](#)
13. Iyer JS, Juyal D, Le Q, Shanis Z, Pokkalla H, Pouryahya M, et al. AI-based automation of enrollment criteria and endpoint assessment in clinical trials in liver diseases. *Nat Med* 2024;30(10):2914-2923. [\[CrossRef\]](#)
14. Yuan HY, Tong XF, Ren YY, et al. AI-based digital pathology provides newer insights into lifestyle intervention-induced fibrosis regression in MASLD: An exploratory study. *Liver Int* 2024;44(10):2572-2582. [\[CrossRef\]](#)
15. Zhou XD, Fan QY, Byrne CD, Targher G, Muthiah MD, Huang DQ, et al. Combination therapies for metabolic dysfunction-associated steatohepatitis: challenges and opportunities. *Gut* 2026;75(4):815-825. [\[CrossRef\]](#)

## SYSTEMATIC REVIEW

# Embolization of spontaneous portosystemic shunts for refractory hepatic encephalopathy in cirrhosis patients: A meta-analysis

 Parth Patel<sup>1</sup>,  Mohamad Ebrahim<sup>1</sup>,  Eli Zaher<sup>1</sup>,  Himsikhar Khataniar<sup>2</sup>,  Priyadarshini Loganathan<sup>3</sup>,  
 Douglas G. Adler<sup>4</sup>

1: Department of Internal Medicine, Saint Joseph Hospital, Chicago, USA

2: Department of Internal Medicine, Allegheny General Hospital, Pennsylvania, USA

3: Department of Gastroenterology, University of Texas Health Science Center San Antonio, Texas, USA

4: Department of Gastroenterology, Center for Advanced Therapeutic Endoscopy at Porter Adventist Hospital, Colorado, USA

## Points to Note

- **Synthesis of Current Evidence:** SPSS embolization improves refractory/recurrent HE, lowers ammonia, and reduces HE-related hospitalization.
- **Major Controversies:** Its effect on portal hypertension remains uncertain because ascites, varices, and GI bleeding may worsen after embolization.
- **Future Directions:** Larger randomized trials are needed to compare embolization with standard medical therapy and define optimal patient selection.

## ABSTRACT

**Background and Aim:** Hepatic encephalopathy is an important cause of morbidity in cirrhosis patients. The presence of spontaneous portosystemic shunts (SPSS) is associated with an increased risk of recurrent/refractory hepatic encephalopathy (HE). Embolization of SPSS has been shown to improve HE symptoms, but it may worsen portal hypertension and related complications. The aim of this study was to determine the efficacy of SPSS embolization for recurrent/refractory HE.

**Materials and Methods:** Five databases were screened to identify studies assessing the efficacy of SPSS embolization for HE. The random-effects model was used to calculate the pooled rates, and I<sup>2</sup> values were used to assess heterogeneity.

**Results:** Twenty-one studies met the inclusion criteria, comprising a total of 331 patients with recurrent or refractory HE despite medical management. The etiology of cirrhosis included ethanol abuse, chronic viral hepatitis, MASH, and others. Following embolization, 82% of patients had HE-related clinical improvement, and 71% of patients became free from HE-related hospitalization. The mean difference in pre- and post-embolization serum ammonia levels was 104 [77-130],  $p < 0.01$ . Worsening portal hypertension following embolization presented as gastrointestinal bleeding (10%), new or aggravated varices (15%), and new or aggravated ascites (15%).

**Conclusion:** SPSS embolization demonstrated improvement in HE-related clinical symptoms with a decreased need for hospitalization, but it exacerbates portal hypertension, increasing the risks of ascites, varices, and gastrointestinal bleeding. Future randomized controlled trials are needed to evaluate the efficacy of SPSS embolization against standard medical management.

**Keywords:** Cirrhosis, hepatic encephalopathy, spontaneous portosystemic shunts.

**How to cite this article:** Patel P, Ebrahim M, Zaher E, Khataniar H, Loganathan P, Adler DG. Embolization of spontaneous portosystemic shunts for refractory hepatic encephalopathy in cirrhosis patients: A meta-analysis. *Hepatology Forum* 2026; 7(2):91–100.

**Received:** August 13, 2024; **Revised:** January 20, 2025; **Accepted:** March 08, 2025; **Available Online:** April 28, 2026

**Corresponding author:** Douglas G. Adler; Center for Advanced Therapeutic Endoscopy (CATE), Porter Adventist Hospital, Denver, Colorado, USA; **E-mail:** dougraham2001@gmail.com



This work is licensed under a Creative Commons Attribution-NonCommercial 4.0 International License.

## Introduction

Hepatic encephalopathy (HE) is a reversible syndrome encompassing neuropsychiatric pathologies resulting from the accumulation of neurotoxins in the bloodstream.<sup>[1]</sup> HE occurs in patients with acute or advanced liver disease, as well as in those with portosystemic shunting even in the absence of liver disease.

Overt HE, characterized by a noticeable decline in cognitive and neurological function, affects 30–45% of patients with cirrhosis and leads to approximately 20,000 hospitalizations annually in the United States.<sup>[2–4]</sup> Inpatient management of HE is costly, with an average of \$35,000 per hospital stay.<sup>[5]</sup> Morbidity is further complicated by an increased risk of falls, the inability to safely drive, and caregiver burden.<sup>[5]</sup>

Management of HE focuses on identifying precipitating factors, administering ammonia-lowering therapies, and preventing recurrence.<sup>[6]</sup> According to the American Association for the Study of Liver Diseases (AASLD), lactulose is recommended as the first-line therapy for treating overt HE, with rifaximin added to prevent recurrence.<sup>[2]</sup>

Patients with overt HE who do not respond to medical management are classified as having refractory HE. These patients may have developed spontaneous portosystemic shunts (SPSS), which are abnormal connections between the portal vein and systemic circulation.<sup>[6]</sup> While SPSS can act as “release valves” to reduce portal pressure, they bypass normal liver blood flow, increasing the risk of recurrent or refractory HE. Embolization of large SPSS is being investigated as a potential preventive measure for HE recurrence and may offer survival benefits.<sup>[7]</sup>

Although data on the clinical performance of SPSS embolization are currently limited to case series and small studies, we conducted a meta-analysis to comprehensively evaluate the efficacy of shunt embolization in managing persistent or recurrent HE.

## Materials and Methods

This study adhered to the Preferred Reporting Items for Systematic Reviews and Meta-Analysis (PRISMA) checklist to identify the efficacy of SPSS embolization for the management of refractory/recurrent HE (Supplementary Appendix A).

### Search Strategy

The literature was searched by the authors (PP, ME) for the concepts of spontaneous portosystemic shunts, hepatic encephalopathy, embolization, portal hypertension, and cirrhosis. Search strategies were created using a combination of keywords and standardized index terms. Searches were conducted in Embase (81), Scopus (8), PubMed (103), Web of Science (58), and Medline (43). Full search strategies are provided in Supplementary Appendix B.

The titles and abstracts of the identified studies were independently screened by two authors (PP and ME). Based on predetermined inclusion and exclusion criteria, studies that did not address our specific research question were excluded. The full texts of the selected articles were then reviewed for relevant information. Any discrepancy in article selection was resolved by mutual consensus after discussion with the third co-author (EZ). Additional relevant articles were manually searched from the bibliographic section of the selected articles, as well as the systematic and narrative articles on the topic.

### Study Selection

For the purpose of this meta-analysis, we included studies that evaluated the efficacy and safety of SPSS embolization for persistent or recurrent HE. Studies reporting data on adult patients (>18 years) with cirrhosis complicated by persistent or recurrent HE were included.

The exclusion criteria were as follows: (1) single-patient case reports, review articles, and editorials; (2) studies done in the pediatric (<18 years) population; (3) non-English-language studies; (4) non-human/animal studies; (5) non-clinical laboratory studies.

### Data Abstraction and Quality Assessment

Two authors (E.Z. and H.K.) independently abstracted data from the studies using a pre-approved standardized form. Two authors (M.A.E., P.P.) independently assessed the quality of the studies to ascertain the risk of bias. This was done using the National Institute of Health (NIH) quality assessment tool for before-after (pre-post) studies with no control group (Table 1).

### Outcomes Assessed

The outcomes assessed included clinical improvement in HE, changes in HE medication requirements, the need for HE-related hospitalization, changes in Model for End-Stage Liver Disease (MELD) score, serum ammonia levels, and serum creatinine levels. We also evaluated the development or worsening of varices and/or ascites and the incidence of gastrointestinal bleeding (GIB) following SPSS embolization for the management of persistent or recurrent HE.

### Statistical Analysis

Standard meta-analysis statistics were used, following the methods suggested by DerSimonian and Laird. The pooled efficacy rates with the corresponding 95% confidence intervals (CIs) were calculated by logit transformation using a random-effects model. Heterogeneity between study-specific estimates was assessed using the Cochrane Q test and the  $I^2$  statistic. Publication bias assessment is discussed under the validation of meta-analysis. All analyses were performed using Comprehensive Meta-Analysis (CMA) software, version 4 (BioStat, Englewood, NJ).

**Table 1.** Characteristics of the included studies

Study ID	Study type	Patients (n) / Male (n)	Age (mean)	Etiology of cirrhosis/shunt	Shunt anatomy	Embolization method	Embolization route	Follow-up period	Outcomes studied
Sakurabayashi et al. <sup>[9]</sup> 1997	Prospective	7 / 3	66	Etoh(1), HCV(4), cryptogenic(2)	Splenorenal shunts(5); gastrosplenic shunt(1); intrahepatic porto-hepatic vein shunt(1)	Stainless steel coil (7)	Percutaneous transhepatic vein(4); transrenal vein(3)	3-4 m	Improvement in HE, change in ammonia level, new/worsening PHTN
Chikamori et al. <sup>[10]</sup> 2000	Case series	5 / 2	60.2±6	Etoh(2); HCV(2); crypto(2)	Gastrorenal(5)	5% ethanalamine oleate with iopamidol(EOI) and absolute ethanol	Transjugular retrograde obliteration (TJO)	17-74 m	Improvement in HE, change in portal flow volume, change in ammonia level, new/worsening PHTN
Zidi et al. <sup>[11]</sup> 2007	Case series	7 / NR	66±9.2	HCV(4); Etoh(3)	Splenorenal(7)	Steel coils ± histoacryl	Transfemoral(6), transhepatic (1)	3 m	Improvement in HE, survival, new/worsening PHTN
Mukund et al. <sup>[12]</sup> 2012	Retrospective	7 / 7	56	MASH(2), Etoh(2), HBV(1), crypto(2)	Splenorenal(7)	Vascular plug or balloon occluder	BRTO with sodium tetradeceyl sulphate foam	4 m	Improvement in HE, change in ammonia levels, new/worsening PHTN
Laleman et al. <sup>[13]</sup> 2013	Retrospective, multicenter	37 / 21	60±12.7	MASH(3), Etoh(17), HCV(13), PBC(2), AIH(1), cryptogenic(1)	Splenorenal(20), meso-caval(7), periumbilical(9), meso-renal shunt(1)	Coils, Amplatzer plugs, matrix	Transhepatic (7); percutaneous (6); transfemoral or transjugular(23)	23±5 m	Improvement in HE, new/worsening PHTN
Young et al. <sup>[14]</sup> 2013	Retrospective	8 / 2	55.5±10.1	MASH, PBC, HCV, AIH, PSC, cryptogenic	NA	Coil, occluder, liquid agents	Common femoral vein(3); internal jugular vein(1); and transhepatic approach(3); recanalized paraumbilical vein(2)	3-28 mo; mean: 15.5±9.9	Improvement in HE, change in HE medications, new/worsening PHTN
An et al. <sup>[15]</sup> 2014	Retrospective cohort	17 / 11	61.6±2.6	HBV (9) HCV (2) Etoh(5) Others (1)	Splenorenal(14); paraumbilical(3)	Vascular plugs or coils + gelatin sponge	Femoral vein(14); percutaneous for paraumbilical vein(3)	17 m (6-37)	Improvement in HE, survival, change in liver function
Naeshiro et al. <sup>[16]</sup> 2014	Retrospective	14 / 9	68.7±5.6	HBV(1), HCV(9), alcohol(4)	Splenorenal(3); gastrosplenic(4), meso-caval(5); porto-caval(2)	Ethanalamine oleate (EO) OR EO+coils OR EO + coils OR EO, coils + n-butyl 2-cyanoacrylate (NBCA) OR coils+NBCA	Combination of these	27 (12-29 mo)	Improvement in HE, change in ammonia level, new/worsening PHTN, survival
Inoue et al. <sup>[17]</sup> 2014	Retrospective	19 / 8	66.9±2.2	HCV(12), HBV(1), ALD(4), schistosomiasis (1), crypto(1)	Splenorenal(19)	5% ethanalamine oleate with iopamidol(EOI) or coil occluder	BRTO	28.4±2.4 m	Improvement in HE, change in hepatic function reserve, survival, new/worsening PHTN
Parra-Farinas et al. <sup>[18]</sup> 2016	Prospective	35 / 18	60.7±15	MASH(4), Etoh(11), HCV(8), PBC(2), AIH(2), cryptogenic(8)	Spleno-renal shunts (24), meso-caval/renal (7), gastric azygos/renal (3), recanalized paraumbilical veins (1)	Coil or occluder and/or liquid agents	Common femoral vein (21), internal jugular vein (9), transhepatic (3), trans-splenic approaches (1).	3-31 m	Improvement in HE, new/worsening PHTN

**Table 1 (cont).** Characteristics of the included studies

Study ID	Study type	Patients (n) / Male (n)	Age (mean)	Etiology of cirrhosis/shunt	Shunt anatomy	Embolization method	Embolization route	Follow-up period	Outcomes studied
Lynn et al. <sup>[19]</sup> 2016	Retrospective	20 / 10	60.9±8.1	MASH (8), Etoh (5), HCV (2), AIH (1), PSC (1), A1AT (1), cryptogenic (1)	Splenorenal (12); IMV-ovarian (2); SMV-ovarian (1); Portal-right gonadal (1); IMV-left renal (1); Periumbilical-portosystemic (1); Multiple (2)	Coil (15); occluder (4); coil+occluder (1)	Transhepatic (5); right femoral vein (6); internal jugular vein (5); umbilical Vein (1); right axillary vein (3)	12 m	Hospitalization requirements, change in HE medications, change in ammonia level, new/worsening PHTN
Aw et al. <sup>[20]</sup> 2017	Retrospective	7 / 5	62.5	Etoh (3), chronic hepatitis (3), MASH (1)	NR	Combination of a vascular plug, coils and sclerosant	Retrograde transvenous obliteration.	3-6 m	Improvement in HE, change in ammonia level, new/worsening PHTN
Choudhary et al. <sup>[21]</sup> 2017	Retrospective	5 / 5	61±7	MASH (3), Etoh (1), HBV (1)	Splenorenal (4); mesocaval (1)	Vascular plugs ± sclerosant	Right femoral vein(4); right internal jugular vein (2)	9.8 m	Improvement in HE, change in ammonia level, new/worsening PHTN
Philips et al. <sup>[22]</sup> 2017	Retrospective	21 / 17	56±10.6	MASH (13), Etoh (6), crypto (2)	Splenorenal (17); mesocaval (7), other (6)	Coil, cyanoacrylate glue	PARTO, BRTO with or without cyanoacrylate glue embolization, or a combination of these	1-9 m	Improvement in HE, change in ammonia levels, new/worsening PHTN
He et al. <sup>[23]</sup> 2018	Retrospective cohort	44 / 31	51.2±11.6	HBV (29), HCV (2), Alcoholic liver disease (3), Others (2), Cryptogenic (8)	Splenorenal (29); mesocaval(2), gastroesophageal(13), recanalized paraumbilical vein(1)	Coil or vascular plug	Transjugular (44)	20.7 m (15.5–31.0)	Improvement in HE, new/worsening PHTN
Philips et al. <sup>[24]</sup> 2020	Retrospective	45 / 38	57.2±9.1	MASH(28), Etoh(15), HBV(1), HCV(1)	Paraumbilical vein(4); coronary vein(3); splenorenal(25); multiple(13)	Vascular plugs or coils or occluders ± glue	Transfemoral(2); transhepatic(8); transjugular(36)	9 m	Improvement in HE, change in ammonia level, new/worsening PHTN
Álvarez-Lopez et al. <sup>[25]</sup> 2022	Retrospective	5 / 3	57.1±8	HCV (4) Etoh(1)	Mesocaval(2); splenorenal(2); gastroesophageal(1), gastrosrenal(1)	Coils + Onyx 34 (3)/ Glue + Amplatzer (1) / Coils (1) / Glue (1)	Right internal jugular vein(5)	4.4 y (range 1.0-5.0)	Improvement in HE, change in HE medications, new/worsening PHTN
Sahay et al. <sup>[26]</sup> 2017	Retrospective	15 / 7	NR	MASH(4), Etoh(2), HCV(5), multifactorial (2), cryptogenic (2)	Natural shunt or TIPS	NA	NA	12 m	Number of hospitalizations, change in renal function, new/worsening PHTN
Fujimoto et al. <sup>[27]</sup> 2023	Retrospective cohort	30 / NR	NR	NR	NR	NR	NR	24 m	Improvement in HE, new/worsening PHTN
Gurtatta et al. <sup>[28]</sup> 2024	Retrospective	9 / 5	62	NR	NR	NR	NR	3 m	Improvement in HE, new/worsening PHTN
Mukund et al. <sup>[29]</sup> 2023	RCT	18 / 12	55.4±10.9	MASH(10), Etoh(3), viral(3), crypto(2)	Spleno-renal(15); gastro-renal(8), large paraumbilical(5); gastro-spleno-renal shunt(3)	Vascular plug or balloon occluder	BRTO; PARTO	5 m	Improvement in HE, change in liver volume, change in ammonia levels, new/worsening PHTN

m: months; y: years; HBV: Hepatitis B virus; HCV: Hepatitis C virus; Etoh: Ethanol; MASH: Metabolic dysfunction associated steatohepatitis; PBC: Primary biliary cholangitis; AIH: Autoimmune hepatitis; BRTO: Balloon-occluded retrograde transvenous obliteration; PARTO: Plug-assisted retrograde transvenous obliteration; CARTO: Coil-assisted retrograde transvenous occlusion; PHTN: Portal hypertension; TIPS: Transjugular intrahepatic portosystemic shunt.

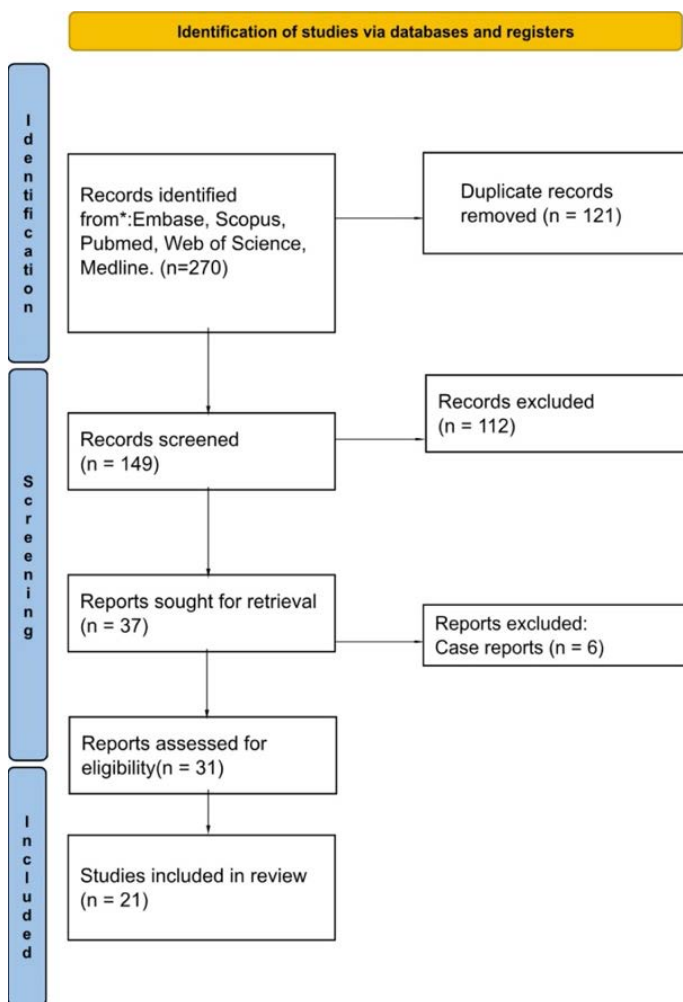


Figure 1. Study selection flow chart.

## Results

### Search Results and Population Characteristics

The initial search yielded 270 references. After the removal of duplicates, a total of 194 studies, including full articles and abstracts, underwent formal title and abstract screening. Based on our inclusion and exclusion criteria, 21 studies involving a total of 331 patients were included (Fig.1).

The final analysis included 331 patients (205 male; mean age:  $60.8 \pm 9.3$ ) with recurrent or refractory HE despite medical management. The most common etiology of cirrhosis was ethanol use/abuse (30%), followed by chronic viral hepatitis (hepatitis B or hepatitis C, 30%), metabolic dysfunction-associated steatohepatitis (27%), and other causes (13%, including primary biliary cholangitis, autoimmune hepatitis, and cryptogenic cirrhosis). Mean MELD and Child-Pugh (CP) scores were  $14.2 \pm 2.3$  and  $8.8 \pm 1.1$ , respectively. One or more types of shunts were present in each patient, and the most common type of shunt was splenorenal, which was present in 64% of patients. One or more procedures for SPSS embolization were performed in each patient,

using techniques including, but not limited to, coils, glue, vascular plugs, and sclerosant injection via various transvenous approaches. Refer to Table 1 for the characteristics of the included studies.

### Characteristics and Quality of Included Studies

Two authors (P.P. and M.E.) conducted an independent and blinded quality assessment of the included studies. Despite encountering some discrepancies, these were resolved by a third author (P.L.) in an independent and blinded manner. Our systematic review employed three types of quality assessment using the NIH scale: pre-post studies without control groups, controlled intervention studies, and case series assessments. The NIH scale was chosen for its comprehensive evaluation criteria suitable for diverse study designs.<sup>[8]</sup> According to the NIH scale, eleven studies received a score of 9, indicating high quality, whereas seven studies were deemed to be of fair quality, with scores ranging from 5 to 8, as shown in Supplementary Table 1 and Table 2. Fair-quality studies had insufficient data, as they were based on abstracts rather than full-text articles. Despite this limitation, these abstracts were included because of their relevance to the research question and the lack of available full-text studies. In the case series studies, two of the included studies were regarded as high quality. Regarding the randomized controlled trial, one study was deemed high quality, with 11 points out of 14 in different aspects, as per the NIH quality assessment for controlled intervention trials.

### Pooled Outcomes

#### Clinical Success

Nineteen of 21 studies reported HE-related clinical improvement. A total of 261 (82%) patients experienced improvement in HE symptoms following one or more embolization procedures ( $I_2=46\%$ ) (Fig. 2). Six studies reported the need for HE-related hospitalization following embolization (Supplementary Fig. 1). A total of 53 (71%) patients became free from HE-related hospitalization ( $I_2=55\%$ ). The change in serum ammonia level was reported by seven studies. There was a significant reduction noted between pre- and post-embolization serum ammonia levels (mean difference= $104 [77-130]$  mcg/dl,  $p<0.01$ ,  $I_2=77\%$ ) (Fig. 3). There was no significant difference in pre- and post-embolization MELD scores ( $0.428 [-2.5-3.3]$ ,  $p=0.8$ ) in 5 studies (Table 2).

#### Adverse Events

Sixteen studies reported the incidence of new or worsening portal hypertension following embolization. A total of 33 (15%) patients developed new or aggravated esophageal and/or gastric varices ( $I_2=62\%$ ), and 34 (15%) patients developed new or worsening ascites ( $I_2=2.5\%$ ) (Supplementary Fig. 2). The post-embolization course was complicated by gastrointestinal bleeding in 15 (10%) patients, as reported by 13 studies ( $I_2=11\%$ ) (Fig. 4). A total of 26 (15%) patients from 12 studies developed post-embolization fever and/or leukocytosis ( $I_2=70\%$ ). No significant difference was noted between pre- and post-embolization serum creatinine levels (mean difference= $0.17 [-0.36-0.03]$  mg/dl,  $p=0.09$ ,  $I_2=56\%$ ) (Table 2).

**Table 2.** Pooled outcomes

Outcomes	Percentage (%)	Mean difference	I <sup>2</sup> %	Studies (n)
Improvement in HE symptoms/clinical success	81.7 (73–87)	–	46	19
Free from HE medications	12.3 (3–37)	–	58	5
Decrease in need for HE medications	17.5 (7–35)	–	42	5
Free from HE related hospitalizations	71.7 (48–87)	–	55	6
No change in HE medications	22.0 (7–51)	–	67	5
Development of new or worsening of pre-existing ascites	15.4 (11–21)	–	2.5	16
Development of new or worsening of pre-existing varices	14.8 (8–26)	–	62	16
Post-embolization gastrointestinal bleeding	10.0 (6–16)	–	11	13
Post-embolization syndrome (fever and leukocytosis)	15.2 (6–32)	–	70	12
Serum creatinine	–	-0.17 (-0.4–0.03), p=0.09	56	5
Serum ammonia	–	104 (77–130), p<0.001	77	7
MELD score	–	0.4 (-2.5–3.4), p=0.7	96	5

HE: Hepatic encephalopathy; MELD: Model for end stage liver disease.

## Validation of Meta-Analysis

### Sensitivity Analysis

To assess whether any one study had a dominant effect on the meta-analysis, we excluded one study at a time and analyzed its effect on the main summary estimate. No single study significantly affected the outcome or heterogeneity.

### Heterogeneity

We assessed the dispersion of the calculated rates using the I<sup>2</sup> percentage values. Based on I<sup>2</sup> analysis for heterogeneity, considerable heterogeneity was noted for the pooled difference in the pre- and post-embolization change in serum ammonia level and MELD score. The I<sup>2</sup> values for the pooled rates are summarized in Table 2.

### Prediction Interval

This meta-analysis was conducted using the random-effects model. Therefore, we calculated the prediction interval, which deals with the dispersion of the effects. The calculated prediction interval for the difference in means between pre- and post-embolization ammonia was 104 (95% interval, 18.5 to 189.5), and for new or aggravated varices, it was 0.148 (95% interval, 0.016 to 0.656).

### Publication Bias

Based on visual inspection of the funnel plot, as well as quantitative measurement using the Egger regression test, there is evidence of publication bias for pre- and post-embolization ammonia (Egger's 2-tailed p-value=0.04). There is also evidence of publication bias for overall clinical success (Egger's 2-tailed p-value=0.001). The funnel plot for publication bias is illustrated in Supplementary Figure 3.

## Discussion

This study evaluated the efficacy of SPSS embolization for patients with HE refractory to medical management. A total of 21 studies meeting the inclusion criteria were analyzed. SPSS embolization demonstrated efficacy through clinical improvement in HE symptoms, reduced need for HE-related hospitalization, and a statistically significant decrease in ammonia levels. Adverse events included post-embolization fever/leukocytosis, GIB, and the development or worsening of pre-existing esophageal or gastric varices and/or ascites.

In our analysis of 19 studies, 82% of patients had clinical improvement in persistent or recurrent HE, reported as an increase in autonomy, improvement in cognitive symptoms, and a decrease in the need for HE medications after SPSS embolization. GIB and the development of new or exacerbated varices were reported in 10% and 15% of patients, respectively, following embolization. GIB following embolization may result from worsened portal hypertension or the progression of underlying cirrhosis. However, it is unclear whether SPSS embolization directly worsens portal hypertension, as the relationship between SPSS and the risk of GIB remains ambiguous.<sup>[30–32]</sup>

In our study, 15% of patients developed new-onset ascites or experienced a worsening of pre-existing ascites after SPSS embolization, likely due to increased portal hypertension. A recent study found that an elevation of the hepatic venous pressure gradient (HVPG) by >4 mm Hg from baseline and an absolute increase to >16 mm Hg immediately post-embolization were significant predictors of early- and late-onset ascites, respectively.<sup>[33]</sup>

Overt HE is one of the major complications of transjugular intrahepatic portosystemic shunt (TIPS).<sup>[34]</sup> Moreover, the presence of SPSS further increases the risk of overt HE following TIPS.<sup>[35]</sup> In their

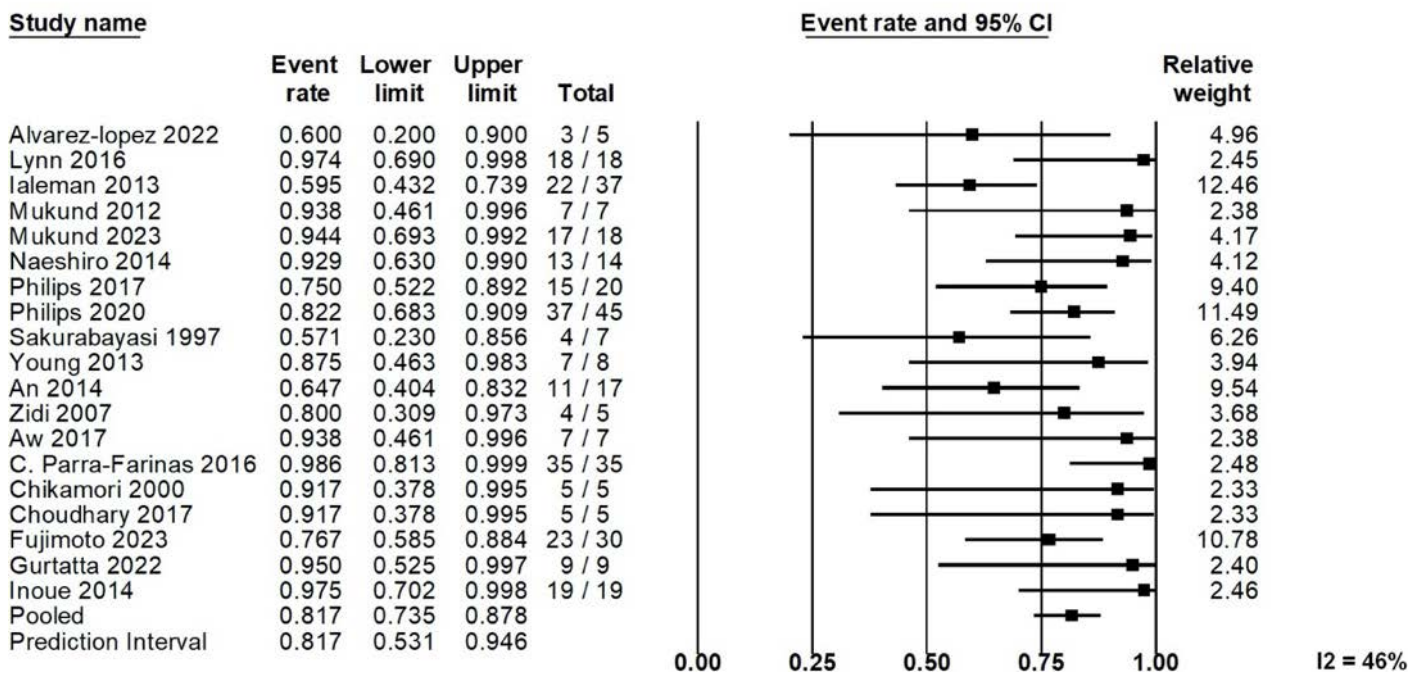


Figure 2. Clinical success.

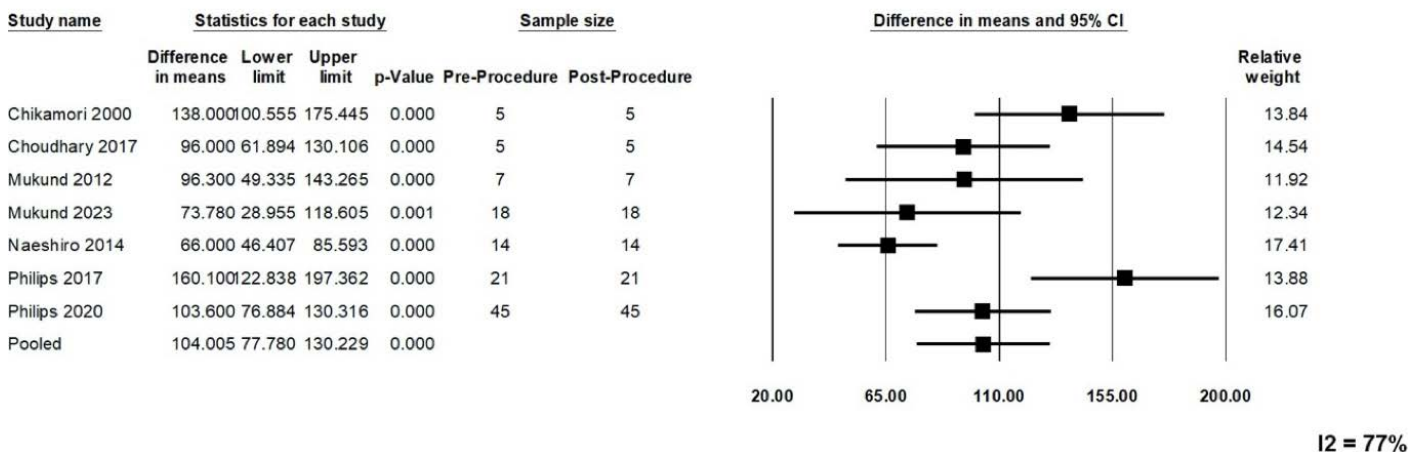


Figure 3. Mean difference in serum ammonia.

meta-analysis, Yang et al.<sup>[35]</sup> reported an increased risk of overt HE in patients undergoing TIPS without concurrent SPSS embolization compared to those with concurrent SPSS embolization, with no significant differences in mortality, variceal bleeding, or shunt dysfunction. A recent meta-analysis reported a decreased risk of overt HE in patients undergoing TIPS along with concurrent large SPSS embolization compared to TIPS alone, without a significant increase in recurrent variceal bleeding.<sup>[36]</sup> Our findings are consistent with these studies in that SPSS embolization decreases the risk of recurrent/refractory HE in patients with or without TIPS.

The presence and size of SPSS increased with liver dysfunction, as indicated by higher MELD scores.<sup>[37]</sup> Our analysis revealed

no significant difference in MELD scores before and after SPSS embolization (Table 2). However, the MELD score does not account for post-SPSS embolization complications related to portal hypertension, and its impact on other serious outcomes remains uncertain.<sup>[7]</sup>

In our analysis, 15% of patients developed fever and/or leukocytosis following SPSS embolization. Post-embolization fever is a common occurrence, primarily attributed to transient bacteremia following the injection of sclerosing agents.<sup>[38]</sup> In the majority of patients, fever subsided with conservative management.

To our knowledge, this is the first meta-analysis investigating the efficacy of SPSS embolization for patients with persistent or

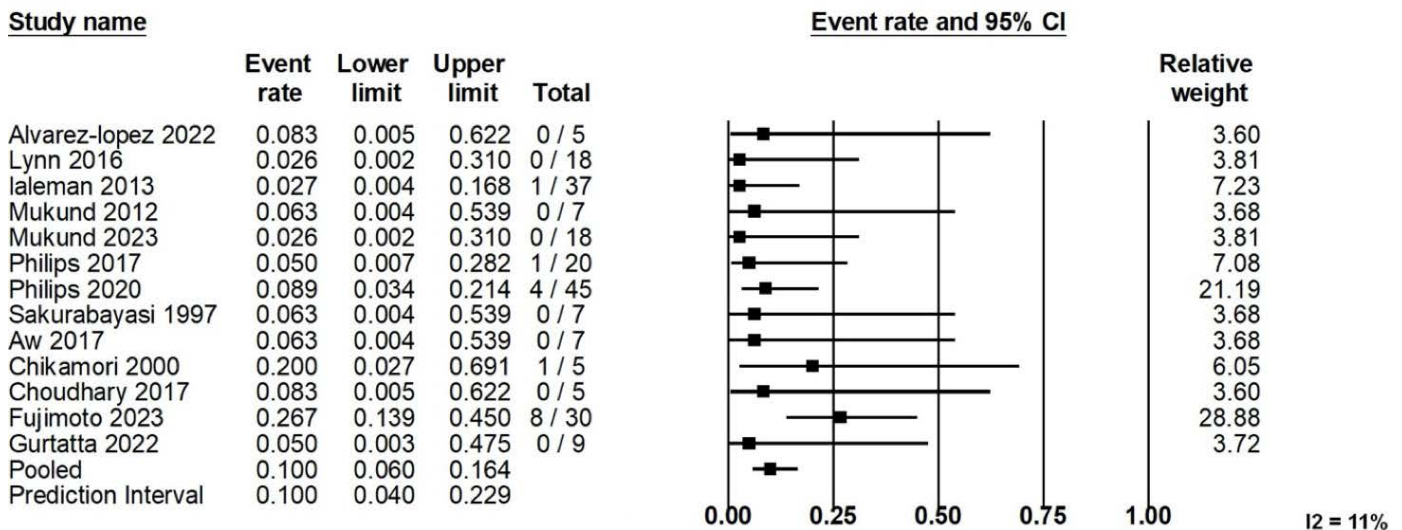


**Figure 4.** Post-embolization gastrointestinal bleeding.

recurrent HE. This analysis includes a diverse patient population with various shunt types and encompasses different embolization techniques. Given that embolization remains a key treatment option for many patients in the absence of liver transplantation, our results demonstrating acceptable levels of heterogeneity are particularly significant. This consistency across the included studies enhances the robustness of our findings in this patient group.

Our study is constrained by the following limitations. First, the prevalence of retrospective studies introduces inherent biases from historical data, which may affect the robustness of our findings. Second, 6 out of 21 studies included in the analysis originate from conference abstracts, which, by their nature, lack the comprehensive scrutiny and peer-review process characteristic of full-length publications. Third, the limited data on long-term and survival-related outcomes highlight the need for further research. Finally, data on shunt diameter, post-procedure changes in HVPG, and stratified outcomes based on MELD score were unavailable in the included studies and thus could not be analyzed. This highlights the need for further research to address these critical gaps in understanding.

## Conclusion

In conclusion, SPSS embolization is an effective treatment for patients with recurrent or refractory HE. Careful patient selection is important to balance long-term benefits with potential complications. Future randomized controlled trials are needed to compare its efficacy against standard medical management and to address technical factors and outcomes.

**Online Appendix Link:** <https://hepatologyforum.org/storage/upload/files/1776156571-appendix-en.pdf>

**Conflict of Interest:** The authors declare that they have nothing to disclose.

**Financial Disclosure:** The authors declare that they have no financial disclosures.

**Use of AI for Writing Assistance:** The authors affirm that no artificial intelligence (AI)-assisted technologies, including Large Language Models (LLMs), chatbots, or image generators, were used in the production of this work.

**Author Contributions:** Concept: PP, ME, EZ, HK, PL, DGA; Design: PP, ME, EZ, HK, PL, DGA; Supervision: PP, ME, EZ, HK, PL, DGA; Data Collection and/or Processing: PP, EZ, HK; Analysis and/or Interpretation: PP, ME, PL, DGA; Literature Review: PP, ME, EZ, HK; Writing: PP, ME, EZ, DGA; Critical Review: PP, ME, EZ, HK, PL, DGA.

**Peer-review:** Externally peer-reviewed.

## References

- Mandiga P, Kommu S, Bollu PC. Hepatic Encephalopathy. 2025 Jan 20. In: StatPearls [Internet]. Treasure Island (FL): StatPearls Publishing; 2026.
- Rahimi RS, Brown KA, Flamm SL, Brown RS. Overt hepatic encephalopathy: Current pharmacologic treatments and improving clinical outcomes. *Am J Med* 2021;134(11):1330-1338. [CrossRef]
- Stepanova M, Mishra A, Venkatesan C, Younossi ZM. In-hospital mortality and economic burden associated with hepatic encephalopathy in the United States From 2005 to 2009. *Clin Gastroenterol Hepatol* 2012;10(9):1034-1041.e1. [CrossRef]
- Duah A, Agyei-Nkansah A, Osei-Poku F, Duah F, Ampofo-Boobi D, Peparah B. The prevalence, predictors, and in-hospital mortality of hepatic encephalopathy in patients with liver cirrhosis admitted at St. Dominic Hospital in Akwatia, Ghana. *Can J Gastroenterol Hepatol* 2020;2020:8816522. [CrossRef]
- Louissaint J, Deutsch-Link S, Tapper EB. Changing epidemiology of cirrhosis and hepatic encephalopathy. *Clin Gastroenterol Hepatol* 2022;20(8S):S1-S8. [CrossRef]
- Hoilat GJ, Suhail FK, Adhami T, John S. Evidence-based approach to management of hepatic encephalopathy in adults. *World J Hepatol* 2022;14(4):670-681. [CrossRef]

7. Nardelli S, Riggio O, Gioia S, Puzzone M, Pelle G, Ridola L. Spontaneous porto-systemic shunts in liver cirrhosis: Clinical and therapeutical aspects. *World J Gastroenterol* 2020;26(15):1726-1732. [CrossRef]
8. National Heart, Lung, and Blood Institute. Study Quality Assessment Tools. Available at: <https://www.nhlbi.nih.gov/health-topics/study-quality-assessment-tools> Accessed on Mar 23, 2024.
9. Sakurabayashi S, Sezai S, Yamamoto Y, Hirano M, Oka H. Embolization of portal-systemic shunts in cirrhotic patients with chronic recurrent hepatic encephalopathy. *Cardiovasc Intervent Radiol* 1997;20(2):120-124. [CrossRef]
10. Chikamori F, Kuniyoshi N, Shibuya S, Takase Y. Transjugular retrograde obliteration for chronic portosystemic encephalopathy. *Abdom Imaging* 2000;25(6):567-571. [CrossRef]
11. Zidi SH, Zanditenas D, Gelu-Siméon M, Rangheard A, Valla DC, Vilgrain V, et al. Treatment of chronic portosystemic encephalopathy in cirrhotic patients by embolization of portosystemic shunts. *Liver Int* 2007;27(10):1389-1393. [CrossRef]
12. Mukund A, Rajesh S, Arora A, Patidar Y, Jain D, Sarin SK. Efficacy of balloon-occluded retrograde transvenous obliteration of large spontaneous lienorenal shunt in patients with severe recurrent hepatic encephalopathy with foam sclerotherapy: Initial experience. *J Vasc Interv Radiol* 2012;23(9):1200-1206. [CrossRef]
13. Laleman W, Simon-Talero M, Maleux G, Perez M, Ameloot K, Soriano G, et al. Embolization of large spontaneous portosystemic shunts for refractory hepatic encephalopathy: a multicenter survey on safety and efficacy. *Hepatology* 2013;57(6):2448-2457. [CrossRef]
14. Young M, Yu H, Zacks SL, Kim KR, Stavas JM. Embolization of spontaneous portosystemic shunt for treatment of refractory hepatic encephalopathy. *J Vasc Interv Radiol* 2013;(Suppl 4):S27-S28. [CrossRef]
15. An J, Kim KW, Han S, Lee J, Lim YS. Improvement in survival associated with embolisation of spontaneous portosystemic shunt in patients with recurrent hepatic encephalopathy. *Aliment Pharmacol Ther* 2014;39(12):1418-1426. [CrossRef]
16. Naeshiro N, Kakizawa H, Aikata H, Kan H, Fujino H, Fukuhara T, et al. Percutaneous transvenous embolization for portosystemic shunts associated with encephalopathy: Long-term outcomes in 14 patients. *Hepatol Res* 2014;44(7):740-749. [CrossRef]
17. Inoue H, Emori K, Toyonaga A, Oho K, Kumamoto M, Haruta T, et al. Long term results of balloon-occluded retrograde transvenous obliteration for portosystemic shunt encephalopathy in patients with liver cirrhosis and portal hypertension. *Kurume Med J* 2014;61(1-2):1-8. [CrossRef]
18. Parra-Fariñas C, Perez LM, Diez-Miranda I, Gonzalez-Junyent C, Hernandez MD, Ordi CQ, et al. A single-centre experience in spontaneous portosystemic shunt embolisation: what do we know after a decade of work? *Cardiovascular and Interventional Radiological Society of Europe (CIRSE)* 2016: Barcelona, Spain. September 10-14, 2016.
19. Lynn AM, Singh S, Congly SE, Khemani D, Johnson DH, Wiesner RH, et al. Embolization of portosystemic shunts for treatment of medically refractory hepatic encephalopathy. *Liver Transpl* 2016;22(6):723-731. [CrossRef]
20. Aw G, Rogan C, Shackel N, Strasser S. Radiology-guided occlusion of portosystemic shunts for treatment of medically refractory hepatic encephalopathy. *J Clin Exp Hepatol* 2017;(Suppl 7):S33-S34. [CrossRef]
21. Choudhary NS, Bajjal SS, Saigal S, Agarwal A, Saraf N, Khandelwal R, et al. Results of portosystemic shunt embolization in selected patients with cirrhosis and recurrent hepatic encephalopathy. *J Clin Exp Hepatol* 2017;7(4):300-304. [CrossRef]
22. Philips CA, Kumar L, Augustine P. Shunt occlusion for portosystemic shunt syndrome related refractory hepatic encephalopathy-A single-center experience in 21 patients from Kerala. *Indian J Gastroenterol* 2017;36(5):411-419. [CrossRef]
23. He C, Lv Y, Wang Z, Yin Z, Fan D, Han G, et al. Association between non-variceal spontaneous portosystemic shunt and outcomes after TIPS in cirrhosis. *Dig Liver Dis* 2018;50(12):1315-1323. [CrossRef]
24. Philips CA, Rajesh S, George T, Ahamed R, Mohanan M, Augustine P, et al. Early, late, or no shunt embolization in patients with cirrhosis- and portosystemic shunt-related hepatic encephalopathy. *Indian J Gastroenterol* 2020;39(4):377-387. [CrossRef]
25. Álvarez-López P, Campos-Varela I, Quiroga S, Díez I, Charco R, Simon-Talero M, et al. Spontaneous portosystemic shunt embolization in liver transplant recipients with recurrent hepatic encephalopathy. *Ann Hepatol* 2022;27(3):100687. [CrossRef]
26. Sahay T, Cheong J, Bittner K, Audi A, Sharma A, Huang JC. A Reduction in Hepatic Encephalopathy-Related Hospitalizations following Natural Shunt Embolization and TIPS Diminution. *Gastroenterology* 2017;152(5):S1145-S1146. [CrossRef]
27. Fujimoto K, Kondo T, Fujiwara K, Kobayashi K, Kiyono S, Nakamura M, et al. The impact of embolization of large portosystemic shunt on the clinical course in patients with cirrhosis. *Asian Pacific Association for the Study of the Liver (APASL) 2023: Taipei, Taiwan. February 15-19, 2023.*
28. Gurtatta RS, Gaba RC, Herren JL. Combined Spontaneous Portosystemic Shunt Embolization and Transjugular Intrahepatic Portosystemic Shunt Creation for Treatment of Hepatic Encephalopathy. *J Vasc Interv Radiol* 2024;35(5):659-663. [CrossRef]
29. Mukund A, Choudhury SP, Tripathy TP, Ananthashayana VH, Jagdish RK, Arora V, et al. Influence of shunt occlusion on liver volume and functions in hyperammonemic cirrhosis patients having large porto-systemic shunts: a randomized control trial. *Hepatol Int* 2023;17(1):150-158. [CrossRef]
30. Lam KC, Juttner HU, Reynolds TB. Spontaneous portosystemic shunt: relationship to spontaneous encephalopathy and gastrointestinal hemorrhage. *Dig Dis Sci* 1981;26(4):346-352. [CrossRef]
31. Aseni P, Beati C, Brambilla G, Bertini M, Belli L. Does large spontaneous portal systemic shunt in cirrhosis protect from the risk of gastroesophageal bleeding? *J Clin Gastroenterol* 1986;8(3 Pt 1):235-238. [CrossRef]
32. Riggio O, Efrati C, Catalano C, Pediconi F, Mecarelli O, Accornero N, et al. High prevalence of spontaneous portal-systemic shunts in persistent hepatic encephalopathy: A case-control study. *Hepatology* 2005;42(5):1158-1165. [CrossRef]
33. Rajesh S, Philips CA, Ahamed R, Abduljaleel JK, Nair DC, Augustine P, et al. Clinical outcomes related to portal pressures before and after embolization of large portosystemic shunts in cirrhosis. *SAGE Open Med* 2023;11:20503121231208655. [CrossRef]
34. Yang C, Zhu X, Liu J, Shi Q, Du H, Chen Y, et al. Development and validation of prognostic models to estimate the risk of overt hepatic encephalopathy after TIPS creation: A multicenter study. *Clin Transl Gastroenterol* 2022;13(3):e00461. [CrossRef]
35. Yang M, Qiu Y, Wang W. Concurrent spontaneous portosystemic shunt embolization for the prevention of overt hepatic encephalopathy after TIPS: A systematic review and meta-analysis. *Dig Liver Dis* 2024;56(6):978-985. [CrossRef]
36. Lv Y, Chen H, Luo B, Bai W, Li K, Wang Z, et al. Concurrent large spontaneous portosystemic shunt embolization for the prevention of overt hepatic

- encephalopathy after TIPS: A randomized controlled trial. *Hepatology* 2022;76(3):676-688. [\[CrossRef\]](#)
37. Simón-Talero M, Roccarina D, Martínez J, Lampichler K, Baiges A, Low G, et al. Association between portosystemic shunts and increased complications and mortality in patients with cirrhosis. *Gastroenterology* 2018;154(6):1694-1705.e4. [\[CrossRef\]](#)
38. Croffie J, Somogyi L, Chuttani R, DiSario J, Liu J, Mishkin D, et al. Sclerosing agents for use in GI endoscopy. *Gastrointest Endosc* 2007;66(1):1-6. [\[CrossRef\]](#)

## ORIGINAL RESEARCH

# Assessment of GALAD score as a diagnostic and prognostic factor of *de novo* hepatitis C–related hepatocellular carcinoma post treatment with direct-acting antivirals

 Ahmed Ramadan<sup>1</sup>,  Ashraf Omar Abdelaziz<sup>1</sup>,  Mohamed Mahmoud Nabeel<sup>1</sup>,  Mirna Atef<sup>1</sup>,  Mai Hamed Kamel<sup>2</sup>,  Tamer Mahmoud Elbaz<sup>1</sup>,  Ammar Hatem<sup>1</sup>,  Eman Medhat<sup>1</sup>,  Ahmed Hosni Abdelmaksoud<sup>3</sup>,  Rania Lithy<sup>1</sup>,  Rabab Maher<sup>4</sup>,  Sabrin AA Mohamed<sup>5</sup>,  Amgad Hamed Kamel<sup>6</sup>,  Hend Ibrahim Shousha<sup>1</sup>

1: Department of Endemic Medicine, School of Medicine, Cairo University, Cairo, Egypt

2: Department of Clinical and Chemical Pathology, School of Medicine Cairo University, Cairo, Egypt

3: Department of Diagnostic and Interventional Radiology, School of Medicine, Cairo University, Cairo, Egypt

4: Department of Endemic Medicine, School of Medicine, Cairo University Students Hospital, Cairo, Egypt

5: Department of Biochemistry, School of Medicine, Cairo University Student Hospital, Cairo, Egypt

6: Department of Tropical Medicine, School of Medicine, Ain Shams University, Cairo, Egypt

## Highlights & Insights

- **Scientific Gap:** HCC may still occur or recur after successful DAA therapy for hepatitis C. This study assessed whether the GALAD score can help diagnose HCC and predict outcomes in these patients.
- **Key Finding:** The GALAD score showed good diagnostic accuracy for HCC (AUC=0.849). Liver stiffness and GALAD were independent predictors, but GALAD poorly predicted mortality.
- **Clinical Impact:** GALAD may support post-DAA HCC diagnosis, but better tools are needed for mortality prediction.

## ABSTRACT

**Background and Aim:** The GALAD score (Gender, Age, AFP, AFP-L3, and Des-gamma-carboxy prothrombin) is a mathematical model that incorporates gender, age, alpha-fetoprotein (AFP), the lens culinaris agglutinin-reactive fraction of AFP (AFP-L3), and des-gamma-carboxy prothrombin (DCP). It has been developed to assess the presence of hepatocellular carcinoma (HCC) in patients with chronic liver disease. This study aimed to evaluate the efficacy of the GALAD score in predicting HCC and assessing its prognosis in patients with hepatitis C–related HCC who had received prior direct-acting antiviral (DAA) treatment.

**Materials and Methods:** This case-control study included patients with hepatitis C virus (HCV)-related liver cirrhosis who had been treated with DAAs, with or without HCC, recruited from the HCC clinic at Kasr Al-Ainy Hospital, Cairo University. Patients were followed until death or the end of the study period. Collected data included clinical and laboratory parameters, levels of DCP, AFP, and AFP-L3, imaging findings, treatment response, and survival outcomes. Logistic regression analysis was used to identify independent predictors of HCC, mortality, and recurrence.

**Results:** Eighty-eight patients with HCV-related HCC following DAA treatment and 88 patients without HCC were recruited, with no significant differences in gender or age between the two groups. Participants with HCC had a higher mean GALAD score than those without HCC ( $4.32 \pm 2.47$  vs.  $1.32 \pm 1.46$ ,  $p < 0.001$ ). The area under the receiver operating characteristic (ROC) curve (AUC) for the GALAD score in diagnosing HCC at a cut-off value of 3.805 was 0.849 (95% confidence interval [CI]: 0.794–0.905,  $p < 0.001$ ), with a sensitivity of 59.3% and a specificity of 97.7%. Multivariate logistic regression identified liver stiffness (odds ratio [OR]=1.140, 95% CI: 1.007–1.291,  $p = 0.038$ ) and the GALAD score

**How to cite this article:** Abdelaziz AO, Nabeel MM, Atef M, Kamel MH, Elbaz TM, Hatem A, et al. Assessment of GALAD score as a diagnostic and prognostic factor of *de novo* hepatitis C–related hepatocellular carcinoma post treatment with direct-acting antivirals. *Hepatology Forum* 2026; 7(2):101–107.

**Received:** January 27, 2025; **Revised:** August 07, 2025; **Accepted:** September 25, 2025; **Available Online:** May 11, 2026

**Corresponding author:** Ahmed Ramadan; Department of Endemic Medicine, School of Medicine, Cairo University, Cairo, Egypt; **E-mail:** ahmed.ramadan@kasralainy.edu.eg



This work is licensed under a Creative Commons Attribution-NonCommercial 4.0 International License.

(OR=2.378, 95% CI: 1.171–4.831,  $p=0.017$ ) as independent predictors of HCC. The GALAD score demonstrated low prognostic value for mortality, with an AUC of 0.564 (95% CI: 0.434–0.693). Patients with HCC recurrence had a slightly higher baseline GALAD score than those without recurrence (6.16 vs. 4.18,  $p=0.032$ ).

**Conclusion:** The GALAD score demonstrated adequate diagnostic performance for predicting HCC following DAA therapy but showed low prognostic value.

**Keywords:** Hepatitis C virus, direct-acting antivirals, hepatocellular carcinoma, GALAD score.

## Introduction

Hepatocellular carcinoma (HCC) is the fourth most prevalent malignancy in Egypt and the sixth most common malignancy worldwide.<sup>[1]</sup> Because chronic hepatitis B and C infections are more prevalent in Africa than in most other regions, the incidence of HCC is higher in Africa, reaching 8.9 cases per 100,000 person-years.<sup>[2]</sup> Despite advancements in treatment, the global incidence of HCC continues to rise, with no corresponding improvement in survival.<sup>[3]</sup> The Barcelona Clinic Liver Cancer (BCLC) classification is widely used to stage HCC and guide treatment decisions.<sup>[4]</sup> Treatment of chronic hepatitis C infection with direct-acting antivirals (DAAs) has demonstrated excellent efficacy.<sup>[5]</sup> However, regardless of whether sustained virologic response (SVR) is achieved, several recent studies have reported unexpected rates of *de novo* and recurrent HCC following DAA treatment.<sup>[6–8]</sup>

Several research trials have investigated potential molecular pathways through which DAAs may contribute to hepatocarcinogenesis. These mechanisms include the stimulation of angiogenesis, cytokine imbalance, and immune cell dysfunction.<sup>[9]</sup> The aim of HCC surveillance programs is to detect cancer at an early stage to allow curative treatment and thereby improve survival rates.<sup>[10]</sup> In the context of screening and surveillance, the GALAD model (Gender, Age, Alpha-fetoprotein, AFP-L3, and Des-gamma-carboxy prothrombin) has the potential to serve as a cost-effective tool.<sup>[11]</sup> Its high sensitivity and specificity have been demonstrated in several studies across diverse ethnic populations.<sup>[12]</sup> The diagnostic accuracy of the GALAD score has been evaluated across various underlying etiologies of chronic liver disease, with adequate performance reported in patients with nonalcoholic fatty liver disease (NAFLD)-related HCC, as well as hepatitis B- and C-related HCC.<sup>[13–15]</sup> The present study aimed to evaluate the role of the GALAD score in predicting the occurrence of HCC following DAA treatment and in assessing HCC treatment outcomes, survival, and mortality.

## Patients and Methods

### Study Design and Patient Selection Criteria

This case-control study included adult patients ( $\geq 18$  years) with hepatitis C virus (HCV)-related liver cirrhosis who had been treated with DAAs, with or without HCC. Patients were recruited from the

multidisciplinary HCC clinic between January 2016 and January 2022 and were followed until death or the end of the study period in June 2023. All procedures were conducted after approval by the Faculty of Medicine, Cairo University Ethics Committee and in accordance with the Declaration of Helsinki (1975), as revised in 2008 (MS-524-2021/27.02.2022). Patients were excluded if they had recurrent HCC, had not received DAAs for HCV before developing HCC, had concomitant malignancies other than HCC, or had concomitant hepatitis B virus or human immunodeficiency virus (HIV) infection.

### Data Collection

After providing written informed consent, all participants underwent a comprehensive clinical evaluation, including a full medical history and complete physical examination. Basic demographic data, manifestations of liver decompensation, history of DAA treatment, sustained virological response, and retreatment history were recorded. Laboratory investigations included complete blood count, liver function tests, international normalized ratio (INR), serum creatinine, alpha-fetoprotein (AFP), HCV antibodies, the Lens culinaris agglutinin-reactive fraction of alpha-fetoprotein (AFP-L3), and des-gamma-carboxy prothrombin (DCP). These markers were measured using enzyme-linked immunosorbent assay (ELISA) kits supplied by SinoGeneClon Biotech Co., Ltd., and readings were obtained using the STAT FAX 2000 ELISA Reader. HCV RNA was assessed by reverse transcriptase real-time polymerase chain reaction (PCR) using the QIAGEN Rotor-Gene Q RT-PCR System. HCV RNA levels were measured before treatment and three months after completion of DAA therapy. All laboratory analyses were conducted at the Clinical and Chemical Pathology Department, Kasr Al-Ainy Hospital, Cairo University. The Child-Turcotte-Pugh score and Model for End-Stage Liver Disease (MELD) score were calculated, and performance status was assessed using the Eastern Cooperative Oncology Group (ECOG) performance status scale.<sup>[16]</sup>

Hepatocellular carcinoma was diagnosed according to American Association for the Study of Liver Diseases (AASLD) guidelines using triphasic computed tomography (CT), with or without magnetic resonance imaging (MRI). Tumor site, size, number of focal lesions, and the presence of vascular or nodal metastases were recorded. Participants with HCC were treated according to international guidelines and followed to assess treatment outcomes, recurrence, and survival.

**Table 1.** Basic characteristics of studied groups

	HCC group (n=88)		HCV group (n=88)		p
	Mean (SD)		Mean (SD)		
Age	62.20±8.12		62.86±8.43		<b>0.338</b>
Duration between DAAs intake and HCC development in months	19.93±16.01				
	Count	%	Count	%	
Sex					<b>0.748</b>
Male	<b>58</b>	<b>65.9</b>	<b>60</b>	<b>68.2</b>	
Female	<b>30</b>	<b>34.1</b>	<b>28</b>	<b>31.8</b>	
DAA					
Yes	<b>88</b>	<b>100</b>	<b>88</b>	<b>100</b>	
SVR					<b>0.001</b>
Yes	<b>76</b>	<b>89.4</b>	<b>88</b>	<b>100</b>	
No	<b>8</b>	<b>9.4</b>	<b>0</b>	<b>0.0</b>	
Unknown	<b>1</b>	<b>1.2</b>	<b>0</b>	<b>0.0</b>	
CHILD score					<b>0.012</b>
A	<b>64</b>	<b>72.7</b>	<b>72</b>	<b>81.8</b>	
B	<b>20</b>	<b>22.7</b>	<b>8</b>	<b>9.1</b>	
C	<b>4</b>	<b>4.5</b>	<b>8</b>	<b>9.1</b>	
Performance status					
0	53	64.6	–	–	
1	24	29.3	–	–	
2	4	4.9	–	–	
3	1	1.2	–	–	
Variables with normal values	HCC group		HCV group		p
	Mean	SD	Mean	SD	
Hb	12.18	<b>2.08</b>	12.30	<b>2.26</b>	<b>0.501</b>
Albumin	3.68	<b>0.58</b>	3.84	<b>0.63</b>	<b>0.037</b>
Creatinine	0.96	0.23	1.00	0.63	<b>0.214</b>
INR	1.18	0.19	1.19	0.20	<b>0.859</b>
CHILD score	6.55	5.40	6.13	2.35	0.215
MELD score	9.67	3.2	9.83	3.41	0.904
Total Bilirubin	1.21	<b>1.10</b>	1.20	<b>1.45</b>	<b>0.269</b>
ALT	37.23	<b>27.91</b>	30.83	<b>32.20</b>	<b>0.001</b>
AFP	<b>806.58</b>	<b>2343.22</b>	<b>4.62</b>	<b>3.21</b>	<b>&lt;0.001</b>
GALAD score	<b>4.32</b>	<b>2.47</b>	<b>1.32</b>	<b>1.46</b>	<b>&lt;0.001</b>
	Median		Median		
AFP-L3	7.25		9.50		<b>&lt;0.001</b>
DCP	551.00		277.00		<b>&lt;0.001</b>
	HCC group (n=88)		HCV group (n=88)		p
	Count	%	Count	%	
Portal vein thrombosis					<b>&lt;0.001</b>
Thrombosis	17	19.3	1	1.1	
Patent	71	80.7	74	84.1	
Dilated	0	0.0	8	9.1	
Attenuated	0	0.0	5	5.7	
Hepatic focal lesion number					
Single	51	58.0	0	0.0	
Two	15	17.0	0	0.0	
Multiple	22	25.0	0	0.0	
BCLC stage					
0	4	4.9	0	0.0	
A	20	24.4	0	0.0	
B	36	43.9	0	0.0	
C	18	22.0	0	0.0	
D	4	4.9	0	0.0	

DAA: Direct-acting antiviral; SVR: Sustained virologic response; Hb: Hemoglobin; INR: International normalized ratio; CHILD score: Child-Turcotte-Pugh score; MELD score: Model for End-Stage Liver Disease score; AFP: Alpha-fetoprotein; GALAD score: Gender, Age, AFP, AFP-L3, and Des-gamma-carboxy prothrombin; AFP-L3: The lens culinaris agglutinin-reactive fraction of AFP; DCP: Des-gamma-carboxy prothrombin; BCLC: Barcelona Clinic Liver Cancer; HCC: Hepatocellular carcinoma; HCV: Hepatitis C virus.

**Table 2.** Baseline characteristics of patients with HCC according to survival status (alive vs dead)

	Alive (n=49)		Dead (n=35)		p
	Mean	SD	Mean	SD	
Age	62.57	8.77	61.77	7.61	0.467
Duration between DAAs intake and HCC development in months	21.86	16.56	18.02	15.71	0.354
	Count	%	Count	%	
Sex					<b>0.817</b>
Male	<b>32</b>	<b>65.3</b>	<b>22</b>	<b>62.9</b>	
Female	<b>17</b>	<b>34.7</b>	<b>13</b>	<b>37.1</b>	
DAA					
Yes	<b>48</b>	<b>100.0</b>	<b>35</b>	<b>100.0</b>	-----
SVR					<b>0.691</b>
Yes	<b>41</b>	<b>89.1</b>	<b>31</b>	<b>88.6</b>	
No	<b>5</b>	<b>10.9</b>	<b>3</b>	<b>8.6</b>	
Unknown	<b>0</b>	<b>0.0</b>	<b>1</b>	<b>2.9</b>	
CHILD score					0.317
A	38	77.6	22	62.9	
B	9	18.4	11	31.4	
C	2	4.1	2	5.7	
Performance status					0.026
0	28	63.6	23	65.7	
1	16	36.4	7	20.0	
2	0	0.0	4	11.4	
3	0	0.0	1	2.9	
Variables	Alive		Dead		p
	Mean	SD	Mean	SD	
Hb	12.22	2.36	12.09	1.67	0.530
Albumin	3.78	0.59	3.53	0.56	0.033
Creatinine	0.96	0.21	0.95	0.26	0.852
INR	1.15	0.16	1.22	0.23	0.296
MELD score	9.11	3.04	10.56	3.38	0.028
CHILD Score	6.76	7.15	6.37	1.50	0.025
Total Bilirubin	1.21	1.33	1.26	0.74	0.116
ALT	34.29	31.26	40.76	24.44	0.116
AFP	396.93	1045.35	1457.29	3430.82	0.087
GALAD	4.13	2.32	4.65	2.68	0.327
	Median		Median		
AFP-L3	7.50		7.00		0.471
DCP	564.00		544.50		0.430
	Alive		Dead		p
	Count	%	Count	%	
Portal vein thrombosis					0.001
Thrombosis	4	8.2	13	37.1	
Patent	45	91.8	22	62.9	
BCLC stage					0.022
0	4	9.1	0	0.0	
A	12	27.3	7	20.0	
B	21	47.7	13	37.1	
C	7	15.9	11	31.4	
D	0	0.0	4	11.4	

DAA: Direct-acting antiviral; SVR: sustained virologic response; Hb: Hemoglobin; INR: International normalized ratio; CHILD score: Child-Turcotte-Pugh score; MELD score: Model for End-Stage Liver Disease score; AFP: Alpha-fetoprotein; GALAD score: Gender, Age, AFP, AFP-L3, and Des-gamma-carboxy prothrombin; AFP-L3: The lens culinaris agglutinin-reactive fraction of AFP; DCP: Des-gamma-carboxy prothrombin; BCLC: Barcelona Clinic Liver Cancer; HCC: Hepatocellular carcinoma; HCV: Hepatitis C virus.

Overall survival was calculated from the date of HCC diagnosis to the date of death or the end of the study. All procedures were conducted in compliance with the Declaration of Helsinki (1975), as revised in 2008,

and the ethical standards of the national and institutional committees responsible for human experimentation. The GALAD score was calculated using the following formula:

**Table 3.** Diagnostic accuracy of GALAD score in early prediction of HCC

Test result variable(s)	Area under curve	p	95% CI		Cut-off value	Sensitivity %	Specificity %
			Lower bound	Upper bound			
AFP	0.854	<0.001	0.794	0.915	7.9	74.4	94.3
DCP	0.860	<0.001	0.800	0.920	366	82.6	86.4
AFP-LP3	0.796	<0.001	0.730	0.862	8.25	68.2	77.3
GALAD	0.849	<0.001	0.794	0.905	3.805	59.3	97.7

AFP: Alpha-fetoprotein; CI: Confidence interval; DCP: desgamma-carboxy prothrombin; GALAD: Gender, Age, AFP, AFP-L3, and Des-gammacarboxy prothrombin.

**Table 4.** Multivariate logistic regression for factors associated with the development of HCC

	p	OR	95% CI	
			Lower	Upper
HCC				
GALAD		2.378	1.171	4.831
Liver stiffness by fibroscan	0.038	1.140	1.007	1.291

OR: Odd ratios; CI: Confidence interval; HCC: Hepatocellular carcinoma; GALAD: Gender, Age, AFP, AFP-L3, and Des-gammacarboxy prothrombin.

$$\text{GALAD} = -10.08 + 0.09 \times \text{age} + 1.67 \times \text{gender} + 2.34 \log_{10}(\text{AFP}) + 0.04 \times \text{AFP-L3} + 1.33 \times \log_{10}(\text{DCP}),$$

where gender is coded as 0 for female and 1 for male.<sup>[17]</sup> HCC was staged according to the Barcelona Clinic Liver Cancer classification.<sup>[4]</sup> Response to therapy in patients with HCC was evaluated using the mRECIST criteria (modified Response Evaluation Criteria in Solid Tumors).<sup>[18]</sup>

### Statistical Analysis

Data were entered and analyzed using the Statistical Package for the Social Sciences (SPSS), version 28 (IBM Corp., Armonk, NY, USA). Quantitative data were expressed as mean ± standard deviation, whereas categorical data were expressed as frequency and percentage. The non-parametric Mann-Whitney test was used to compare quantitative variables. The chi-square ( $\chi^2$ ) test was used to compare categorical variables; however, when the expected frequency was less than five, an exact test was applied. The Spearman correlation coefficient was used to assess associations between quantitative variables. Logistic regression analysis was performed to identify independent predictors of HCC, mortality, and recurrence. To determine the optimal GALAD score cut-off value for identifying HCC and predicting mortality, a receiver operating characteristic (ROC) curve was constructed using the area under the curve analysis. A p value <0.05 was considered statistically significant.

### Results

This study included 88 patients with HCV-related HCC following DAA treatment and 88 patients without HCC. The two groups were matched for age and gender. Patients with HCC exhibited significantly

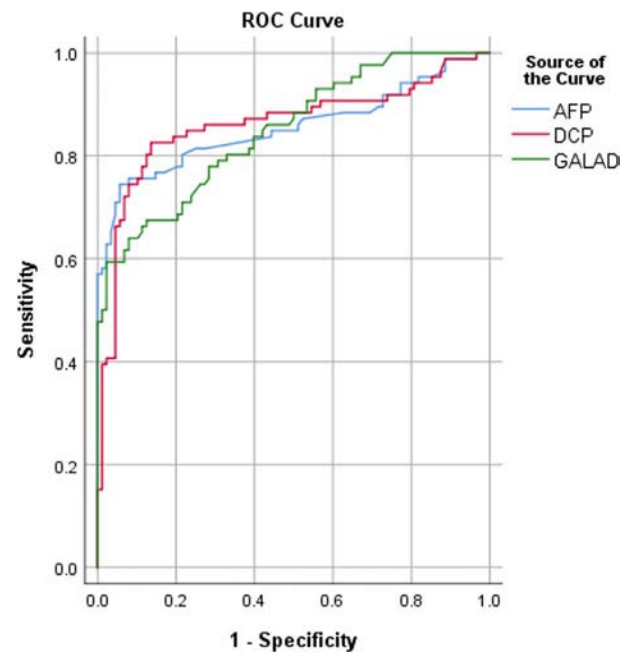


**Figure 1.** ROC curve for testing the diagnostic accuracy of GALAD score in early detection of HCC in comparison with AFP, AFP-L3, DCP.

ROC: Receiver operating characteristic; GALAD score: Gender, Age, AFP, AFP-L3, and Des-gamma-carboxy prothrombin; AFP-L3: The lens culinaris agglutinin-reactive fraction of AFP; DCP: Des-gamma-carboxy prothrombin.

higher median liver stiffness values, as measured by FibroScan. SVR was achieved in all patients without HCC and in 89.4% of patients with HCC (p=0.001) (Table 1). Median levels of AFP, DCP, and the GALAD score were significantly higher in patients with HCC (Table 2). The median duration between the end of DAA therapy and the development of HCC was one year.

Table 3 shows the diagnostic accuracy of the GALAD score and each of the studied markers independently using ROC curve analysis. The area under the ROC curve of the GALAD score for diagnosing HCC following DAA treatment at a cut-off value of 3.805 was 0.849 (95% confidence interval [CI]: 0.794–0.905, p<0.001), with a sensitivity of 59.3% and specificity of 97.7% (Fig. 1). Independent predictors of HCC following DAA treatment identified by multivariate logistic regression were liver stiffness (odds ratio [OR]=1.140, 95% CI: 1.007–1.291, p=0.038) and GALAD score (OR=2.378, 95% CI: 1.171–4.831, p=0.017) (Table 4).

**Table 5.** Multivariate logistic regression for predictors of recurrence

	p	OR	95% CI	
			Lower	Upper
Recurrence				
CHILD score (B)	0.815	0.764	0.080	7.284
CHILD score (C)	0.020	13.750	1.513	124.989

OR: Odd ratios; CI: Confidence interval; CHILD score: Child-Turcotte-Pugh score.

**Table 6.** Prediction of recurrence using GALAD score

Area under the curve	p	95% CI		Cut-off	Sen. (%)	Spe. (%)
		Lower bound	Upper bound			
0.746	0.002	0.590	0.901	4.485	85.7	65.3

GALAD score: Gender, Age, AFP, AFP-L3, and Des-gamma-carboxy prothrombin; CI: Confidence interval; Sen: Sensitivity; Spe: Specificity.

## HCC Treatment and Outcomes

Transarterial chemoembolization (TACE) was the most frequently used treatment modality, applied in 39 patients (44.3%), followed by transarterial radioembolization (TARE) and best supportive care, each used in nine patients (10.11%). According to the modified RECIST criteria, 38 patients (45.0%) had progressive disease, 20 patients (23.8%) had a partial response, and five patients (6.0%) had stable disease. By the end of the study, the mortality rate was 41.7% (n=35). Hepatic encephalopathy was the most common cause of death (n=27, 79.4%). Recurrence of HCC was identified in eight patients (9.5%) (Table 5). The GALAD score demonstrated poor predictive ability for mortality, with an area under the curve (AUC) of 0.564 (95% CI: 0.434–0.693). Factors affecting mortality in univariate analysis included ECOG performance status, portal vein status, BCLC stage, serum albumin level, MELD score, and liver stiffness measured by FibroScan (Table 6). Multivariate regression analysis identified portal vein thrombosis (OR=7.366, 95% CI: 2.022–26.835, p=0.002) and MELD score (OR=1.198, 95% CI: 1.027–1.398, p=0.022) as independent predictors of mortality.

Univariate analysis of parameters influencing HCC recurrence is presented in Supplementary Table 1. These parameters included diabetes mellitus, Child-Pugh score, and GALAD score. The baseline GALAD score was significantly higher in patients who experienced HCC recurrence (6.16 vs. 4.18, p=0.032).

## Discussion

Hepatocellular carcinoma is a major global health concern, with chronic viral hepatitis B and C being the most frequently reported causes due to a variety of direct and indirect carcinogenic mechanisms.<sup>[19]</sup> Over the past several years, debate has emerged regarding the impact of DAAs on HCC development. Several studies have suggested that treatment of chronic HCV infection with direct-acting antivirals may be associated with an increased risk of *de novo* and recurrent HCC.<sup>[20]</sup>

In the current study, the median levels of AFP and DCP were higher among patients with HCC compared to those without HCC, which is consistent with the findings of Dating et al.<sup>[21]</sup> (p<0.0001). However, in contrast to the findings of Dating et al.<sup>[21]</sup> and Best et al.,<sup>[22]</sup> who reported elevated AFP-L3 levels in patients with HCC, our study demonstrated a significantly lower median AFP-L3 level among patients with HCC.<sup>[21,22]</sup> Furthermore, liver stiffness measured by FibroScan was significantly higher among patients with HCC following DAA therapy compared with HCV patients without HCC following DAA therapy (32.63±24.3 vs. 11.24±4.71, p=0.001). This may be explained by the presence of tumor masses, which likely contribute to increased liver stiffness.

In our study, the GALAD score demonstrated poor prognostic performance for predicting mortality among patients with HCC (AUC=0.564, 95% CI: 0.434–0.693).

Our study also evaluated the diagnostic accuracy of the GALAD score using ROC curve analysis, yielding an AUC of 0.849 (95% CI: 0.794–0.905, p<0.001), with a sensitivity of 59.3% and specificity of 97.7%. These findings are consistent with those of Best et al.,<sup>[22]</sup> who reported an area under the receiver operating characteristic curve (AUROC) of 0.9242 (95% CI: 0.8925–0.9559, p<0.0001) for the GALAD score. Similarly, a study by Huang et al.<sup>[23]</sup> demonstrated good diagnostic performance of the GALAD score, with an AUC of 0.869 (95% CI: 0.845–0.891), sensitivity of 85.6%, and specificity of 93.3%. The adequate diagnostic accuracy of the GALAD score may be attributed to its incorporation of multiple biomarkers (AFP, AFP-L3, and DCP), which reflect intratumoral heterogeneity, in addition to demographic factors (age and sex) associated with increased HCC risk. Thus, the GALAD score offers higher sensitivity and specificity compared to the use of individual markers alone.

Kushner et al.<sup>[24]</sup> proposed that modifications in the interferon gene expression environment and natural killer cell activity resulting from HCV eradication may underlie tumor recurrence following DAA therapy. Interferon genes may be suppressed by DAA therapy, potentially leading to enhanced cell proliferation and subsequent tumor growth. Furthermore, DAA therapy eliminates the inflammatory response associated with chronic HCV infection, which may increase the risk of liver carcinogenesis.<sup>[24]</sup>

The primary limitation of this study is its relatively small sample size. Additionally, all participants were of Egyptian ethnicity, which may limit the generalizability of the results to other populations. The high mortality rate observed in this study may be attributed to several factors, including the frequent diagnosis of HCC at advanced stages (BCLC B or C), the advanced age of many patients, and recurrent episodes of hepatic encephalopathy, all of which adversely affected survival.

## Conclusion

The GALAD score demonstrated adequate diagnostic performance for predicting *de novo* HCC following DAA therapy and was associated with HCC recurrence. However, it showed limited ability to predict mortality.

**OnlineAppendixLink:**<https://hepatologyforum.org/storage/upload/files/1775573474-appendix-en.pdf>

**Ethics Committee Approval:** All procedures were conducted after approval by the Faculty of Medicine, Cairo University Ethics Committee and in accordance with the Declaration of Helsinki (1975), as revised in 2008 (MS-524-2021/27.02.2022).

**Informed Consent:** After providing written informed consent, all participants underwent a comprehensive clinical evaluation, including a full medical history and complete physical examination.

**Conflict of Interest:** The authors have no conflict of interest to declare.

**Financial Disclosure:** The authors declared that this study has received no financial support.

**Use of AI for Writing Assistance:** The authors declared that they did not use artificial intelligence (AI)- assisted technologies.

**Author Contributions:** Concept: AOA, TME; Design: MMN; Supervision: HIS, AHK, AHA; Funding: AH; Materials: MHK; Data Collection and/or Processing: MA, AH; Analysis and/or Interpretation: SAAM, AOA; Literature Search: RM; Writing: AR; Critical Reviews: AOA, EM, RL.







**Peer-review:** Externally peer-reviewed.

## References

- Rashed WM, Kandeil MAM, Mahmoud MO, Ezzat S. Hepatocellular carcinoma (HCC) in Egypt: A comprehensive overview. *J Egypt Natl Canc Inst* 2020;32(1):5. [CrossRef]
- Bray F, Ferlay J, Soerjomataram I, Siegel RL, Torre LA, Jemal A. Global cancer statistics 2018: GLOBOCAN estimates of incidence and mortality worldwide for 36 cancers in 185 countries. *CA Cancer J Clin* 2018;68(6):394-424. Erratum in: *CA Cancer J Clin* 2020;70(4):313. [CrossRef]
- Labadie K, M. Sullivan K, O. Park J. Surgical Resection in HCC. In: Lasfar A (editor). *Liver Cancer*. London: IntechOpen; 2018. [CrossRef]
- European Association for The Study of the Liver; European Organisation For Research and Treatment of Cancer. EASL-EORTC clinical practice guidelines: management of hepatocellular carcinoma. *J Hepatol* 2012;56(4):908-943. Erratum in: *J Hepatol* 2012;56(6):1430. [CrossRef]
- Franco RA, Galbraith JW, Overton ET, Saag MS. Direct-acting antivirals and chronic hepatitis C: towards elimination. *Hepatoma Res* 2018;4:74. [CrossRef]
- Conti F, Buonfiglioli F, Scuteri A, Crespi C, Bolondi L, Caraceni P, et al. Early occurrence and recurrence of hepatocellular carcinoma in HCV-related cirrhosis treated with direct-acting antivirals. *J Hepatol* 2016;65(4):727-733. [CrossRef]
- Nakao Y, Hashimoto S, Abiru S, Komori A, Yamasaki K, Nagaoka S, et al. Rapidly growing, moderately differentiated HCC: A clinicopathological characteristic of HCC occurrence after IFN-free DAA therapy? *J Hepatol* 2018;68(4):854-855. [CrossRef]
- Abdelaziz AO, Nabil MM, Abdelmaksoud AH, Shousha HI, Cordie AA, Hassan EM, et al. De-novo versus recurrent hepatocellular carcinoma following direct-acting antiviral therapy for hepatitis C virus. *Eur J Gastroenterol Hepatol* 2018;30(1):39-43. [CrossRef]
- Villani R, Vendemiale G, Serviddio G. Molecular mechanisms involved in HCC recurrence after direct-acting antiviral therapy. *Int J Mol Sci* 2018;20(1):49. [CrossRef]
- Prasad V, Lenzer J, Newman DH. Why cancer screening has never been shown to "save lives"--and what we can do about it. *BMJ* 2016;352:h6080. [CrossRef]
- Nomura S. Use of the GALAD score for serological prediction of hepatocellular carcinoma. UC San Diego Independent Study Projects. UC San Diego: University of California; 2018.
- Li L, Lu F, Chen P, Song H, Xu W, Guo J, et al. Validation of the GALAD model and establishment of a new model for HCC detection in Chinese patients. *Front Oncol* 2022;12:1037742. Erratum in: *Front Oncol* 2023;13:1170066. [CrossRef]
- Li H, Liu H, Yan LJ, Ding ZN, Zhang X, Pan GQ, et al. Performance of GALAD score and serum biomarkers for detecting NAFLD-related HCC: a systematic review and network meta-analysis. *Expert Rev Gastroenterol Hepatol* 2023;17(11):1159-1167. [CrossRef]
- Schotten C, Ostertag B, Sowa JP, Manka P, Bechmann LP, Hilgard G, et al. GALAD Score Detects Early-Stage Hepatocellular Carcinoma in a European cohort of chronic Hepatitis B and C patients. *Pharmaceuticals (Basel)* 2021;14(8):735. [CrossRef]
- Guan MC, Zhang SY, Ding Q, Li N, Fu TT, Zhang GX, et al. The Performance of GALAD score for diagnosing hepatocellular carcinoma in patients with chronic liver Diseases: A systematic review and meta-analysis. *J Clin Med* 2023;12(3):949. [CrossRef]
- Hsu CY, Lee YH, Hsia CY, Huang YH, Su CW, Lin HC, et al. Performance status in patients with hepatocellular carcinoma: determinants, prognostic impact, and ability to improve the Barcelona Clinic Liver Cancer system. *Hepatology* 2013;57(1):112-119. [CrossRef]
- Berhane S, Toyoda H, Tada T, Kumada T, Kagebayashi C, Satomura S, et al. Role of the GALAD and BALAD-2 serologic models in diagnosis of hepatocellular carcinoma and prediction of survival in patients. *Clin Gastroenterol Hepatol* 2016;14(6):875-886.e6. [CrossRef]
- Sato Y, Watanabe H, Sone M, Onaya H, Sakamoto N, Osuga K, et al; Japan Interventional Radiology in Oncology Study Group-JIVROSG. Tumor response evaluation criteria for HCC (hepatocellular carcinoma) treated using TACE (transcatheter arterial chemoembolization): RECIST (response evaluation criteria in solid tumors) version 1.1 and mRECIST (modified RECIST): JIVROSG-0602. *Ups J Med Sci* 2013;118(1):16-22. [CrossRef]
- European Association for the Study of the Liver. EASL Clinical Practice Guidelines: Management of hepatocellular carcinoma. *J Hepatol* 2018;69(1):182-236.
- Guarino M, Sessa A, Cossiga V, Morando F, Caporaso N, Morisco F; Special Interest Group on "Hepatocellular carcinoma and new anti-HCV therapies" of the Italian Association for the Study of the Liver. Direct-acting antivirals and hepatocellular carcinoma in chronic hepatitis C: A few lights and many shadows. *World J Gastroenterol* 2018;24(24):2582-2595. [CrossRef]
- Dating MJP, Relente MJL, Junio DZG, Tiangco BJ, Tripon ES, Albia JR. A baseline validation study of the GALAD model for diagnosis of hepatocellular carcinoma among philippine patients. Research Square. Preprint, 2022. doi: 10.21203/rs.3.rs-1583117/v1 [CrossRef]
- Best J, Bilgi H, Heider D, Schotten C, Manka P, Bedreli S, et al. The GALAD scoring algorithm based on AFP, AFP-L3, and DCP significantly improves detection of BCLC early stage hepatocellular carcinoma. *Z Gastroenterol* 2016;54(12):1296-1305. [CrossRef]
- Huang C, Fang M, Xiao X, Wang H, Gao Z, Ji J, et al. Validation of the GALAD model for early diagnosis and monitoring of hepatocellular carcinoma in Chinese multicenter study. *Liver Int* 2022;42(1):210-223. [CrossRef]
- Kushner T, Dieterich D, Saberi B. Direct-acting antiviral treatment for patients with HCC. *Curr Opin Gastroenterol* 2018;34(3):132-139. [CrossRef]

## ORIGINAL RESEARCH

# High expression of USP15 affects tumor progression and immune infiltration in hepatocellular carcinoma

 Si-Peng Wu<sup>1</sup>,  Xue-Yuan Zhang<sup>1</sup>,  Hui-Dan Chen<sup>1</sup>,  Fu-Zhi Jin<sup>2</sup>,  Nan Jiang<sup>1</sup>,  Jia-Xing Zhang<sup>1</sup>,  Zhe-Long Liang<sup>2</sup>

1: Medical College of Yanbian University, Jilin, China

2: Department of Anesthesia, Hospital of Yanbian University, Jilin, China

## Highlights & Insights

- **Scientific Gap:** The role of USP15 in shaping the tumor immune microenvironment and immunotherapy response in hepatocellular carcinoma remains unclear.
- **Key Finding:** High USP15 expression is associated with advanced stage, reduced T-cell and NK-cell infiltration, and increased PD-L1 expression and macrophage presence, indicating an immunosuppressive milieu.
- **Clinical Impact:** USP15 may serve as a prognostic biomarker and its inhibition, especially with PD-1/PD-L1 blockade, may enhance immunotherapy response.

## ABSTRACT

**Background and Aim:** Ubiquitin-specific protease 15 (USP15) is closely associated with the occurrence and progression of hepatocellular carcinoma (HCC). However, its role in shaping the immune landscape of HCC remains unclear.

**Materials and Methods:** The expression levels, proportions, and spatial distributions of USP15 and specific immune cell subsets in HCC tissues were evaluated using multiplex immunohistochemistry (mIHC).

**Results:** In the tumor parenchyma of HCC tissues, the infiltration of immune cells, particularly natural killer (NK) cells, was significantly reduced ( $p < 0.05$ ). Further analyses revealed that USP15 expression levels were significantly associated with clinical stage and other clinicopathological parameters ( $p < 0.05$ ). In particular, NK cell infiltration was significantly correlated with N stage, M stage, and overall tumor–node–metastasis (TNM) stage ( $p < 0.05$ ).

**Conclusion:** USP15 contributes to the establishment of an immunosuppressive tumor microenvironment in HCC by inhibiting T cell and NK cell infiltration, facilitating programmed death-ligand 1 (PD-L1)-mediated immune evasion, and enhancing macrophage recruitment. These findings indicate that USP15 may serve as a potential therapeutic target for HCC.

**Keywords:** Hepatocellular carcinoma, immune cell infiltrates, tumor immune microenvironment, ubiquitin-specific peptidase 15 (USP15).

**How to cite this article:** Wu S-P, Zhang X-Y, Chen H-D, Jin F-Z, Jiang N, Zhang J-X, et al. High expression of USP15 affects tumor progression and immune infiltration in hepatocellular carcinoma. *Hepatology Forum* 2026; 7(2):108–117.

**Received:** June 19, 2025; **Revised:** October 23, 2025; **Accepted:** January 16, 2026; **Available Online:** April 08, 2026

**Corresponding author:** Zhe-Long Liang, Department of Anesthesia, Affiliated Hospital of Yanbian University, Jilin, China; **E-mail:** zlliang@ybu.edu.cn



This work is licensed under a Creative Commons Attribution-NonCommercial 4.0 International License.

## Introduction

Hepatocellular carcinoma (HCC) is the most common primary liver malignancy and is characterized by abnormal cell proliferation and dysregulation of the immune system. Consequently, HCC is often diagnosed at an advanced stage, which limits treatment options and contributes to a persistently high mortality rate.<sup>[1,2]</sup> Although various therapeutic strategies, including surgical resection, locoregional ablation, and systemic therapies, are available, the overall prognosis of patients with HCC remains poor. Because the efficacy of programmed cell death protein 1 (PD-1)/programmed death-ligand 1 (PD-L1)-based immunotherapies critically depends on the tumor microenvironment (TME), it is essential to elucidate the key factors that regulate the TME to optimize therapeutic responses, improve prognostic accuracy, and develop novel treatment strategies.

The liver is an immune-rich organ that contains numerous immune-active cells and defense mechanisms against pathogens. However, its ability to combat cancer is often compromised by tumor cell-mediated evasion mechanisms and the establishment of an immunosuppressive TME.<sup>[3]</sup> The composition of the TME is highly complex and heterogeneous, consisting of various cellular and acellular components, as well as the molecules they produce. These components can modulate immune function, ultimately suppressing effective antitumor immune responses while creating a microenvironment that favors tumor survival.

The dynamic interaction between the immune microenvironment and tumor cells drives tumorigenesis, progression, metastasis, and treatment response.<sup>[4]</sup> Immune cell populations within the immune microenvironment play crucial roles in the development of HCC by regulating antitumor immune responses. When the antitumor activity of immunocytes in HCC is impaired, the TME promotes cancer cell growth and metastasis while limiting the immune system's ability to eliminate tumor cells.<sup>[5]</sup> Therefore, exploring changes in the TME during HCC progression, particularly alterations in the aforementioned immune cell populations, is essential for guiding HCC treatment strategies.

Ubiquitin-specific proteases (USPs) constitute the largest family of deubiquitinases (DUBs) and play pivotal roles in regulating tumor progression, immune cell function, immune responses, and the establishment of an immunosuppressive TME.<sup>[6,7]</sup> Ubiquitin-specific protease 15 (USP15) has been reported to be overexpressed in various malignancies, including glioblastoma, ovarian cancer, myeloma, and pancreatic cancer.<sup>[8]</sup> Our previous research demonstrated that USP15 expression is relatively low in normal liver tissue but markedly elevated in metastatic HCC. In addition, increased USP15 in HCC tissues is strongly associated with unfavorable clinical outcomes and negatively correlated with patient survival time.<sup>[9]</sup> These findings suggest that USP15 expression may be closely linked to inflammatory and immune-mediated pathways that promote HCC metastatic spread, highlighting the pivotal role of USP15 in driving HCC progression and disease deterioration. Furthermore, some studies have suggested that ubiquitin-specific peptidase 6 (USP6) in

pancreatic ductal adenocarcinoma is strongly associated with various immune cell infiltrations.<sup>[10]</sup> Therefore, we hypothesize that members of the USP family may influence the immune response in the TME of HCC. Exploring the relationship between USP15 and the TME holds considerable clinical significance and may provide deeper insights into the critical roles of USP15 in tumor development and immune regulation in patients with HCC.

This study aims to explore USP15 expression in HCC and analyze its impact on the TME, particularly on the infiltration of immune cell subpopulations such as T cells and natural killer (NK) cells. Additionally, we investigated the association between USP15 expression levels and the clinical characteristics of HCC patients to evaluate its potential as a therapeutic target.

## Materials and Methods

### Clinical Samples

Tumor tissue microarrays (TMAs; HLivH060CD03) were obtained from Shanghai Outdo Biotechnology. The array consists of 60 tissue cores, each with a diameter of 2.0 mm. The cohort includes two normal liver tissue samples, six cirrhotic specimens, 17 primary HCC lesions, and 15 metastatic HCC samples. For the majority of HCC cases, paired sampling was performed between the central region of the primary tumor and the adjacent peritumoral liver tissue. In addition, a subset of advanced-stage cases included distant hepatic tissue specimens. This study was conducted in accordance with the Declaration of Helsinki. All patients provided informed consent, and the study was approved by the Shanghai Outdo Ethics Committee (No: SHYJS-CP-1601006) on January 4, 2016. USP15 expression levels across the HCC cohort were ranked in ascending order, and the median value (50<sup>th</sup> percentile) was used as the stratification threshold. The cohort was subsequently divided into two subgroups: those with above-median USP15 expression (high-expression group) and those with below-median expression (low-expression group).

### Antibody Information

The antibodies used in multiplex immunohistochemistry (mIHC) were as follows: PD-L1 antibody (AD80167) from Abcepta; USP15 antibody (14354-1-AP) from Proteintech; cluster of differentiation 56 (CD56) antibody (ZM0057) from Beijing Zhong Shan Golden Bridge Biological Technology Co., Ltd.; cluster of differentiation 4 (CD4) antibody (PA285); cluster of differentiation 68 (CD68) antibody (PA014); cluster of differentiation 8 (CD8) antibody (PA577); forkhead box P3 (FoxP3) antibody (PA448); and cytokeratin (CK) antibody (PA125) from Suzhou Abcarta Medtech Co., Ltd.

### Multiplex Immunohistochemistry

The experimental protocols were verified by the EACRI IHC Core (Providence Cancer Institute, Portland, OR) following established guidelines.<sup>[11]</sup> Briefly, tissue microarray (TMA) sections underwent sequential processing: initial baking at 63°C for one hour, followed by dewaxing in xylene and rehydration through graded ethanol.

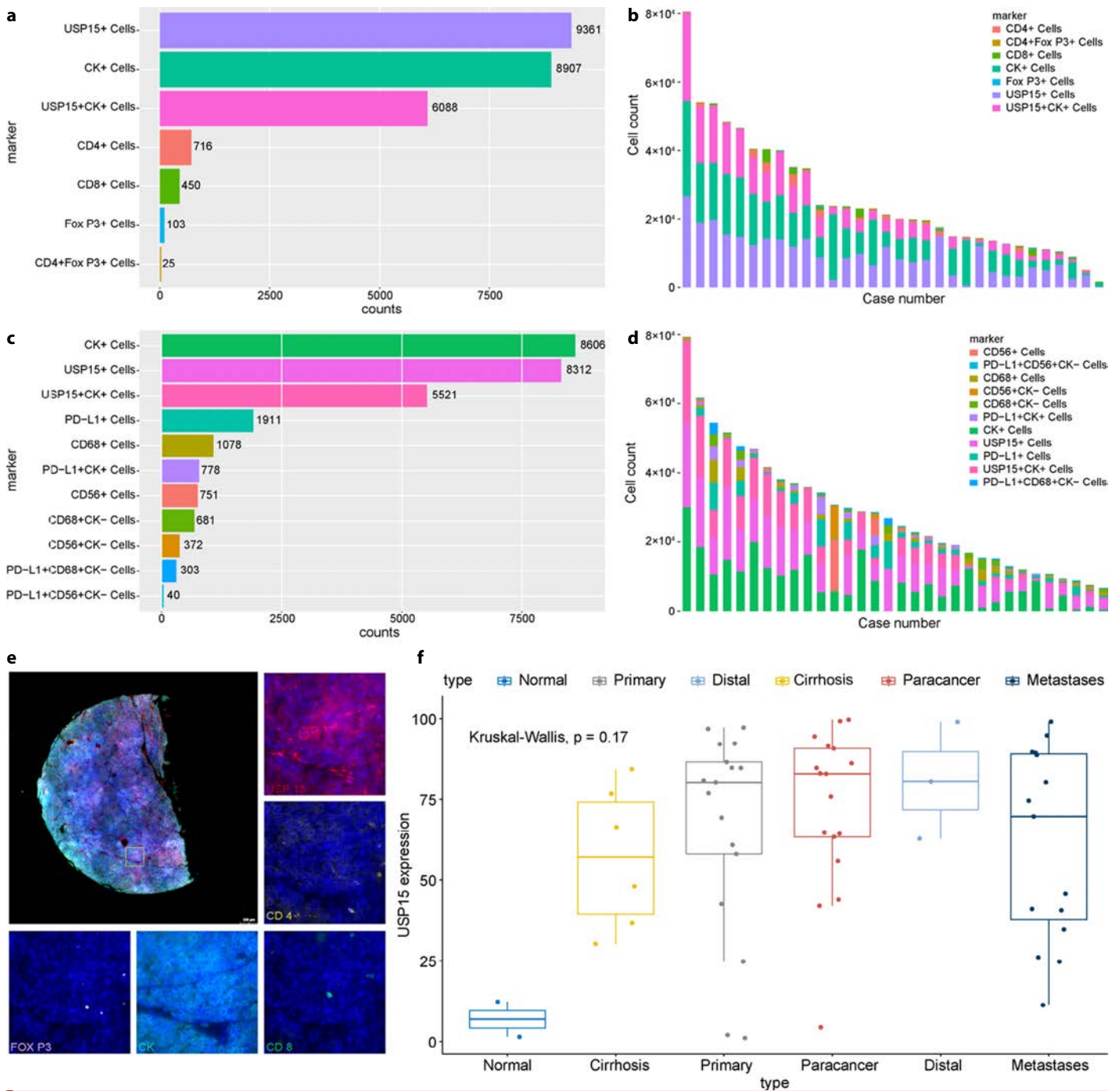


**Figure 1.** (a, c) Statistical demonstration of overall expression levels of various cell types in TMA in the two mIHC panels respectively. (b, d) Statistical demonstration of the expression levels of various cell types in each clinical sample in the two mIHC panels respectively. (e). Representative multiplex immunofluorescence image of a HCC tissue core selected for analysis of USP15-high peritumoral regions. Markers: USP15 (red), CD8 (T cells, green), CD4 (T cells, yellow), CK (tumor epithelial cells, cyan), FOX P3 (purple). Scale bar =200 μm. (f) The difference of USP15 infiltration between different progression of HCC.

Antigen unmasking was performed using an automated staining platform (Leica ST5020; Leica Biosystems). To neutralize endogenous peroxidase activity, slides were treated with 3% hydrogen peroxide for 10 minutes. Subsequent blocking with 5% bovine serum albumin (BSA) preceded a 60-minute incubation with primary antibodies targeting PD-L1 (ready to use), USP15 (1:200 dilution), CD56 (ready to

use), CD4 (ready to use), CD68 (ready to use), CD8 (ready to use), FoxP3 (ready to use), and cytokeratin (ready to use). Following three washes with Tris-buffered saline with Tween 20 (TBST), a secondary antibody (SM802; Dako; ready to use) was applied for 10 minutes. Fluorescent labeling was performed using Opal 7-color dye (PerkinElmer; NEL801001KT) diluted 1:100, with a 10-minute incubation at room

temperature. Antibody stripping between markers was achieved via microwave treatment in the citrate buffer. Sequential staining cycles were repeated for all targets, followed by nuclear counterstaining with DAPI for 5 minutes and mounting with antifade medium. Two independent antibody panels were processed.

Whole-slide imaging was conducted using a TissueFAXS Spectra system (TissueGnostics GmbH, Austria). Acquired multispectral data were analyzed using StrataQuest software (v7.1.129; TissueGnostics), employing spectral unmixing to resolve individual fluorescence channels. Nuclear segmentation was performed using DAPI signals, and cytoplasmic or membrane markers were quantified within a user-defined radius from the nuclei. Threshold parameters were dynamically adjusted for each marker to classify positive cells based on fluorescence intensity and spatial distribution. Multiplex positivity was determined through co-localization analysis of two or more markers, with cell counts and signal intensities recorded for statistical evaluation.

### Statistical Analysis

USP15 expression and the levels of TME cells in HCC tumor tissues and paracancerous tissues were compared using the Wilcoxon test. Comparisons among multiple groups were performed using the Kruskal–Wallis test. The relationship between USP15 expression and immunohistochemical factors was examined using the Spearman rank correlation coefficient. All statistical analyses were performed using SPSS version 22.0 (IBM Corporation, Armonk, NY, USA), and  $p < 0.05$  was considered statistically significant.

## Results

### USP15 Expression Level Correlates with Clinical Characteristics and Progression in Patients with HCC

To investigate the regulatory role of USP15 within the TME of HCC, mIHC was used to detect USP15 expression and specific immune markers, including CD4 (a marker of CD4<sup>+</sup> T cells), CD8 (a marker of CD8<sup>+</sup> T cells), CD56 (a marker of NK cells), and CD68 (a marker of macrophages), in HCC tissues. The infiltration of various immune cells in HCC tissues with high USP15 expression was analyzed (Fig. 1A–D), and their correlation with USP15 expression levels was assessed.

According to the mIHC results, USP15 staining was predominantly observed on the tumor cell membrane and in the cytoplasm, with a red positive signal (Fig. 1E). In contrast, USP15 staining varied among paracancerous tissues, with some samples showing strong staining and others weak staining. These findings indicate that USP15 may play a specific role in tumor cells, and its expression is upregulated during the progression of HCC (Fig. 1F), consistent with our previous research.

Our previous studies have revealed that USP15 expression is positively correlated with HCC recurrence.<sup>[9]</sup> To further investigate whether differential USP15 expression in HCC tissues is associated with

**Table 1.** Expression of USP15 in HCC of patients with different clinical characteristics

Character	Group	Low	High	Total	p value	r value
Age(year)	≤52	1	16	17	0.319	-0.213
	>52	3	12	15		
Tumor size	≤6.25 cm	2	6	8	1	0.16
	>6.25 cm	1	7	8		
T stage	I-II	3	6	9	0.585	0.218
	III	1	6	7		
N stage	N0	0	16	16	0.066	0.149
	N1	4	11	15		
M stage	M0	0	1	1	0.038	0.402
	M1	4	11	15		
Pathological grade	I	0	17	17	1	-0.203
	II-III	0	2	2		
TNM stage	I-III	2	8	10	0.028	0.429
	IV	4	10	14		

USP15: Ubiquitin-specific protease 15; HCC: Hepatocellular carcinoma; TNM: Tumor node metastasis.

clinical characteristics, we analyzed the clinical data of all patients with HCC. Our analysis revealed a strong association between high USP15 expression and advanced disease stages, showing a marked trend with M stage and a statistically significant association with tumor–node–metastasis (TNM) stage ( $p < 0.05$ ) (Table 1). These results are consistent with our previous findings and suggest that USP15 expression may serve as a therapeutic target in HCC.

### USP15 as a Negative Regulatory Factor for T-Cell Infiltration

The activation and function of T cells are tightly regulated by various negative regulators to ensure that the immune system effectively combats foreign pathogens while preventing abnormal immune responses and autoimmune diseases.<sup>[12]</sup> Our results indicated significant differences in the staining of CD4<sup>+</sup> T cells, CD8<sup>+</sup> T cells, and regulatory T (Treg) cells between HCC tissues and paracancerous tissues ( $p < 0.05$ ) (Fig. 2A–C). The observed low densities of CD4<sup>+</sup> T cells and CD8<sup>+</sup> T cells suggest limited infiltration into the tumor parenchyma. These findings imply that USP15 may function as a negative regulator of T cells in HCC, with high USP15 expression correlating with reduced T-cell activation and infiltration.

Furthermore, we observed a strong association between tumor epithelial cells (cytokeratin-positive, CK<sup>+</sup>) and both CD4<sup>+</sup> T-cell expression and USP15<sup>+</sup> CK<sup>+</sup> cells. Specifically, CD4<sup>+</sup> T-cell expression showed a significant negative correlation ( $p < 0.001$ ) (Fig. 2D–E), whereas USP15<sup>+</sup> CK<sup>+</sup> cells showed a significant positive correlation ( $p < 0.001$ ) (Fig. 2F). However, although a negative correlation was

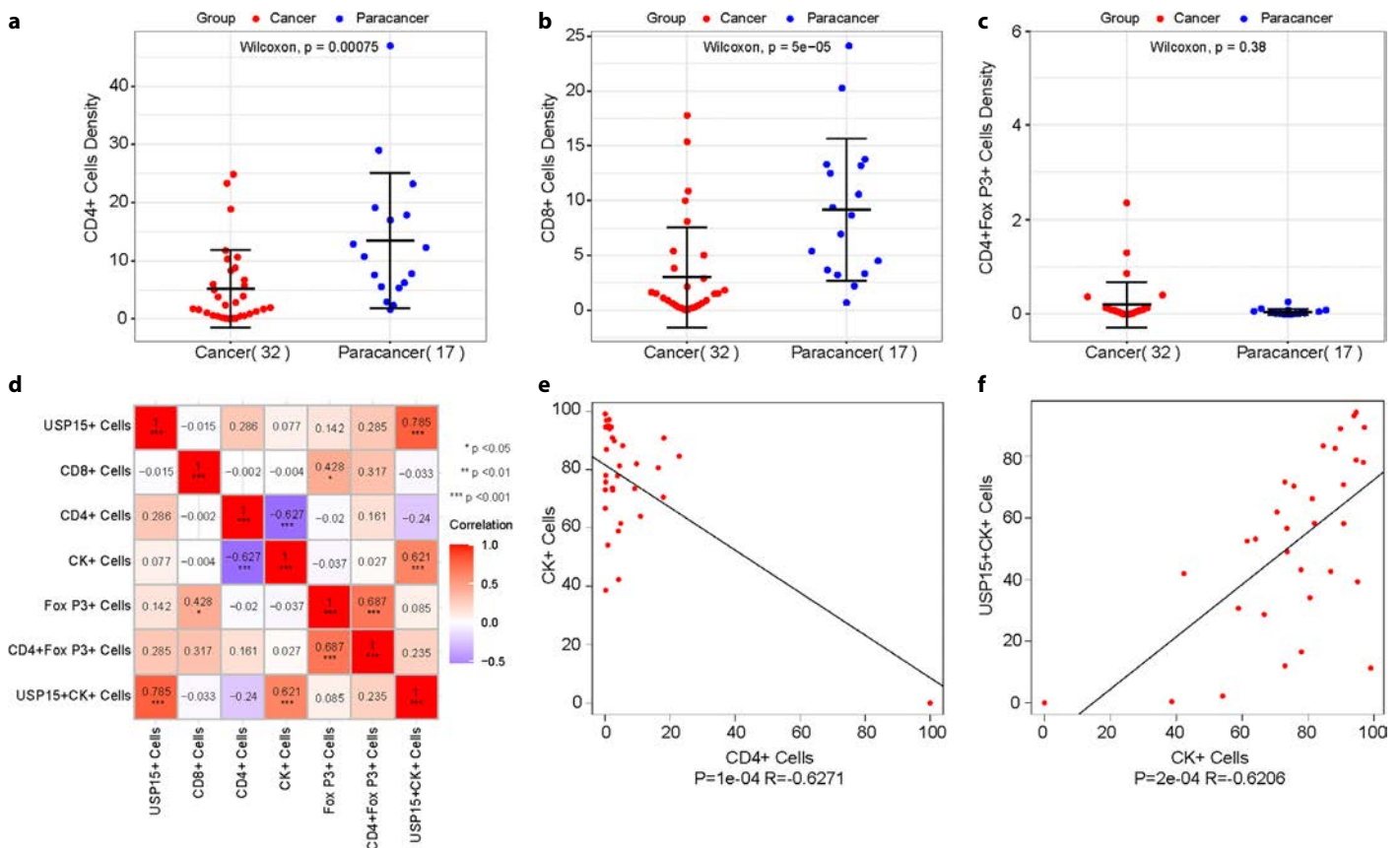


**Figure 2.** (a–c) Differential analysis of the percentage of CD4<sup>+</sup> T cells, CD8<sup>+</sup> T cells and Treg cells between cancer tissues and adjacent normal tissues. (d) Heat map of correlation analysis between indicators in panel 1. (e) Correlation analysis of Tumor epithelial cells (CK<sup>+</sup>) and CD4<sup>+</sup> T cell expression,  $p < 0.001$ ,  $R = -0.627$ . (f) Correlation analysis of Tumor epithelial cells (CK<sup>+</sup>) and USP15<sup>+</sup> Tumor epithelial cells expression,  $p < 0.001$ ,  $R = 0.621$ .

observed between USP15<sup>+</sup> CK<sup>+</sup> cells and CD4<sup>+</sup> T cells, it was not statistically significant ( $p > 0.05$ ). Therefore, we speculate that USP15 may influence CD4<sup>+</sup> T cells indirectly through modulation of the tumor microenvironment rather than through direct interaction.

### The Degree of NK Cell Infiltration Is Correlated with USP15 Expression and the Clinical Features of Patients with HCC

To better evaluate NK-cell infiltration, we selected tumor peripheral regions exhibiting high USP15 expression for detailed analysis (Fig. 3A). The mIHC data revealed a significant difference in NK-cell infiltration between HCC tissues and paracancerous tissues ( $p < 0.001$ ) (Fig. 3B). The low density of CD56<sup>+</sup> cells indicates minimal NK-cell infiltration in the tumor parenchyma (Fig. 3C). In addition, mIHC analysis revealed a significant negative association between the level of NK-cell infiltration and USP15<sup>+</sup> cells ( $p < 0.05$ ) (Fig. 3D–E). Similarly, the expression level of CD56<sup>+</sup> cells was significantly negatively correlated with USP15<sup>+</sup> tumor epithelial cells ( $p < 0.05$ ) (Fig. 3F). To investigate potential associations between NK-cell infiltration in HCC tissues and clinical characteristics, we analyzed the clinicopathological data of all patients with HCC. The results showed that NK-cell infiltration was significantly associated with the N stage, M stage, and TNM stage ( $p < 0.05$ ) (Table 2). Therefore, these findings

suggest that high USP15 expression may inhibit NK-cell infiltration, activation, and cytotoxic function within the TME.

### USP15 Exhibits a Positive Correlation with PD-L1<sup>+</sup> Cells and Tumor-Associated Macrophages

PD-L1, an important target for tumor immunotherapy, is expressed not only on tumor cells but also on tumor-associated macrophages (TAMs). Our mIHC analysis revealed a modest correlation between USP15 expression and PD-L1<sup>+</sup> cells (Fig. 4A). Although the proportion of PD-L1<sup>+</sup> cells showed no significant difference between HCC tissues and adjacent normal tissues (Fig. 3C), we observed a significant negative correlation between PD-L1<sup>+</sup> cell infiltration and tumor epithelial cell expression levels ( $p < 0.05$ ) (Fig. 4B). Concurrently, a significant positive correlation was observed with the expression of PD-L1<sup>+</sup> tumor epithelial cells ( $p < 0.05$ ) (Fig. 4C). These findings suggest that USP15 may be involved in regulating PD-L1<sup>+</sup> cells, particularly PD-L1<sup>+</sup> tumor epithelial cells.

Notably, our data demonstrated a modest positive correlation between PD-L1<sup>+</sup> tumor epithelial cells and CD68<sup>+</sup> cell infiltration ( $p < 0.05$ ) (Fig. 4D). Therefore, the sequential chain of correlations from USP15<sup>+</sup> cells to CD68<sup>+</sup> cells may suggest that USP15<sup>+</sup> tumor cells influence macrophage infiltration indirectly via PD-L1 co-expression.

**Table 2.** Expression of NK cells in hepatocellular carcinoma tissues of patients with different clinical characteristics

Character	Group	Low	High	Total	p value	r value
Age(year)	≤52	8	9	17	0.735	0.071
	>52	6	9	15		
Tumor size	≤6.25cm	6	2	8	0.608	0.258
	>6.25cm	4	4	8		
T stage	I-II	6	3	9	1	0.098
	III	4	3	7		
N stage	N0	4	12	16	0.031	0.333
	N1	10	5	15		
M stage	M0	0	1	1	0.031	0.434
	M1	10	5	15		
Pathological grade	I	4	13	17	1	-0.112
	II-III	1	1	2		
TNM stage	I-III	7	3	10	0.011	0.492
	IV	10	4	14		

NK: Natural killer; TNM: Tumor node metastasis.

## Discussion

In recent years, the TME has gradually emerged as a major focus of cancer research. In this study, we explored the relationship between USP15 and the TME by performing mIHC staining to analyze the expression of USP15 and various immune cell subsets associated with the TME in tissues from patients with HCC (Fig. 4E-F). Our findings revealed that USP15 significantly influences tumor cell expression and shows negative correlations with the infiltration of most immune cell types. Furthermore, our study demonstrated that USP15 is overexpressed in HCC tissues and is associated with adverse clinicopathological parameters. These findings suggest that USP15 may function as an important immunomodulatory regulator in HCC and highlight its potential as a therapeutic target in HCC.

The therapeutic value of combining USP inhibitors with tumor immunotherapy has been increasingly recognized. For example, combination therapy strategies that synergistically enhance the efficacy of anti-PD-1/PD-L1 immunotherapy by inhibiting deubiquitinating enzymes can reshape the inflammatory TME. In addition, inhibition of USP22 expression has been shown to enhance the sensitivity of patients with pancreatic ductal adenocarcinoma to immunotherapy.<sup>[13,14]</sup> Therefore, our study provides a theoretical basis for the development of novel USP inhibitors.

The observed correlations between USP15 and immune cell infiltration provide important insights into the potential role of USPs as therapeutic targets for HCC. Numerous mechanisms involved in tumorigenesis and tumor progression, including regulation of the TME, are closely associated with ubiquitination processes. Previous

studies have reported that USP15 functions as a negative regulator of T-cell activation, and targeting USP15 may induce tumor cell apoptosis while enhancing the antitumor T-cell response.<sup>[15]</sup> These findings are consistent with our mIHC results. High USP15 expression was associated with reduced T-cell infiltration and increased metastasis in HCC. This suggests that USP15 may promote tumorigenesis and disease progression through both intrinsic tumor-cell mechanisms and suppression of host antitumor immune defense.

Natural killer cells, as essential innate immune effector cells, play a critical role in defense against infections and tumor progression.<sup>[16]</sup> However, the functional activity of NK cells within the TME can be inhibited by certain cytokines, such as interleukin-6 (IL-6), IL-10, and indoleamine 2,3-dioxygenase (IDO), which suppress NK-cell activity by promoting immunosuppressive cells and cytokines that antagonize NK-cell activation.<sup>[16,17]</sup> To examine the relationship between immune infiltration and clinicopathological features of HCC, we performed a comprehensive clinical correlation analysis using patient-derived clinical data. Our results demonstrated significant associations between NK-cell infiltration and multiple clinicopathological features in patients with HCC. Therefore, we believe that the immunosuppressive TME represents one of the main limiting factors preventing NK cells from exerting effective immune responses. Future studies will further investigate the intrinsic mechanisms by which USP15 regulates NK-cell activity, with the aim of optimizing NK cell-based immunotherapy and identifying new therapeutic strategies for tumor immunotherapy.

Currently, TAMs are important targets for cancer therapy. Their two main subtypes, M1 and M2, can transform into each other in response to changes in the microenvironment. Among them, M2 macrophages promote the formation of an immunosuppressive TME by secreting various immunosuppressive factors, including transforming growth factor- $\beta$  (TGF- $\beta$ ) and IL-10, thereby exacerbating the immunosuppressive state of the TME and leading to HCC metastasis and resistance to immunotherapy.<sup>[18-20]</sup> Previous studies have shown that downregulation of USP7 expression can induce phenotypic transformation of TAMs from the M2 to the M1 subtype through the p38 mitogen-activated protein kinase (MAPK) pathway, while also upregulating PD-L1 expression in the TME.<sup>[21]</sup> Both USP7 and USP15 belong to the USP family and play similar roles in regulating intracellular ubiquitination processes. Therefore, USP15 could be a new therapeutic target and prognostic factor. In this study, we initially attempted to determine the relationship between USP15 and macrophages; however, no significant changes in macrophage infiltration were observed. We suspect that macrophages may instead undergo polarization changes, which provides a direction for our subsequent research. Furthermore, in both the tumor parenchyma and stroma of HCC, the co-expression of USP15 and PD-L1, as well as the co-expression of macrophages and PD-L1, was significant, indicating a close relationship among these three factors. Therefore, we speculate that macrophages may alter their polarization state due to the combined effects of USP15 and PD-L1, thereby promoting tumor growth. Over the past decade, PD-L1/PD-1 monoclonal antibodies have been widely used in cancer treatment; however, anti-

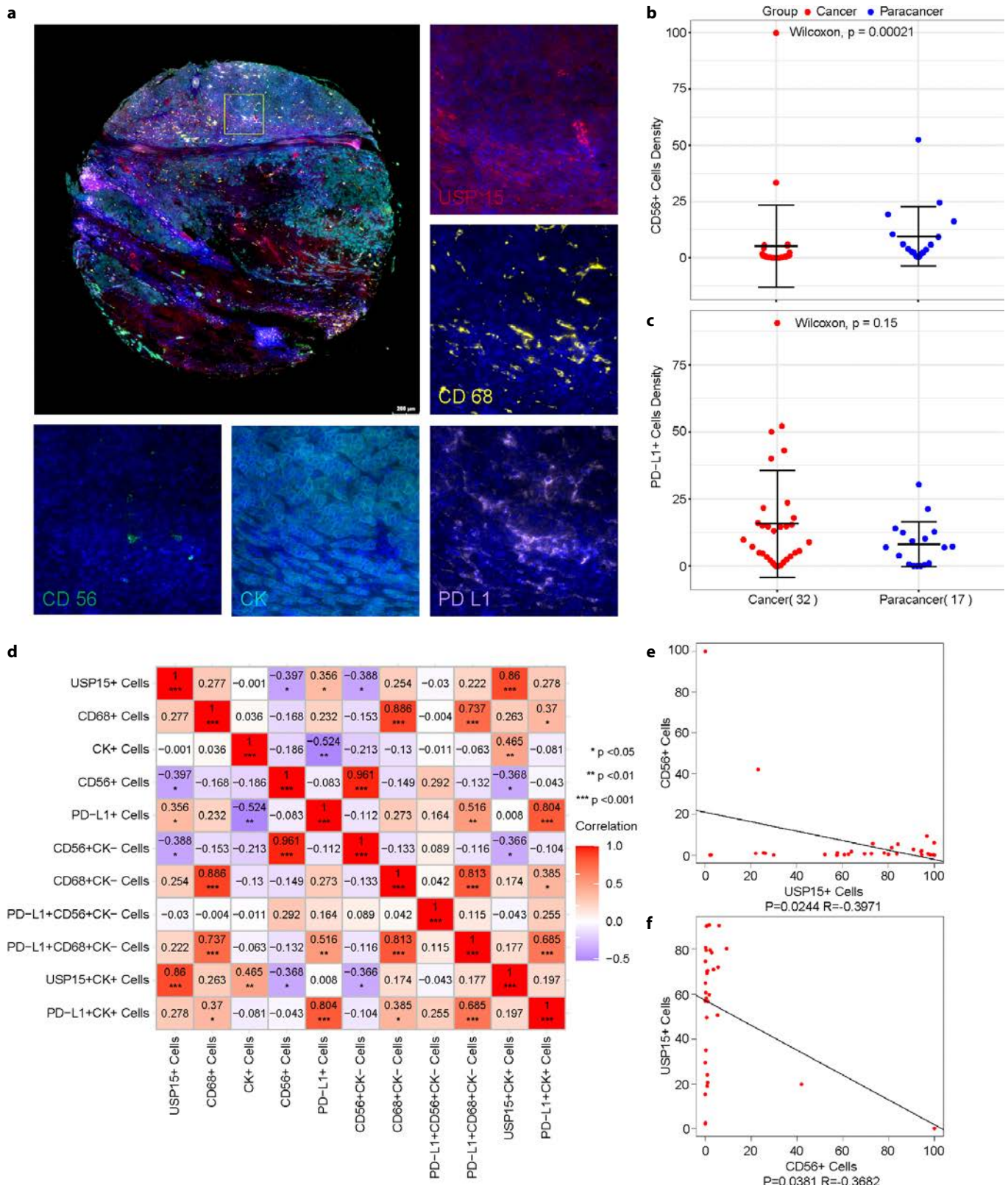


**Figure 3.** (a) Representative immunohistochemical staining of peritumoral regions in HCC tissue microarray. Markers: USP15 (red), CD68 (macrophages, yellow), CD56 (NK cells, green), CK (tumor epithelial cells, cyan), PD-L1 (purple). Scale bar =200 μm. (b, c) Differential analysis of the percentage of NK cells and PD-L1<sup>+</sup> cells between HCC tissues and adjacent normal tissues respectively. (d) Heat map of correlation analysis between indicators in panel 1. (e) Correlation analysis of USP15<sup>+</sup> cells and NK cells expression,  $p < 0.05$ ,  $R = -0.397$ . (f) Correlation analysis of NK cells and USP15<sup>+</sup> Tumor epithelial cells expression,  $p < 0.05$ ,  $R = -0.368$ .

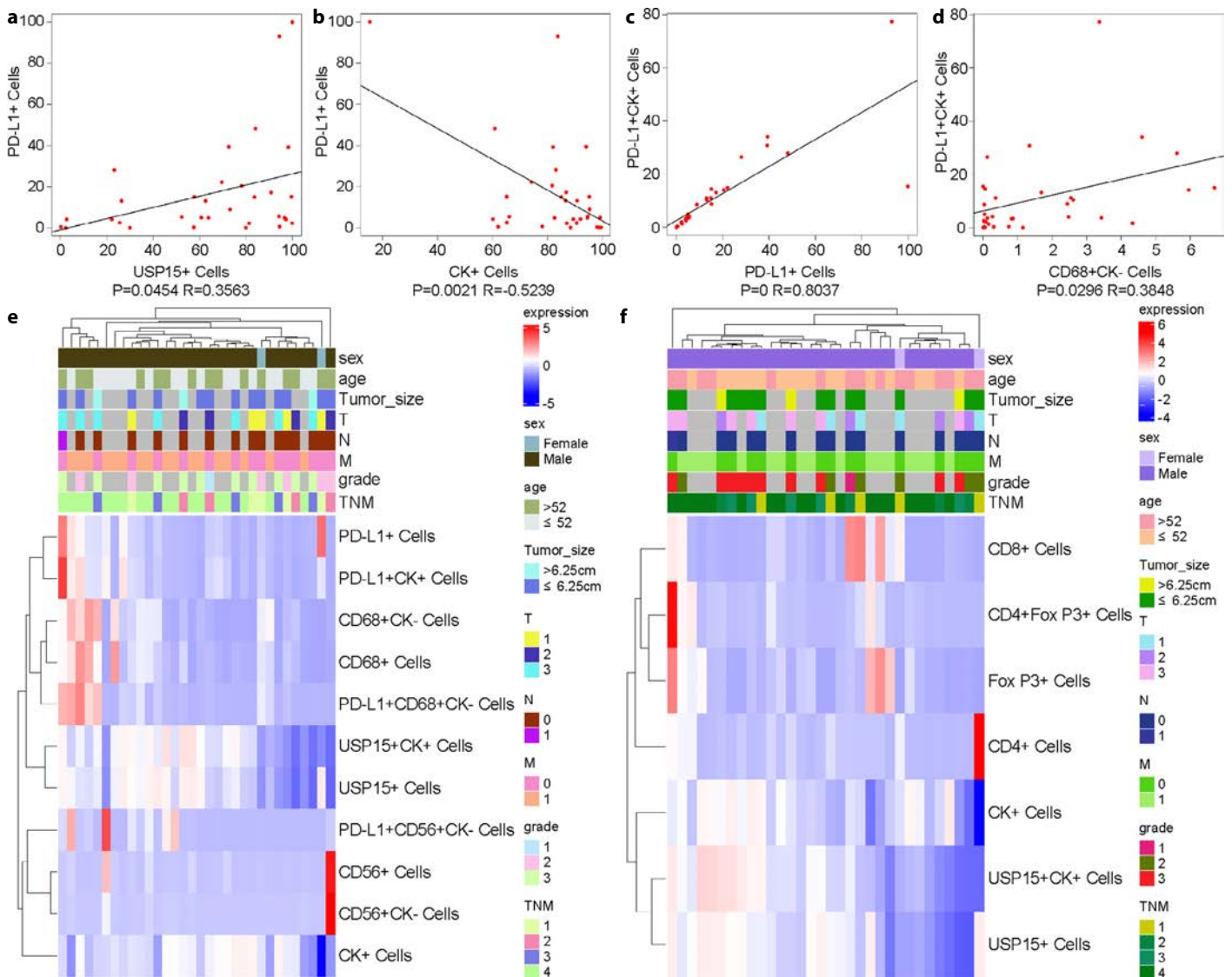


**Figure 4.** (a) Correlation analysis of USP15<sup>+</sup> cells and PD-L1<sup>+</sup> cells expression,  $p<0.05$ ,  $R=0.356$ . (b) Correlation analysis of tumor cells and PD-L1<sup>+</sup> cells expression,  $p<0.005$ ,  $R=-0.524$ . (c) Correlation analysis of PD-L1<sup>+</sup> cells and PD-L1<sup>+</sup> tumor epithelial cells expression,  $p<0.05$ ,  $R=0.804$ . (d) Correlation analysis of PD-L1<sup>+</sup> tumor epithelial cells and macrophages expression,  $p<0.05$ ,  $R=0.385$ . (e, f) Complex Heatmap based on the expression of different cells in different samples and the corresponding clinical information of each sample of two mIHC panels.

PD-L1/PD-1 monotherapy still has unavoidable limitations. It has been reported that the immunotherapeutic effect of PD-1/PD-L1 inhibitors can be enhanced by inhibiting macrophage infiltration in the TME.<sup>[22]</sup> Our findings suggest that combining USP15-targeted inhibition with PD-1/PD-L1 blockade may represent a novel therapeutic strategy for the treatment of hepatocellular carcinoma.

Our findings demonstrate that USP15 functions as a crucial immune regulatory factor in hepatocellular carcinoma, underscoring its potential as a therapeutic target. However, it is necessary to note that this study has several limitations. First, the cohort size is limited and the group distribution is imbalanced. For example, the M0 group contains only one patient, rendering statistical comparisons between M0 and M1 highly unstable and unreliable. Similarly, regarding lymph node stage, all N0 cases exhibited high USP15 expression, while 11 of

15 N1 cases showed high expression ( $p=0.066$ ). This indicates that the observed associations with M and N stages—although biologically suggestive—require validation in larger and more balanced independent cohorts. Second, although TMA technology enables efficient high-throughput analysis, its limited sampling range may fail to fully capture intratumoral heterogeneity. To address this limitation, we conducted paired sampling of “peritumoral liver tissue - primary tumor site” for most HCC cases. For some advanced cases, we further included “distal liver tissue - peritumoral liver tissue - primary tumor site” for three-point sampling. However, this technical compensation still cannot fully overcome the challenges posed by intratumoral heterogeneity. Finally, although the present data support the potential of USP15 as a therapeutic target, the limited sample size, absence of survival analysis, and lack of functional validation

preclude definitive clinical recommendations at this stage. In future studies, we will expand the cohort size, integrate comprehensive survival data, and perform in-depth mechanistic investigations to further elucidate the role of USP15 and robustly validate its potential as a viable therapeutic target in HCC. In summary, this study provides novel evidence supporting the role of USP15 in modulating the immune microenvironment of HCC. However, the aforementioned limitations underscore the need for larger and more diverse cohorts in future investigations for further validation.

## Conclusion

In summary, our study investigated the role and regulatory effects of USP15 within the TME and characterized the tumor microenvironment of primary and metastatic liver tumors under different USP15 expression levels. We elucidated the critical role of USP15 in shaping the TME and driving the progression of HCC. Our findings demonstrate that high USP15 expression in HCC tissues is strongly associated with advanced clinical stages, including M stage and TNM stage, and correlates with reduced infiltration of immune cells, particularly T cells and NK cells. Furthermore, USP15 shows a positive association with PD-L1<sup>+</sup> cells and TAMs, suggesting its dual role in promoting immune evasion and fostering an immunosuppressive TME. These results underscore USP15 as a pivotal regulator of tumor-immune interactions in HCC, highlighting its potential as a therapeutic target.

**Ethics Committee Approval:** All patients gave their consent, and the Shanghai outdo Ethical Committee authorized this study (No: SHYJS-CP-1601006), on January 4, 2016. Informed Consent: Written informed consent was obtained from participants.

**Informed Consent:** All patients gave their consent.

**Conflict of Interest:** The authors declare that they have no competing interests.

**Financial Disclosure:** This project received funding from Jilin Provincial Department of Science and Technology (No. YDZJ202201ZYTS203).

**Use of AI for Writing Assistance:** No AI-assisted technologies were used in the preparation of this manuscript.

**Author Contributions:** Concept: Z-LL; Design: Z-LL; Supervision: Z-LL; Analysis and/or Interpretation: Z-LL; Writing: S-PW; Critical Reviews: X-YZ, H-DC, F-ZJ, NJ, J-XZ.

**Peer-review:** Externally peer-reviewed.

## References

- Ganesan P, Kulik LM. Hepatocellular carcinoma: New developments. *Clin Liver Dis* 2023;27(1):85-102. [\[CrossRef\]](#)
- Bicer F, Kure C, Ozluk AA, El-Rayes BF, Akce M. Advances in immunotherapy for hepatocellular carcinoma (HCC). *Curr Oncol* 2023;30(11):9789-9812. [\[CrossRef\]](#)
- Mittal D, Gubin MM, Schreiber RD, Smyth MJ. New insights into cancer immunoediting and its three component phases—elimination, equilibrium and escape. *Curr Opin Immunol* 2014;27:16-25. [\[CrossRef\]](#)
- Xiao Y, Yu D. Tumor microenvironment as a therapeutic target in cancer. *Pharmacol Ther* 2021;221:107753. [\[CrossRef\]](#)
- Donne R, Lujambio A. The liver cancer immune microenvironment: Therapeutic implications for hepatocellular carcinoma. *Hepatology* 2023;77(5):1773-1796. [\[CrossRef\]](#)
- Li J, Yuan S, Norgard RJ, Yan F, Yamazoe T, Blanco A, Stanger BZ. Tumor cell-intrinsic USP22 suppresses antitumor immunity in pancreatic cancer. *Cancer Immunol Res* 2020;8(3):282-291. [\[CrossRef\]](#)
- Liu WT, Huang KY, Lu MC, Huang HL, Chen CY, Cheng YL, et al. TGF- $\beta$  upregulates the translation of USP15 via the PI3K/AKT pathway to promote p53 stability. *Oncogene* 2017;36(19):2715-2723. [\[CrossRef\]](#)
- Jiang B, Zhou L, Lu J, Wang Y, Liu C, Liang Z, et al. Clinicopathological and prognostic significance of ubiquitin-specific peptidase 15 and its relationship with transforming growth factor- $\beta$  receptors in patients with pancreatic ductal adenocarcinoma. *J Gastroenterol Hepatol* 2021;36(2):507-515. [\[CrossRef\]](#)
- Yao XQ, Li L, Piao LZ, Zhang GJ, Huang XZ, Wang Y, et al. Overexpression of ubiquitin-specific protease 15 (USP15) promotes tumor growth and inhibits apoptosis and correlated with poor disease-free survival in hepatocellular carcinoma. *Technol Cancer Res Treat* 2020;19:1533033820967455. [\[CrossRef\]](#)
- Wang Y, Zhou D, Kong Y, Yang Q, Ding Y, Wang W. USPs in pancreatic ductal adenocarcinoma: A comprehensive bioinformatic analysis of expression, prognostic significance, and immune infiltration. *Biomed Res Int* 2022;2022:6109052. [\[CrossRef\]](#)
- Baird JR, Bell RB, Troesch V, Friedman D, Bambina S, Kramer G, et al. Evaluation of explant responses to STING ligands: Personalized immunosurgical therapy for head and neck squamous cell carcinoma. *Cancer Res* 2018 1;78(21):6308-6319. [\[CrossRef\]](#)
- Zou Q, Jin J, Xiao Y, Zhou X, Hu H, Cheng X, et al, Sun SC. T Cell Intrinsic USP15 deficiency promotes excessive IFN- $\gamma$  production and an immunosuppressive tumor microenvironment in MCA-induced fibrosarcoma. *Cell Rep* 2015;13(11):2470-2479. [\[CrossRef\]](#)
- Xiong W, Gao X, Zhang T, Jiang B, Hu MM, Bu X, et al. USP8 inhibition reshapes an inflamed tumor microenvironment that potentiates the immunotherapy. *Nat Commun.* 2022;13(1):1700. [\[CrossRef\]](#)
- Li J, Yuan S, Norgard RJ, Yan F, Yamazoe T, Blanco A, et al. Tumor cell-intrinsic USP22 suppresses antitumor immunity in pancreatic cancer. *Cancer Immunol Res* 2020;8(3):282-291. [\[CrossRef\]](#)
- Zou Q, Jin J, Hu H, Yamazoe T, Blanco A, Stanger BZ. USP15 stabilizes MDM2 to mediate cancer-cell survival and inhibit antitumor T cell responses. *Nat Immunol* 2014;15(6):562-570. [\[CrossRef\]](#)
- Terrén I, Orrantía A, Vitallé J, Zenarruzabeitia O, Borrego F. NK Cell Metabolism and Tumor Microenvironment. *Front Immunol* 2019;10:2278. [\[CrossRef\]](#)
- Stojanovic A, Correia MP, Cerwenka A. Shaping of NK cell responses by the tumor microenvironment. *Cancer Microenviron* 2013;6(2):135-146. [\[CrossRef\]](#)
- Cai H, Zhang Y, Wang J, Gu J. Defects in macrophage reprogramming in cancer therapy: The negative impact of PD-L1/PD-1. *Front Immunol* 2021;12:690869. [\[CrossRef\]](#)
- Lu Y, Han G, Zhang Y, Zhang L, Li Z, Wang Q, et al. M2 macrophage-secreted exosomes promote metastasis and increase vascular permeability in hepatocellular carcinoma. *Cell Commun Signal* 2023;21(1):299. [\[CrossRef\]](#)

20. Yang Q, Guo N, Zhou Y, Chen J, Wei Q, Han M. The role of tumor-associated macrophages (TAMs) in tumor progression and relevant advance in targeted therapy. *Acta Pharm Sin B* 2020;10(11):2156-2170. [\[CrossRef\]](#)
21. Dai X, Lu L, Deng S, Meng J, Wan C, Huang J, et al. USP7 targeting modulates anti-tumor immune response by reprogramming tumor-associated macrophages in lung cancer. *Theranostics* 2020;10(20):9332-9347. [\[CrossRef\]](#)
22. Pu Y, Ji Q. Tumor-associated macrophages regulate PD-1/PD-L1 immunosuppression. *Front Immunol* 2022;13:874589. [\[CrossRef\]](#)

## ORIGINAL RESEARCH

# The usefulness of a simultaneous immunoassay for hepatitis C virus antigen-antibody using the ELECSYS HCV Duo assay

Keisuke Amano<sup>1,2</sup>, Tomoya Sano<sup>1,2</sup>, Tatsuya Ide<sup>1,2</sup>, Dan Nakano<sup>1</sup>, Shigemune Bekki<sup>1</sup>, Teruko Arinaga-Hino<sup>1,3</sup>, Takumi Kawaguchi<sup>1</sup>

1: Division of Gastroenterology, Department of Medicine, Kurume University School of Medicine, Kurume, Japan

2: Fukuoka Consulting & Support Center for Liver Diseases, Kurume University Hospital, Kurume, Japan

3: School of Medical Technology, Kurume University, Kurume, Japan

## Highlights & Insights

- Scientific Gap:** Despite the goal of eliminating HCV by 2030, many HCV patients remain undiagnosed. The ELECSYS® HCV Duo immunoassay (Duo assay) detects both antibodies and core antigens, but its sensitivity and specificity in real-world practice are unclear.
- Key Finding:** The Duo assay identified 100% of HCV carriers via antibody detection and 78% via core antigen detection, with fewer false negatives in high viral load patients.
- Clinical Impact:** The Duo assay is a rapid, cost-effective screening tool for diagnosing HCV without RNA testing, aiding early diagnosis and treatment.

## ABSTRACT

**Background and Aim:** The World Health Organization has a goal to eliminate the hepatitis C virus (HCV) by 2030. To achieve this, effective screening for HCV is essential. We evaluated the utility of the ELECSYS® HCV Duo immunoassay (Duo assay) for HCV screening.

**Materials and Methods:** This single-center retrospective study included 184 HCV patients from 2014 to 2017. We measured HCV antibody (Duo/Ab) and HCV core antigen (Duo/cAg) using the Duo assay in HCV RNA-positive samples obtained before DAA therapy. We compared Duo/cAg positivity rates according to host and viral factors. We also performed logistic regression analysis and decision tree analysis to identify independent factors and profiles for Duo/cAg false-negative results, respectively.

**Results:** Duo/Ab positivity rates were 100%, and Duo/cAg positivity rates were 78% in all subjects. Duo/cAg positivity rates were 40.0%, 78.6%, and 92.9% at HCV RNA levels  $\leq 4.9$ , 5.0–5.9, and  $\geq 6.0$  log IU/mL, respectively ( $p < 0.0001$ ). There were no significant differences in Duo/cAg positivity rates by gender, age, body mass index, ALT  $> 30$  U/L, and HCV genotype. In multivariate analysis, the HCV RNA level (Unit  $-1.0$  log IU/mL, OR 5.49, CI 3.12–10.56,  $p < 0.0001$ ) was the only independent factor associated with Duo/cAg false-negative results. Decision tree analysis revealed that HCV RNA  $\geq 5.7$  log IU/mL was the profile associated with the lowest false-negative rate (7.4%). In contrast, HCV RNA  $< 4.4$  log IU/mL was the profile associated with the highest false-negative rate (100%).

**Conclusion:** The Duo assay identified approximately 80% of HCV carriers without HCV RNA measurement, regardless of patient background, providing substantial clinical, economic, and time-saving benefits. However, clinicians should be aware of limitations in patients with low HCV RNA levels.

**Keywords:** HCV, HCV antibody, HCV antigen, HCV duo.

**How to cite this article:** Amano K, Sano T, Ide T, Nakano D, Bekki S, Arinaga-Hino T, et al. The usefulness of a simultaneous immunoassay for hepatitis C virus antigen-antibody using the ELECSYS HCV duo assay. *Hepatology Forum* 2026; 7(2):118–124.

**Received:** July 25, 2025; **Revised:** October 24, 2025; **Accepted:** December 06, 2025; **Available Online:** April 14, 2026

**Corresponding author:** Keisuke Amano; Division of Gastroenterology, Department of Medicine, Kurume University School of Medicine, Kurume, Japan;

**E-mail:** amano\_keisuke@kurume-u.ac.jp



This work is licensed under a Creative Commons Attribution-NonCommercial 4.0 International License.

## Introduction

Chronic hepatitis C virus (HCV) infection is a leading cause of liver cirrhosis, liver failure, and hepatocellular carcinoma (HCC).<sup>[1–3]</sup> Direct-acting antiviral agents (DAA) have contributed to high rates of sustained virological response (SVR) in patients with HCV-related chronic liver disease.<sup>[4,5]</sup> However, in Japan, it is estimated that 300,000–600,000 untreated patients with HCV remain, and the eradication of HCV has not yet been achieved.<sup>[6]</sup>

The World Health Organization (WHO) has set a goal of eliminating HCV by 2030 in World.<sup>[7]</sup> An obstacle to achieving this goal is that HCV RNA is not measured in a large number of individuals with positive HCV antibody tests.<sup>[8,9]</sup> Therefore, they have not been diagnosed as HCV carriers and are missing the opportunity to receive treatment. Thus, it is crucial to efficiently identify patients eligible for treatment among those who test positive for HCV antibodies.

The ELECSYS® HCV Duo immunoassay (Duo assay) was developed in 2022. The Duo assay is designed for the detection of HCV carriers through a simultaneous immunoassay for HCV antibodies (Duo/Ab) and HCV core antigens (Duo/cAg) within a single platform. This assay provides rapid results with a processing time of only 27 minutes. Notably, a positive Duo/cAg test result makes it possible for individuals to be diagnosed as HCV carriers on the same day their blood sample is collected.<sup>[10]</sup> Consequently, the Duo assay may reduce the need for additional HCV RNA measurement to identify infected individuals. Furthermore, the rapid identification of HCV-infected individuals is expected to improve medical consultation and increase the number of patients receiving antiviral therapy. However, there are still few reports on the diagnostic sensitivity and specificity of the Duo assay as applied to real-world clinical practice.<sup>[10–12]</sup>

The aim of this study was to evaluate the usefulness of the Duo assay in the diagnosis of HCV carriers. In addition, we also identified independent factors and profiles for Duo/cAg false-negative results.

## Materials and Methods

### Study Design and Ethics

This study is a single-center retrospective study. The study was performed in accordance with the ethical principles described in the Declaration of Helsinki. It was approved by the Clinical Research Ethics Committee of our hospital on November 11, 2024 (approval no. 24152). An opt-out approach was used to obtain informed consent from the patients, and personal information was protected during data collection.

### Patients

The subjects were 184 HCV patients who visited our hospital between January 2014 and December 2017. All patients were infected with HCV genotypes 1 or 2. HCV RNA-positive samples obtained before DAA treatment were used for analysis. According to the results of the Duo assay, all patients were classified into Duo/cAg-positive or false-negative groups. In this study, a “false-negative” result for Duo/cAg was defined as a negative Duo/cAg test in an HCV RNA-positive

patient. We excluded patients who met any of the following criteria: HBV co-infection, HIV co-infection, or other liver diseases.

## Laboratory Assessment

### Measurement of Duo Assay

The Duo assay was measured using electrochemiluminescence immunoassay (ECLIA) for qualitative detection of HCV antibodies and HCV core antigens (ELECSYS® HCV Duo immunoassay; Roche Diagnostics GmbH, Mannheim, Germany). Stored serum samples were processed using the Cobas 8000 e801 machine following the manufacturer's instructions (Roche Diagnostics GmbH). The results were reported as cutoff index (COI) values in three categories: the main result (Duo) and two modules consisting of Duo/Ab and Duo/cAg. The Duo result was automatically calculated from Duo/Ab and Duo/cAg values, with a COI of less than 1.0 indicating a non-reactive result and a COI of 1.0 or greater indicating reactivity. Similarly, for both Duo/Ab and Duo/cAg, COI values below 1.0 indicate non-reactive results, while values of 1.0 or higher indicate reactivity for Duo/Ab and Duo/cAg, respectively.

### Measurement of HCV RNA

HCV RNA was measured using a quantitative real-time polymerase chain reaction (Cobas TaqMan HCV Test, version 3.0; Roche Diagnostics, Basel, Switzerland). The results of the HCV RNA test were based on the clinical data at the time of blood collection.

### Data Collection

Information on gender, age, body mass index (BMI), obesity, and history of cirrhosis or interferon (IFN) therapy or HCC treatment was collected from medical records. We measured the following laboratory tests: aspartate aminotransferase (AST), alanine aminotransferase (ALT), gamma-glutamyl transpeptidase (GGT), albumin, total bilirubin, prothrombin time, creatinine, white blood cell count, hemoglobin, platelet count, fibrosis-4 (FIB-4) index, alpha fetoprotein, and des-γ-carboxy prothrombin.

### Statistical Analysis

Chi-square tests were used to analyze the association between categorical variables, and the Wilcoxon test was used for continuous variables. Factors associated with Duo/cAg false-negative results were statistically evaluated by univariate logistic regression models. Odds ratios and their 95% confidence intervals with corresponding P values are presented. All statistical analyses were performed using JMP® Pro version 16.0 (SAS Institute Inc., Cary, North Carolina, USA). Statistical significance was defined as  $p < 0.05$ , as described previously.<sup>[13,14]</sup>

### Comparison of Duo/cAg Positivity According to Host, Hepatic, and Viral Factors between the Duo/cAg-Positive and False-Negative Groups

We compared the Duo/cAg positivity rate according to host factors, including age, gender, and BMI. We also compared the Duo/cAg positivity rate according to hepatic and viral factors, including ALT >30 U/L, HCV genotype, and HCV RNA levels.

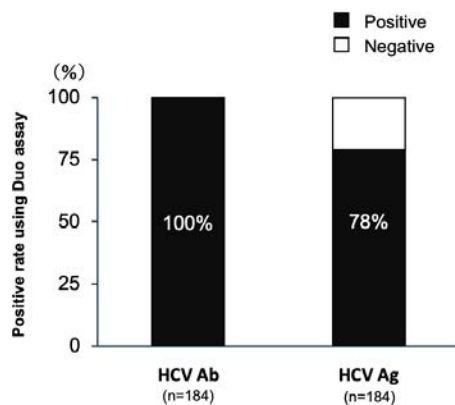


**Figure 1.** Positivity rate of Duo/Ab and Duo/cAg using Duo assay.

### Independent Factors and Profiles of Duo/cAg False-Negative Results

A logistic regression model was used to identify independent variables associated with Duo/cAg false-negative results in multivariate analysis. Explanatory variables were selected based on age, sex, creatinine, and HCV RNA levels in a stepwise manner, minimizing the Bayesian information criterion as previously described.<sup>[15]</sup>

The stepwise selection procedure was chosen because it provides an objective and algorithmic method for selecting the most statistically significant set of variables.

### Decision-Tree Algorithm

A decision-tree algorithm was constructed to reveal the profiles associated with Duo/cAg false-negative results, as previously described.<sup>[15,16]</sup> The initial classification was the most important factor associated with Duo/cAg false-negative results. The patients were classified according to the cutoff values indicated for each variable. The cutoff value was determined by decision tree analysis, which gave the best split of variables.<sup>[15]</sup> The following variables were used in the decision tree analysis: gender, age, BMI, AST, ALT, GGT, albumin, total bilirubin, prothrombin time, white blood cell count, hemoglobin, platelet count, FIB-4 index, alpha fetoprotein, des-gamma-carboxy prothrombin, HCV genotype, history of IFN therapy, history of HCC treatment, and HCV RNA.

## Results

### Usefulness of the Duo Assay to Identify Patients with HCV RNA Positive

Among the 184 HCV RNA-positive samples measured with the Duo assay, Duo/Ab positivity rates were 100% (184/184), and Duo/cAg positivity rates were 78% (143/184) (Fig. 1).

### Comparison of the Patient Characteristics between Duo/cAg-Positive and False-negative Groups

Table 1 shows a comparison of the patient characteristics between the Duo/cAg-positive group (n=143) and the Duo/cAg false-negative

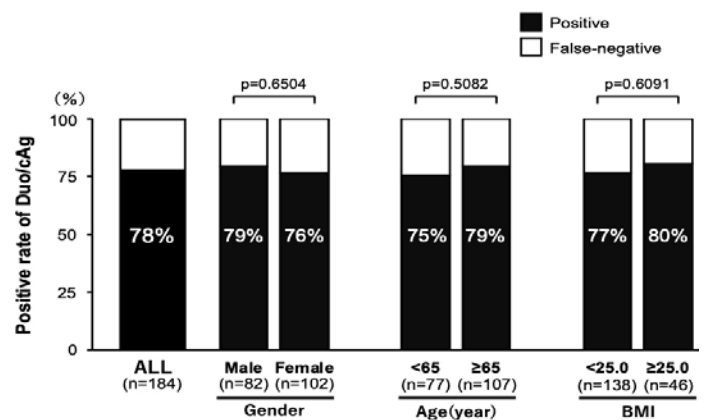


**Figure 2.** Duo/cAg positivity rate by patient background (gender, age, and BMI).

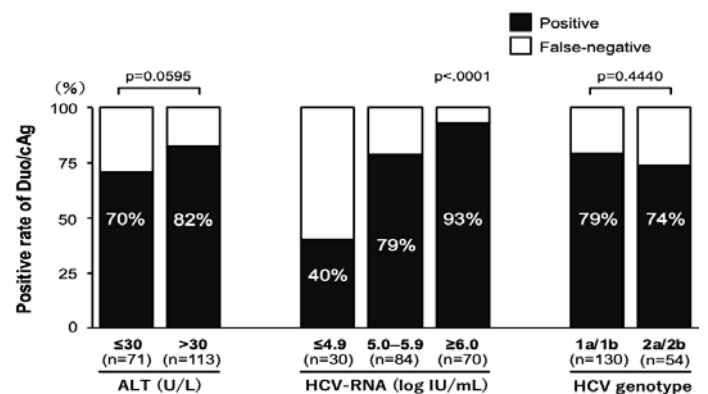


**Figure 3.** Duo/cAg positivity rate by patient background (ALT, HCV RNA, and HCV genotype).

group (n=41) in the Duo assay. No significant difference was observed in gender, age, and BMI between the two groups (Fig. 2).

No significant difference was also observed in ALT levels, albumin levels, bilirubin levels, prothrombin time, and FIB-4 index between the Duo/cAg-positive and false-negative groups (Fig. 3). There was no significant difference in HCV genotype between the Duo/cAg-positive and false-negative groups (Fig. 3). However, Duo/cAg positivity rates were lower according to the low HCV RNA viral load ( $p<0.0001$ ) (Fig. 3).

### Logistic Regression Analysis for Duo/cAg False Negative

There was a significant difference in serum creatinine and HCV RNA levels between the Duo/cAg-positive and false-negative groups in univariate analysis. However, only the HCV RNA level was identified as an independent factor (OR 5.49, CI 3.12–10.56,  $p<0.0001$ ) related to Duo/cAg false-negative results in multivariate analysis (Table 2).

### Decision Tree Analysis for Duo/cAg False Negative

The most impacted factor for Duo/cAg false-negative results was HCV RNA. In patients with HCV RNA  $\geq 5.7$  log IU/mL, 7.4% had false-negative results. On the other hand, 43.4% had false-negative results

**Table 1.** Comparison of host, hepatic, and viral factors between the Duo/cAg positive and false negative groups

	Positive (HCV RNA+, Duo/cAg+) (n=143)		False-negative (HCV RNA+, Duo/cAg-) (n=41)		p
	Median (IQR)	Range (min–max)	Median (IQR)	Range (min–max)	
Gender (female/male)	54.5%/45.5% (78/65)	N/A	58.5%/41.5% (24/17)	N/A	0.6504
Age (years)	67 (57–73)	27–91	65 (57–73)	32–82	0.3387
Proportion of age ≥65 years old (%)	59.4% (85/143)	N/A	53.7% (22/41)	N/A	0.5082
Body mass index (kg/m <sup>2</sup> )	23.0 (21.0–25.4)	16.6–32.9	22.3 (20.3–24.3)	16.8–28.7	0.0903
Prevalence of obesity (BMI ≥25 kg/m <sup>2</sup> )	25.9% (37/143)	N/A	22.0% (9/41)	N/A	0.6091
AST (U/L)	41 (29–59)	9–213	39 (28–71)	19–125	0.8593
ALT (U/L)	36 (26–54)	6–427	30 (21–72)	16–226	0.2984
GGT (U/L)	30 (20–43)	10–323	30 (18–66)	13–230	0.5287
Albumin (g/dL)	4.0 (3.7–4.3)	2.4–4.9	4.0 (3.7–4.2)	3.1–4.7	0.9536
Total bilirubin (mg/dL)	0.8 (0.6–1.0)	0.3–3.8	0.7 (0.6–0.9)	0.2–2.5	0.7658
Prothrombin time (%)	98 (86–108)	34–140	100 (84–110)	52–130	0.9104
Creatinine (mg/dL)	0.67 (0.56–0.79)	0.41–8.34	0.58 (0.47–0.74)	0.36–6.36	0.0067
White blood cell count (/μL)	4450 (3300–5600)	1600–9500	5000 (3800–6000)	1900–11200	0.1856
Hemoglobin (g/dL)	13.3 (12.2–14.4)	8.6–18.2	13.8 (12.7–15.0)	9.7–16.4	0.2001
Platelet count (×10 <sup>4</sup> /μL)	15.3 (10.3–19.6)	2.0–34.8	16.1 (11.6–21.5)	4.6–28.6	0.2427
FIB-4 index	3.06 (1.92–5.44)	0.57–29.44	2.82 (1.71–4.55)	0.63–13.94	0.3444
Alpha fetoprotein (ng/mL)	4.6 (2.8–11.3)	1.0–157.5	4.4 (2.7–7.7)	0.9–43.7	0.3636
Des-gamma-carboxy prothrombin (mAU/mL)	17 (14–22)	4–195	17 (15–23)	6–41	0.6964
HCV RNA (log IU/mL)	5.9 (5.5–6.5)	4.4–7.3	5.1 (4.4–5.6)	3.6–6.9	<0.0001
HCV genotype (1a+1b/2a+2b)	103/40	N/A	27/14	N/A	0.4440
Prevalence of pre-existing cirrhosis	44.1% (63/143)	N/A	34.1% (14/41)	N/A	0.2568
History of IFN therapy (%) (no/yes/unknown)	14.7% (105/21/17)	N/A	7.3% (36/3/2)	N/A	0.1571
History of HCC treatment	16.8% (24/143)	N/A	17.1% (7/41)	N/A	0.9651

Data are expressed as median (interquartile range [IQR]), range, or number. N/A: Not applicable; AST: Aspartate aminotransferase; ALT: Alanine aminotransferase; GGT: Gamma-glutamyl transpeptidase; FIB-4: Fibrosis-4; HCV RNA: Hepatitis C virus ribonucleic acid; IFN: Interferon; HCC: Hepatocellular carcinoma.

in patients with HCV RNA <5.7 log IU/mL. Of these patients, the second impacted factor was also HCV RNA, and 100% had false-negative results in patients with HCV RNA <4.4 log IU/mL (Fig. 4).

## Discussion

The present study demonstrated that the Duo assay can identify 100% of HCV carriers by HCV antibody detection and approximately 80% of HCV carriers by HCV antigen detection without measuring HCV RNA. We also demonstrated that the HCV RNA level was the only independent factor and the most impacted factor influencing Duo/cAg false-negative results in the Duo assay.

In this study, we examined 184 cases of HCV-RNA-positive patients. Of these, HCV genotype 1 is the major genotype and accounts for 70.7% (130/184) of all subjects. Toyoda et al.<sup>[17]</sup> also reported that

**Table 2.** Independent factor for Duo/cAg false negative results

Variable	Unit	OR	95% CI	p
HCV RNA	-1.0 log IU/mL	5.49	3.12–10.56	<0.0001
Creatinine	1.0 mg/dL	0.75	0.37–1.20	0.2567

OR: Odds ratios; CI: Confidence interval; HCV RNA: Hepatitis C virus ribonucleic acid.

72.1% (7,706/10,688) of the cases were genotype 1. Thus, our database appears to have the general characteristics of HCV carriers before DAA treatment in Japan. However, we have to be cautious that this is a single-center, retrospective study on a Japanese cohort with only HCV genotypes 1 and 2. Kanokudom et al.<sup>[11]</sup> reported that the detection rate of HCV antigen was lower in HCV genotype 3a. Accordingly, our results may differ from those of HCV genotype 3/4 and other genotypes.

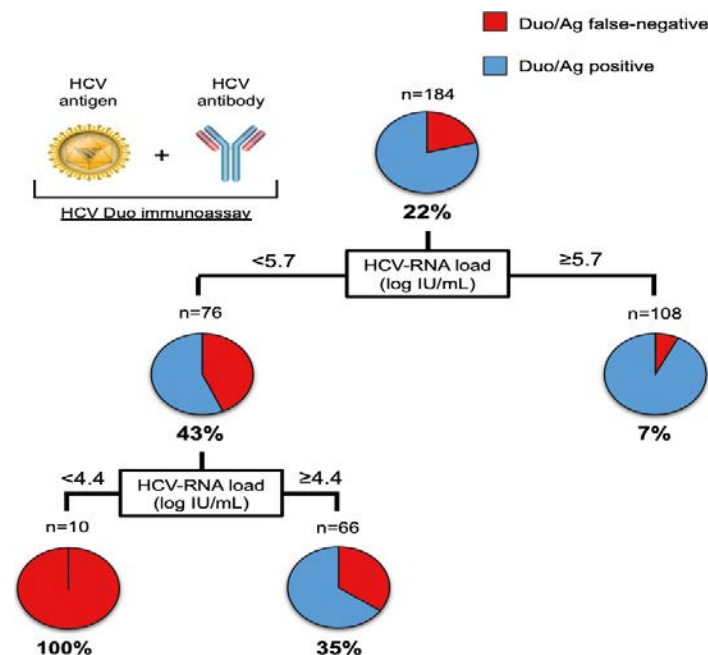


**Figure 4.** The profile of Duo/cAg false negative using decision tree analysis. The patients were classified according to the indicated cut-off values of the variables. The pie graphs indicate the percentage of patients with Duo/cAg positive (white)/patients with Duo/cAg false negative (black) in each group.

We demonstrated that the Duo assay can identify 100% of HCV carriers by HCV antibody detection and approximately 80% of HCV carriers by HCV antigen detection without the need for HCV RNA measurement. HCV antibody detection using the Duo assay has been reported in some studies to identify 100% of HCV carriers.<sup>[11,12]</sup> This demonstrates its viability as a screening method equivalent to conventional approaches. On the other hand, Inoue et al.<sup>[12]</sup> reported that the Duo assay identified only 55% of patients who showed positive results of HCV core antigen. This lower identification rate may be due to the high proportion (36.7%) of cases with HCV RNA  $\leq 4$  log IU/mL. Their study demonstrated a detection rate of 87.5% (48/55) for HCV RNA  $\geq 5.6$  log IU/mL. Thus, our findings are in good agreement with the detection rates of Duo/Ab and Duo/cAg in previous studies.

We also demonstrated that the assay was effective at detecting HCV infection regardless of host factors such as gender, age, BMI, liver enzyme levels, and severity of liver disease. Unfortunately, we did not evaluate the impact of HIV co-infection on the detection rate of HCV antibody and antigen using the Duo assay. Juniastuti et al.<sup>[18]</sup> reported a high rate of seronegative HCV antibody in HIV-positive patients. On the other hand, Ananchuensook et al.<sup>[19]</sup> reported that the HCV Duo immunoassay effectively diagnosed HCV infection regardless of HIV status. These findings suggest that the HCV Duo is useful for the detection of HCV carriers in patients with HIV co-infection.

We identified that the HCV RNA level was the only independent factor influencing Duo/cAg false-negative results. In addition, decision tree analysis revealed that the Duo/cAg false-negative rate for cases with HCV RNA levels  $< 4.4$  log IU/mL was 100%. These findings are consistent with previous studies suggesting that the sensitivity of HCV Ag detection assays is highly dependent on viral load.<sup>[10]</sup> The reason

why higher viral loads result in more positive Ag results is thought to be due to increased production and release of HCV core Ag into the systemic blood circulation. Some studies have reported that Abbott's HCV Ag assay demonstrates a higher positivity rate even in patients with low viral load.<sup>[20,21]</sup> Therefore, further improvements are needed to reduce false negatives in the Duo assay.

HCV-PCR is the current standard for evaluating direct-acting antiviral (DAA) efficacy. However, if post-DAA initiation strategies using core antigen testing are validated,<sup>[22]</sup> the HCV Duo assay may offer significant medical-economic benefits. Simultaneous measurement of Duo/Ab and Duo/cAg incurs the same cost as conventional HCV Ab testing (USD 6.84 per test) and identifies approximately 80% of HCV carriers without requiring HCV RNA testing. Given the high sustained virologic response (SVR) rate among HCV Ab-positive individuals,<sup>[23]</sup> this approach could reduce the cost of HCV RNA measurement (USD 27.61 per test). Moreover, the Duo assay may be especially useful for non-hepatology specialists, who often do not order HCV RNA testing.<sup>[8]</sup> Core antigen testing also shows adequate sensitivity in high-risk populations, such as people living with HIV or those who inject drugs, particularly in resource-limited settings, as recognized by the WHO. In addition to economic advantages, the Duo assay is time-efficient, requiring only 27 minutes and allowing for same-day HCV Ab and Ag testing. This contrasts with RNA testing, which is typically ordered later. Thus, the Duo assay may promote earlier detection and increase referrals to hepatologists, offering an effective and practical tool for identifying HCV-infected individuals across diverse clinical settings.

This study has several limitations. First, it was a retrospective single-center design. Second, the study focused exclusively on a Japanese cohort with genotypes 1 and 2, limiting generalizability.

Third, the use of stored serum samples may have impacted antigen stability and assay performance. HCV Ag degradation may occur, especially in cases with low viral load. Thus, an international prospective multi-center study with multi-genotypic HCV is required to confirm the broader applicability of the Duo assay. However, the strongest point of this study was that we assessed the usefulness in clinical practice and the characteristics of Duo/cAg false-negative results.

## Conclusion

In conclusion, we demonstrated that Duo assay screening can identify approximately 80% of HCV carriers with no HCV RNA measurement. Additionally, the test offers significant medical economic and time-saving benefits by reducing HCV RNA measurement. Thus, the Duo assay may become an important screening test toward the elimination of HCV.

**Ethics Committee Approval:** The study was performed in accordance with the ethical principles described in the Declaration of Helsinki. It was approved by the Kurume University Clinical Research Ethics Committee of our hospital on November 11, 2024 (approval no. 24152).

**Informed Consent:** An opt-out approach was used to obtain informed consent from the patients, and personal information was protected during data collection.

**Conflicts of Interest:** Takumi Kawaguchi has received lecture fees from ASKA Pharmaceutical Co., Ltd., Taisho Pharmaceutical Co., Ltd., Kowa Company, Ltd., AbbVie GK., Eisai Co., Ltd., EA Pharma Co., Ltd., Nippon Boehringer Ingelheim Co., Ltd., Sumitomo Pharma Co., Ltd., Novo Nordisk Pharma Ltd., Otsuka Pharmaceutical Co., Ltd., Janssen Pharmaceutical K.K. Keisuke Amano, Tomoya Sano, Tatsuya Ide, Dan Nakano, Shigemune Bekki, and Teruko Arinaga-Hino have no conflicts of interest to declare.

**Financial Disclosure:** The authors declared that this study has received no financial support.

**Use of AI for Writing Assistance:** No artificial intelligence (AI)-assisted technologies (such as Large Language Models [LLMs], chatbots, or image creators) were used in the production of this manuscript.

**Author Contributions:** Concept: KA, DN; Design: KA, TI; Supervision: KA, SB; Funding: KA, SB, TK; Materials: KA, TS, TK; Data Collection and/or Processing: KA, TS, DN, TK; Analysis and/or Interpretation: KA, TS; Literature Search: KA, TI, TAH; Writing: KA, TI, TAH; Critical Reviews: KA, DN, TAH.

**Peer-review:** Externally peer-reviewed.






## References

1. El-Serag HB. Epidemiology of viral hepatitis and hepatocellular carcinoma. *Gastroenterology* 2012;142(6):1264-1273.e1. [\[CrossRef\]](#)
2. Hoshida Y, Fuchs BC, Bardeesy N, Baumert TF, Chung RT. Pathogenesis and prevention of hepatitis C virus-induced hepatocellular carcinoma. *J Hepatol* 2014;61(Suppl 1):S79-S90. [\[CrossRef\]](#)
3. Chuaypen N, Chittmitrapap S, Avihingsanon A, Siripongsakun S, Wongpiyabovorn J, Tanpowpong N, et al. Liver fibrosis improvement assessed by magnetic resonance elastography and Mac-2-binding protein glycosylation isomer in patients with hepatitis C virus infection receiving direct-acting antivirals. *Hepatol Res* 2021;51(5):528-537. [\[CrossRef\]](#)
4. Chayama K, Suzuki F, Karino Y, Kawakami Y, Sato K, Atarashi T, et al. Efficacy and safety of glecaprevir/pibrentasvir in Japanese patients with chronic genotype 1 hepatitis C virus infection with and without cirrhosis. *J Gastroenterol* 2018;53(4):557-565. [\[CrossRef\]](#)
5. Feld JJ, Jacobson IM, Hezode C, Asselah T, Ruane PJ, Gruener N, et al. Sofosbuvir and Velpatasvir for HCV Genotype 1, 2, 4, 5, and 6 Infection. *N Engl J Med* 2015;373(27):2599-2607. [\[CrossRef\]](#)
6. Tanaka J, Kurisu A, Ohara M, Ouoba S, Ohisa M, Sugiyama A, et al. Burden of chronic hepatitis B and C infections in 2015 and future trends in Japan: A simulation study. *Lancet Reg Health West Pac* 2022;22:100428. [\[CrossRef\]](#)
7. Razavi H, Sanchez Gonzalez Y, Yuen C, Cornberg M. Global timing of hepatitis C virus elimination in high-income countries. *Liver Int* 2020;40(3):522-529. [\[CrossRef\]](#)
8. McGibbon E, Bornschlegel K, Balter S. Half a diagnosis: gap in confirming infection among hepatitis C antibody-positive patients. *Am J Med* 2013;126(8):718-722. [\[CrossRef\]](#)
9. Spradling PR, Tong X, Rupp LB, Moorman AC, Lu M, Teshale EH, et al. Trends in HCV RNA testing among HCV antibody-positive persons in care, 2003-2010. *Clin Infect Dis* 2014;59(7):976-981. [\[CrossRef\]](#)
10. Majchrzak M, Bronner K, Laperche S, Riester E, Bakker E, Bollhagen R, et al. Multicenter performance evaluation of the Elecsys HCV Duo immunoassay. *J Clin Virol* 2022;156:105293. [\[CrossRef\]](#)
11. Kanokudom S, Poovorawan K, Nilyanimit P, Suntronwong N, Aemjinda R, Honsawek S. Comparison of anti-HCV combined with HCVcAg (Elecsys HCV Duo immunoassay) and anti-HCV rapid test followed by HCV RNA analysis using qRT-PCR to identify active infection for treatment. *PLoS One* 2024;19(11):e0313771. [\[CrossRef\]](#)
12. Inoue T, Setoyama H, Watanabe T, Suzuki T, Nagaoka K, Iio E, et al. Innovative hepatitis C screening: Clinical utility of the HCV antigen-antibody assay in Japan. *Jpn J Infect Dis* 2025;78(6):192-198. [\[CrossRef\]](#)
13. Fukunaga S, Mukasa M, Nakane T, Nakano D, Tsutsumi T, Chou T, et al. Impact of non-obese metabolic dysfunction-associated fatty liver disease on risk factors for the recurrence of esophageal squamous cell carcinoma treated with endoscopic submucosal dissection: A multicenter study. *Hepatol Res* 2024;54(2):201-212. [\[CrossRef\]](#)
14. Nakane T, Fukunaga S, Nakano D, Tsutsumi T, Tanaka H, Chou T, et al. Impact of metabolic dysfunction-associated fatty liver disease on the incidence of Helicobacter pylori-negative gastric cancer. *Hepatol Res* 2024;54(6):540-550. [\[CrossRef\]](#)
15. Nakano M, Kawaguchi M, Kawaguchi T, Yoshiji H. Profiles associated with significant hepatic fibrosis consisting of alanine aminotransferase >30 U/L, exercise habits, and metabolic dysfunction-associated steatotic liver disease. *Hepatol Res* 2024;54(7):655-666. [\[CrossRef\]](#)
16. Sano T, Amano K, Ide T, Isoda H, Honma Y, Morita Y, et al. Metabolic management after sustained virologic response in elderly patients with hepatitis C virus: A multicenter study. *Hepatol Res* 2024;54(4):326-335. [\[CrossRef\]](#)
17. Toyoda H, Atsukawa M, Uojima H, Nozaki A, Tamai H, Takaguchi K, et al. Trends and efficacy of interferon-free anti-hepatitis C virus therapy in the region of high prevalence of elderly patients, cirrhosis, and hepatocellular carcinoma: A real-World, Nationwide, multicenter study of 10 688 patients in Japan. *Open Forum Infect Dis* 2019;6(5):ofz1185. [\[CrossRef\]](#)

18. Juniastuti, Utsumi T, Nasronudin, Alimsardjono L, Amin M, Adianti M, et al. High rate of seronegative HCV infection in HIV-positive patients. *Biomed Rep* 2014;2(1):79-84. [\[CrossRef\]](#)
19. Ananchuensook P, Wongpiyabovorn J, Avihingsanon A, Tangkijvanich P. Performance of elecsys((R)) HCV duo immunoassay for diagnosis and assessment of treatment response in HCV patients with or without HIV infection. *Diagnostics (Basel)* 2024;14(19):2179. [\[CrossRef\]](#)
20. Flores GL, Mota JC, da Silva Andrade LT, Lopes RS, Bastos FI, Villar LM. Performance of HCV antigen testing for the diagnosis and monitoring of antiviral treatment: A systematic review and meta-analysis. *Biomed Res Int* 2022;2022:7348755. [\[CrossRef\]](#)
21. Prostko J, Rothman R, Hsieh YH, Pearce S, Kilbane M, McAuley K, et al. Performance evaluation of the Abbott alinity hepatitis C antigen next assay in a US urban emergency department population. *J Clin Virol* 2024;175:105743. [\[CrossRef\]](#)
22. van Tilborg M, Al Marzooqi SH, Wong WWL, Maan R, Vermehren J, Maasoumy B, et al. HCV core antigen as an alternative to HCV RNA testing in the era of direct-acting antivirals: retrospective screening and diagnostic cohort studies. *Lancet Gastroenterol Hepatol* 2018;3(12):856-864. [\[CrossRef\]](#)
23. Enomoto H, Akuta N, Hikita H, Suda G, Inoue J, Tamaki N, et al. Etiological changes of liver cirrhosis and hepatocellular carcinoma-complicated liver cirrhosis in Japan: Updated nationwide survey from 2018 to 2021. *Hepatol Res* 2024;54(8):763-772. [\[CrossRef\]](#)

## ORIGINAL RESEARCH

# Plasma *PDGFRβ* and *PSD4* methylation levels for non-invasive staging of liver fibrosis

 Burge Ulukan<sup>1†</sup>,  Hong Yang<sup>2</sup>,  Hande Uludag<sup>1</sup>,  Cheng Zhang<sup>2</sup>,  Ali Mutlu<sup>3</sup>,  Murat Dayangac<sup>4</sup>,  Murat Akyildiz<sup>1</sup>,  Buket Yigit<sup>1</sup>,  Shaghayegh Soleimani<sup>1</sup>,  Hale Kirimlioglu<sup>5</sup>,  Burcu Saka<sup>6</sup>,  Cigdem Ataizi Celikel<sup>7</sup>,  Fatih Eren<sup>8–10</sup>,  Adil Mardinoglu<sup>2,11</sup>,  Yusuf Yilmaz<sup>9</sup>,  Mujdat Zeybel<sup>1</sup>

1: Department of Gastroenterology and Hepatology, School of Medicine, Koc University, Istanbul, Turkiye

2: Science for Life Laboratory, KTH- Royal Institute of Technology, Stockholm, Sweden

3: School of Medicine, Koc University, Istanbul, Turkiye

4: Department of General Surgery, Faculty of Medicine, Medipol University, Istanbul, Turkiye

5: Department of Pathology, School of Medicine, Acibadem Mehmet Ali Aydinlar University, Istanbul, Turkiye

6: Department of Pathology, School of Medicine, Koc University, Istanbul, Turkiye

7: Department of Medical Pathology, School of Medicine, Marmara University, Istanbul, Turkiye

8: Institute of Gastroenterology, Marmara University, Istanbul, Turkiye

9: Department of Gastroenterology and Hepatology, School of Medicine, Recep Tayyip Erdogan University, Rize, Turkiye

10: Liver Research Unit, Institute of Gastroenterology, Marmara University, Istanbul, Turkiye

11: Centre for Host-Microbiome Interactions, Faculty of Dentistry, Oral & Craniofacial Sciences, King's College London, London, UK

## Highlights & Insights

- **Scientific Gap:** Liver biopsy remains an imperfect gold standard for fibrosis assessment due to sampling errors and inter-observer variability. Although non-invasive methods have improved evaluation, they cannot fully replace biopsy; accurate, timely fibrosis detection in MASLD remains needed.
- **Key Finding:** Machine learning using cell-free epigenetic markers and clinical data identified significant differences in plasma *PDGFRβ* and *PSD4* methylation by MASLD status and fibrosis stage
- **Clinical Impact:** These methylation signatures may offer a promising non-invasive approach for assessing fibrosis in MASLD.

## ABSTRACT

**Background and Aim:** While liver biopsy remains the reference standard for assessing hepatic fibrosis, the major prognostic factor in metabolic dysfunction-associated steatotic liver disease (MASLD), its inherent limitations have driven the search for innovative non-invasive diagnostic tests. In this study, we sought to evaluate the diagnostic accuracy of plasma *PDGFRβ* and *PSD4* methylation levels, integrated within machine learning algorithms, for non-invasive staging of hepatic fibrosis in patients with MASLD, and to compare its performance against established non-invasive biomarkers.

**Materials and Methods:** Patients with biopsy-proven MASLD and healthy controls were recruited from the three institutions. Quantitative methylation of circulating cell-free DNA was assessed using bisulfite modification and pyrosequencing. The resulting data were used to develop linear discriminant analysis, random forest, and support vector machine algorithms to identify patients at different stages of fibrosis.

**Results:** The study included 234 patients with histologically confirmed MASLD and 43 healthy controls. Each dataset was validated using an independent cohort. Advanced fibrosis was associated with elevated plasma *PDGFRβ* and *PSD4* methylation levels in both the discovery and validation cohorts. The integration of plasma DNA methylation markers with clinical parameters demonstrated performance comparable to that of existing noninvasive biomarkers for detecting both significant and advanced fibrosis, achieving area under the curve scores exceeding 0.75 across all models.

**Conclusion:** Supervised machine learning algorithms incorporating plasma *PDGFRβ* and *PSD4* DNA methylation levels show promise as a non-invasive approach for assessing hepatic fibrosis in MASLD.

**Keywords:** Cell-free DNA, DNA methylation, liver fibrosis, machine learning algorithms, MASLD, predictive models.

<sup>†</sup>Current Address: Department of Biochemistry and Molecular Biology, Hollings Cancer Center, Medical University of South Carolina, Charleston, USA

**How to cite this article:** Ulukan B, Yang H, Uludag H, Zhang C, Mutlu A, Dayangac M, et al. Plasma *PDGFRβ* and *PSD4* methylation levels for non-invasive staging of liver fibrosis. *Hepatology Forum* 2026; 7(2):125–132.

**Received:** September 25, 2025; **Revised:** November 21, 2025; **Accepted:** December 30, 2025; **Available Online:** May 11, 2026

**Corresponding author:** Mujdat Zeybel; Department of Gastroenterology and Hepatology, School of Medicine, Koc University, Istanbul, Turkiye; **E-mail:** mzeybel@ku.edu.tr



This work is licensed under a Creative Commons Attribution-NonCommercial 4.0 International License.

## Introduction

Metabolic dysfunction-associated steatotic liver disease (MASLD), is a complex and prevalent clinical condition, affecting over 30% of the global population.<sup>[1]</sup> It is closely associated with obesity, type 2 diabetes, dyslipidemia and metabolic syndrome, which collectively contribute to hepatic injury and increase the risk of severe hepatic complications, including advanced fibrosis, cirrhosis and hepatocellular carcinoma (HCC).<sup>[2,3]</sup> Notably, MASLD has emerged as the leading cause of chronic liver disease worldwide and is a significant contributor to liver-related morbidity and mortality.

Until recently, no pharmacological treatment had received regulatory approval for MASLD. However, the U.S. Food and Drug Administration (FDA) has recently granted accelerated approval to resmetirom for the treatment of Metabolic dysfunction-associated steatohepatitis (MASH) in patients with moderate-to-advanced liver fibrosis (stages F2 and F3). Notably, resmetirom, an oral thyroid hormone receptor- $\beta$ -agonist, has demonstrated efficacy in reducing hepatic fibrosis and improving key histopathological features of MASH, including hepatic fat content and inflammation.<sup>[4]</sup>

Fibrosis represents a critical prognostic determinant in chronic liver diseases of various etiologies. The early detection and accurate staging of hepatic fibrosis are essential to prevent the progression to more advanced stages, such as decompensated cirrhosis.<sup>[5]</sup> While liver biopsy remains the reference standard for fibrosis assessment, its invasive nature, susceptibility to sampling errors, and inter-observer variability highlight the need for alternative diagnostic approaches.<sup>[3,6–8]</sup> Non-invasive techniques (NIT), including serum biomarkers, routine laboratory tests, scoring systems (e.g., FIB-4 index, the NAFLD fibrosis score), and imaging-based methods such as vibration-controlled Transient Elastography (VCTE; FibroScan®, Echosens, Paris, France), have emerged as valuable and effective tools for excluding advanced fibrosis. Among these, VCTE is particularly effective for assessing liver stiffness and staging fibrosis in patients with MASLD. Nevertheless, limitations such as higher failure rates in obese individuals and practical challenges related to its application and stability restrict its broader feasibility.<sup>[9]</sup> Despite their utility, NITs cannot fully replace liver biopsy in clinical practice.<sup>[9,10]</sup>

The mechanisms driving the development and progression of MASLD are intricate and remain incompletely understood. Multiple factors, including dietary habits, lifestyle, genetic predisposition, and epigenetic modifications, have been implicated in the pathophysiology of MASLD.<sup>[11,12]</sup> Among these, DNA methylation, a key epigenetic modification, predominantly occurs at cytosine-guanine dinucleotides, known as CpG sites, and is closely linked to alterations in gene expression. DNA methylation is mediated by DNA methyltransferases (DNMTs), which catalyze the addition of a methyl group to the fifth carbon of the cytosine ring, forming 5-methylcytosine. It plays a significant role in the pathogenesis of metabolic disorders including obesity, diabetes, and MASLD.<sup>[13]</sup> Extensive research has demonstrated the association between DNA methylation patterns and liver diseases.<sup>[3,14–17]</sup> For example, Gerhard

et al.<sup>[14]</sup> identified the correlation between DNA methylation levels in patients with MASLD and key signaling pathways. Similarly, Xu et al.<sup>[16]</sup> identified ten methylation markers for diagnosing HCC. Furthermore, our previous studies revealed significantly higher DNA methylation levels within the PPAR $\gamma$  and PPAR $\alpha$  promoters, two genes with anti-fibrogenic effects, in patients with severe MASLD.<sup>[17,18]</sup>

Predictive models are widely employed in the diagnosis and prognosis of liver diseases. For instance, Batista et al.<sup>[19]</sup> applied Linear Discriminant Analysis (LDA) to develop a model for predicting fibrosis stages. Similarly, recent research has highlighted the effectiveness of the support vector machine (SVM) model in predicting fibrosis risk based on the patients' radiomics data.<sup>[20]</sup> Building on the significance of predictive modeling, we evaluated whether methylation levels of circulating cell-free plasma DNA at specific CpG sites could serve as biomarkers to stratify fibrosis stages in MASLD. Two genes, *PDGFR $\beta$*  and Pleckstrin and Sec7 Domain Containing 4 (*PSD4*), were selected due to their potential association with liver disease or fibrosis biology.<sup>[16,21]</sup> Subsequently, three predictive models were developed and compared to identify the most effective approach for fibrosis stage stratification. These findings are anticipated to contribute to the development of novel NITs for liver fibrosis, offering valuable insights for future diagnostic advancements.

## Material and Methods

### Study Cohorts

The study was conducted on MASLD patients (Discovery Cohort n=115, Validation Cohort n=119) and healthy individuals (Discovery Cohort n=21, Validation Cohort n=22). Blood samples and clinical data were collected after obtaining informed consent from participants in compliance with ethical standards and approved by Koc University Research Ethics Committees [approval number: 2015.053. IRB1.014 (30.03.2015), 2016.024.IRB2.005 (15.02.2016), 2017.139. IRB2.048 (10.09.2017), 2022.246.IRB2.040 (30.07.2022), 09.2018.086 (24.09.2018)]. The study adhered to the ethical principles outlined in the Declaration of Helsinki. The diagnosis of MASLD was established based on the guidelines of American Association for the Study of Liver Diseases.<sup>[22]</sup> The fibrosis severity in the study participants was assessed using histopathological evaluation.

### DNA Methylation and Pyrosequencing Analysis

200  $\mu$ L of plasma was used for DNA extraction with the QIAamp DNA Blood Mini Kit (Qiagen, Hilden, Germany). The DNA was then treated with bisulfite using the EZ DNA Methylation Gold kit (Zymo Research, Irvine, CA, US) according to the manufacturer's instructions. The bisulfite-modified DNA was amplified using custom-designed primers. The primers were designed using PyroMark Assay Design Software 2.0, and their sequences are provided in Supplementary Table 1. Amplification was performed using the PyroMark-PCR kit (Qiagen) according to conditions in Supplementary Table 2. After thermal cycling, all samples were loaded onto a 1.5% agarose gel and run at 100 volts for 30 minutes. Samples were processed for the

**Table 1.** Demographic and clinical characteristics of patients

	Discovery cohort (n=136)		Validation cohort (n=141)	
	Healthy (n=21)	MASLD (n=115)	Healthy (n=22)	MASLD (n=119)
Male, n (%)	11 (52.3)	69 (60.0)	7 (31.8)	57 (47.9)
Female, n (%)	10 (47.6)	46 (40.0)	15 (68.2)	62 (52.1)
Age (years)	37 (24, 42)	55 (47, 61)	35 (25, 40)	53 (46, 59)
Diabetes, n (%)	0	69 (60.0)	0	85 (71.4)
BMI (kg/m <sup>2</sup> )	23.9±2.1	29.5 (26.7, 34.2)****	23.86±2.4	33.3 (29.7, 36.6)
Albumin (g/dL)	4.82±0.1**	4.5 (4, 4.8)	4.65±0.1	4.4 (4.1, 4.7)
ALT (IU/L)	22.0±10.0	40 (25.5, 69.5)*	19.93±7.3	49 (31.0, 98.0)
AST (IU/L)	21.68±7.6	32.7 (25.0, 47.0)**	19.10±5.3	41 (29.0, 62.0)
Platelet (x10 <sup>9</sup> ),	258.5±56.4	213.5 (133.0, 285.0)	240.0±46.4	208.0 (148.0, 248.0)
FIB-4 Index	0.6±0.2	1.2 (0.7, 3.2)*	0.6±0.2	1.4 (1.0, 2.3)
Fibrosis stage, n (%)				
0	–	16 (13.91)	–	0 (0.00)
1	–	23 (20.00)	–	25 (21.00)
2	–	16 (13.91)	–	35 (29.41)
3	–	27 (23.48)	–	30 (25.21)
4	–	33 (28.70)	–	29 (24.37)
NAS score	–	3.0 (2.0, 4.0)****	–	6.0 (5.0, 7.0)

Categorical variables are shown as frequencies (percentages). Normally distributed data are presented as “mean±standard deviation” and non-normally distributed data are presented as “median (interquartile range)”. Comparisons between cohorts of each subgroup were made using the Student’s t-test for continuous and Fisher’s exact test for categorical variables. Statistically significant variables are annotated on the discovery cohort and p-values are given as p<0.05 (\*), 0.01 (\*\*), 0.0001 (\*\*\*\*). ALT: Alanine aminotransferase; AST: Aspartate aminotransferase; BMI: Body mass index; MASLD: Metabolic dysfunction-associated steatotic liver disease; NAS: NAFLD Activity score.

pyrosequencing experiment only after their band intensities shown in Supplementary Figure 1 had been checked. Sample preparation and pyrosequencing were subsequently carried out on the PyroMark Q96 ID instrument (Qiagen). Unmethylated and methylated EpiTect DNA controls (Qiagen) and negative PCR templates were used for each experiment. The average methylation percentages were analyzed using PyroMark software (version 2.5.8; Supplementary Fig. 2–6).

### Predictive Models for Staging Fibrosis and Statistical Analysis

The discovery dataset was used to develop three binary classification models aimed at distinguishing between different stages of fibrosis. The first model was designed to differentiate patients with significant fibrosis ( $F \geq 2$ ) from healthy subjects and those with mild or no fibrosis ( $F \leq 1$ ). The second model focused on identifying patients with advanced fibrosis ( $F \geq 3$ ), while the third model aimed to differentiate patients with cirrhosis ( $F=4$ ). To construct these models, three machine-learning algorithms were employed. Linear Discriminant Analysis was implemented using the LDA () function from the MASS package (version 7.3-60.0.1). The Random Forest algorithm was implemented using the random Forest () function in the randomForest R package (version 4.7-1.1). Finally, the SVM algorithm was implemented using the SVM () function from the

e1071 package (version 1.7-14). These algorithms were selected to assess their accuracy in classifying fibrosis stages using the provided data. Initially, the discovery dataset, consisting of 85 patients with MASLD and 21 healthy controls, was divided into a training set (70%) and a testing set (30%) using the create Data Partition () function from the caret R package (v 6.0-94). Hyperparameter optimization was performed through 5-fold cross-validation on the training set to maximize the area under the receiver operating characteristic (AUC ROC) curve. Once the models were trained and stabilized, the predict () function in caret was employed to estimate the class probabilities for the samples in the test set. The trained models were then independently validated on an external dataset comprising 103 patients with MASLD and 22 healthy controls. Samples with missing feature data were excluded from the model training and prediction procedures. The pROC R package (v 1.18.5) was used to visualize the ROC curve. Performance metrics, including sensitivity, specificity, positive predictive value (PPV), negative predictive value (NPV), precision, recall, and F1 scores, were calculated and presented in Supplementary Tables 3 and 4.

All statistical analyses were performed using GraphPad Prism version 9.0 (GraphPad Software, San Diego, CA, USA). For comparisons between cohorts, descriptive statistics were used. The Shapiro-Wilk test was used to check the normality of continuous

variables. Normally distributed variables were analyzed using the Student's t-test and presented as "mean±standard deviation" whereas non-normally distributed variables were analyzed using the Mann-Whitney U test and presented as median (interquartile range). Categorical variables were analyzed with Fisher's exact test and presented as frequencies (percentages). Two-tailed p-values <0.05 were considered statistically significant.

## Results

The study cohort included 43 healthy subjects and 234 patients diagnosed with MASLD. The histological assessments and Fibroscan evaluations revealed that 115 patients exhibited mild fibrosis (stages F0-F2), whereas 119 had advanced fibrosis (stages F3-F4). The general characteristics of study participants are summarized in Table 1.

Higher plasma *PDGFRβ* and *PSD4* DNA methylation are associated with advanced hepatic fibrosis.

We investigated DNA methylation profiles at specific CpG sites within *PSD4*, a locus recently implicated in HCC, and *PDGFRβ*, a receptor for *PDGF* strongly expressed in hepatic stellate cells and activated myofibroblasts.<sup>[16,21]</sup> Cell-free DNA was extracted from blood samples, and pyrosequencing assays were optimized for targeted CpG sites (Supplementary Table 1). Plasma DNA methylation levels were quantified at five CpG loci within the *PDGFRβ* promoter and three CpG loci within the *PSD4* promoter (Fig. 1, 2). The discovery cohort consisted of patients recruited from two centers. In this study, all CpG sites within *PDGFRβ* exhibited higher DNA methylation levels in patients with MASLD than in healthy controls (Fig. 1a-e). Notably, methylation levels at *PDGFRβ* CpGs 5 and 6 were significantly higher in patients with MASLD and advanced fibrosis (F3-F4) compared with those with mild fibrosis (F0-F2) and healthy controls (Fig. 1a, b). Other CpG sites (CpG 7–9) showed higher methylation levels in MASLD groups than in healthy controls (Fig. 1c–e). These findings were validated in an independent patient cohort recruited from the third center (Fig. 2). The elevated methylation levels at *PDGFRβ* CpG sites 5 and 6 in F3-4 MASLD remained significant but were less pronounced in the validation cohort (Fig. 2a, b).

For the *PSD4* promoter, plasma DNA methylation levels at all targeted CpG loci were considerably higher in patients with MASLD than in healthy controls in both the discovery and validation cohorts (p<0.001) (Fig. 1f-h, Fig. 2f-h). Remarkably, patients with advanced fibrosis exhibited higher methylation levels than those with mild fibrosis in both cohorts.

## Machine Learning Algorithms for Accurate Staging of Liver Fibrosis

To identify fibrosis stages, we developed predictive models integrating plasma DNA methylation data and clinical parameters. Four diagnostic approaches were assessed across four distinct datasets: the FIB-4 index, clinical data alone, DNA methylation levels alone, and a combination of clinical data and DNA methylation levels. Patients were stratified into four fibrosis categories for comparison:

mild/no fibrosis (F0-1), significant fibrosis (≥F2), advanced fibrosis (≥F3), and cirrhosis (F4). To benchmark the models' performance, we conducted AUC analyses using three supervised machine learning approaches: (i) *lda()*, (ii) *randomForest()*, (iii) *svm()*.

Among the three supervised machine learning algorithms tested, SVM achieved the best diagnostic performance for detecting significant fibrosis, advanced fibrosis, and cirrhosis (Fig. 3). For identifying or excluding significant fibrosis, algorithms based on DNA methylation with or without clinical parameters performed comparably to the FIB-4 index, achieving AUC values of 0.84, 0.87, and 0.81 in the discovery cohort, and 0.63, 0.81, and 0.76 in the validation cohort, respectively (Fig. 3a, b). In detecting advanced fibrosis, SVM-based models outperformed the FIB-4 index, with higher positive predictive values of 0.87 and 0.74 compared with 0.66. For exclusion of advanced fibrosis, all three methods demonstrated excellent negative predictive values (Supplementary Tables 3 and 4). Additionally, models based on plasma DNA methylation levels of *PSD4* and *PDGFRβ* showed excellent diagnostic accuracy for detecting and ruling out stage 4 fibrosis (cirrhosis) (Supplementary Tables 3 and 4).

Overall, combining clinical data with DNA methylation levels yielded promising results for diagnosing or ruling out various stages of fibrosis, with AUC values consistently exceeding 0.75. Detailed comparisons of cohort performance across predictive models are presented in Figure 3 and Supplementary Figures 7 and 8; sensitivity and specificity metrics are provided in Supplementary Tables 3 and 4.

## Discussion

Early and accurate identification of hepatic fibrosis is crucial for determining the clinical prognosis of chronic liver diseases and plays a vital role in preventing and treating advanced liver diseases.<sup>[5]</sup> Significant efforts have been directed towards developing novel NITs, including blood-based biomarkers, for fibrosis assessment.<sup>[9]</sup> In this study, we explored the potential of cell-free DNA methylation signatures as biomarkers for liver fibrosis in MASLD. Specifically, we analyzed DNA methylation levels in two candidate genes (*PDGFRβ* and *PSD4*) and identified significant differences across distinct fibrosis stages (significant fibrosis, advanced fibrosis, and cirrhosis).

*PDGFRβ* is the receptor for PDGF-B, a well-established pro-fibrotic growth factor predominantly produced by Kupffer cells, pericytes, and hepatic stellate cells. PDGF has a pivotal role in the extracellular matrix remodeling, particularly collagen synthesis and is implicated in various fibroproliferative disorders.<sup>[23]</sup> In this study, a significant increase in *PDGFRβ* methylation levels at 5 CpG sites was observed in patients with mild or advanced fibrosis compared with healthy controls in the discovery cohort. Notably, CpG 5-6 methylation levels of *PDGFRβ* showed marked differences between MASLD F0-2 and MASLD F3-4 patients in the discovery data; in the validation cohort, the difference was modest but statistically significant. Previous research by Lambrecht et al.<sup>[24]</sup> indicated that extracellular vesicles derived from activated murine and human hepatic stellate cells are enriched for *PDGFRβ* expression. Furthermore, circulating *PDGFRβ*

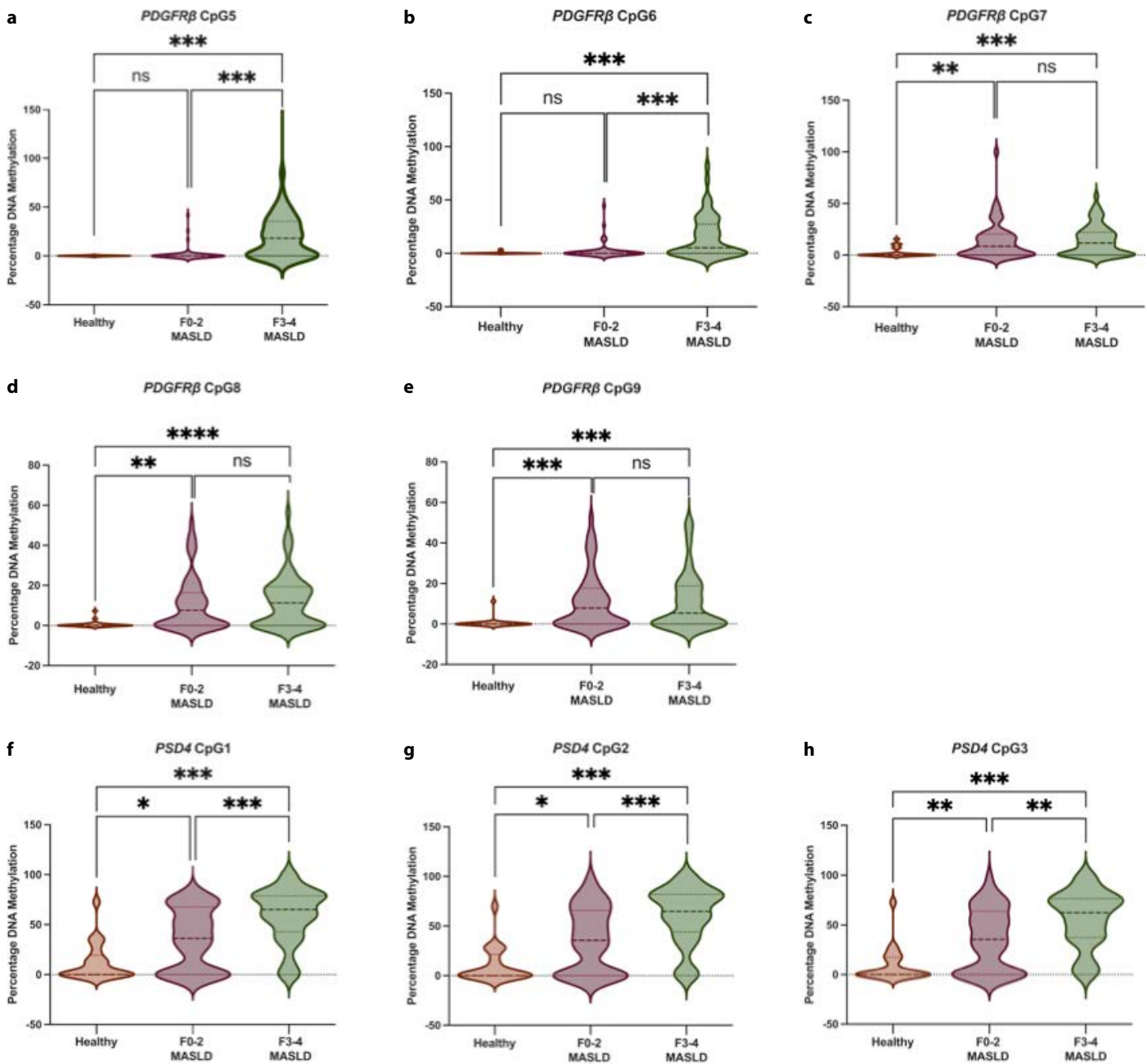


**Figure 1.** Plasma DNA methylation level of MASLD patients in the discovery cohort. Plots were shown as the correlation between the CpG methylation and fibrosis stage of the MASLD. The analysis examines the plasma DNA methylation levels across fibrosis stages F0-2 and F3-4, alongside those of healthy subjects. Bisulfite modification and pyrosequencing were used to assess the plasma CpG methylation at five loci in *PDGFRβ* and three loci in the *PSD4* gene. Changes in *PDGFRβ* (a–e) and *PSD4* (f–h) CpG methylation levels are associated with the fibrosis stage in the discovery cohort. DNA methylation is quantified and represented as a percentage.

\*p<0.05, \*\*p<0.01 and \*\*\*p<0.001.

protein levels, combined with a PDGFR  $\beta$ -based (PRTA) score, were identified as biomarkers of hepatic fibrosis, achieving AUROC values of 0.78 for significant fibrosis, 0.74 for advanced fibrosis, and 0.79 for cirrhosis across three different etiologies. In our study, apoptotic or necrotic myofibroblasts might have contributed to the circulating cell-free DNA methylation pool, thereby leading to an increase in *PDGFRβ* methylation in association with hepatic fibrosis.

*PSD4* was previously identified as a prominent circulating cell-free methylation marker for HCC in a large cohort study.<sup>[16]</sup> Additionally, prior research has demonstrated that TNF- $\alpha$ -induced phospho-p65 activation leads to the recruitment of DNMT1, resulting in hypermethylation of the *PSD4* promoter. This epigenetic modification is associated with carcinogenesis, particularly in individuals with excessive alcohol consumption.<sup>[25]</sup> Based on these

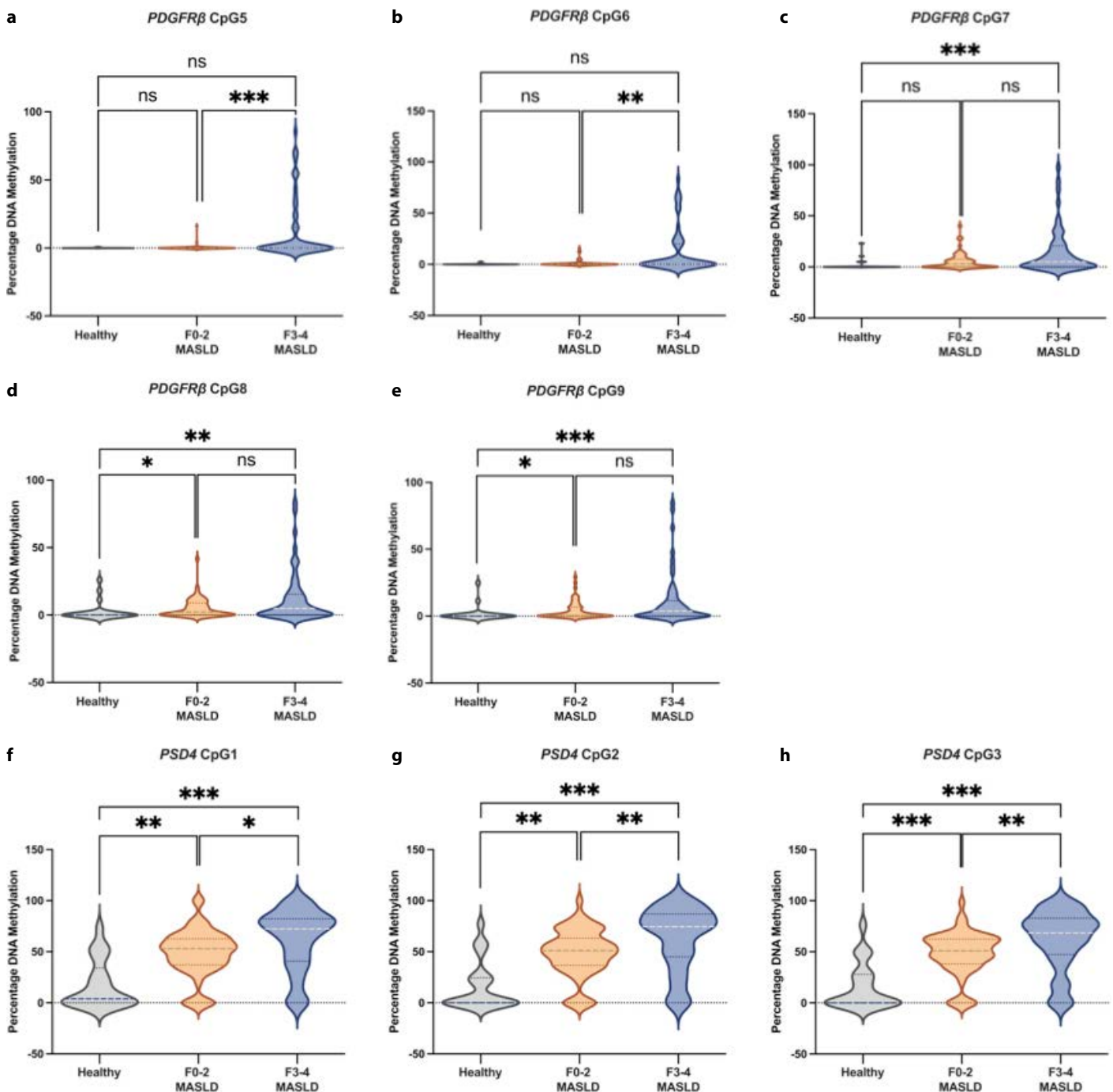


**Figure 2.** Plasma DNA methylation level of MASLD patients in the validation cohort. Plots were shown as the correlation between the CpG methylation and fibrosis stage of the MASLD. The analysis examines the plasma DNA methylation levels across fibrosis stages F0-2 and F3-4, alongside those of healthy subjects in the validation cohort. Bisulfite modification and pyrosequencing were used to assess the plasma CpG methylation at five loci in *PDGFRβ* and three loci in the *PSD4* gene. Changes in *PDGFRβ* (a–e) and *PSD4* (f–h) CpG methylation levels are associated with the fibrosis stage in the validation cohort. DNA methylation is quantified and represented as a percentage.

\* $p < 0.05$ , \*\* $p < 0.01$  and \*\*\* $p < 0.001$ .

findings, we investigated whether plasma methylation levels of the *PSD4* gene are associated with fibrosis stages in MASLD. Our analysis revealed that changes in cell-free DNA methylation within the *PSD4* promoter region were remarkably consistent across

cohorts and notably higher in MASLD patients than in healthy controls (Fig. 1f-h, Fig. 2f-h). These results suggest that *PSD4* methylation levels could serve as reliable predictors not only for hepatic fibrosis but also for HCC.

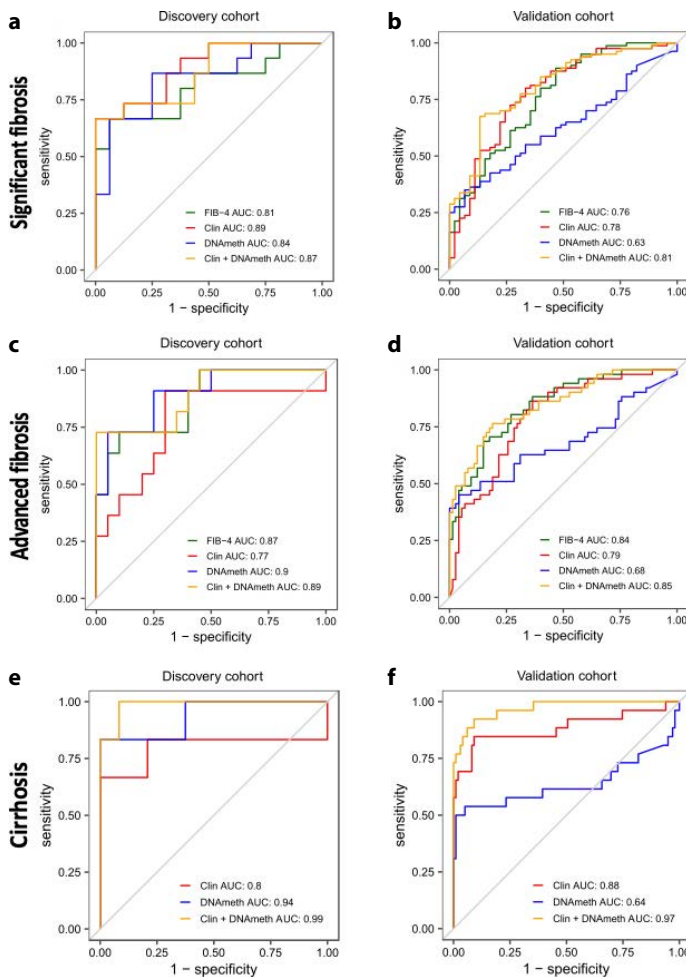


**Figure 3.** SVM analysis model in MASLD patients. This figure shows the SVM analysis in patients with different stages of fibrosis. (a–b) ROC curves of four markers (FIB-4, Clinical parameters, DNA Methylation, and Clinical Parameters + DNA methylation combination) in the discovery and validation cohort of patients with significant fibrosis. (c–d) ROC curves of four markers (FIB-4, Clinical parameters, DNA Methylation, and Clinical Parameters + DNA methylation combination) in the discovery and validation cohort of patients with advanced fibrosis. (e–f) ROC curves of four markers (FIB-4, Clinical parameters, DNA Methylation, and Clinical Parameters + DNA methylation combination) in cirrhotic patients' discovery and validation cohort.

We next evaluated whether DNA methylation markers outperformed other biomarkers, including the FIB-4 index. To this end, we applied three widely used supervised machine learning algorithms: LDA, Random Forest, and SVM.<sup>[20,26,27]</sup> While differences were observed between cohorts for each marker, the AUROC scores consistently favored the combination of DNA methylation and clinical data in SVM analyses. The observed discrepancies between cohorts may be attributed to differences in sample size and fibrosis severity among patients. Notably, SVM results demonstrated that combining DNA methylation markers with clinical data yielded strong diagnostic performance, as reflected by AUROC scores and NPVs.<sup>[28–30]</sup> Importantly, even DNA methylation-based algorithms without incorporating clinical parameters showed robust

performance in ruling out fibrosis. These algorithms achieved an NPV of 0.83 for significant fibrosis and an NPV of 1 for advanced fibrosis, highlighting their potential utility in primary care settings for stratifying MASLD patients and identifying those who require referral to specialized centers.

There are several limitations to this study. First, the relatively modest sample size may constrain the generalizability of our findings. Second, although multicenter, the data collection was limited to three medical centers within a single country, potentially introducing geographical and ethnic biases that may affect the generalizability of our results. Another significant limitation concerns participant selection: study included only a subset of metabolic profiles, which may not fully represent the diverse spectrum of metabolic manifestations observed in clinical practice. From an analytical perspective, although pyrosequencing provides highly accurate methylation analysis, its labor-intensive nature may present challenges for widespread clinical implementation. This methodological constraint could affect the immediate translation of our findings into routine clinical practice, particularly in resource-limited settings.

## Conclusion

In conclusion, we explored the potential of machine learning algorithms as a non-invasive diagnostic tools for assessing fibrosis in patients with MASLD. Our findings demonstrate that methylation levels in circulating cell-free DNA are significantly altered in this patient group, aligning with prior research.<sup>[3]</sup> Collectively, our findings underscore the potential of DNA methylation as a biomarker for fibrosis staging.

**Online Appendix Link:** <https://hepatologyforum.org/storage/upload/files/1773648500-appendix-en.pdf>

**Ethics Committee Approval:** Blood samples and clinical data were collected after obtaining informed consent from participants in compliance with ethical standards and approved by Koc University Research Ethics Committees [approval number: 2015.053.IRB1.014 (30.03.2015), 2016.024.IRB2.005 (15.02.2016), 2017.139.IRB2.048 (10.09.2017), 2022.246.IRB2.040 (30.07.2022), 09.2018.086 (24.09.2018)].

**Informed Consent:** Blood samples and clinical data were collected after obtaining informed consent from participants in compliance with ethical standards.

**Conflict of Interest:** Yusuf Yilmaz has received honoraria for lectures from Echosens and consulting fees from Zydus, Akero, and Novo Nordisk. Adil Mardinoglu is the founder of SZA Longevity, Trustlife Therapeutics, ScandiBio Therapeutics, and ScandiEdge Therapeutics. All other authors have no conflicts of interest to declare.

**Financial Disclosure:** This work was supported by grants from the European Commission, Horizon 2020 Marie Curie Sklodowska Individual Fellowship (to MZ) and Newton-Katip Celebi Fund 2551 (to MZ).

**Use of AI for Writing Assistance:** The authors declare that no artificial intelligence was used in this study.

**Author Contributions:** Concept: MZ, YY; Design: MZ, YY; Supervision: YY; Data Collection and/or Processing: MZ, MD, MA, FE, YY; Analysis and/or Interpretation: BU, BY, SS, AM, HY, CZ, BS, HK, CAC, AMA; Literature Review: BU, HU; Writing: BU, HU, MZ; Critical Review: BU, HY, HU, CZ, AM, MD, MA, BY, SS, HK, BS, CAC, FE, AMA, YY, MZ.

**Acknowledgement:** The authors acknowledge the use of the facilities at the Koc University Research Center for Translational Medicine (KUTTAM), funded by the Presidency of Turkiye, Head of Strategy and Budget.

**Peer-review:** Externally peer-reviewed.

## References

- Teng ML, Ng CH, Huang DQ, Chan KE, Tan DJ, Lim WH, Y, et al. Global incidence and prevalence of nonalcoholic fatty liver disease. *Clin Mol Hepatol* 2023;29(Suppl):S32-S42. [\[CrossRef\]](#)
- Grander C, Grabherr F, Tilg H. Non-alcoholic fatty liver disease: pathophysiological concepts and treatment options. *Cardiovasc Res* 2023;119(9):1787-1798. [\[CrossRef\]](#)
- Hardy T, Zeybel M, Day CP, Dipper C, Masson S, McPherson S, et al. Plasma DNA methylation: a potential biomarker for stratification of liver fibrosis in non-alcoholic fatty liver disease. *Gut* 2017;66(7):1321-1328. [\[CrossRef\]](#)
- Kingwell K. NASH field celebrates ‘hurrah moment’ with a first FDA drug approval for the liver disease. *Nat Rev Drug Discov* 2024;23(4):235-237. [\[CrossRef\]](#)
- Ravndal L, Lindvig KP, Jensen EL, Sunde A, Nassehi D, Thiele M, et al. Algorithms for early detection of silent liver fibrosis in the primary care setting - a scoping review. *Expert Rev Gastroenterol Hepatol* 2023;17(10):985-997. [\[CrossRef\]](#)
- Anstee QM, Castera L, Loomba R. Impact of non-invasive biomarkers on hepatology practice: Past, present and future. *J Hepatol* 2022;76(6):1362-1378. [\[CrossRef\]](#)
- European Association for the Study of the Liver. EASL Clinical Practice Guidelines on non-invasive tests for evaluation of liver disease severity and prognosis - 2021 update. *J Hepatol* 2021;75(3):659-689. [\[CrossRef\]](#)
- Tincopa, M.A Loomba R. Non-invasive diagnosis and monitoring of non-alcoholic fatty liver disease and non-alcoholic steatohepatitis. *Lancet Gastroenterol Hepatol* 2023;8(7):660–670. [\[CrossRef\]](#)
- Wang J, Qin T, Sun J, Li S, Cao L, Lu X. Non-invasive methods to evaluate liver fibrosis in patients with non-alcoholic fatty liver disease. *Front Physiol* 2022;13:1046497. [\[CrossRef\]](#)
- van Kleef LA, Sonneveld MJ, de Man RA, de Knegt RJ. Poor performance of FIB-4 in elderly individuals at risk for chronic liver disease - implications for the clinical utility of the EASL NIT guideline. *J Hepatol* 2022;76(1):245-246. [\[CrossRef\]](#)
- Ali H, Shahzil M, Moond V, Shahzad M, Thandavaram A, Sehar A, et al. Non-pharmacological approach to diet and exercise in metabolic-associated fatty liver disease: Bridging the gap between research and clinical practice. *J Pers Med* 2024;14(1):61. [\[CrossRef\]](#)
- Yang H, Atak D, Yuan M, Li M, Altay O, Demirtas E, et al. Integrative proteo-transcriptomic characterization of advanced fibrosis in chronic liver disease across etiologies. *Cell Rep Med* 2025;6(2):101935. [\[CrossRef\]](#)
- Wu YL, Lin ZJ, Li CC, Lin X, Shan SK, Guo B, et al. Epigenetic regulation in metabolic diseases: mechanisms and advances in clinical study. *Signal Transduct Target Ther* 2023;8(1):98. [\[CrossRef\]](#)
- Gerhard GS, Malenica I, Llaci L, Chu X, Petrick AT, Still CD, DiStefano JK. Differentially methylated loci in NAFLD cirrhosis are associated with key signaling pathways. *Clin Epigenetics* 2018;10(1):93. [\[CrossRef\]](#)
- Ulukan B, Sila Ozkaya Y, Zeybel M. Advances in the epigenetics of fibroblast biology and fibrotic diseases. *Curr Opin Pharmacol* 2019;49:102–109. [\[CrossRef\]](#)
- Xu RH, Wei W, Krawczyk M, Wang W, Luo H, Flagg K, et al. Circulating tumour DNA methylation markers for diagnosis and prognosis of hepatocellular carcinoma. *Nat Mater* 2017;16(11):1155-1161. [\[CrossRef\]](#)
- Zeybel M, Hardy T, Robinson SM, Fox C, Anstee QM, Ness T, et al. Differential DNA methylation of genes involved in fibrosis progression in non-alcoholic fatty liver disease and alcoholic liver disease. *Clin Epigenetics* 2015;7(1):25. [\[CrossRef\]](#)
- Zeybel M, Hardy T, Wong YK, Mathers JC, Fox CR, Gackowska A, et al. Multigenerational epigenetic adaptation of the hepatic wound-healing response. *Nat Med* 2012;18(9):1369-1377. [\[CrossRef\]](#)
- Batista AD, Barros CJP, Costa TBBC, de Godoy MMG, Silva RD, Santos JC, et al. Proton nuclear magnetic resonance-based metabolomic models for non-invasive diagnosis of liver fibrosis in chronic hepatitis C: Optimizing the classification of intermediate fibrosis. *World J Hepatol* 2018;10(1):105-115. [\[CrossRef\]](#)
- Meng F, Wu Q, Zhang W, Hou S. Application of interpretable machine learning models based on ultrasonic radiomics for predicting the risk of fibrosis progression in diabetic patients with nonalcoholic fatty liver disease. *Diabetes Metab Syndr Obes* 2023;16:3901-3913. [\[CrossRef\]](#)
- Bonner JC. Regulation of PDGF and its receptors in fibrotic diseases. *Cytokine Growth Factor Rev* 2004;15(4):255-273. [\[CrossRef\]](#)
- Kanwal F, Neuschwander-Tetri BA, Loomba R, Rinella ME. Metabolic dysfunction-associated steatotic liver disease: Update and impact of new nomenclature on the American Association for the Study of Liver Diseases practice guidance on nonalcoholic fatty liver disease. *Hepatology* 2024;79(5):1212-1219. [\[CrossRef\]](#)
- Kocabayoglu P, Lade A, Lee YA, Dragomir AC, Sun X, Fiel MI, et al.  $\beta$ -PDGF receptor expressed by hepatic stellate cells regulates fibrosis in murine liver injury, but not carcinogenesis. *J Hepatol* 2015;63(1):141-147. [\[CrossRef\]](#)
- Lambrecht J, Verhulst S, Mannaerts I, Sowa JP, Best J, Canbay A, et al. A *PDGFR $\beta$* -based score predicts significant liver fibrosis in patients with chronic alcohol abuse, NAFLD and viral liver disease. *EBioMedicine* 2019;43:501-512. [\[CrossRef\]](#)
- Shi J, Song S, Li S, Zhang K, Lan Y, Li Y. TNF- $\alpha$ /NF- $\kappa$ B signaling epigenetically represses *PSD4* transcription to promote alcohol-related hepatocellular carcinoma progression. *Cancer Med* 2021;10(10):3346-3357. [\[CrossRef\]](#)
- Gorden DL, Myers DS, Ivanova PT, Fahy E, Maurya MR, Gupta S, et al. Biomarkers of NAFLD progression: a lipidomics approach to an epidemic. *J Lipid Res* 2015;56(3):722-736. [\[CrossRef\]](#)
- Wu CC, Yeh WC, Hsu WD, Islam MM, Nguyen PAA, Poly TN, et al. Prediction of fatty liver disease using machine learning algorithms. *Comput Methods Programs Biomed* 2019;170:23-29. [\[CrossRef\]](#)
- European Association for the Study of the Liver. EASL Clinical Practice Guidelines on non-invasive tests for evaluation of liver disease severity and prognosis - 2021 update. *J Hepatol* 2021;75(3):659-689. [\[CrossRef\]](#)
- Loomba R, Adams LA. Advances in non-invasive assessment of hepatic fibrosis. *Gut* 2020;69(7):1343-1352. [\[CrossRef\]](#)
- Polo TCF, Miot HA. Use of ROC curves in clinical and experimental studies. *J Vasc Bras* 2020;19:e20200186. [\[CrossRef\]](#)

## ORIGINAL RESEARCH

# Evaluation of percutaneous endobiliary punch biopsy in suspected malignant biliary strictures: Five-year experience from a tertiary center

 **Ufuk Avcioglu**<sup>1</sup>,  **Hakan Demiroz**<sup>1</sup>,  **Aysegul Idil Soylu**<sup>2</sup>,  **Fatih Uzunkaya**<sup>2</sup>,  **Huseyin Akkaya**<sup>2</sup>,  **Ibrahim Goren**<sup>1</sup>,  **Talat Ayyildiz**<sup>1</sup>,  **Muge Ustaoglu Dede**<sup>1</sup>,  **Ahmet Bektas**<sup>1</sup>

1: Department of Gastroenterology, Ondokuz Mayis University School of Medicine, Samsun, Turkiye

2: Department of Radiology, Ondokuz Mayis University School of Medicine, Samsun, Turkiye

## Highlights & Insights

- **Scientific Gap:** Evidence regarding the diagnostic performance of percutaneous endobiliary punch biopsy (PEPB) in biliary strictures remains limited.
- **Key Finding:** In this single-center study, PEPB demonstrated high specificity and moderate sensitivity for detecting malignancy, with no false-positive results. False-negative findings were mainly associated with subepithelial growth and limited tissue sampling due to fibrosis or necrosis.
- **Clinical Impact:** PEPB is a safe and effective diagnostic option, particularly when sampling via endoscopic retrograde cholangiopancreatography (ERCP) is not feasible or yields inconclusive results.

## ABSTRACT

**Background and Aim:** To evaluate the diagnostic performance, technical feasibility, and safety of percutaneous endobiliary punch biopsy (PEPB) in patients with suspected malignant biliary strictures, particularly when endoscopic approaches are not feasible.

**Materials and Methods:** This retrospective, single-center study included 23 patients with radiologically confirmed biliary strictures who underwent PEPB between January 2020 and January 2025. All procedures were conducted under fluoroscopic guidance following percutaneous biliary drainage. Clinical, laboratory, and procedural data were reviewed.

**Results:** Biopsy samples were adequate for histopathological analysis in all cases. The technical success rate was 100%. Malignancy was detected by PEPB in 17 patients, while 3 cases were confirmed as benign and 3 were false-negative results later proven malignant. PEPB demonstrated a sensitivity of 85%, specificity of 100%, and an overall accuracy of 86.96%. Fisher's exact test showed a significant association between biopsy results and final diagnosis ( $p=0.011$ ). Two minor complications (8.7%)—cholangitis and hemobilia—occurred and were managed conservatively.

**Conclusion:** PEPB is a safe, technically viable, and diagnostically accurate method for tissue sampling in biliary strictures. It offers a valuable alternative when endoscopic biopsy fails or is not feasible.

**Keywords:** Biliary obstruction, percutaneous intervention, punch biopsy.

**How to cite this article:** Avcioglu U, Demiroz H, Soylu AI, Uzunkaya F, Akkaya H, Goren I, et al. Evaluation of percutaneous endobiliary punch biopsy in suspected malignant biliary strictures: Five-year experience from a tertiary center. *Hepatology Forum* 2026; 7(2):133–138.

**Received:** July 21, 2025; **Revised:** January 07, 2026; **Accepted:** January 12, 2026; **Available Online:** April 28, 2026

**Corresponding author:** Hakan Demiroz; Department of Gastroenterology, Ondokuz Mayis University School of Medicine, Samsun, Turkiye; **E-mail:** hakandemiroz.90@gmail.com



This work is licensed under a Creative Commons Attribution-NonCommercial 4.0 International License.

## Introduction

Biliary system diseases are significant clinical conditions that may develop due to benign or malignant causes and can lead to severe complications if not diagnosed early. Among these diseases, biliary obstruction holds a special place in terms of both diagnosis and treatment. Although various imaging and laboratory methods are used to determine the etiology of the obstruction, interventional procedures are often required for definitive diagnosis and treatment. These include Endoscopic Retrograde Cholangiopancreatography (ERCP), percutaneous transhepatic intervention, and surgical approaches.

Percutaneous transhepatic intervention serves as an alternative method in patients for whom endoscopic procedures are unsuitable or unsuccessful. Through percutaneous transhepatic access, not only can biliary drainage be established via catheter or stent placement, but therapeutic interventions such as stone removal and endobiliary ablation can also be performed. Recently, the introduction of endobiliary punch biopsy has expanded the diagnostic capabilities of percutaneous transhepatic procedures.

This study aims to evaluate the effectiveness and safety of percutaneous endobiliary punch biopsy (PEPB).

## Materials and Methods

This retrospective, single-center, single-arm study included 23 patients over the age of 18 with biliary stenosis. The cohort consisted of 14 males and 9 females, with a mean age of 67.

The study covers patients who underwent PEPB between January 2020 and January 2025 after imaging and laboratory results indicated obstructive jaundice. Prior to the procedure, clinical, laboratory, and imaging results of the patients were reviewed. All patients underwent imaging with CT, MRI, or ultrasound. Retrospective analysis confirmed biliary obstruction in all 23 patients before the intervention. The procedures were performed by two interventional radiologists experienced in biliary interventions, either during or after biliary decompression via percutaneous transhepatic access. Data obtained through histopathological analysis were recorded in a Microsoft Excel spreadsheet.

### Ethical Approval

This study was approved by the Clinical Research Ethics Committee of Ondokuz Mayıs University (Application No: 2024/544; Date: March 28, 2025). The research was conducted in accordance with the principles of the Declaration of Helsinki.

### Patient Selection

The indication for biopsy was suspicion of malignant obstruction. Medical records, histopathology reports, diagnostic imaging, surgical reports (if applicable), and patient prognoses were retrospectively reviewed. Collected data included age, gender, technical success of the biopsy, lesion location, stricture length, complications, number of samples taken, laboratory values (ALP,



**Figure 1.** Confirmation of the distal choledochal obstruction by cholangiography.

GGT, direct and indirect bilirubin), imaging findings, pathology results, and surgical reports if available.

Clinical features included varying degrees of jaundice observed in mucous membranes and sclera, dark urine, epigastric pain, fatigue, abdominal distension, anorexia, pruritus, and acholic stool. Laboratory tests showed signs of liver injury with elevated total and direct bilirubin levels.

Some patients had pre-existing conditions. Five patients (21.7%) had a history of malignancy, including three with gastric cancer (13%), one with pancreatic cancer (4%), and one with colon cancer (4%). Informed consent was obtained from all patients before the procedure.

Histopathological diagnosis was established in all patients using PEPB. A pathological diagnosis was considered positive when compatible with radiological, clinical, surgical, or prognostic findings. If no tumor was found in pathology but imaging, clinical evidence, surgical report, or prognosis suggested malignancy, the pathology was considered negative.

### Technique

PEPB procedures were conducted in our hospital's Interventional Radiology Unit using a Digital Subtraction Angiography system (Innova, General Electric). Biopsies were performed under sedoanalgesia using midazolam and tramadol, along with local anesthesia via prilocaine at the skin entry site.

Biopsies were conducted in sessions following the placement of internal-external biliary drainage catheters. In cases with hilar strictures, two catheters were placed along the right and



**Figure 2.** (a) Collection of multiple tissue samples from the obstruction site using endoscopic biopsy forceps. (b) Placement of internal and external drainage catheters.

left intrahepatic bile ducts. For extrahepatic obstructions distal to the hilum, a single catheter was usually placed via the right intrahepatic duct. During biopsy, existing catheters were removed over guidewires. A 7 Fr, 45 cm long introducer sheath was inserted via the planned biopsy route, and a shorter sheath was placed on the alternate route if applicable. Cholangiography confirmed the stricture site. Biopsy forceps were advanced through the long sheath to the proximal side of the stricture (Fig. 1). In cases where re-accessing the stricture post-biopsy might be challenging due to bleeding or edema, a guidewire was positioned through the sheath extending to the jejunum. Multiple tissue samples were obtained using endoscopic biopsy forceps through the stricture (Fig. 2). After sampling, double or single internal-external drainage catheters were re-inserted depending on stricture location. For some inoperable patients, metallic stents were placed upon request. Tissue samples were fixed in formalin. Specimens measuring at least 1–2 mm and structurally intact were considered suitable for histopathological examination.

Primary endpoints were technical success and complication rates. Additional metrics included the average number of biopsy samples, total procedure time (from start to obtaining suitable tissue), mean fluoroscopy time, and mean radiation exposure (in mSv).

Complications were classified according to SIR standards for percutaneous biliary interventions: minor complications included those requiring no treatment (class A) or minimal treatment with overnight observation (class B). Major complications were those requiring short hospital stays under 48 hours (class C), major treatment or hospitalization over 48 hours (class D), permanent adverse sequelae (class E), or death.<sup>[1]</sup>

**Table 1.** Radiological classification of the biliary strictures and status of the prior ERCP attempts

Bismuth type	n	ERCP not attempted (n)	ERCP attempted but failed (n)
Type I	2	1	1
Type II	9	6	3
Type IIIa	2	2	0
Type IIIb	1	1	0
Type IV	9	7	2
Total	23	17	6

ERCP: Endoscopic retrograde cholangiopancreatography.

## Statistics

Statistical analysis was performed using SPSS version 22.0 (IBM Corp., Armonk, NY, USA). Categorical variables were expressed as counts and percentages. Due to the small sample size and expected cell counts below five, associations between PEPB pathology results and final diagnosis were analyzed using Fisher's Exact Test. A two-tailed p value <0.05 was considered statistically significant.

## Results

PEPB was technically successful in all 23 patients. Each patient yielded at least two and up to eleven samples. The localization of the biliary obstructions was determined to be in the intrahepatic bile ducts in 2 patients and at the hepatic hilum or distal bile ducts in 21 patients. The detailed information for the biliary obstruction according to Bismuth–Corlette Classification is given in Table 1. The mean

fluoroscopy time was  $18.2 \pm 5.2$  minutes, and the mean radiation dose (air kerma) was  $680 \pm 210$  mGy.

Laboratory values prior to PEPB showed: mean age  $67.4 \pm 10.2$  years, total bilirubin  $6.9 \pm 4.6$  mg/dL, direct bilirubin  $6.1 \pm 4.5$  mg/dL, GGT  $287.0 \pm 217.5$  IU/L, and ALP  $443.1 \pm 264.0$  IU/L.

All biopsy specimens were adequate for histopathological evaluation. Malignancy was detected by PEPB in 17 patients, including 16 cases of cholangiocarcinoma and one case of metastatic colon cancer. Three patients were reported as benign by PEPB but were later confirmed to have malignancy based on surgical, radiological, or clinical follow-up findings, constituting false-negative results.

Accordingly, PEPB demonstrated a sensitivity of 85%, specificity of 100%, accuracy of 86.96%, positive predictive value of 100%, and negative predictive value of 50%. Fisher's exact test showed a statistically significant association between PEPB pathology results and final diagnosis ( $p=0.011$ ).

Detailed evaluation of the three false-negative cases revealed potential procedural and pathological limitations. In two patients, histopathological examination showed fibrotic or necrotic tissue without viable tumor cells, suggesting sampling from non-representative areas of the stricture. In the remaining case, the tumor demonstrated predominantly submucosal growth with intact biliary epithelium, which may have limited the diagnostic yield of superficial forceps biopsy. These findings highlight that false-negative results are more likely in tumors with subepithelial growth patterns or extensive necrosis.

Two complications (8.7%) were observed: the first was post-procedural cholangitis, which was treated successfully with antibiotics. The second was a hemobilia that regressed spontaneously without the need for surgical or other intervention, as confirmed through multiple follow-up CT scans.

## Discussion

The location of bile duct obstruction can be rapidly and accurately identified using non-invasive imaging modalities such as ultrasound, CT, or MRI. However, tumors originating from the biliary epithelium are often very small and lack specific imaging characteristics.<sup>[2]</sup> Obtaining tissue samples for histological and pathological evaluation remains a cornerstone in the diagnosis of neoplasms.<sup>[3,4]</sup> While a lesion may be benign, the lower the differentiation of a malignant tumor, the higher its grade of malignancy, with increased potential for local invasion and metastasis.<sup>[5,6]</sup> Therefore, pathological diagnosis is crucial for accurate identification of neoplasms and for guiding subsequent management.<sup>[7-9]</sup>

Nevertheless, obtaining biopsy samples in biliary system neoplasms continues to pose challenges. In cases where pathological diagnosis cannot be established through ERCP in biliary strictures, percutaneous transhepatic biopsy using forceps is employed. Percutaneous endobiliary punch biopsy (PEPB) not only provides diagnostic information for cancer but also offers a therapeutic approach for

obstructive disease.<sup>[10]</sup> This technique, involving biopsy forceps via a percutaneous approach, was first reported in 1980<sup>[11]</sup> and has since undergone continuous development.<sup>[12-16]</sup> Studies have suggested that histological diagnosis with forceps biopsy is more successful than bile cytology or fine-needle aspiration, with reported sensitivity ranging from 71% to 93%.<sup>[7,8,17-19]</sup> Accordingly, PEPB is a technically simple, minimally invasive procedure with low complication rates and high diagnostic yield compared to other established techniques.<sup>[2,10,19,20]</sup>

Although diagnostic and technical success rates of PEPB vary across the literature, in our study, the technical success rate was 100% and the diagnostic success rate was 86.96%. In three cases (13%), false-negative results were obtained, though malignancy was confirmed by clinical, radiological, or surgical findings. In our cohort, complications were observed in  $2/23 = 8.7\%$ : one case of post-procedural cholangitis and one case of hemobilia. Theoretically, bile leakage or severe bleeding due to injury to adjacent vascular structures can occur as complications of PEPB.<sup>[21]</sup> However, such complications have not been reported in the literature. A recent meta-analysis including 14 studies and 1,762 patients reported a sensitivity of 81%, specificity of 100%, and a major complication rate of 3.1% for PEPB.<sup>[22]</sup> In a single-center retrospective study by Zhang et al.<sup>[23]</sup> involving 194 patients, the sensitivity, specificity, and false-positive rate of PEPB were reported as 81.8%, 100%, and 0%, respectively. In a retrospective case series by Ozdemir et al.,<sup>[24]</sup> a 100% technical success rate, 87.5% diagnostic success rate, and 12.5% complication rate were reported.

Although the study period spanned five years, the number of included patients was relatively limited. This reflects the highly selective indication for percutaneous endobiliary punch biopsy (PEPB) in our institution. The procedure was reserved for patients with suspected malignant biliary strictures in whom ERCP-based tissue acquisition was unsuccessful or not feasible due to anatomical constraints, prior interventions, or technical failure. Consequently, PEPB represents a niche diagnostic approach rather than a routinely performed procedure, explaining the low annual case volume. Given the descriptive nature of this case series, the primary objective of the study was to report the diagnostic performance of PEPB rather than to establish comparative superiority over ERCP-based tissue acquisition techniques.

One important limitation inherent to forceps-based biopsy techniques is the limited depth of tissue acquisition. Tumors exhibiting predominantly subepithelial growth patterns, extensive fibrosis, or central necrosis may not be adequately sampled despite technically successful biopsy procedures. This limitation was also evident in our cohort, where false-negative results were primarily attributed to histopathological characteristics rather than procedural failure.

Several additional limitations should be acknowledged. This study has a retrospective design and lacks a direct control group using endoscopic sampling techniques, precluding direct comparative analysis. Furthermore, the relatively small sample size limits the statistical power of subgroup analyses. Despite these limitations, our findings provide clinically relevant real-world data on the diagnostic performance and safety of PEPB in a carefully selected patient population.

## Conclusion

From a technical perspective, PEPB is a simple, minimally invasive procedure with low complication rates and high diagnostic accuracy compared to other techniques. It has broadened the scope of biliary diagnostics and proved to be a reliable and accurate method for histopathological diagnosis of biliary neoplasms. PEPB is a safe, feasible, and effective technique that yields a high rate of true-positive results in diagnosing obstructive jaundice.

**Ethics Committee Approval:** This study was approved by the Clinical Research Ethics Committee of Ondokuz Mayıs University (Application No: 2024/544; Date: March 28, 2025).

**Informed Consent:** Informed consent was obtained from all patients before the procedure.

**Conflict of Interest:** The authors declare that they have no conflict of interest.

**Financial Disclosure:** No funding was received for this study.

**Use of AI for Writing Assistance:** The authors declare that no artificial intelligence (AI)-assisted technologies (including but not limited to Large Language Models [LLMs], chatbots, or image creators) were used in the preparation of this manuscript. All content was solely generated by the authors.

**Author Contributions:** Concept: UA, HD, IG; Design: AS, AB, HA; Supervision: FU, IG; Funding: TA, MU; Materials: TA, MU; Data Collection and/or Processing: UA, FU; Analysis and/or Interpretation: AS, MU, IG; Literature Review: TA, HA, FU; Writing: MU, HD, HA; Critical Review: UA, AS, AB.

**Acknowledgement:** The authors thank the Interventional Radiology team for their assistance in the procedures.

**Peer-review:** Externally peer-reviewed.

## References

1. Saad WE, Wallace MJ, Wojak JC, Kundu S, Cardella JF. Quality improvement guidelines for percutaneous transhepatic cholangiography, biliary drainage, and percutaneous cholecystostomy. *J Vasc Interv Radiol* 2010;21(6):789-795. [\[CrossRef\]](#)
2. Warnken EM, Uder M, Stein H, Wucherer M, Lell M, Muschweck H, et al. Transhepatic forceps biopsy after PTCO for histological assessment of bile duct stenoses or occlusions. *Z Gastroenterol* 2019;57(2):133-138. [\[English\]](#) [\[CrossRef\]](#)
3. Singh A, Gelrud A, Agarwal B. Biliary strictures: diagnostic considerations and approach. *Gastroenterol Rep (Oxf)* 2015;3(1):22-31. [\[CrossRef\]](#)
4. Valle JW, Borbath I, Khan SA, Huguet F, Gruenberger T, Arnold D; ESMO Guidelines Committee. Biliary cancer: ESMO Clinical Practice Guidelines for diagnosis, treatment and follow-up. *Ann Oncol* 2016;27(Suppl 5):v28-v37. [\[CrossRef\]](#)
5. Su CH, Tsay SH, Wu CC, Shyr YM, King KL, Lee CH, et al. Factors influencing postoperative morbidity, mortality, and survival after resection for hilar cholangiocarcinoma. *Ann Surg* 1996;223(4):384-394. [\[CrossRef\]](#)
6. Kondo S, Hirano S, Ambo Y, Tanaka E, Okushiba S, Morikawa T, et al. Forty consecutive resections of hilar cholangiocarcinoma with no postoperative mortality and no positive ductal margins: results of a prospective study. *Ann Surg* 2004;240(1):95-101. [\[CrossRef\]](#)
7. Tapping CR, Byass OR, Cast JE. Cytological sampling versus forceps biopsy during percutaneous transhepatic biliary drainage and analysis of factors predicting success. *Cardiovasc Intervent Radiol* 2012;35(4):883-889. [\[CrossRef\]](#)
8. Patel P, Rangarajan B, Mangat K. Improved accuracy of percutaneous biopsy using "cross and push" technique for patients suspected with malignant biliary strictures. *Cardiovasc Intervent Radiol* 2015;38(4):1005-1010. [\[CrossRef\]](#)
9. Tibana TK, Grubert RM, Fornazari VAV, Barbosa FCP, Bacelar B, Oliveira A, et al. The role of percutaneous transhepatic biliary biopsy in the diagnosis of patients with obstructive jaundice: an initial experience. *Radiol Bras* 2019;52:222-228. [\[CrossRef\]](#)
10. Li Z, Li TF, Ren JZ, Li WC, Ren JL, Shui SF, et al. Value of percutaneous transhepatic cholangiobiopsy for pathologic diagnosis of obstructive jaundice: analysis of 826 cases. *Acta Radiol* 2017;58(1):3-9. [\[CrossRef\]](#)
11. Elyaderani MK, Gabriele OF. Brush and forceps biopsy of biliary ducts via percutaneous transhepatic catheterization. *Radiology* 1980;135(3):777-778. [\[CrossRef\]](#)
12. Savader SJ, Lynch FC, Radvany MG, Kudryk BT, Andrews RT, Geschwind JF, et al. Single-specimen bile cytology: a prospective study of 80 patients with obstructive jaundice. *J Vasc Interv Radiol* 1998;9(5):817-821. [\[CrossRef\]](#)
13. Nunes TF. Percutaneous biopsy of abdominal lesions: what is currently the best diagnostic strategy? *Radiol Bras* 2018;51(3):V-VI. [\[CrossRef\]](#)
14. Schiavon LHO, Tyng CJ, Travesso DJ, Rocha RD, Schiavon ACSA, Bitencourt AGV. Computed tomography-guided percutaneous biopsy of abdominal lesions: indications, techniques, results, and complications. *Radiol Bras* 2018;51(3):141-146. [\[CrossRef\]](#)
15. Ribeiro KCP, Guimarães JPO, Aidar LB, Guimarães TADS, da Silva JCS. Hemobilia in a patient with arteriohepatic fistula after liver contusion. *Radiol Bras* 2018;51(6):413-414. [\[CrossRef\]](#)
16. Zurstrassen CE, Bitencourt AGV, Guimaraes MD, Cavalcante ACBS, Tyng CJ, Amoedo MK, et al. Percutaneous stent placement for the treatment of malignant biliary obstruction: nitinol versus elgiloy stents. *Radiol Bras* 2017;50(2):97-102. [\[CrossRef\]](#)
17. Jung GS, Huh JD, Lee SU, Han BH, Chang HK, Cho YD. Bile duct: analysis of percutaneous transluminal forceps biopsy in 130 patients suspected of having malignant biliary obstruction. *Radiology* 2002;224(3):725-730. [\[CrossRef\]](#)
18. Ierardi AM, Mangini M, Fontana F, Floridi C, De Marchi G, Petrillo M, et al. Usefulness and safety of biliary percutaneous transluminal forceps biopsy (PTFB): our experience. *Minim Invasive Ther Allied Technol* 2014;23(2):96-101. [\[CrossRef\]](#)
19. Boos J, Yoo RJ, Steinkeler J, Ayata G, Ahmed M, Sarwar A, et al. Fluoroscopic percutaneous brush cytology, forceps biopsy and both in tandem for diagnosis of malignant biliary obstruction. *Eur Radiol* 2018;28(2):522-529. [\[CrossRef\]](#)
20. Park JG, Jung GS, Yun JH, Yun BC, Lee SU, Han BH, et al. Percutaneous transluminal forceps biopsy in patients suspected of having malignant biliary obstruction: factors influencing the outcomes of 271 patients. *Eur Radiol* 2017;27(10):4291-4297. [\[CrossRef\]](#)

21. Terasaki K, Wittich GR, Lycke G, Walter R, Nowels K, Swanson D, et al. Percutaneous transluminal biopsy of biliary strictures with a biptome. *AJR Am J Roentgenol* 1991;156(1):77-78. [\[CrossRef\]](#)
22. Jeon TY, Choi MH, Yoon SB, Soh JS, Moon SH. Systematic review and meta-analysis of percutaneous transluminal forceps biopsy for diagnosing malignant biliary strictures. *Eur Radiol* 2022;32(3):1747-1756. [\[CrossRef\]](#)
23. Zhang C, Li Y, Song M, Sun Z, Han X, Ren J, et al. False-negative factors of percutaneous transluminal clamp biopsy for suspected malignant biliary stricture: 194 cases analyzed from a single center. *Insights Imaging* 2024;15(1):108. [\[CrossRef\]](#)
24. Ozdemir M, Dertli T, Faruk Sevinc O, Taydas O, Danisan G, Faruk Ates O, et al. An alternative method in the diagnosis of intrabiliary lesions: Percutaneous endobiliary brush biopsy. *Hepatol Forum* 2024;5(4):167-170. [\[CrossRef\]](#)

## ORIGINAL RESEARCH

# Empagliflozin versus dapagliflozin in patients with liver cirrhosis: A comparative real-world study on hepatic decompensation

 Hatem Ahmed<sup>1</sup>,  Imad Alabdul Razzak<sup>1</sup>,  Eyad Abdulrazzak<sup>2</sup>,  Sameh Gomaa<sup>1</sup>,  Joelle Lauchner<sup>3</sup>

1: Department of Internal Medicine Residency, Phoenixville Hospital, Pennsylvania, USA

2: Beth Israel Deaconess Medical Center- Boston, Massachusetts, USA

3: Tower Health Medical Group Internal Medicine, Douglassville, Pennsylvania, USA

## Highlights & Insights

- **Scientific Gap:** Sodium-glucose cotransporter-2 inhibitors (SGLT2i) may benefit cirrhosis patients, but comparative real-world data on empagliflozin and dapagliflozin are limited. This study compares their outcomes.
- **Key Finding:** Empagliflozin and dapagliflozin showed similar five-year mortality and hospitalization rates. However, empagliflozin was associated with fewer hepatic decompensation events, such as hepatic encephalopathy and hepatorenal syndrome.
- **Clinical Impact:** Empagliflozin may offer additional hepatic benefits over dapagliflozin without increasing adverse events. Further research is needed to confirm these findings.

## ABSTRACT

**Background and Aim:** Sodium-glucose cotransporter-2 inhibitors may improve outcomes in liver cirrhosis, but comparative evidence between individual agents is limited. We compared real-world outcomes of empagliflozin versus dapagliflozin in adults with liver cirrhosis.

**Materials and Methods:** We conducted a multicenter retrospective cohort study using the TriNetX US Collaborative Network (69 healthcare organizations). Adults with cirrhosis who were newly prescribed empagliflozin or dapagliflozin after the diagnosis of cirrhosis between March 1, 2013 and January 1, 2025, were included. Propensity score matching (1:1) was used to balance baseline characteristics. Outcomes were assessed from day 1 after the index prescription through 5 years. Primary outcomes were all-cause mortality and all-cause hospitalization. Secondary outcomes included hepatic decompensation events. Tertiary outcomes included prognostic hepatic and renal biomarkers. Safety outcomes included the incidence of acute kidney injury, urinary tract infection, and diabetic ketoacidosis.

**Results:** Before matching, 17,700 empagliflozin users and 8,619 dapagliflozin users were identified; 7,852 patients remained in each cohort after matching. Five-year mortality was similar between groups (12.7% vs. 12.6%; odds ratio [OR]: 1.012, 95% confidence interval [CI]: 0.921–1.112;  $p=0.8075$ ), as was the risk of hospitalization (14.7% vs. 13.4%; OR: 1.105, 95% CI: 0.94–1.30;  $p=0.216$ ). Empagliflozin was associated with lower rates of hepatic encephalopathy (4.0% vs. 4.7%; OR: 0.84;  $p=0.0295$ ), hepatorenal syndrome (1.0% vs. 1.6%; OR: 0.614;  $p=0.0007$ ), and paracentesis (2.9% vs. 3.7%; OR: 0.785;  $p=0.0083$ ). Albumin levels were higher and bilirubin levels were lower with empagliflozin ( $p<0.01$  for both). Safety outcomes were similar between groups.

**Conclusion:** In matched adults with cirrhosis, empagliflozin and dapagliflozin demonstrated comparable five-year mortality and hospitalization rates. However, empagliflozin was associated with fewer selected decompensation events without an increase in adverse events.

**Keywords:** Cirrhosis, empagliflozin, dapagliflozin.

**How to cite this article:** Ahmed H, Razzak IA, Abdulrazzak E, Gomaa S, Lauchner J. Empagliflozin versus dapagliflozin in patients with liver cirrhosis: A comparative real-world study on hepatic decompensation. *Hepatology Forum* 2026; 7(2):139–145.

**Received:** December 16, 2025; **Revised:** February 10, 2026; **Accepted:** February 16, 2026; **Available Online:** April 14, 2026

**Corresponding author:** Hatem Ahmed; Department of Internal Medicine Residency, Phoenixville Hospital, Pennsylvania, USA; **E-mail:** hatem.sayedahmed@towerhealth.org



This work is licensed under a Creative Commons Attribution-NonCommercial 4.0 International License.

## Introduction

Liver cirrhosis remains a major global health burden and is associated with substantial morbidity and mortality driven by hepatic decompensation, hepatocellular carcinoma (HCC), and progression to end-stage liver disease.<sup>[1]</sup> Despite advances in understanding the pathophysiology of cirrhosis, disease-modifying therapies remain limited, particularly for patients with decompensated disease.<sup>[2]</sup> The emerging concept of recompensated cirrhosis—defined as the resolution of prior decompensating events with improvement in hepatic function—has been linked to better long-term outcomes and represents a potential therapeutic target.<sup>[3]</sup> Concurrently, the rising prevalence of metabolic dysfunction–associated steatotic liver disease (MASLD) and its inflammatory subtype, metabolic dysfunction–associated steatohepatitis (MASH), further underscores the need for novel strategies to improve outcomes in the cirrhosis population.<sup>[4]</sup>

Sodium-glucose cotransporter-2 inhibitors (SGLT2i), initially developed for the treatment of type 2 diabetes mellitus (T2DM), have demonstrated pleiotropic benefits extending beyond glycemic control, including cardioprotective, nephroprotective, and anti-inflammatory effects.<sup>[5,6]</sup> These agents are now routinely incorporated into the management of heart failure and chronic kidney disease (CKD), including in individuals without diabetes, supported by evidence from large clinical trials across diverse clinical settings.<sup>[7]</sup>

Increasing evidence suggests that SGLT2 inhibitors may also confer hepatoprotective effects. Preclinical and clinical studies have reported improvements in liver enzymes (alanine aminotransferase [ALT], aspartate aminotransferase [AST], and gamma-glutamyl transferase [GGT]), reductions in hepatic steatosis and fibrosis, and potential mitigation of cirrhosis-related complications such as ascites, portal hypertension, and hepatic encephalopathy.<sup>[8–11]</sup> Proposed mechanisms include attenuation of oxidative stress and suppression of pro-inflammatory cytokines (e.g., tumor necrosis factor alpha [TNF- $\alpha$ ] and interleukin-6 [IL-6]), with downstream anti-inflammatory and antifibrotic effects that may counter pathways implicated in cirrhosis progression.<sup>[12–17]</sup>

Despite these promising observations, comparative real-world data evaluating individual SGLT2i agents in cirrhosis are limited. Accordingly, we used a large real-world electronic health record database (TriNetX) to compare outcomes among patients with liver cirrhosis initiated on empagliflozin versus dapagliflozin. Using propensity score matching, we evaluated mortality, hospitalization, hepatic decompensation events, and safety outcomes to determine whether medication-specific differences exist within the SGLT2i class in this high-risk population.

## Materials and Methods

### Study Design and Data Source

We conducted a multicenter retrospective cohort study using the TriNetX Research Network, a federated health research platform

that aggregates real-time, de-identified electronic health record (EHR) data from more than 120 million patients across 69 healthcare organizations in the United States. This study used the TriNetX US Collaborative Network, which includes both structured and unstructured clinical data (e.g., diagnoses, medications, laboratory results, and procedures). Diagnoses were identified using the International Classification of Diseases, Tenth Revision (ICD-10) codes; medications using RxNorm codes; procedures using Current Procedural Terminology (CPT) codes; and laboratory tests using Logical Observation Identifiers Names and Codes (LOINC). All diagnostic, medication, procedure, laboratory, and encounter codes used for cohort construction and outcome ascertainment are provided in Supplementary Table 1A–E.

### Study Population and Cohort Definition

Eligible patients were adults (aged  $\geq 18$  years) with a documented diagnosis of liver cirrhosis identified using ICD-10 codes. Patients were excluded if they had a history of liver transplantation, renal transplantation, dialysis, primary biliary cholangitis, or primary sclerosing cholangitis. Two exposure cohorts were defined among eligible patients: patients prescribed empagliflozin after cirrhosis diagnosis and patients prescribed dapagliflozin after cirrhosis diagnosis.

The index date was defined as the first prescription for empagliflozin or dapagliflozin occurring after the initial cirrhosis diagnosis. Patients who received both medications or who were exposed to other sodium-glucose cotransporter-2 inhibitors were excluded. Patients who experienced any study outcome prior to the index date were excluded from the analysis of that specific outcome but remained eligible for analyses of other outcomes. The study period extended from March 1, 2013 (initial U.S. Food and Drug Administration [FDA] approval of SGLT2i), through January 1, 2025.

### Covariates and Baseline Characteristics

Baseline characteristics and covariates were assessed during the five years preceding each patient's index date. These included demographics (age, sex, race); comorbidities (type 2 diabetes mellitus, hypertension, heart failure, chronic kidney disease, and obesity); liver disease etiologies (e.g., alcoholic liver disease, nonalcoholic steatohepatitis, and chronic viral hepatitis); and medication exposures, including diuretics, beta-blockers, angiotensin-converting enzyme (ACE) inhibitors, angiotensin receptor blockers (ARBs), statins, insulin, metformin, glucagon-like peptide-1 (GLP-1) receptor agonists, dipeptidyl peptidase-4 (DPP-4) inhibitors, and sulfonylureas. Procedural history, including transjugular intrahepatic portosystemic shunt (TIPS) placement, was also captured.

Laboratory parameters used to characterize baseline liver and renal function included aspartate aminotransferase, alanine aminotransferase, gamma-glutamyl transferase, total bilirubin, serum albumin, serum creatinine, estimated glomerular filtration rate (eGFR), international normalized ratio (INR), hemoglobin A1c (HbA1c), platelet count, serum sodium, and body mass index (BMI).

**Table 1.** Hepatic and prognostic laboratory markers in the empagliflozin and dapagliflozin cohorts at five-year follow-up

Laboratory marker	Empagliflozin (n=7,852) Mean±SD	Dapagliflozin (n=7,852) Mean±SD	p
Aspartate aminotransferase (AST)	57.86±336.33	57.37±227.51	0.9266
Alanine aminotransferase (ALT)	39.51±135.45	41.37±141.22	0.4636
Gamma-glutamyl transferase (GGT)	164.89±274.91	141.66±231.12	0.1013
Total bilirubin	1.22±2.36	1.34±2.83	0.0094
Serum albumin	3.69±0.72	3.61±0.74	<0.0001
International normalized ratio (INR)	1.37±0.67	1.39±0.68	0.1429
Platelets	181.43±92.25	179.72±91.88	0.302
Creatinine	1.26±0.94	1.29±0.83	0.0681
Glomerular filtration rate (eGFR)	66.88±31.75	66.37±32.34	0.3654
Serum sodium	137.93±4.08	137.76±4.16	0.02

Values are presented as mean±standard deviation (SD).

## Study Outcomes

The primary outcomes were all-cause mortality and all-cause hospitalization during follow-up. Secondary outcomes were hepatic decompensation events, including ascites, need for peritoneal drainage, spontaneous bacterial peritonitis (SBP), jaundice, esophageal variceal bleeding, hepatic encephalopathy, hepatorenal syndrome (HRS), and hepatocellular carcinoma. Tertiary outcomes included laboratory markers reflecting hepatic and renal function (e.g., AST, ALT, INR, serum albumin, serum creatinine, and eGFR). Safety outcomes included acute kidney injury (AKI), urinary tract infections (UTIs), and diabetic ketoacidosis (DKA).

## Statistical Analysis

To reduce confounding, 1:1 propensity score matching (PSM) was performed using greedy nearest-neighbor matching without replacement and a caliper width of 0.1 pooled standard deviations within the TriNetX Analytics Platform (TriNetX LLC, Cambridge, MA, USA). Propensity scores were estimated via logistic regression including all prespecified covariates. Balance after matching was evaluated using standardized mean differences (SMDs), with an absolute SMD<0.1 indicating acceptable balance.

All analyses were conducted within the TriNetX analytics platform using its built-in modules. For binary outcomes within the follow-up window, TriNetX “Measure of Association” analyses were used to compute risk, risk difference, risk ratio, and odds ratios (OR), with corresponding 95% confidence intervals (CI). Time-to-event outcomes were evaluated using TriNetX Kaplan–Meier survival analyses with log-rank testing; censoring was applied according to the platform rule that patients are censored after the last recorded clinical fact in their EHR. For laboratory outcomes, TriNetX laboratory analyses were used, which incorporated only the most recent laboratory value within the specified time window; group means were compared using t-tests. All tests were two-sided, and p-values <0.05 were considered statistically significant.

## Ethical Approval/Waiver

This study was reviewed by a Phoenixville Hospital Institutional Review Board and determined to be exempt (No. 2025-109, September 10, 2025) because it involved the secondary analysis of de-identified data obtained through the TriNetX platform. Our article was written in accordance with the Helsinki declaration.

## Results

### Cohort Selection and Baseline Characteristics

Among 720,923 adults with cirrhosis, 604,728 remained after exclusions. We identified 17,700 empagliflozin users (Group A) and 8,619 dapagliflozin users (Group B). After 1:1 propensity score matching, 7,852 patients remained in each cohort. Baseline characteristics were well balanced after matching (absolute SMD<0.1 across covariates), with a small residual imbalance in serum albumin (SMD=0.102). Full baseline characteristics are shown in Supplementary Table 1.

### Primary Outcomes: Mortality and Hospitalization

At five years, all-cause mortality did not differ significantly between cohorts (12.7% vs. 12.6%; OR: 1.012; 95% CI: 0.921–1.112; p=0.8075). Kaplan–Meier analysis similarly showed no significant difference in time to death between empagliflozin and dapagliflozin (hazard ratio: 0.970; 95% CI: 0.888–1.060; log-rank p=0.500) (Fig. 1). The risk of all-cause hospitalization was also similar (14.7% vs. 13.4%; OR: 1.105; 95% CI: 0.94–1.30; p=0.216).

### Secondary Outcomes: Hepatic Decompensation Events

Composite hepatic decompensation was similar between groups (11% vs. 10.6%; OR: 1.004; 95% CI: 0.886–1.137; p=0.9516). However, empagliflozin was associated with lower rates of hepatic

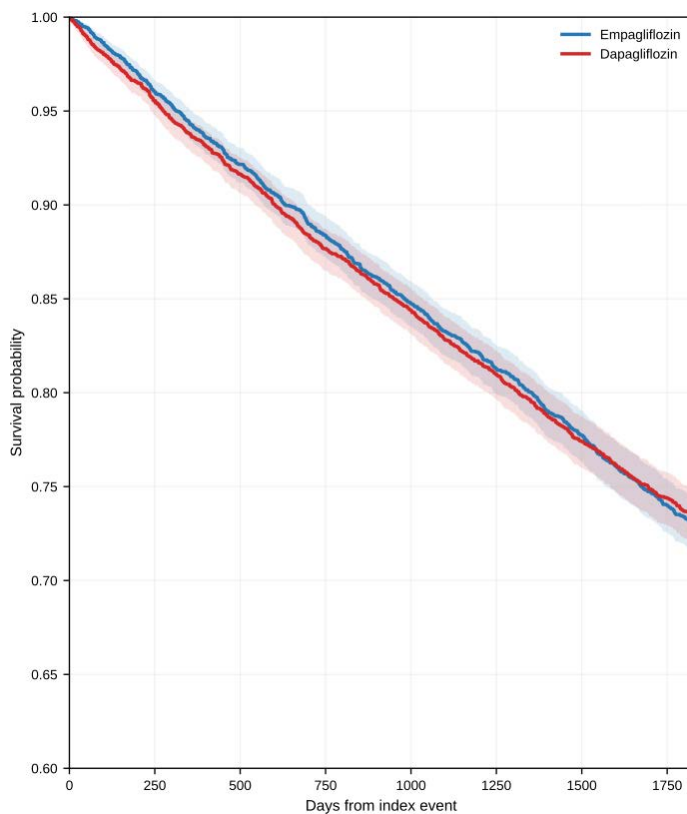


**Figure 1.** Kaplan–Meier survival curves for all-cause mortality after initiation of empagliflozin versus dapagliflozin in propensity score–matched adults with cirrhosis. Shaded areas indicate 95% confidence intervals (CI). Groups were compared using the log-rank test ( $\chi^2=0.455$ ;  $p=0.500$ ); hazard ratio of 0.970 (95% CI: 0.888–1.060). Note: The y-axis is truncated (0.60–1.00) to improve visualization of between-group differences.

encephalopathy (4.0% vs. 4.7%; OR: 0.84; 95% CI: 0.717–0.983;  $p=0.0295$ ), hepatorenal syndrome (1.0% vs. 1.6%; OR: 0.614; 95% CI: 0.462–0.816;  $p=0.0007$ ), and paracentesis (2.9% vs. 3.7%; OR: 0.785; 95% CI: 0.656–0.94;  $p=0.0083$ ). Other hepatic outcomes were not significantly different (Table 2). These associations are summarized in Figure 2.

### Tertiary Outcomes: Prognostic Markers

At five years, empagliflozin users had higher albumin levels ( $3.69\pm 0.72$  vs.  $3.61\pm 0.74$  g/dL;  $p<0.0001$ ) and lower total bilirubin levels ( $1.22\pm 2.36$  vs.  $1.34\pm 2.83$  mg/dL;  $p=0.0094$ ). Serum sodium was also statistically, though modestly, higher with empagliflozin ( $137.93\pm 4.08$  vs.  $137.76\pm 4.16$  mmol/L;  $p=0.02$ ). Other laboratory markers were similar (Table 1).

### Adverse Events

Safety outcomes were comparable between cohorts: AKI (12.8% vs. 13.6%; OR: 0.927; 95% CI: 0.823–1.045;  $p=0.214$ ), UTI (6.5% vs. 6.9%; OR: 0.95; 95% CI: 0.825–1.095;  $p=0.4783$ ), and DKA (0.8% vs. 0.8%; OR: 0.966; 95% CI: 0.674–1.383;  $p=0.849$ ).

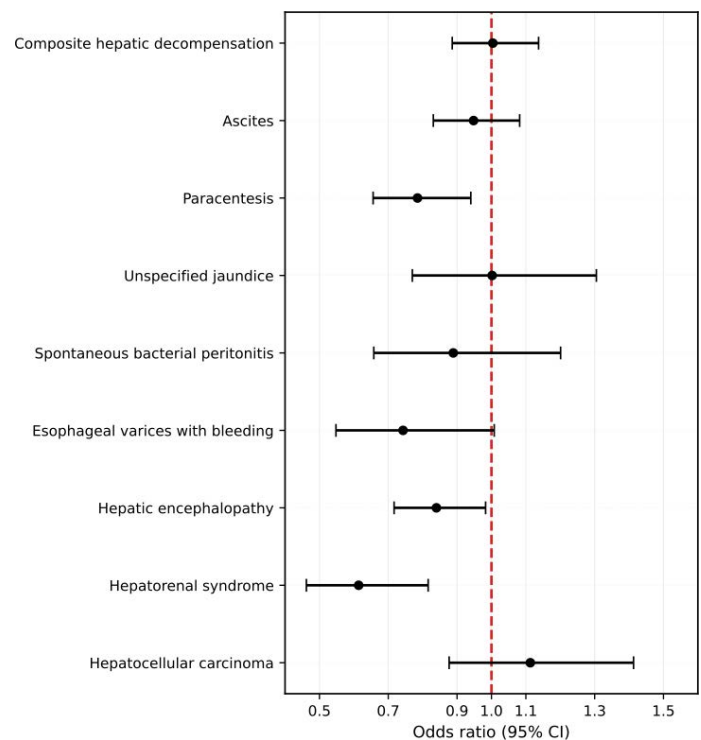


**Figure 2.** Forest plot of hepatic decompensation outcomes comparing empagliflozin and dapagliflozin. Odds ratios (OR) with 95% confidence intervals are shown for five-year outcomes after propensity score matching. The vertical reference line indicates OR=1.0.

## Discussion

In this real-world retrospective cohort study, empagliflozin and dapagliflozin were associated with comparable five-year risks of mortality and all-cause hospitalization in matched adults with cirrhosis. However, empagliflozin was associated with fewer selected hepatic decompensation events—particularly hepatic encephalopathy, hepatorenal syndrome, and paracentesis—along with modest differences in albumin and bilirubin levels, without an observed increase in AKI, UTI, or DKA. To our knowledge, this is the first large-scale real-world comparison of these two agents in liver cirrhosis.

In the cirrhosis literature, empagliflozin has been most consistently linked to improved ascites control and reduced need for therapeutic drainage, aligning with the lower paracentesis rates observed in our cohort.<sup>[18–20]</sup> A case report described resolution of refractory ascites and hepatic hydrothorax after empagliflozin initiation in primary biliary cirrhosis;<sup>[18]</sup> a pilot study showed improved natriuresis and circulatory, cardiac, and renal parameters in cirrhotic patients with refractory ascites;<sup>[19]</sup> and a randomized trial demonstrated reduced large-volume paracentesis requirements and complete ascites resolution in a subset of patients when empagliflozin was added to standard care.<sup>[20]</sup> Safety data in cirrhosis, though limited, support feasibility and are consistent with our similar rates of AKI, UTI, and DKA between cohorts.<sup>[21]</sup>

**Table 2.** Five-year hepatic outcomes in the empagliflozin and dapagliflozin cohorts after propensity score matching

Secondary outcome	Empagliflozin (n=7,852) n (%)	Dapagliflozin (n=7,852) n (%)	OR	95% CI	p
Composite hepatic decompensation	564 (11)	555 (10.6)	1.004	(0.886, 1.137)	0.9516
Ascites	466 (7.9)	489 (8.3)	0.948	(0.831, 1.082)	0.4311
Paracentesis	221 (2.9)	277 (3.7)	0.785	(0.656, 0.94)	0.0083
Unspecified jaundice	112 (1.5)	112 (1.5)	1.002	(0.77, 1.305)	0.988
Spontaneous bacterial peritonitis	81 (1.0)	91 (1.2)	0.889	(0.658, 1.201)	0.4417
Esophageal varices with bleeding	73 (0.9)	98 (1.3)	0.743	(0.548, 1.008)	0.0554
Hepatic encephalopathy	299 (4.0)	353 (4.7)	0.84	(0.717, 0.983)	0.0295
Hepatorenal syndrome	78 (1.0)	126 (1.6)	0.614	(0.462, 0.816)	0.0007
Hepatocellular carcinoma	145 (1.9)	131 (1.7)	1.113	(0.877, 1.413)	0.3779

Values are presented as n (%). OR: Odds ratio; CI, Confidence interval.

Beyond cirrhosis, randomized trials in metabolic dysfunction-associated steatotic liver disease populations show that empagliflozin reduces hepatic fat content and improves liver-related biomarkers, providing a broader hepatometabolic rationale for differences in liver-related outcomes.<sup>[22–25]</sup> Across E-LIFT (Effect of Empagliflozin on Liver Fat in Patients with Type 2 Diabetes Mellitus) and subsequent placebo-controlled studies in type 2 diabetes, mixed diabetic and nondiabetic populations, and nondiabetic MASLD, empagliflozin consistently reduced liver fat on imaging and was associated with favorable metabolic changes.<sup>[22–25]</sup>

Taken together, existing evidence most directly supports empagliflozin's role in ascites and volume-related management and hepatic steatosis reduction, which is directionally consistent with our findings of reduced paracentesis and modestly more favorable liver synthetic and cholestatic markers. The observed differences in hepatic encephalopathy and hepatorenal syndrome warrant prospective validation, as empagliflozin-specific data for these endpoints remain limited.

The literature on dapagliflozin in cirrhosis is more limited and mixed. A small randomized trial in cirrhotic patients with ascites reported improved natriuresis and ascites control but no survival or disease severity benefit, along with higher rates of AKI and infections,<sup>[26]</sup> whereas a retrospective study in cirrhotic patients with diabetes found better ascites control, reduced diuretic requirements, and fewer complications, including hepatic encephalopathy, variceal bleeding, and infections.<sup>[27]</sup> These data suggest that dapagliflozin may provide hepatic benefits in selected populations, but its safety profile in cirrhosis requires further clarification.

In our analysis, empagliflozin was associated with slightly more favorable hepatic laboratory parameters, including higher serum albumin and lower bilirubin levels, suggesting better preservation of hepatic synthetic function and fluid homeostasis. This pattern is consistent with reports of reduced liver fat and improved metabolic and nutritional parameters with empagliflozin in cirrhosis and MASLD.<sup>[19,24]</sup> Overall, our findings add comparative effectiveness evidence and

support the possibility that empagliflozin may confer hepatic benefits beyond glycemic and cardiorenal effects, particularly with respect to hepatic decompensation events and selected hepatic biomarkers.

### Limitations

This study has several limitations. First, its retrospective design and reliance on EHR-based administrative coding introduce the possibility of residual confounding and misclassification. Although propensity score matching balanced measured covariates, unmeasured factors—such as cirrhosis severity (e.g., Model for End-Stage Liver Disease [MELD] or Child-Pugh scores), medication adherence, and alcohol consumption patterns—could not be assessed. Second, due to platform limitations, we could not ascertain cause-specific mortality or indications for hospitalization, nor could we determine the timing of SGLT2i discontinuation. Finally, generalizability may be limited to the healthcare systems represented in TriNetX.

### Conclusion

In this large, real-world multicenter cohort study of patients with liver cirrhosis, empagliflozin and dapagliflozin were associated with comparable five-year risks of all-cause mortality and hospitalization after propensity score matching. However, empagliflozin use was associated with a lower risk of key hepatic decompensation events—particularly hepatic encephalopathy and hepatorenal syndrome—and a reduced need for paracentesis, along with modestly more favorable liver function markers (higher albumin and lower bilirubin levels). Adverse event rates were similar between groups, supporting comparable short-term safety in this population. Collectively, these findings provide novel comparative effectiveness evidence suggesting that empagliflozin may confer additional hepatic benefits within the SGLT2 inhibitor class in patients with cirrhosis. Prospective randomized studies are needed to confirm these observations, clarify mechanisms, and guide optimal SGLT2 inhibitor selection in patients with advanced liver disease.

**Online Appendix Link:** <https://hepatologyforum.org/storage/upload/files/1775572025-appendix-en.pdf>

**Ethics Committee Approval:** This study was reviewed by a Phoenixville Hospital Institutional Review Board and determined to be exempt (No. 2025-109, September 10, 2025) because it involved the secondary analysis of de-identified data obtained through the TriNetX platform.

**Conflict of Interest:** The authors declare no potential conflicts of interest.

**Financial Disclosure:** No financial support was received for the preparation of this research article.

**Use of AI for Writing Assistance:** The authors declare that no artificial intelligence (AI)-assisted technologies, including large language models, chatbots, or image-generation tools, were used in the conception, writing, analysis, or preparation of this manuscript.

**Author Contributions:** Concept: HA; Design: HA; Supervision: SG, JL; Funding: HA, SG; Materials: HA, IAR; Data Collection and/or Processing: HA, IAR, EA, SG; Analysis and/or Interpretation: HA, IAR, EA, SG; Literature Review: HA, IAR, EA, SG; Writing: HA; Critical Review: IAR, EA, SG, JL.

**Acknowledgement:** A preliminary abstract based on this work was submitted to the American College of Gastroenterology (ACG) Annual Meeting in October 2025 (Arizona) and was accepted as a poster presentation. The abstract was subsequently published by the American College of Gastroenterology (DOI: 10.14309/01.ajg.0001139060.76824.1f). The full manuscript has not been published previously and is not under consideration by any other journal.

**Peer-review:** Externally peer-reviewed.

## References

- Liu YB, Chen MK. Epidemiology of liver cirrhosis and associated complications: Current knowledge and future directions. *World J Gastroenterol* 2022;28(41):5910-5930. [CrossRef]
- Lee S, Saffo S. Evolution of care in cirrhosis: Preventing hepatic decompensation through pharmacotherapy. *World J Gastroenterol* 2023;29(1):61-74. [CrossRef]
- Piano S, Reiberger T, Bosch J. Mechanisms and implications of recompensation in cirrhosis. *JHEP Reports* 2024;6(12):101233. [CrossRef]
- Targher G, Valenti L, Byrne CD. Metabolic dysfunction-associated steatotic liver disease. *N Engl J Med* 2025;393(7):683-698. [CrossRef]
- Vallon V. The mechanisms and therapeutic potential of SGLT2 inhibitors in diabetes mellitus. *Annu Rev Med* 2015;66(1):255-270. [CrossRef]
- Youssef ME, Yahya G, Popoviciu MS, Cavalu S, Abd-Eldayem MA, Saber S. Unlocking the full potential of SGLT2 inhibitors: Expanding applications beyond glycemic control. *Int J Mol Sci* 2023;24(7):6039. [CrossRef]
- Fonseca-Correa JI, Correa-Rotter R. Sodium-glucose cotransporter 2 inhibitors mechanisms of action: A review. *Front Med (Lausanne)* 2021;8:777861. [CrossRef]
- Inoue M, Hayashi A, Taguchi T, Arai R, Sasaki S, Takano K, et al. Effects of canagliflozin on body composition and hepatic fat content in type 2 diabetes patients with non-alcoholic fatty liver disease. *J Diabetes Investig* 2019;10(4):1004-1011. [CrossRef]
- Leiter LA, Forst T, Polidori D, Balis DA, Xie J, Sha S. Effect of canagliflozin on liver function tests in patients with type 2 diabetes. *Diabetes Metab* 2016;42(1):25-32. [CrossRef]
- Taheri H, Malek M, Ismail-Beigi F, Zamani F, Sohrabi M, Reza Babaei M, et al. Effect of empagliflozin on liver steatosis and fibrosis in patients with non-alcoholic fatty liver disease without diabetes: A randomized, double-blind, placebo-controlled Trial. *Adv Ther* 2020;37(11):4697-4708. [CrossRef]
- Coelho F dos S, Borges-Canha M, von Hafe M, Neves JS, Vale C, Leite AR, et al. Effects of sodium-glucose co-transporter 2 inhibitors on liver parameters and steatosis: A meta-analysis of randomized clinical trials. *Diabetes Metab Res Rev* 2021;37(6):e3413. [CrossRef]
- Kronsten VT, Shawcross DL. Clinical implications of inflammation in patients with cirrhosis. *Am J Gastroenterol* 2025;120(1):65-74. [CrossRef]
- Arroyo V, Angeli P, Moreau R, Jalan R, Clària J, Trebicka J, et al. The systemic inflammation hypothesis: Towards a new paradigm of acute decompensation and multiorgan failure in cirrhosis. *J Hepatol* 2021;74(3):670-685. [CrossRef]
- Bray JJH, Foster-Davies H, Stephens JW. A systematic review examining the effects of sodium-glucose cotransporter-2 inhibitors (SGLT2is) on biomarkers of inflammation and oxidative stress. *Diabetes Res Clin Pract* 2020;168:108368. [CrossRef]
- Schönberger E, Mihaljević V, Steiner K, Šarić S, Kurevija T, Majnarić LT, et al. Immunomodulatory effects of SGLT2 inhibitors-targeting inflammation and oxidative stress in aging. *Int J Environ Res Public Health* 2023;20(17):6671. [CrossRef]
- Theofilis P, Sagris M, Oikonomou E, Antonopoulos AS, Siasos G, Tsioufis K, et al. The anti-inflammatory effect of novel antidiabetic agents. *Life (Basel)* 2022;12(11):1829. [CrossRef]
- Ahmed H, Gomaa S, Abdulrazzak E, Alabdul Razzak I, Kovalovich KK. Therapeutic potential of sodium-glucose cotransporter 2 (SGLT2) inhibitors in liver disease: Focus on cirrhosis. *Cureus* 2025;17(5):e84768. [CrossRef]
- Kalambokis GN, Tsiakas I, Filippas-Ntekuan S, Christaki M, Despotis G, Milionis H. Empagliflozin eliminates refractory ascites and hepatic hydrothorax in a patient with primary biliary cirrhosis. *Am J Gastroenterol* 2021;116(3):618-619. [CrossRef]
- Kalambokis G, Tsiakas I, Filippas-Ntekouan S, Christaki M, Milionis H. Empagliflozin controls cirrhotic refractory ascites along with improvement of natriuresis and circulatory, cardiac, and renal function: A pilot study. *Eur J Intern Med* 2024;130:162-164. [CrossRef]
- Bakosh MF, Ghazy RM, Ellakany WI, Kamal A. Empagliflozin as a novel therapy for cirrhotic refractory ascites: a randomized controlled study. *Egypt Liv J* 2024;14(1):76. [CrossRef]
- Shen I, Stojanova J, Yeo M, Olsen N, Lockart I, Wang M, et al. A potential novel treatment for cirrhosis-related ascites: Empagliflozin is safe and tolerable in advanced chronic liver disease. *Br J Clin Pharmacol* 2024;90(10):2529-2538. [CrossRef]
- Kuchay MS, Krishan S, Mishra SK, Farooqui KJ, Singh MK, Wasir JS, et al. Effect of empagliflozin on liver fat in patients with type 2 diabetes and nonalcoholic fatty liver disease: A randomized controlled trial (E-LIFT Trial). *Diabetes Care* 2018;41(8):1801-1808. [CrossRef]
- Kahl S, Gancheva S, Straßburger K, Herder C, Machann J, Katsuyama H, et al. Empagliflozin effectively lowers liver fat content in well-controlled type 2 diabetes: A randomized, double-blind, phase 4, placebo-controlled trial. *Diabetes Care* 2020;43(2):298-305. [CrossRef]

24. Abdelgani S, Khattab A, Adams J, Baskoy G, Brown M, Clarke G, et al. Empagliflozin reduces liver fat in individuals with and without diabetes. *Diabetes Care* 2024;47(4):668-675. [\[CrossRef\]](#)
25. Cheung KS, Ng HY, Hui RWH, Lam LK, Mak LY, Ho YC, et al. Effects of empagliflozin on liver fat in patients with metabolic dysfunction-associated steatotic liver disease without diabetes mellitus: A randomized, double-blind, placebo-controlled trial. *Hepatology* 2024;80(4):916-927. [\[CrossRef\]](#)
26. Singh V, De A, Aggrawal R, Singh A, Charak S, Bhagat N. Safety and efficacy of dapagliflozin in recurrent ascites: A pilot study. *Dig Dis Sci* 2025;70(2):835-842. [\[CrossRef\]](#)
27. Seif El-Din Z, Afify M, Zayed E, Elsabaawy D, Tharwa ES, Elsharawy A, et al. Dapagliflozin as an oral antihyperglycemic agent in the management of diabetes mellitus in patients with liver cirrhosis. *World J Exp Med* 2024;14(4):95272. [\[CrossRef\]](#)

## REVIEW ARTICLE

# Occult hepatitis B infection

 Mikha Eliana Wati,  Yusra

*Department of Clinical Pathology, Universitas Indonesia, Jakarta, Indonesia*

## Points to Note

- **Synthesis of Current Evidence:** Occult Hepatitis B Infection (OBI) is marked by undetectable HBsAg but detectable HBV DNA in the liver. It poses risks of transmission, reactivation, and hepatocellular carcinoma (HCC), particularly in immunocompromised patients. Prevalence is higher in Southeast Asia. Diagnosis relies on liver HBV DNA testing.
- **Major Controversies:** There are controversies regarding false OBI detection due to HBsAg mutations. The necessity of antiviral therapy for OBI remains debated.
- **Future Directions:** Future research should focus on improving diagnostics, exploring antiviral treatments, and understanding long-term risks like liver cancer.

## ABSTRACT

Occult Hepatitis B Infection (OBI) is a condition in which HBsAg tests are negative, but Hepatitis B virus (HBV) DNA is detectable in the liver, with or without low levels of HBV DNA in the blood (<200 IU/mL). The Hepatitis B surface antigen (HBsAg) negative status in OBI may result from the absence or low production of HBsAg due to immune system defense mechanisms or mutations in the S genome of HBV DNA, which make HBsAg undetectable. The gold standard for diagnosing OBI is testing for HBV DNA from liver tissue, with an alternative method being HBV DNA testing from serum. Patients with OBI may be at risk of transmitting HBV to others through blood transfusions or organ transplants. Reactivation may occur, especially in OBI patients who are immunocompromised or undergoing immunosuppressive therapy. Antiviral prophylaxis may be considered for OBI patients at risk of reactivation. Additionally, OBI patients also carry a risk of developing hepatocellular carcinoma (HCC), similar to those with non-occult hepatitis B infection. Antiviral therapy for OBI is generally not required unless the case represents false OBI due to HBsAg mutation.

**Keywords:** Hepatitis B surface antigen, hepatitis B virus, occult hepatitis B infection.

**How to cite this article:** Wati ME, Yusra. Occult hepatitis B infection. Hepatology Forum 2026; 7(2):146–153.

**Received:** March 14, 2025; **Revised:** September 10, 2025; **Accepted:** September 18, 2025; **Available Online:** April 14, 2026

**Corresponding author:** Mikha Eliana Wati; Department of Clinical Pathology, Universitas Indonesia, Jakarta, Indonesia; **E-mail:** mikhaeliana@gmail.com



This work is licensed under a Creative Commons Attribution-NonCommercial 4.0 International License.

## Introduction

Hepatitis B is a disease caused by the Hepatitis B virus (HBV). This disease has a wide spectrum, ranging from occult infection to fulminant hepatitis with cirrhosis and hepatocellular carcinoma (HCC).<sup>[1]</sup> In 2019, the World Health Organization (WHO) reported that 296 million people were living with HBV infection, with 1.5 million new cases and 820,000 deaths annually due to complications such as cirrhosis and HCC.<sup>[2]</sup> The majority of HBV-related deaths occurred in Asia (74%). In Indonesia, the prevalence of HBV infection was 7.1%, based on data from Riskesdas in 2013. Occult Hepatitis B Infection (OBI) plays a significant role in Hepatitis B cases in Indonesia.<sup>[3]</sup>

OBI is a condition in which Hepatitis B surface antigen (HBsAg) is negative, but viral replication is present in the liver, with low levels of HBV DNA (<200 IU/mL). Although HBV DNA is detected at low levels, patients with OBI can still transmit the virus.<sup>[4]</sup> The global prevalence of OBI among blood donors who tested negative for HBsAg was found to be 6.2% in a sample of 6,757,391 blood donors. Southeast Asia showed a higher prevalence of 16.73% among 2,243 blood donors.<sup>[5]</sup> In Indonesia, OBI prevalence was 8.1% among 309 blood donors with negative HBsAg. This variation is attributed to differences in the endemicity of HBV infection.<sup>[1]</sup>

OBI was first reported in the 1970s in a post-transfusion patient who developed HBV infection despite receiving HBsAg-negative blood. In 1999, HBV DNA was detected in a liver biopsy from a patient with chronic liver disease who tested negative for HBsAg. Since then, the term OBI has appeared in numerous medical publications. The primary concern regarding OBI is its clinical impact. Blood transfusion or liver transplantation from OBI donors places recipients at risk of Hepatitis B infection, similar to transfusions from donors who test positive for HBsAg. OBI can reactivate into full-blown Hepatitis B infection and progress to cirrhosis and HCC, particularly in immunosuppressed patients.<sup>[4]</sup> This paper explores the virology of HBV and the definition of OBI, disease progression, diagnosis, transmission risk, reactivation, complications, and treatment.

## Definition of OBI

OBI is defined as the presence of competent HBV capable of replication, indicated by the detection of HBV DNA in the liver with or without the presence of HBV DNA in the patient's blood, along with a negative HBsAg result using currently available HBsAg tests. The HBV DNA detected in OBI is typically intermittent and at low levels, usually less than 200 IU/mL or 1,000 viral copies/mL. This characteristic distinguishes OBI from overt Hepatitis B infection, in which a positive HBsAg result is accompanied by a high viral load.

OBI can be classified based on antibody profiles against HBV into seropositive and seronegative OBI. In seropositive OBI, antibodies against the HBV core (anti-HBc) are present. Approximately 80% of OBI cases are seropositive. In contrast, anti-HBc is absent in seronegative OBI. The undetectable HBsAg in OBI may result from HBsAg levels being too low to be detected, failure of HBsAg production, or

mutations in HBsAg itself. Mutations in HBsAg cause "false OBI," in which HBsAg tests are negative despite high levels of HBV DNA due to active viral replication.<sup>[4,6]</sup>

## Hepatitis B Virology

Hepatitis B virus is an enveloped virus of small size (42–50 nm) containing partially double-stranded circular DNA. The viral envelope consists of lipids and HBsAg proteins on the surface, which vary in size (small, medium, and large). The nucleocapsid has an icosahedral shape with 90–120 Hepatitis B core (HBc) proteins or Hepatitis B core antigen (HBcAg). Inside the nucleocapsid are the HBV genome and viral polymerase. Hepatitis B e-antigen (HBeAg) is a product generated during the translation process and serves as a marker of viral replication.<sup>[7,8]</sup>

The genomic structure of HBV consists of the S, P, C, and X genes, which overlap with each other. The S gene, comprising the pre-S1, pre-S2, and S open reading frames (ORF), is responsible for the production of HBsAg. The P gene, the longest gene, encodes the viral polymerase. The C gene consists of the pre-C ORF and C ORF, which contribute to the formation of the HBc protein and the secretion of HBeAg. The X gene encodes the HBx protein, a non-structural protein of HBV.

## Disease Progression

The absence of HBsAg in OBI is caused by several mechanisms, including recovery from acute and chronic Hepatitis B infections, the absence of Hepatitis B infection markers in early infection (as seen in seronegative OBI), and mutations in the HBV S variant. A positive result for HBsAg and IgM antibodies against HBcAg (anti-HBc) can be found during acute Hepatitis B infection. The persistence of HBsAg for more than six months indicates chronic infection. Recovery from Hepatitis B infection may result in HBsAg becoming negative. In addition to anti-HBc, anti-HBs may also be detected as a marker of prior acute infection. However, it should be noted that in some cases of Hepatitis B infection, HBsAg may disappear spontaneously without any treatment.<sup>[1,6,9]</sup>

Seronegative OBI may result from the loss of anti-HBc or anti-HBs during disease progression or from the complete absence of serological markers except for HBV DNA.<sup>[6,10]</sup> A summary of OBI progression is shown in Figure 1.

The persistence of HBV DNA in the hepatocytes of OBI patients is caused by the suppression of viral replication and protein expression by the host immune system. However, the immune system cannot completely eradicate the virus from infected hepatocytes. Suppression of HBV DNA transcription and replication results in low plasma HBV DNA levels. Nevertheless, the covalently closed circular DNA (cccDNA) of HBV in OBI remains capable of viral replication. Factors involved in suppressing HBV replication in OBI include the host immune response, coinfection, and epigenetic mechanisms. The immune system limits antigen expression through efficient

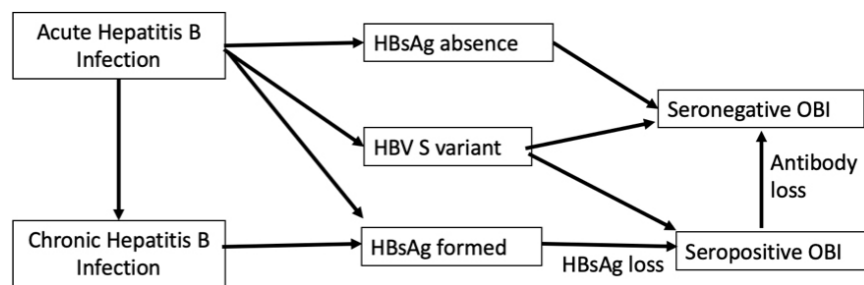


**Figure 1.** Progression from hepatitis B infection to seropositive and seronegative OBI.

T-cell responses. Coinfection with other viruses, such as Hepatitis C, can inhibit HBV replication. Epigenetic modification, such as CpG methylation of cccDNA, can enhance histone methylation of cccDNA. This alteration modifies transcriptional activity and reduces HBV mRNA formation, ultimately resulting in decreased HBV protein synthesis.<sup>[4,6,11]</sup>

Overt HBV infection begins with the presence of circulating virus in the bloodstream. The HBs protein on the viral surface initially binds to heparan sulfate proteoglycan (HSPG) with low affinity. High-affinity binding occurs between the HBs protein and sodium taurocholate co-transporting polypeptide (NTCP), forming the HBV–NTCP complex. The HBV–NTCP complex then enters hepatocytes via endocytosis. Inside the hepatocyte, the relaxed circular DNA (rcDNA) is released into the nucleus, where it is converted into cccDNA or integrated into host DNA. The cccDNA is transcribed into HBV mRNA, which is then translated into viral proteins. The viral proteins, including HBsAg, are released into circulation and become detectable by diagnostic tests.<sup>[6,11,12]</sup>

In OBI, the infection starts with HBV nucleocapsids already present within hepatocytes, which then enter the nucleus to form rcDNA. The rcDNA is converted into cccDNA. The cccDNA undergoes methylation, specifically CpG methylation by DNA methyltransferase (DNMT), which prevents its expression. DNA methylation leads to the binding of DNA methyl-binding proteins (DNA MBP) to the methylated DNA, which then recruits transcriptional corepressors such as histone deacetylase (HDAC). Elevated levels of HDAC, along with histone methyltransferase (HMT) and Sirtuin 1 (Sirt1), enhance histone methylation, further suppressing cccDNA expression. This process results in HBx-mutated HBV, which produces less HBV mRNA. In HBx-mutated HBV, the increase in apolipoprotein B mRNA-editing enzyme catalytic polypeptide-like 3 (APOBEC3) inhibits heterogeneous nuclear ribonucleoprotein K (hnRNPK), further decreasing HBV mRNA synthesis. The reduced HBV mRNA leads to the production of fewer HBV proteins. Additionally, increased microRNA (miRNA) activity also inhibits HBV protein synthesis, further decreasing the amount of protein formed.<sup>[6,11,12]</sup>

There are some cases in which HBsAg may not be detected by assays due to mutations. These conditions are referred to as “false OBI.” HBV DNA detected in false OBI cases can be high—comparable to that in overt Hepatitis B infection—but with negative HBsAg due to mutation. HBV with mutations in the S gene, particularly in the

pre-S region, is referred to as the S variant. The S variant HBV can form modified HBsAg with low antigenicity. This modified HBsAg in HBV S variants cannot be detected by some commercial HBsAg tests, although cases of OBI due to S gene mutations are rare. S gene mutations most frequently occur in the  $\alpha$  determinant sequence region. The substitution of glycine with arginine at position 145 (G145R) is the most frequently reported mutation. This mutation was first identified by Carman in 1990 in an infant born to a carrier mother who had been vaccinated and given immunoglobulin therapy since birth, yet the baby developed HBV infection.<sup>[13]</sup> A study by Araujo et al.<sup>[14]</sup> in Brazil, which sequenced DNA from OBI patients, found S mutations in the E164D, I195M, P217L, and P120S regions, with E164D and P120S located in the  $\alpha$  determinant sequence region.

## Diagnosis of OBI

The diagnosis of OBI is based on the detection of HBV DNA from a patient’s liver biopsy along with a negative HBsAg result. The gold standard for diagnosing OBI is testing for HBV DNA in liver biopsy samples; however, this test has not yet been standardized or validated. Other tests that may be performed include testing for HBV DNA in blood samples, as well as HBsAg, anti-HBc, and anti-HBs.<sup>[6,15]</sup> The diagnostic pathway for suspected OBI is illustrated in Figure 2.

## HBV DNA

The recommended method for HBV DNA testing in liver tissue samples is nested PCR (Polymerase Chain Reaction) or real-time PCR, which amplifies at least three regions of the viral genome.<sup>[4,6]</sup> A study by Faria et al.<sup>[16]</sup> compared nested PCR from liver biopsy using two protocols. Protocol 1 amplified four regions of the viral genome, while Protocol 2 amplified two regions to confirm the diagnosis of OBI in 104 HBsAg-negative patients with chronic liver disease. Protocol 1 demonstrated higher sensitivity in detecting HBV DNA (12.5%) compared to Protocol 2 (8.7%).

HBV DNA testing from blood samples is more commonly used than liver tissue testing due to the ease of obtaining blood samples, whereas liver biopsy is more invasive. However, HBV DNA found in liver tissue remains the gold standard for diagnosing OBI. This is supported by a study conducted by Wang et al.,<sup>[15]</sup> which compared HBV DNA testing from liver tissue. Table 1 presents the results of three studies compiled by Wang et al.,<sup>[15]</sup> showing that HBV DNA detection

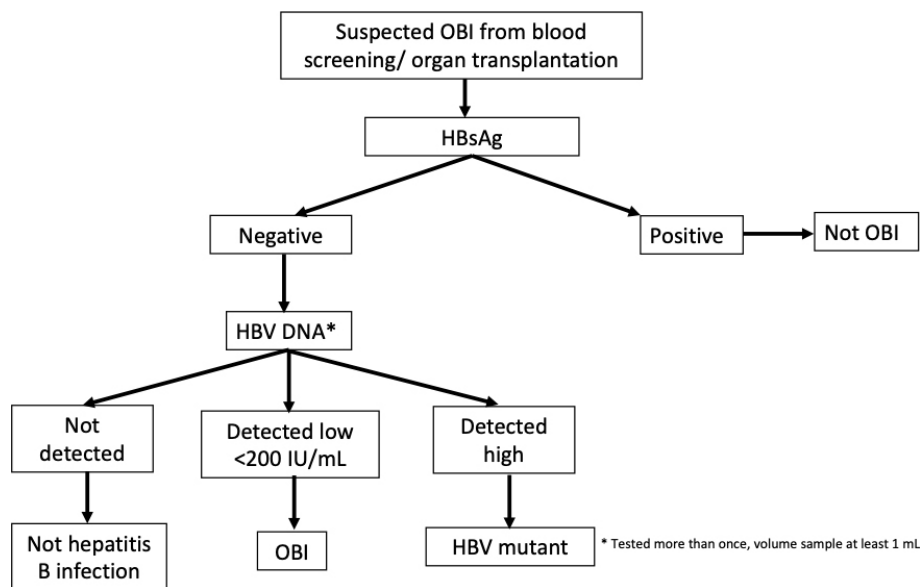


**Figure 2.** Diagnosis pathway of OBI.

**Table 1.** OBI incidence based on detected HBV DNA from liver tissue compared to blood<sup>[15]</sup>

Study	Country	Year	Sample size	OBI incidence	
				Liver tissue	Blood
Yuki et al. <sup>[17]</sup>	Japan	2003	13	100%	21%
Komori et al. <sup>[18]</sup>	Japan	2001	15	100%	13.3%
Knöll et al. <sup>[19]</sup>	Germany	2006	545	41%	8.1%

HBV: Hepatitis B virus; OBI: Occult hepatitis B infection.

in liver tissue had higher sensitivity for OBI than detection in blood samples.<sup>[17-19]</sup> This finding is also supported by another study from Cakal et al.,<sup>[20]</sup> which assessed the presence of OBI in 59 patients with chronic Hepatitis C and negative HBsAg. In that study, 16 patients with negative HBsAg had positive HBV DNA in their liver tissue, but none of these patients had positive serum HBV DNA.<sup>[20]</sup>

HBV DNA detected in the blood of OBI patients is typically at low levels, usually <200 IU/mL, and 80–90% of cases show levels <20 IU/mL. Meanwhile, the detection limit of current commercial HBV DNA tests is 10–20 IU/mL. HBV DNA in the blood is also detected intermittently, making it harder to identify. Therefore, it is recommended that blood HBV DNA testing be performed more than once, using a sample volume of at least 1 mL. HBV DNA testing is crucial for distinguishing between true occult infection and “false OBI.”<sup>[15,21]</sup>

## HBsAg

The detection limit for HBsAg testing ranges from 0.005–0.05 IU/mL (Table 2). HBsAg testing with a minimum detection limit of 0.005 IU/mL can detect HBsAg in 5–48% of patients who were previously HBsAg-negative.<sup>[4,11,22-24]</sup> Although current commercial HBsAg tests

**Table 2.** Lower limit of detection of HBsAg test<sup>[11]</sup>

HBsAg test	Manufacturer	Lower limit detection (IU/mL)
Architect HBsAg QT	Abbott Laboratories	0.05
Elecsys HBsAg II	Roche Diagnostics	0.05
Liaison XL Murex HBsAg Quant	DiaSorin	0.03
Lumipulse HBsAg-Quant	Fujirebio, Inc.	0.005
Ultrahigh sensitive HISCL HBsAg	Symex Co, Ltd	0.0005

HBsAg: Hepatitis B surface antigen; HISCL: Highly sensitive chemiluminescent.

can detect small amounts of HBsAg, they still have limited ability to identify HBsAg S variants. Therefore, the use of anti-HBs conjugates targeting multiple epitopes of HBsAg improves the ability to detect HBV S variants.<sup>[4,6]</sup>

Kuhns et al.<sup>[24]</sup> found in their study that the latest prototype HBsAg test with a lower detection limit could detect OBI in 3 of 7 HBV samples carrying HBsAg escape mutations. In the remaining four samples that were not detected, it was likely due to HBsAg levels being below the detection threshold rather than due to the mutations themselves. These mutations were detectable in other studies using HBsAg tests with the same prototype.<sup>[24,25]</sup>

## Anti-HBc

The anti-HBc test can serve as an alternative for diagnosing OBI in organ or blood donors, patients who are about to receive immunosuppressive therapy, or for use in epidemiological studies. This test is particularly useful when liver tissue is unavailable and access to HBV DNA testing is limited or delayed. A negative result for HBV DNA in the blood on the

**Table 3.** Incidence of OBI based on HBV serology<sup>[26]</sup>

Anti-HBs	Anti-HBc	Anti-HBe	OBI incidence
+	+	-	1.87% (13/695)
-	+	-	3.73% (10/268)
+	+	+	6.27% (53/845)
-	+	+	15.61% (32/205)

HBs: Hepatitis B surface; HBc: Hepatitis B core; HBe: Hepatitis B e antigen; OBI: Occult hepatitis B infection.

first test does not rule out the diagnosis of OBI; therefore, additional anti-HBc testing is necessary. However, a negative anti-HBc result also does not exclude OBI, as seronegative OBI cases exist.<sup>[6,11]</sup>

This is supported by a study conducted by Cakal et al.,<sup>[20]</sup> which found that 18.71% of OBI patients were seronegative for both anti-HBc and anti-HBs. A positive anti-HBc result indicates past or current HBV infection; however, confirming the diagnosis of OBI still requires HBV DNA testing.<sup>[6,11]</sup>

### Anti-HBs

Anti-HBs is a protective marker against HBsAg infection. Its presence can neutralize the virus and resolve OBI, thereby reducing the likelihood of OBI.<sup>[11]</sup> This was demonstrated in a study by Cai et al.,<sup>[26]</sup> which showed that the incidence of OBI was higher in patients who were anti-HBs negative, as shown in Table 3. The data in Table 3 highlight the role of anti-HBs in neutralizing HBV infection, resulting in a lower OBI incidence in individuals who are anti-HBs positive.

### HBeAg

HBeAg is a circulating HBV antigen found in patient serum. Although HBeAg is not required for replication, its presence indicates active viral replication. Therefore, a negative HBeAg result does not rule out the diagnosis of OBI. A positive HBeAg in OBI cases contradicts the typically negative HBsAg result.<sup>[7]</sup> In a case report by Han et al.,<sup>[27]</sup> two patients were HBsAg negative but both HBV DNA and HBeAg were positive. They were later found to have HBV escape mutations.

### HBcrAg

Hepatitis B core-related antigen (HBcrAg) consists of HBcAg, HBeAg, and the 22 kDa precore protein (p22cr). According to the European Association for the Study of the Liver<sup>[28]</sup> and a systematic review by Mak et al.<sup>[29]</sup> (Table 4), HBcrAg reflects intrahepatic DNA and cccDNA. This is also supported by a case report by Yokoyama et al.<sup>[30]</sup> in Japan. In that case, a patient who was negative for HBsAg, HBeAg, anti-HBc, anti-HBs, and anti-HBe, and had undetectable HBV DNA (<1300 IU/mL), was found to have elevated HBcrAg levels and experienced recurrence of hepatocellular carcinoma (HCC).

The use of HBcrAg to detect HCC complications in patients with negative HBsAg is also supported by a study by Hsieh et al.,<sup>[31]</sup> which found that positive HBcrAg significantly increased the risk of developing HCC compared to patients with negative HBcrAg (OR 9.3

**Table 4.** HBcrAg correlation with intrahepatic HBV DNA and cccDNA<sup>[29]</sup>

	Sample size	Correlation coefficient	p
HBcrAg with HBV DNA	93	0.7	<0.001
	305	0.67	<0.0001
HBcrAg with cccDNA	93	0.64	<0.001
	138	0.7	<0.0001
	31	0.482	<0.006

HBV: Hepatitis B virus; HBcrAg: Hepatitis B core-related antigen.

**Table 5.** Post-transplantation HBV infection incidence in recipient from HBsAg negative donor<sup>[35]</sup>

Recipient serology		HBV incidence without prophylaxis	HBV incidence with prophylaxis
Anti-HBs	Anti-HBc		
-	-	47.8%	12% <sup>c</sup>
-	+	13.1% <sup>ab</sup>	3.4% <sup>c</sup>
+	-	9.7% <sup>a</sup>	0%
+	+	1.4% <sup>a</sup>	N/A

a: Statistically significant compared with naive HBV (negative anti-HBs and anti-HBc) without prophylaxis; b: Statistically significant compared with positive anti-HBs and anti HBc without prophylaxis; c: Statistically significant compared with group without prophylaxis; HBV: Hepatitis B virus; HBsAg: Hepatitis B surface antigen; HBs: Hepatitis B surface; HBc: Hepatitis B core.

[3.3–26.4];  $p < 0.001$ ). This demonstrates that HBcrAg can help monitor the progression of OBI toward HCC. However, since HBcrAg testing is relatively new and studies on its correlation are still limited, it cannot yet be routinely used to diagnose OBI.

## Transmission of OBI

In OBI, cccDNA can persist in hepatocytes for a long time, even when HBsAg is not detectable. Various studies related to blood donation from patients with OBI have shown that it can lead to Hepatitis B infection in the recipient. Blood product screening to prevent the transmission of HBV infection through transfusion usually relies on HBsAg testing. However, HBV infection from an OBI donor will not be detected using this parameter alone. Therefore, some blood transfusion units implement PCR screening for HBV DNA using a pooling system to reduce costs. Six to fifty HBsAg-negative donor samples are collected, pooled, and tested for HBV DNA by PCR. If a positive result is found, further HBV DNA testing is conducted on each sample to identify the positive one.<sup>[32]</sup>

The transmission rate of OBI through blood products is highest with fresh frozen plasma (FFP) and thrombocyte concentrate (TC), at 85% and 51%, respectively. Blood products such as packed red cells (PRC) have a lower transmission rate, at 24%.<sup>[33]</sup> This is because FFP and TC contain more plasma volume than PRC, resulting in a higher

number of virions being transfused. This is supported by a case report by Candotti et al.,<sup>[34]</sup> which identified nine cases of HBV infection in recipients from OBI donors. Seven of these cases involved FFP recipients, while two involved PRC recipients.

The risk of HBV transmission from OBI patients can also occur through organ transplantation. Liver transplant recipients are at a similar risk of HBV infection whether the organ donor has overt HBV infection or OBI.<sup>[4]</sup> A systematic review conducted by Cholongitas et al.<sup>[35]</sup> found that the incidence of HBV transmission from OBI donors was highest in recipients who had never been infected with HBV. The administration of prophylaxis, such as lamivudine, significantly reduced the proportion of recipients who developed HBV infection. The most significant reduction was observed in recipients who were HBV naïve, as shown in Table 5. Table 5 also highlights the protective effect of anti-HBs, with populations positive for anti-HBs showing a lower incidence of HBV infection compared to those who were anti-HBs negative.

## Reactivation and Complications of OBI

Patients with OBI are at risk of reactivation. The reactivation of HBV in OBI patients is defined as seroconversion to HBsAg positivity or an increase in serum HBV DNA by at least 1 log above the lower detection limit in patients who were previously undetectable, or a 1-log increase in those who previously had low HBV DNA levels. Reactivation typically occurs in patients receiving chemotherapy or immunosuppressive therapy. Approximately 40% of OBI patients experience HBV reactivation during immunosuppressive treatment, with the highest risk observed in those receiving anti-CD20 therapy.

HBV reactivation can also occur in patients with immunodeficiency due to HIV infection. The American Association for the Study of Liver Diseases (AASLD) and the Infectious Diseases Society of America (IDSA) recommend that HIV patients undergo HBV DNA testing and Hepatitis B serology to detect potential OBI and assess the risk of reactivation. Antiviral prophylaxis, such as nucleotide analogs, may be given to OBI patients who are at risk of HBV reactivation. Patients considered at low risk do not require prophylaxis but should be closely monitored.<sup>[6,36]</sup>

OBI patients are also at risk of progressing to hepatocellular carcinoma (HCC), particularly those with chronic Hepatitis B. A study by Mak et al.<sup>[11]</sup> found that 60–70% of patients with HCC of unknown etiology in Asia and Europe had OBI in their liver tissue. Furthermore, among 82 patients with cirrhosis of unknown cause who had OBI, 100% developed HCC within 5.8 years, while cirrhosis patients without OBI had only a 17.6% risk of developing HCC within 10 years.

Co-infection of OBI with Hepatitis C virus (HCV) further increases the risk of developing HCC. This co-infection leads to more severe liver damage compared to OBI without HCV co-infection.<sup>[4,7,11]</sup>

The presence of HBV DNA in OBI patients contributes to HCC progression because HBV DNA is proto-oncogenic within hepatocytes. HBV can integrate into the host genome and produce proteins with carcinogenic properties, such as the HBx protein, and also induce liver

inflammation. The integration of HBV into the host genome disrupts the cell cycle and promotes tumor progression. The HBx protein, a non-structural protein of HBV, can regulate the cell cycle, leading to dysregulation. This dysregulation causes mitochondrial dysfunction and uncontrolled cell proliferation, which supports HCC carcinogenesis.

Chronic liver inflammation can result in continuous hepatocellular damage, progressing to liver cirrhosis. In cases of OBI with HBsAg mutations, HBsAg becomes undetectable and may accumulate within cells. This accumulation induces endoplasmic reticulum stress, leading to DNA damage, genomic instability, and progression toward cancer.<sup>[4,7,11]</sup>

## Treatment

Treatment of OBI patients currently does not require antiviral therapy. If the goal is to completely eliminate HBV from the hepatocytes of OBI patients, strategies involving the direct elimination of cccDNA in hepatocytes can be considered. One such approach includes gene-editing techniques, such as CRISPR/Cas9, which specifically target cccDNA.

In addition to cccDNA elimination, another potential strategy is to enhance T-cell responses to eliminate infected hepatocytes in the liver. However, this therapeutic approach still requires further research. Therefore, current OBI management focuses primarily on preventing reactivation, transmission, and complications such as HCC.

It is important to note that in cases of false OBI, where HBsAg has mutated and is undetectable with current HBsAg tests, treatment should follow the same approach as for non-occult HBV infection, including the administration of antiviral therapy. Suspicion of mutation is particularly supported by a reactive HBeAg, which indicates active viral replication.<sup>[6,11]</sup>

Prophylactic therapy, such as lamivudine, may be given to OBI patients at risk of reactivation, especially those with detectable serum HBV DNA, even in small amounts. Prophylactic therapy should be continued for up to six months after the end of immunosuppressive treatment, or for 12 months after therapies targeting B cells. Monitoring should include liver function tests, HBV DNA, and HBsAg every three months.<sup>[37–39]</sup>

## Conclusion

It is important to consider OBI when HBsAg is found to be negative, especially in endemic areas. Patients with OBI are at risk of transmitting HBV infection through blood transfusion and organ transplantation. Reactivation may occur, particularly in patients with HIV or those receiving immunosuppressive therapy, leading to overt HBV infection. They are also at risk of developing hepatocellular carcinoma due to persistent HBV infection.

**Conflict of Interest:** The authors have no conflict of interest to declare.

**Financial Disclosure:** The authors declared that this study has received no financial support.

**Use of AI for Writing Assistance:** Artificial intelligence was not used in the preparation of the article.

**Author Contributions:** Concept: MEW, Y; Design: MEW, Y; Supervision: MEW, Y; Funding: MEW, Y; Materials: MEW, Y; Data Collection and/or Processing: MEW, Y; Analysis and/or Interpretation: MEW, Y; Literature Search: MEW, Y; Writing: MEW, Y; Critical Reviews: MEW, Y.

**Peer-review:** Externally peer-reviewed.

## References

- Thedja MD, Roni M, Harahap AR, Siregar NC, Muljono DH. Occult hepatitis B in blood donors in Indonesia: Altered antigenicity of the hepatitis B virus surface protein. *Hepatol Int* 2010;4(3):608-614. [CrossRef]
- Teo EK, Lok ASF. Epidemiology, transmission, and prevention of hepatitis B virus infection. UpToDate; 2024. Available at: <https://www.uptodate.com/contents/epidemiology-transmission-and-prevention-of-hepatitis-b-virus-infection> Accessed on Feb 23, 2024.
- Muljono DH. Epidemiology of hepatitis B and C in republic of Indonesia. *Euroasian J Hepatogastroenterol* 2017;7(1):55-59. [CrossRef]
- Saitta C, Pollicino T, Raimondo G. Occult hepatitis B virus infection: an update. *Viruses* 2022;14(7):1504. [CrossRef]
- Takuissu GR, Kenmoe S, Atsama MA, Okobalemba EA, Mbaga DS, Ebo-go-Belobo JT, et al. Global epidemiology of occult hepatitis B virus infections in blood donors, a systematic review and meta-analysis. *PLoS One* 2022;17(8):e0272920. [CrossRef]
- Raimondo G, Locarnini S, Pollicino T, Levrero M, Zoulim F, Lok AS, et al. Update of the statements on biology and clinical impact of occult hepatitis B virus infection. *J Hepatol* 2019;71:397-408. [CrossRef]
- Chapus L, Martinez MG, Testoni B, Zoulim F. Molecular virology and life cycle of hepatitis B virus. In: Kao JH, editor. *Hepatitis B virus and liver disease*. Edisi 2. Springer: Singapore; 2021. p. 1-508. [CrossRef]
- Anand P, Singh S, Schelonka RL, Tekleab AM, Upadhyay A. Hepatitis B infections in neonates. *Newborn* 2022;1(4):368-375. [CrossRef]
- Almeida NAA, Paula VS. Occult Hepatitis B virus (HBV) infection and challenges for hepatitis elimination: a literature review. *J Appl Microbiol* 2022;132(3):1616-1635. [CrossRef]
- Gherlan GS. Occult hepatitis B - the result of the host immune response interaction with different genomic expressions of the virus. *World J Clin Cases* 2022;10(17):5518-5530. [CrossRef]
- Mak LY, Wong DKH, Pollicino T, Raimondo G, Hollinger FB, Yuen MF. Occult hepatitis B infection and hepatocellular carcinoma: epidemiology, virology, hepatocarcinogenesis and clinical significance. *J Hepatol* 2020;73(4):952-964. [CrossRef]
- He P, Zhang P, Fang Y, Han N, Yang W, Xia Z, et al. The role of HBV cccDNA in occult hepatitis B virus infection. *Mol Cell Biochem* 2023;478(10):2297-2307. [CrossRef]
- Lalana Garcés M, Ortiz Pastor O, Solé Enrech G, Guerra-Ruiz AR, Casals Mercadal G, Almería Lafuente A, et al. Control of occult hepatitis B virus infection. *Adv Lab Med* 2022;3(4):321-341. [CrossRef]
- Araújo S dos R, Malheiros AP, Sarmiento VP, Nunes HM, Freitas PEB. Molecular investigation of occult hepatitis B virus infection in a reference center in Northern Brazil. *Braz J Infect Dis* 2022;26(3):102367. [CrossRef]
- Wang C, Xue R, Wang X, Xiao L, Xian J. High-sensitivity HBV DNA test for the diagnosis of occult HBV infection: commonly used but not reliable. *Front Cell Infect Microbiol* 2023;13:1186877. [CrossRef]
- Faria AC, Correa BHM, Faria LC, Vidigal PVT, Xavier MAP, Ferrari TCA. Occult hepatitis B virus infection in patients with chronic liver disease of different etiology in a Brazilian referral center: comparison of two different hepatitis B virus deoxyribonucleic acid amplification protocols: a cross-sectional study. *Sao Paulo Med J* 2022;141(3):e2022147. [CrossRef]
- Yuki N, Nagaoka T, Yamashiro M, Mochizuki K, Kaneko A, Yamamoto K, et al. Long-term histologic and virologic outcomes of acute self-limited hepatitis B. *Hepatology* 2003;37(5):1172-1179. [CrossRef]
- Komori M, Yuki N, Nagaoka T, Yamashiro M, Mochizuki K, Kaneko A, et al. Long-term clinical impact of occult hepatitis B virus infection in chronic hepatitis B patients. *J Hepatol* 2001;35(6):798-804. [CrossRef]
- Knöll A, Hartmann A, Hamoshi H, Weislaeber K, Jilg W. Serological pattern anti-HBc alone: characterization of 552 individuals and clinical significance. *World J Gastroenterol* 2006;12(8):255. [CrossRef]
- Cakal B, Cavus B, Atasoy A, Poda M, Bulakci M, Gulluoglu M, et al. What is the clinical impact of occult HBV infections and anti-HBc positivity in patients with chronic hepatitis C. *Microbiol Immunol* 2022;66(8):386-393. [CrossRef]
- Pollicino T, Raimondo G. Occult hepatitis B infection. *J Hepatol* 2014;61(3):688-689. [CrossRef]
- Ozeki I, Nakajima T, Suii H, Tatsumi R, Yamaguchi M, Kimura M, et al. Analysis of hepatitis B surface antigen (HBsAg) using high-sensitivity HBsAg assays in hepatitis B virus carriers in whom HBsAg seroclearance was confirmed by conventional assays. *Hepatol Res* 2018;48(3):E263-E274. [CrossRef]
- Wong DKH, Chen C, Mak LY, Fung J, Seto WK, Yuen MF. Detection of the hepatitis B surface antigen in patients with occult hepatitis B by use of an assay with enhanced sensitivity. *J Clin Microbiol* 2022;60(2):e0220421. [CrossRef]
- Kuhns MC, Holzmayer V, McNamara AL, Sickinger E, Schultess J, Cloherty GA. Improved detection of early acute, late acute, and occult hepatitis B infections by an increased sensitivity HBsAg assay. *J Clin Virol* 2019;118:41-45. [CrossRef]
- Lou S, Taylor R, Pearce S, Kuhns M, Leary T. An ultra-sensitive Abbott ARCHITECT® assay for the detection of hepatitis B virus surface antigen (HBsAg). *J Clin Virol* 2018;105:18-25. [CrossRef]
- Cai J, Wu W, Wu J, Chen Z, Wu Z, Tang Y, et al. Prevalence and clinical characteristics of hepatitis B surface antigen-negative/hepatitis B core antibody-positive patients with detectable serum hepatitis B virus DNA. *Ann Transl Med* 2022;10(1):25. [CrossRef]
- Han Z, Liu Y, Pan J, Bi Y, Liu J, Zhou YH. Occult hepatitis B virus infection with positive hepatitis B e antigen. *Clin Chim Acta* 2015;438:266-268. [CrossRef]
- Lampertico P, Agarwal K, Berg T, Buti M, Janssen HLA, Papatheodoridis G, et al. EASL 2017 Clinical Practice guidelines on the management of hepatitis B virus infection. *J Hepatol* 2017;67(2):370-398. [CrossRef]
- Mak LY, Wong DKH, Cheung KS, Seto WK, Lai CL, Yuen MF. Review article: hepatitis B core-related antigen (HBcrAg): an emerging marker for chronic hepatitis B virus infection. *Aliment Pharmacol Ther* 2018;47(1):43-54. [CrossRef]
- Yokoyama K, Yamauchi E, Uchida Y, Kitaguchi T, Fukuda H, Yamauchi R, et al. Hepatitis B virus core-related antigen is useful for surveillance of hepatocellular carcinoma recurrence in a patient with occult hepatitis B virus infection: case report. *Clin Case Rep* 2020;8(12):3032-3037. [CrossRef]
- Hsieh YC, Pan MH, Jeng WJ, Hu HH, Liu J, Mizokami M, et al. Serum HBcrAg and hepatocellular carcinoma in a taiwanese population seronegative for HBsAg and anti-HCV. *Clin Gastroenterol Hepatol* 2023;21(5):1303-1313. [CrossRef]

32. Esposito A, Sabia C, Iannone C, Nicoletti GF, Sommese L, Napoli C. Occult Hepatitis infection in transfusion medicine: screening policy and assessment of current use of anti-HBc testing. *Transfus Med Hemother* 2017;44(4):263-272. [\[CrossRef\]](#)
33. Candotti D, Boizeau L, Laperche S. Occult hepatitis B infection and transfusion-transmission risk. *Transfus Clin Biol* 2017;24(3):189-195. [\[CrossRef\]](#)
34. Candotti D, Assennato SM, Laperche S, Allain JP, Levicnik-Stezinar S. Multiple HBV transfusion transmissions from undetected occult infections: revising the minimal infectious dose. *Gut* 2019;68(2):313-321. [\[CrossRef\]](#)
35. Cholongitas E, Papatheodoridis GV, Burroughs AK. Liver grafts from anti-hepatitis B core positive donors: A systematic review. *J Hepatol* 2010;52(2):272-279. [\[CrossRef\]](#)
36. Lee BT, Perumalswami PV. Diagnosis and management of occult hepatitis b infection. *Curr Hepatol Rep* 2020;19(4):354-361. [\[CrossRef\]](#)
37. Raimondo G, Filomia R, Maimone S. Therapy of occult hepatitis b virus infection and prevention of reactivation. *Intervirology* 2014;57(3-4):189-195. [\[CrossRef\]](#)
38. Cendrero RMR, Castellano BC, Martín MVH, Parra MCC, González JG, Solís MAF, et al. When can it be useful to look for occult HBV in haemodialysis patients. *Nefrología* 2020;40(2):115-119. [\[CrossRef\]](#)
39. Lau G, Yu ML, Wong G, Thompson A, Ghazianian H, Hou JL, et al. APASL clinical practice guideline on hepatitis B reactivation related to the use of immunosuppressive therapy. *Hepatol Int* 2021;15(5):1031-1048. [\[CrossRef\]](#)

## REVIEW ARTICLE

# A traditional herbal remedy in liver diseases: *Momordica charantia* L. (kudret narı/bitter melon)

 Dudu Altintas Gunduz<sup>1</sup>,  Yasemin Balaban<sup>2</sup>,  Ufuk Koca Caliskan<sup>1,3</sup>

1: Department of Pharmacognosy, Duzce University Faculty of Pharmacy, Duzce, Turkiye

2: Division of Gastroenterology, Department of Internal Medical Sciences, Hacettepe University School of Medicine, Ankara, Turkiye

3: Department of Pharmacognosy and Pharmaceutical Botany, Gazi University Faculty of Pharmacy, Ankara, Turkiye

## Points to Note

- **Synthesis of Current Evidence:** This review examines whether bitter melon (*Momordica charantia*) has hepatoprotective effects.
- **Major Controversies:** Preclinical studies show *M. charantia* improves fatty liver, alcohol-related liver injury, and hepatocellular damage through antioxidant, anti-inflammatory, and lipid-lowering effects, though clinical evidence is limited.
- **Future Directions:** Bitter melon may support liver health, but it should not be routinely recommended due to insufficient human trials, dosing, and safety data.

## ABSTRACT

The liver is the central organ regulating the body's metabolism; therefore, liver diseases negatively affect metabolic activities as well as the immune system. *Momordica charantia* L. is one of the medicinal plants used in folk medicine to prevent or treat liver diseases. *M. charantia* contains compounds with antioxidant and anti-inflammatory properties that protect liver cells from free radical damage and reduce inflammation. In addition, the phytochemicals of *M. charantia* may help regulate blood sugar levels, thereby supporting metabolism and reducing fat accumulation in the liver. Previous studies indicate that *M. charantia* has the potential to enhance liver function while reducing the incidence of fatty liver disease. This study aimed to summarize data from *in vivo* studies investigating the hepatoprotective mechanisms of *M. charantia* at various application doses, highlighting its potential as a future dietary supplement candidate. However, due to insufficient evidence regarding its safety, the possibility of hepatotoxic effects should not be disregarded.

**Keywords:** Bitter melon, hepatoprotective effect, liver diseases, *Momordica charantia*, non-alcoholic fatty liver disease (NAFLD).

**How to cite this article:** Altintas Gunduz D, Balaban Y, Koca Caliskan U. A traditional herbal remedy in liver diseases: *Momordica charantia* L. (kudret narı/bitter melon). Hepatology Forum 2026; 7(2):154–162.

**Received:** January 16, 2025; **Revised:** August 06, 2025; **Accepted:** August 18, 2025; **Available Online:** April 08, 2026

**Corresponding author:** Dudu Altintas Gunduz; Department of Pharmacognosy, Duzce University, Duzce, Turkiye; **E-mail:** duduaaltintas@gmail.com



This work is licensed under a Creative Commons Attribution-NonCommercial 4.0 International License.

## Introduction

The liver is responsible for several vital functions, including detoxification, protein synthesis, the bile production and secretion, glucose metabolism, bilirubin metabolism, blood clotting, and control of immune function.<sup>[1]</sup> Several diseases and conditions are frequently associated with liver dysfunction, including hepatitis A, hepatitis B, hepatitis C, hepatitis E, alcohol-related liver diseases, autoimmune hepatitis, non-alcoholic fatty liver disease (NAFLD), drug-induced liver injury, and hepatocellular carcinoma.<sup>[2]</sup> Given the rising prevalence of liver diseases, there is an increasing need to identify plants and plant-derived compounds that can provide hepatoprotective benefits. Studies indicate that green tea, resveratrol, milk thistle, garlic, and artichoke are among the plants that demonstrate hepatoprotective properties.<sup>[3]</sup> Although these plants exhibit hepatoprotective effects, they may also become hepatotoxic when consumed in excessive amounts. Green tea, for instance, can induce hepatotoxicity due to its content of epigallocatechin gallate (EGCG). The safe dose of EGCG has been established as less than 338 mg per day. When this threshold is exceeded, EGCG may trigger oxidative damage and potentially lead to mutations.<sup>[4]</sup> The use of herbs in maintaining human health has a history spanning several centuries. In recent years, there has been a significant increase in interest in the potential of medicinal plants for the protection and enhancement of liver health.

The fruits of *Momordica charantia* L. have been traditionally used for the prevention or treatment of liver diseases, particularly in Asian countries.<sup>[5]</sup> Therefore, this study focuses on investigating the hepatoprotective effects of *M. charantia*. Due to the limited number of clinical studies evaluating the hepatoprotective effects of *M. charantia*, the present study primarily focuses on evidence from *in vivo* and *in vitro* experiments. Although *M. charantia* has been used medicinally for a long time, recent studies suggest that the alpha-momorcharin compound isolated from its seeds may cause toxicity.<sup>[6]</sup> In addition, triterpenic compounds, namely 22-hydroxy-23,24,24,25,26,27-pentanorcucurbit-5-en-3-one and 3,7-dioxo-23,24,25,26,27-pentanorcucurbit-5-en-22-oic acid, isolated from *M. charantia* stems, have also been shown to cause toxicity in the HepG2 cell line.<sup>[7]</sup>

## Search Strategy

Electronic literature sources were used to prepare this narrative review. The keywords *Momordica charantia*, bitter melon, hepatoprotective effect, bitter melon, liver health, preclinical studies, and clinical studies were searched in the PubMed®, Scopus, Web of Science, Google Scholar, and EBSCOhost databases and combined using the search terms "AND," "OR," and "NOT." As the study focused on hepatoprotective effects, other liver diseases were not included. Database searches were updated weekly. Clinical trials and *in vivo* studies were primarily included. As this research is a narrative review, no formal assessment of study quality was performed.

## *M. charantia*

*M. charantia*, commonly known as "bitter melon" or "bitter gourd," is a species belonging to the Cucurbitaceae family. *M. charantia* has a long history of use in traditional medicine for the treatment of various conditions, including anemia, diabetes, intestinal parasites, digestive system diseases, skin wounds, and liver diseases.<sup>[5]</sup> In Turkish traditional medicine, an oily macerate prepared by soaking the fruits in olive oil is used to treat gastrointestinal disorders and as a wound-healing agent.<sup>[8]</sup> In India, the fruits have been traditionally used for various therapeutic purposes, including the treatment of diabetes, psoriasis, and scabies, as well as for their abortifacient and antihelmintic effects.<sup>[9]</sup> *M. charantia* fruits are also frequently used for the treatment of jaundice in India.<sup>[10]</sup>

The pharmacological efficacy of *M. charantia* has been demonstrated in scientific studies investigating its diverse chemical composition and traditional medicinal uses. These studies have examined its analgesic effect,<sup>[11]</sup> antidiabetic activity,<sup>[12]</sup> anti-inflammatory activity,<sup>[13]</sup> hepatoprotective activity,<sup>[14]</sup> hypolipidemic effect,<sup>[15]</sup> and wound-healing activity.<sup>[16]</sup> The present study aims to review the literature on hepatoprotection, which is defined as the ability of a substance or treatment to protect the liver from damage or disease (Table 1).

The plant is a rich source of phytochemicals, consisting of various phytochemical groups found in different parts of the plant in varying concentrations. It has been demonstrated that the roots of *M. charantia* contain a variety of phenolic compounds, including flavonoids and triterpene saponins (Fig. 1).<sup>[7]</sup>

## Non-Alcoholic Fatty Liver Disease

Non-alcoholic fatty liver disease has been reclassified under the umbrella term *steatotic liver disease*. Metabolic dysfunction-associated *steatotic liver disease* is the new name for the liver disease formerly known as NAFLD.<sup>[34]</sup> In recent times, there has been an alarming rise in the prevalence of NAFLD, which is now considered one of the most common forms of liver disease, affecting approximately 25% of the global population. The incidence of this disease is closely associated with the increasing prevalence of obesity.<sup>[35]</sup> NAFLD is a broad category that encompasses a spectrum of conditions ranging from simple steatosis (hepatic steatosis) to inflammation (steatohepatitis), with or without fibrosis, known as non-alcoholic steatohepatitis (NASH). Additionally, evidence suggests that NAFLD is associated with the development of cirrhosis and hepatocellular carcinoma (HCC).<sup>[36]</sup>

In a study utilizing a mouse model of NAFLD, the effect of *M. charantia* extract on the progression of NAFLD was examined following the administration of a high-fat diet for five days. When the experimental and control groups were compared, blood glucose, cholesterol, and low-density lipoprotein levels were found to decrease in the experimental group fed a high-fat diet. Histological examinations also revealed improvements in liver structure and function.<sup>[37]</sup> In

**Table 1.** Phytochemical constituents identified in different parts of *Momordica charantia* L.

Plant part	Chemical components	Chemical groups
Root	Quercetin <sup>[17]</sup>	Flavonoid
	Kaempferol <sup>[17]</sup>	Flavonoid
	Catechin <sup>[17]</sup>	Flavonoid
	Chlorogenic acid <sup>[17]</sup>	Flavonoid
	Momordicoside X	Cucurbitane-type triterpene saponin
	3 $\beta$ , 7 $\beta$ , 25-trihydroxycucurbita-5 23(E)-dien-19-al <sup>[18]</sup>	Cucurbitane-type triterpene saponin
	Momordicin I <sup>[18]</sup>	Cucurbitane-type triterpene saponin
	Momordicin II <sup>[18]</sup>	Cucurbitane-type triterpene saponin
	Kuguaglycoside G <sup>[18]</sup>	Cucurbitane-type triterpene saponin
Leaves	Caffeic acid <sup>[19]</sup>	Phenolic compounds
	Gallic acid <sup>[19]</sup>	Phenolic compounds
	Chlorogenic acid <sup>[19]</sup>	Phenolic compounds
	Karavilagenin F <sup>[20]</sup>	Cucurbitane-type triterpene saponin
	Karaviloside XII <sup>[20]</sup>	Cucurbitane-type triterpene saponin
	Karaviloside XIII <sup>[20]</sup>	Cucurbitane-type triterpene saponin
	Momordicine VI <sup>[20]</sup>	Cucurbitane-type triterpene saponin
	Momordicine VII <sup>[20]</sup>	Cucurbitane-type triterpene saponin
	Momordicine VIII <sup>[20]</sup>	Cucurbitane-type triterpene saponin
	(19R,23E)-5 $\beta$ ,19-epoxy-19-methoxycucurbita-6,23,25-trien-3 $\beta$ -ol <sup>[20]</sup>	Cucurbitane-type triterpene saponin
Kuguacin R <sup>[20]</sup>	Cucurbitane-type triterpene saponin	
Fruits	Lycopene <sup>[21]</sup>	Carotenoids
	$\beta$ -carotene <sup>[21]</sup>	Carotenoids
	Zeaxanthin <sup>[21]</sup>	Carotenoids
	Lutein <sup>[21]</sup>	Carotenoids
	Charantadiol A <sup>[22]</sup>	Triterpene saponin
	Charantagenin E <sup>[22]</sup>	Triterpene saponin
	Stigmasterol <sup>[22]</sup>	Sterols
	7,25-dihydroxycholesterol <sup>[22]</sup>	Sterols
	Goyaglycoside B <sup>[22]</sup>	Triterpene saponin
	Charantagenin D <sup>[22]</sup>	Triterpene saponin
	Kuguaglycoside C <sup>[22]</sup>	Triterpene saponin
	Momordicoside K <sup>[22]</sup>	Triterpene saponin
	Quinic acid <sup>[23]</sup>	Phenolic compounds
	Benzoic acid <sup>[23]</sup>	Phenolic compounds
	Gallic acid <sup>[23]</sup>	Phenolic compounds
Seeds	$\alpha$ -eleostearic acid (45.60%) <sup>[24]</sup>	Fatty acids
	Stearic acid (28%) <sup>[24]</sup>	Fatty acids
	Oleic acid (12.45%) <sup>[24]</sup>	Fatty acids
	Linoleic acid (8.90%) <sup>[24]</sup>	Fatty acids
	trans-Nerolidol (61.6%) <sup>[25]</sup>	Sesquiterpene
	Apiole (8.9%) <sup>[25]</sup>	Phenylpropene
	cis-Dihydrocarveol (4.9%) <sup>[25]</sup>	Monoterpenoids
	Germacrene D (4.4%) <sup>[25]</sup>	Sesquiterpene

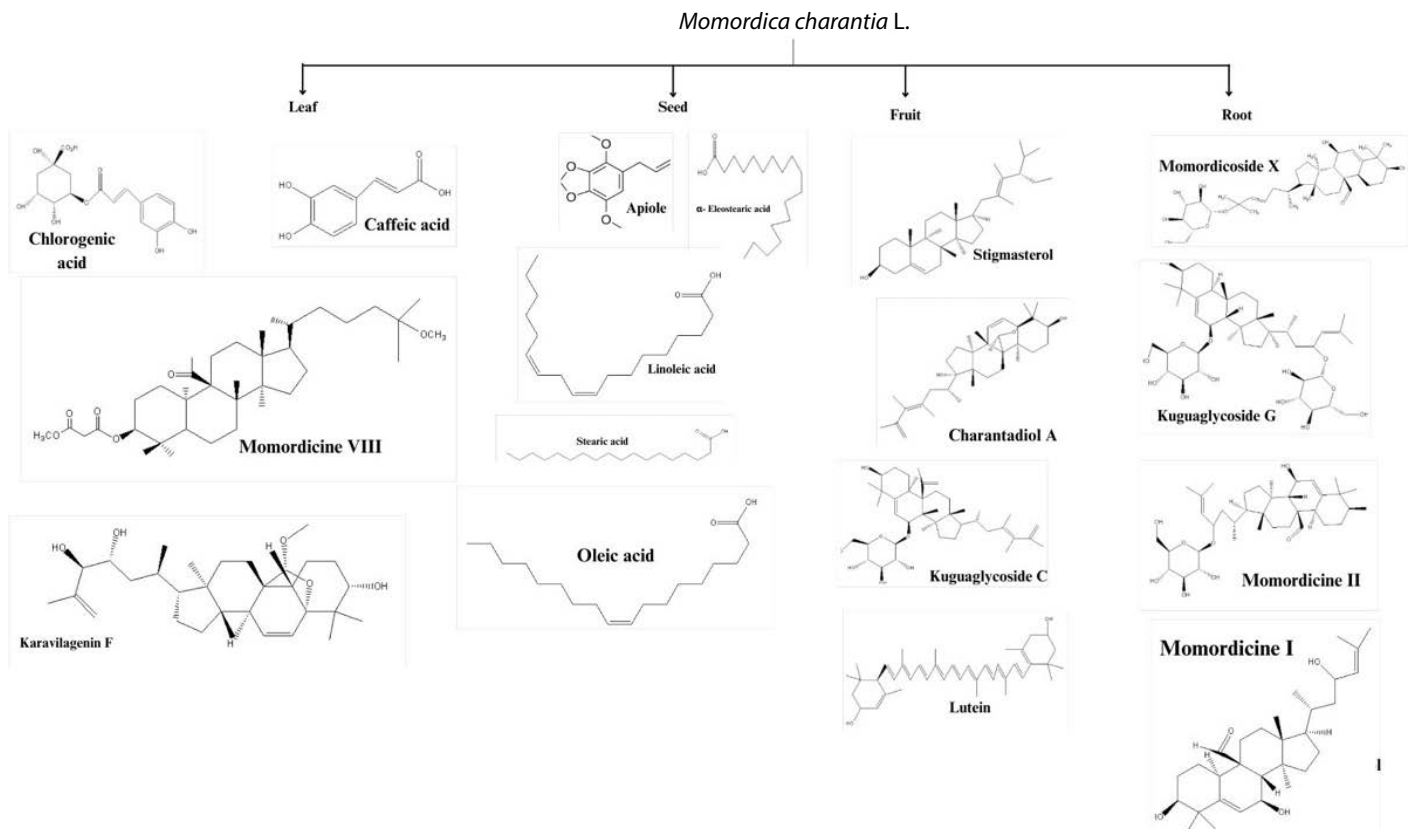


**Figure 1.** Molecular structure of *M. charantia* components (illustrated by the authors).

a further study, the efficacy of *M. charantia* compounds on the liver was evaluated by isolating the triterpenic saponins 3 $\beta$ , 7 $\beta$ , 25-trihydroxycucurbita-5,23(E)-dien-19-al and momordicine II, which were observed to inhibit lipid accumulation in HepG2 cells.<sup>[38]</sup>

The impact of protein derived from *M. charantia* fruits on NAFLD was examined in both *in vitro* and *in vivo* assays. It was observed that pretreatment of HepG2 cells with this isolated protein protected them from cellular changes such as steatosis. It was also demonstrated that intracellular triglyceride levels decreased and bile acid production increased. In addition, while findings such as liver discoloration and swelling were observed in rats fed a high-fat diet, lipid accumulation was significantly reduced and no hepatocyte growth was observed in the groups that received *M. charantia* protein at doses of 400 and 800 mg/kg.<sup>[39]</sup>

The effect of *M. charantia* juice on NAFLD development was investigated in mice at doses of 0.5 and 5 g/kg. In the *M. charantia*-treated group, kidney fat mass and liver weight were significantly lower than those in the fat-only diet group ( $p < 0.05$ ).<sup>[40]</sup>

## Alcohol-Related Liver Disease

Chronic alcohol consumption can result in a range of liver damage, from fatty liver with microvesicular steatosis to cirrhosis and HCC. Furthermore, alcohol consumption has been shown to induce mitochondrial DNA damage in hepatocytes.<sup>[41]</sup> As the duration of

alcohol consumption increases, there is a corresponding increase in lipid accumulation in hepatocytes, along with the activation of inflammatory damage, fibrogenesis, and carcinogenesis pathways.<sup>[42]</sup>

An 80% ethanol extract prepared from *M. Charantia* fruits was investigated for its protective effects against alcohol-induced liver damage in mice. The results of the analyses indicated a statistically significant reduction in liver weight and in the levels of alanine aminotransferase and aspartate aminotransferase, which are biochemical markers of liver damage ( $p < 0.05$ ). Histological examinations also demonstrated a reduction in lipid accumulation within hepatocytes.<sup>[43]</sup>

## Hepatocellular Carcinoma

Hepatocellular carcinoma is the most common primary liver cancer and its incidence is increasing. Diseases such as hepatitis B, hepatitis C, and NASH, as well as alcohol consumption, have been implicated in its etiology. Cirrhosis is known to be one of the strongest risk factors for HCC.<sup>[44]</sup>

A lectin isolated from *M. charantia* was investigated using *in vitro* and *in vivo* methods. In a study conducted using the HepG2 cell line, increased apoptosis was observed at higher doses ( $p < 0.01$ ). Histological evaluations in mice also revealed a significant decrease in tumor volume ( $p < 0.01$ ).<sup>[45]</sup>

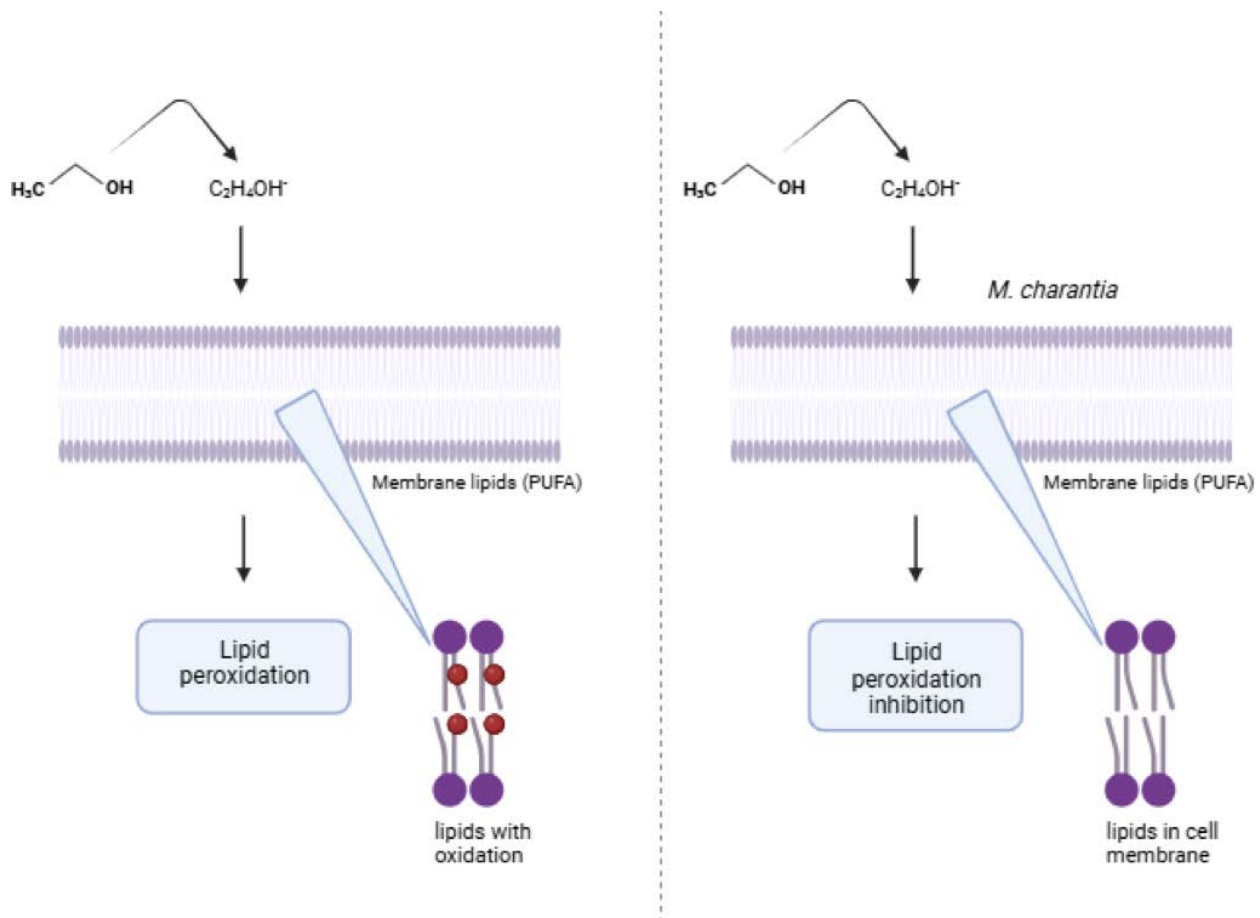


**Figure 2.** Antioxidant effect mechanism of *M. charantia* (original creations). The effectiveness of *Momordica charantia* in protecting the membrane integrity of liver cells has been demonstrated by its ability to inhibit the alcohol-mediated lipid peroxidation process in the liver (illustrated by the author).

Cucurbitan-type saponosides extracted from *M. charantia* fruits were assessed for their antiproliferative effects on Hep3B and HepG2 liver cell lines. The half maximal inhibitory concentration (IC<sub>50</sub>) values for caraviloside III were determined to be 16.68 μM for Hep3B and 4.12 μM for HepG2, indicating that it is the most effective saponoside. The IC<sub>50</sub> values for 5-fluorouracil, which was used as the positive control, were determined to be 15.49 μM for Hep3B and 33.58 μM for HepG2.<sup>[46]</sup>

The *in vitro* and *in vivo* effects of Momordica anti-HIV protein of 30 kDa (MAP30) protein, isolated from *M. charantia* seeds, were evaluated in cancer cells. *In vitro* studies demonstrated that the compound induced cell cycle arrest at the S phase in the HepG2 cell line. In a mouse model of liver cancer, a dose of 2 mg/kg of MAP30 was administered every two days. Consequently, a notable reduction in tumor volume and size was observed, as confirmed by histological analysis ( $p < 0.05$ ).<sup>[47]</sup>

The oral administration of *M. charantia* seed oil to rats yielded statistically significant outcomes. These included a reduction ( $p < 0.05$ ) in the mean number, diameter, and area of dysplastic nodules in the liver, as well as a reduction in the size of neoplastic lesions compared to the control group.<sup>[48]</sup>

## Hepatoprotective Mechanisms of *M. charantia*

The use of plants in natural medical treatments has a long history spanning thousands of years. Advances in science and technology have enabled the efficacy and safety of herbal products to be studied in greater detail, and these products are now available in a variety of formulations. Formulation development is a crucial step in enhancing the efficacy of herbal products while reducing their potential adverse effects on the human body. The components of each herbal product may have different mechanisms of action; therefore, it is necessary to determine how these components can be used most effectively.<sup>[49]</sup>

Given that herbal extracts contain complex mixtures of phytochemicals, they exhibit a wide range of pharmacological effects through various mechanisms. Hazardous agents such as alcohol can damage hepatocytes and impair the normal functioning of their membranes. Consequently, the activities of transaminases and alkaline phosphatase increase as a result of this damage.<sup>[50]</sup>

Chronic alcohol consumption can lead to lipid oxidation, resulting in the disruption of membrane permeability. This process involves the formation of hydroxylethyl radicals, which primarily target

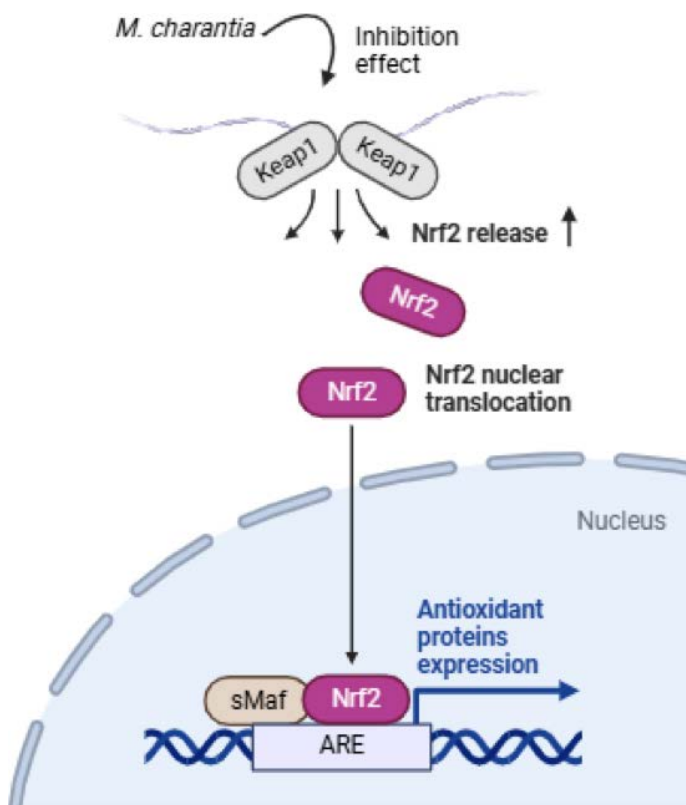


**Figure 3.** Nrf2-related antioxidant mechanisms (original creations).

polyunsaturated fatty acids. Certain fractions of *M. charantia* have been shown to maintain the membrane integrity of liver cells by inhibiting alcohol-induced lipid peroxidation in the liver.<sup>[31]</sup> The oxidative mechanism is illustrated in Figure 2.<sup>[51]</sup>

The use of antioxidants has been shown to inhibit the progression of liver disease and improve the effectiveness of current therapies by reducing oxidative stress. Antioxidants may promote the dissociation of nuclear factor erythroid 2–related factor 2 (Nrf2) from the complex by altering the phosphorylation of Kelch-like ECH-associated protein-1 (Keap1) or Nrf2, leading to Nrf2 activation. Activation of Nrf2 results in its translocation to the nucleus, where it interacts with the antioxidant response element. This process results in increased expression of genes encoding antioxidant enzymes and phase II detoxifying enzymes, which are essential for cellular protection and recovery. Moreover, several studies have shown that certain antioxidants or plant extracts rich in antioxidants protect against hepatotoxin-induced liver injury by enhancing Nrf2 activation.<sup>[52]</sup> The oxidative mechanism is illustrated in Figure 3.

Under unstressed conditions, the protein Keap1 represses Nrf2. However, in the presence of oxidative stress, Nrf2 is released from repression, thereby activating antioxidant genes and strengthening cellular defense mechanisms. In a study examining the hepatoprotective effects of *M. charantia* on NAFLD, serum concentrations of C-reactive protein and interleukin-6 were significantly reduced following supplementation ( $p < 0.05$ ). Similarly, sterol regulatory element-binding protein 1 (SREBP-1),

a principal regulator of lipogenesis and a potential contributor to the development of fatty liver, was reduced following *M. charantia* supplementation, accompanied by decreased expression of fatty acid synthase (FAS) and acetyl-CoA carboxylase 1 (ACC-1) proteins, as well as reduced cholesterol and triglyceride (TG) concentrations. Inflammatory processes have been shown to induce the production of tumor necrosis factor- $\alpha$  (TNF- $\alpha$ ), which may stimulate the maturation of SREBP-1 and contribute to lipid accumulation in hepatocytes. Therefore, it can be suggested that the effects of *M. charantia* on SREBP-1 and its target genes may help reduce inflammation. These findings indicate that *M. charantia* may serve as a promising agent for the prevention and treatment of NAFLD.<sup>[40]</sup>

The hepatoprotective properties of a formulation containing *Ferula asafoetida*, *M. charantia*, and *Nardostachys jatamansi* were examined in carbon tetrachloride-induced injury in rats. Enzymes including glutamate oxaloacetate transaminase, glutamate pyruvate transaminase, and alkaline phosphatases were selected as markers for the investigation. A statistically significant decrease was observed in the levels of these enzymes ( $p < 0.01$ ).<sup>[53]</sup>

The acute toxicity of *M. charantia* fruits was investigated, and the median lethal dose (LD<sub>50</sub>) value was calculated to be  $> 5000$  mg/kg. Consequently, the fruit is considered relatively safe.<sup>[54]</sup> Nevertheless, research indicates that bitter melon may potentially interact with hypoglycemic drugs.<sup>[55]</sup> Furthermore, because *M. charantia* exhibits cytochrome P450 3A4 (CYP3A4) activity, there is a possibility of interaction with drugs metabolized by this enzyme.<sup>[56,57]</sup> The most frequently observed adverse effects are hypoglycemia and headaches.<sup>[55]</sup> Its use is not recommended during pregnancy and lactation. Studies in rats demonstrated the occurrence of cardiac hypertrophy in embryos, although no instances of lethality were observed.<sup>[58]</sup> Therefore, formulations containing *M. charantia* may potentially have adverse effects on the developing fetus.

## Bioavailability

Bioavailability is one of the major challenges associated with herbal products.<sup>[59]</sup> It is important to investigate advanced technologies, such as nanoparticles and phytosomes, for bitter melon. Owing to the unpleasant flavor and limited bioavailability of *M. charantia*, innovative technologies such as nanoparticles and phytosomes may be utilized to enhance stability and bioavailability.<sup>[60]</sup> Studies involving nanoparticles have shown that herbal extracts may reduce toxicity while increasing activity.<sup>[61]</sup> The antibacterial efficacy of silver nanoparticles synthesized from *M. charantia* extract has been examined. The nanoparticle-treated group exhibited a notable increase in activity ( $p < 0.005$ ).<sup>[62]</sup> A study using the Huh-7 liver cancer cell line showed that *M. charantia* copper-iron nanoparticles promoted apoptosis. The IC<sub>50</sub> was determined to be 324  $\mu\text{g/mL}$ , indicating potential effectiveness.<sup>[63]</sup> Because nanoparticles are extremely small, they may also pose potential safety risks. Nanoparticle safety is a controversial subject due to the lack of evidence regarding both acute and chronic toxicity.<sup>[64]</sup>

**Table 2.** *In vivo* studies investigating the hepatoprotective effects of *Momordica charantia* L.

Plant part—solvent used	Research model	Dosage	Results
Leaves—water <sup>[26]</sup>	CCl <sub>4</sub> -induced hepatotoxicity in rats	200 mg/kg and 400 mg/kg	ALT, AST, and ALP ↓ (p<0.05) SOD and CAT ↑ (p<0.05)
Leaves—50% ethanol <sup>[27]</sup>	CCl <sub>4</sub> -induced hepatotoxicity in rats	100 mg/kg and 200 mg/kg	ALT, AST ↓ (p<0.05); histopathological findings showed minimal cellular damage after treatment
Leaves—70% ethanol <sup>[28]</sup>	CCl <sub>4</sub> -induced hepatotoxicity in rats	100 mg/kg and 200 mg/kg	SGOT, SGPT, ALP, and total bilirubin levels improved (p<0.05)
Juice <sup>[29]</sup>	Acetaminophen-induced liver injury in rabbits	5 mL/kg	ALT, AST, and ALP ↓ (p<0.05)
Fruit—95% ethanol <sup>[30]</sup>	Ammonium chloride-induced liver injury in rats	300 mg/kg	AST, ALT, and ALP ↓ (p<0.05); decreased blood ammonia and plasma urea levels
Fruit—80% ethanol <sup>[31]</sup>	Alcohol-induced hepatotoxicity in rats	25, 50, and 100 mg/kg	SOD, GSH, and CAT ↑ (p<0.05)
Fruit—water <sup>[14]</sup>	Restraint-stressed mice	250, 500, and 750 mg/kg	Histopathological findings indicated intact liver cell structure and clearly defined hepatic cords; ALT and AST ↓ (p<0.05)
Fruit—Hexane <sup>[32]</sup>	Rat model of hepatic ischemia-reperfusion injury	200 mg/kg	Prevented increases in SGOT, SGPT, ALP, LDH, and CRP levels (p<0.01); prevented increase in MDA levels (p<0.05)
Leaves—70% methano <sup>[33]</sup>	Cadmium-induced hepatotoxicity in rats	300 mg/kg	Cadmium caused fibrosis around the portal vein and disintegration of hepatocyte nuclei; pretreatment with extracts revealed prominent Kupffer cells

ALP: Alkaline phosphatase; AST: Aspartate aminotransferase; ALT: Alanine aminotransferase; SGOT: Glutamate oxaloacetate transaminase; SGPT: Glutamate pyruvate transaminase; SOD: Superoxide dismutase; CAT: Catalase; GSH: Glutathione; LDH: Lactate dehydrogenase; CRP: C-reactive protein; MDA: Malondialdehyde.

## Conclusion

Bitter melon (*M. charantia*) has a long history of use in traditional medicine spanning several centuries. Because the liver performs numerous essential functions in the body, maintaining liver health is of critical importance. Various pathways may contribute to the development of liver disorders; therefore, herbal compounds and extracts that act through multiple mechanisms play an important role. Studies investigating the hepatoprotective effects of *M. charantia* are summarized in Table 2. However, the lack of clinical trials and safety data represents a significant obstacle to the development of *M. charantia* as a therapeutic agent. Its traditional medicinal use provides valuable insight for modern drug development, particularly in elucidating its chemical constituents and determining their mechanisms of action through scientific investigation. *M. charantia* may be used in combination with other herbs, such as milk thistle, and compounds beneficial for liver health, such as curcumin and silymarin. Future studies may investigate potential synergistic effects between these agents. This review aimed to evaluate the hepatoprotective potential of *M. charantia*. However, the current state of clinical research and formulation development is insufficient in several aspects. Moreover, another major limitation is the lack of clinical studies investigating the optimal dosage and duration required to achieve hepatoprotective effects.

**Conflict of Interest:** The authors have no conflict of interest to declare.

**Financial Disclosure:** The authors declared that this study has received no financial support.

**Use of AI for Writing Assistance:** The study did not use artificial intelligence (AI)-supported technologies (such as Large Language Models [LLMs], chatbots or image generators, ChatGPT).

**Author Contributions:** Concept: DAG, YB, UKC; Design: DAG, YB, UKC; Supervision: DAG, YB, UKC; Funding: DAG, YB, UKC; Materials: DAG, YB, UKC; Data Collection and/or Processing: DAG, YB, UKC; Analysis and/or Interpretation: DAG, YB, UKC; Literature Search: DAG, YB, UKC; Writing: DAG, YB, UKC; Critical Reviews: DAG, YB, UKC.

**Peer-review:** Externally peer-reviewed.

## References





- Lala V, Zubair M, Minter D. Liver function tests. *Indian J Pediatr* 2007;74(7):663-671. [\[CrossRef\]](#)
- Tajiri K, Shimizu Y. Liver physiology and liver diseases in the elderly. *World J Gastroenterol* 2013;19(46):8459-8467. [\[CrossRef\]](#)
- Xiao J, So KF, Liong EC, Tipoe GL. Recent advances in the herbal treatment of non-alcoholic fatty liver disease. *J Tradit Complement Med* 2013;3(2):88-94. [\[CrossRef\]](#)

4. Zhao T, Li C, Wang S, Song X. Green tea (*Camellia sinensis*): a review of its phytochemistry, pharmacology, and toxicology. *Molecules* 2022;27(12):1-23. [\[CrossRef\]](#)
5. Ahmad N, Hasan N, Ahmad Z, Zishan M, Zohrameena S. *Momordica charantia*: for traditional uses and pharmacological actions. *J Drug Deliv Ther* 2016;6(2):40-44. [\[CrossRef\]](#)
6. Meng Y, Liu B, Lei N, Zheng J, He Q, Li D, et al. Alpha-momorcharin possessing high immunogenicity, immunotoxicity and hepatotoxicity in SD rats. *J Ethnopharmacol* 2012;139(2):590-598. [\[CrossRef\]](#)
7. Chen CR, Liao YW, Wang L, Kuo YH, Liu HJ, Shih WL, et al. Cucurbitane triterpenoids from *Momordica charantia* and their cytoprotective activity in tert-butyl hydroperoxide-induced hepatotoxicity of HepG2 cells. *Chem Pharm Bull (Tokyo)* 2010;58(12):1639-1642. [\[CrossRef\]](#)
8. Yeşilada E, Gürbüz I, Shibata H. Screening of Turkish anti-ulcerogenic folk remedies for anti-*Helicobacter pylori* activity. *J Ethnopharmacol* 1999;66(3):289-293. [\[CrossRef\]](#)
9. Grover JK, Yadav SP. Pharmacological actions and potential uses of *Momordica charantia*: a review. *J Ethnopharmacol* 2004;93(1):123-132. [\[CrossRef\]](#)
10. Deb D, Datta BK, Debbarma J, Deb S. Ethno-medicinal plants used for herbal medication of jaundice by the indigenous community of Tripura, India. *Biodiversitas* 2016;17(1):256-269. [\[CrossRef\]](#)
11. Ofuegbe S, Akinrinde A, Oyagbemi A, Omobowale T, Yakubu M, Adedapo A. Phytochemical, acute toxicity, analgesic, *in vitro* antioxidant studies and GC-MS investigation of essential oil of the methanol leaf extract of *Momordica charantia*. *J Complement Altern Med Res* 2017;4(4):1-18. [\[CrossRef\]](#)
12. Liu Y, Mu S, Chen W, Liu S, Cong Y, Liu J, et al. Saponins of *Momordica charantia* increase insulin secretion in INS-1 pancreatic  $\beta$ -cells via the PI3K/Akt/FoxO1 signaling pathway. *Endocrinol Diabetes Nutr (Engl Ed)* 2021;68(5):329-337. [\[CrossRef\]](#)
13. Chao CY, Sung PJ, Wang WH, Kuo YH. Anti-inflammatory effect of *Momordica charantia* in sepsis mice. *Molecules* 2014;19(8):12777-12788. [\[CrossRef\]](#)
14. Deng Y, Tang Q, Zhang Y, Zhang R, Wei Z, Tang X, et al. Protective effect of *Momordica charantia* water extract against liver injury in restraint-stressed mice and the underlying mechanism. *Food Nutr Res* 2017;61(1):1-11. [\[CrossRef\]](#)
15. Mahwish, Saeed F, Arshad MS, Nisa M, Nadeem MT, Arshad MU. Hypoglycemic and hypolipidemic effects of different parts and formulations of bitter melon (*Momordica charantia*). *Lipids Health Dis* 2017;16(1):211. [\[CrossRef\]](#)
16. Pişkin A, Altunkaynak BZ, Tümentemur G, Kaplan S, Yazıcı ÖB, Hökelek M. The beneficial effects of *Momordica charantia* (bitter melon) on wound healing of rabbit skin. *J Dermatolog Treat* 2014;25(4):350-357. [\[CrossRef\]](#)
17. Thiruvengadam M, Praveen N, Maria John KM, Yang YS, Kim SH, Chung IM. Establishment of *Momordica charantia* hairy root cultures for the production of phenolic compounds and determination of their biological activities. *Plant Cell Tiss Organ Cult* 2014;118(3):545-557. [\[CrossRef\]](#)
18. Ma J, Whittaker P, Keller AC, Mazzola EP, Pawar RS, White KD, et al. Cucurbitane-type triterpenoids from *Momordica charantia*. *Planta Med* 2010;76(17):1758-1761. [\[CrossRef\]](#)
19. Shodehinde SA, Adefegha SA, Oboh G, Oyeleye SI, Olasehinde TA, Nwanna EE, et al. Phenolic composition and evaluation of methanol and aqueous extracts of bitter melon (*Momordica charantia* L) leaves on angiotensin-I-converting enzyme and some pro-oxidant-induced lipid peroxidation *in vitro*. *J Evid Based Complement Alternat Med* 2016;21(1):67-76. [\[CrossRef\]](#)
20. Zhao GT, Liu JQ, Deng YY, Li HZ, Chen JC, Zhang ZR, et al. Cucurbitane-type triterpenoids from the stems and leaves of *Momordica charantia*. *Fitoterapia* 2014;95(1):75-82. [\[CrossRef\]](#)
21. Lee SH, Jeong YS, Song J, Hwang KA, Noh GM, Hwang IG. Phenolic acid, carotenoid composition, and antioxidant activity of bitter melon (*Momordica charantia* L) at different maturation stages. *Int J Food Prop* 2017;20(3):3078-3087. [\[CrossRef\]](#)
22. Wang X, Sun W, Cao J, Qu H, Bi X, Zhao Y. Structures of new triterpenoids and cytotoxicity activities of the isolated major compounds from the fruit of *Momordica charantia* L. *J Agric Food Chem* 2012;60(16):3927-3933. [\[CrossRef\]](#)
23. Lopes AP, Petenuci ME, Galuch MB, Schneider VVA, Canesin EA, Visentainer JV. Evaluation of effect of different solvent mixtures on the phenolic compound extraction and antioxidant capacity of bitter melon (*Momordica charantia*). *Chem Pap* 2018;72(11):2945-2953. [\[CrossRef\]](#)
24. Gölükçü M, Toker R, Ayas F, Çınar N. Some physical and chemical properties of bitter melon (*Momordica charantia* L) seed and fatty acid composition of seed oil. *Derim* 2014;31(2):17-24. [\[CrossRef\]](#)
25. Braca A, Siciliano T, D'Arrigo M, Germanò MP. Chemical composition and antimicrobial activity of *Momordica charantia* seed essential oil. *Fitoterapia* 2008;79(2):123-125. [\[CrossRef\]](#)
26. Mada S. Hepatoprotective effect of *Momordica charantia* extract against CCl4 induced liver damage in rats. *Br J Pharm Res* 2014;4(3):368-380. [\[CrossRef\]](#)
27. Chaudhari BP, Chaware VJ, Joshi YR, Biyani KR. Hepatoprotective activity of hydroalcoholic extract of *Momordica charantia* Linn leaves against carbon tetrachloride induced hepatopathy in rats. *Int J ChemTech Res* 2009;1(2):355-358.
28. Moharir G, Bharatha A, Ojeh N, Prasad VS. Evaluation of hepatoprotective effect of hydroalcoholic extract of *Momordica charantia* leaves in carbon tetrachloride-induced liver toxicity in wistar rats. *Biomed Pharmacol J* 2019;12(3):1555-1560. [\[CrossRef\]](#)
29. Zahra K, Malik MA, Mughal MS, Arshad M, Sohail MI. Hepatoprotective role of extracts of *Momordica charantia* L in acetaminophen-induced toxicity in rabbits. *J Anim Plant Sci* 2012;22(1):273-277. [\[CrossRef\]](#)
30. Thenmozhi AJ, Subramanian P. Hepatoprotective effect of *Momordica charantia* in ammonium chloride induced hyperammonemic rats. *J Pharm Res* 2011;4(3):700-702. [\[CrossRef\]](#)
31. Hussain MA. Hepatoprotective activity of ethanolic extract fractions of *Momordica charantia* fruit, against alcohol induced hepatotoxic rats. *Adv Pharmacol Toxicol* 2014;15(1):43-48.
32. Parikh M, Patel A, Patel K, Tejal G. Protective effect of *Momordica charantia* against hepatic ischemic reperfusion injury model in rats. *Austin J Pharmacol Ther* 2015;3(1):1-5. [\[CrossRef\]](#)
33. Ajilore BS, Ayannuga OA. Hepatoprotective potentials of methanolic extract of the leaf of *Momordica charantia* Linn on cadmium-induced hepatotoxicity in rats. *J Nat Sci Res* 2012;2(5):41-47.
34. Rinella ME, Lazarus JV, Ratziu V, Francque SM, Sanyal AJ, Kanwal F, et al. A multisociety Delphi consensus statement on new fatty liver disease nomenclature. *Hepatology* 2023;78(6):1966-1986. [\[CrossRef\]](#)
35. Younossi ZM, Koenig AB, Abdelatif D, Fazel Y, Henry L, Wymer M. Global epidemiology of nonalcoholic fatty liver disease - Meta-analytic assessment of prevalence, incidence, and outcomes. *Hepatology* 2016;64(1):73. [\[CrossRef\]](#)
36. Powell EE, Wong VW S, Rinella M. Non-alcoholic fatty liver disease. *Lancet* 2021;397(10290):2212-2224. [\[CrossRef\]](#)

37. Santos MESM, Lemos BSO, Teixeira KB, Silva LN, Souza GA, Pinto FCH, et al. Effects of the *Momordica charantia* (MC) in the alterations caused by administration of a high fat diet (HL) as a model of non-alcoholic fatty liver disease (NAFLD). *FASEB J* 2013;27(Suppl 1):1-9. [CrossRef]
38. Yang LC, Lee YT, Kumaran A, Huang SQ, Su CH, Wu DR, et al. Target and non-target analysis with molecular network strategies for identifying potential index compounds from *Momordica charantia* L for alleviating non-alcoholic fatty liver. *Ind Crops Prod* 2024;219:1-10. [CrossRef]
39. Gao Y, Liu P, Wang D, Liu J, Yang L, Kang Y, et al. Isolation and characterization of a novel protein from *Momordica charantia* L that positively regulates lipid metabolism activity *in vivo* and *in vitro*. *J Funct Foods* 2022;96:1-10. [CrossRef]
40. Xu J, Cao K, Li Y, Zou X, Chen C, Szeto IM Y, et al. Bitter melon inhibits the development of obesity-associated fatty liver in C57BL/6 mice fed a high-fat diet. *J Nutr* 2014;144(3):475-483. [CrossRef]
41. Meza V, Arnold J, Díaz LA, Ayala Valverde M, Idalsoaga F, Ayares G, et al. Alcohol consumption: medical implications, the liver and beyond. *Alcohol* 2022;57(3):283-291. [CrossRef]
42. Arab JP, Roblero JP, Altamirano J, Bessone F, Chaves Araujo R, Higuera De la Tijera F, et al. Alcohol-related liver disease: Clinical practice guidelines by the Latin American Association for the Study of the Liver (ALEH). *Ann Hepatol* 2019;18(4):518-535. [CrossRef]
43. Lu KH, Tseng HC, Liu CT, Huang CJ, Chyuan JH, Sheen LY. Wild bitter melon protects against alcoholic fatty liver in mice by attenuating oxidative stress and inflammatory responses. *Food Funct* 2014;5(4):1027-1037. [CrossRef]
44. Llovet JM, Kelley RK, Villanueva A, Singal AG, Pikarsky E, Roayaie S, et al. Hepatocellular carcinoma. *Nat Rev Dis Primers* 2021;7(1):1-28. [CrossRef]
45. Zhang CZ, Fang EF, Zhang HT, Liu LL, Yun JP. *Momordica charantia* lectin exhibits antitumor activity towards hepatocellular carcinoma. *Invest New Drugs* 2015;33(1):1-11. [CrossRef]
46. Yue J, Sun Y, Xu J, Cao J, Chen G, Zhang H, et al. Cucurbitane triterpenoids from the fruit of *Momordica charantia* L and their anti-hepatic fibrosis and anti-hepatoma activities. *Phytochemistry* 2019;157:21-27. [CrossRef]
47. Fang EF, Zhang CZY, Wong JH, Shen JY, Li CH, Ng TB. The MAP30 protein from bitter melon (*Momordica charantia*) seeds promotes apoptosis in liver cancer cells *in vitro* and *in vivo*. *Cancer Lett* 2012;324(1):66-74. [CrossRef]
48. Ranasinghe KNK, Premarathna AD, Mahakapuge TAN, Wijesundera KK, Ambagaspitiya AT, Jayasooriya AP, et al. *In vivo* anticancer effects of *Momordica charantia* seed fat on hepatocellular carcinoma in a rat model. *J Ayurveda Integr Med* 2021;12(3):435-442. [CrossRef]
49. Choudhary N, Sekhon BS. An overview of advances in the standardization of herbal drugs. *J Pharm Educ Res* 2011;2(2):55-70.
50. Madrigal Santillán E, Madrigal Bujaidar E, Álvarez González I, Sumaya Martínez MT, Gutiérrez Salinas J, Bautista M, et al. Review of natural products with hepatoprotective effects. *World J Gastroenterol* 2014;20(40):14787-14804. [CrossRef]
51. Valgimigli L. Lipid peroxidation and antioxidant protection. *Biomolecules* 2023;13(9):1291. [CrossRef]
52. Rouf R, Ghosh P, Uzzaman MdR, Sarker DK, Zahura FT, Uddin SJ, et al. Hepatoprotective plants from Bangladesh: a biophytochemical review and future prospect. *Evid Based Complement Alternat Med* 2021;2021:1-39. [CrossRef]
53. Dandagi PM, Patil MB, Mastiholmath VS, Gadad AP, Dhumsure RH. Development and evaluation of hepatoprotective polyherbal formulation containing some indigenous medicinal plants. *Indian J Pharm Sci* 2008;70(2):265-268. [CrossRef]
54. Abdillah S, Inayah B, Kartiningsih, Febrianti AB, Nafisa S. Acute and sub-chronic toxicity of *Momordica charantia* L fruits ethanolic extract in liver and kidney. *Syst Rev Pharm* 2020;11(1):2249-2255.
55. Basch E, Gabardi S, Ulbricht C. Bitter melon (*Momordica charantia*): a review of efficacy and safety. *Am J Health Syst Pharm* 2003;60(4):356-359. [CrossRef]
56. Shah PA, Eck P, Nerurkar PV. Modulation of human cytochrome P450 by *Momordica charantia* (bitter melon). *FASEB J* 2009;23(Suppl 1):688.5. [CrossRef]
57. Eichelbaum M, Burk O. CYP3A genetics in drug metabolism. *Nat Med* 2001;7(3):285-287. [CrossRef]
58. Khan MF, Abutaha N, Nasr FA, Alqahtani AS, Noman OM, Wadaan MAM. Bitter melon (*Momordica charantia*) possess developmental toxicity as revealed by screening the seeds and fruit extracts in zebrafish embryos. *BMC Complement Altern Med* 2019;19(1):1-13. [CrossRef]
59. Kesarwani K, Gupta R. Bioavailability enhancers of herbal origin: an overview. *Asian Pac J Trop Biomed* 2013;3(3):253-266. [CrossRef]
60. Çiçek SS. *Momordica charantia* L-diabetes-related bioactivities, quality control, and safety considerations. *Front Pharmacol* 2022;13:904643. [CrossRef]
61. Yavuz İ, Yılmaz EŞ. Nanoparticles with biological systems. *GÜFFD* 2021;2(2):93-108. [Turkish]
62. Rashid MdMO, Akhter KN, Chowdhury JA, Hossen F, Hussain MdS, Hossain MdT. Characterization of phytoconstituents and evaluation of antimicrobial activity of silver-extract nanoparticles synthesized from *Momordica charantia* fruit extract. *BMC Complement Altern Med* 2017;17(1):336. [CrossRef]
63. Alamri RK, Ali D, Alharthi WA, Yaseen KN, Almutairi BO, Alkahtani S, et al. Green synthesis of copper-iron nanoparticles using the peel of *Momordica charantia* and its cytotoxicity and apoptotic effect on human liver and breast cancer cells. *Nat Prod Commun* 2023;18(11). [CrossRef]
64. Najahi Missaoui W, Arnold RD, Cummings BS. Safe nanoparticles: are we there yet? *Int J Mol Sci* 2021;22(1):1. [CrossRef]

## CASE REPORT

# Methylprednisolone for *Swietenia macrophylla* seeds-induced liver injury: A report of two cases

 Ze-yu Huang<sup>1,2</sup>,  Xiu-jun Zhang<sup>1,2</sup>,  Xue-cheng Tong<sup>1,2</sup>,  Yuan Xue<sup>1,2</sup>

1: Department of Infectious Diseases, Changzhou Third People's Hospital, Changzhou Medical Center, Nanjing Medical University, Changzhou, China

2: Institute of Hepatology, Changzhou Third People's Hospital, Changzhou, China

## Clinical Pearls

### • Unique Features of the Case:

Two cases of drug-induced liver injury (DILI) caused by *Swietenia macrophylla* seeds (SMS) are presented. Both patients had elevated liver enzymes and autoimmune-like hepatitis.

One patient recovered fully with methylprednisolone, with normal liver tissue seen in the second biopsy after three years.

No recurrence occurred during one-year follow-up after treatment withdrawal.

### • Primary Lesson for Clinicians:

Clinicians should exercise caution with SMS in patients with potential immune disorders, as it may cause liver damage. Methylprednisolone may be beneficial for SMS-related DILI.

## ABSTRACT

*Swietenia macrophylla* seeds (SMS), as a traditional medicine, are widely used against diabetes, hypertension, and malaria. To date, knowledge about the safety of human consumption remains limited. We herein reported two cases of drug-induced liver injury (DILI) caused by SMS. Both patients had positive antinuclear antibodies. Hepatotoxicity of SMS is characterized by elevated alanine aminotransferase and obvious autoimmune-like hepatitis. Furthermore, the 2<sup>nd</sup> biopsy at the 3<sup>rd</sup> year of methylprednisolone treatment showed normal liver tissue, and then methylprednisolone was withdrawn. No recurrence occurred during one-year follow-up after methylprednisolone withdrawal. SMS may increase the risk of liver damage for patients with potential immune disorders, and patients with SMS-related DILI may benefit from methylprednisolone.

**Keywords:** Autoimmune hepatitis, drug-induced liver injury, hepatotoxicity, methylprednisolone, *Swietenia macrophylla*.

**How to cite this article:** Huang Z-Y, Zhang X-J, Tong X-C, Xue Y. Methylprednisolone for *Swietenia macrophylla* seeds-induced liver injury: A report of two cases. *Hepatology Forum* 2026; 7(2):163–166.

**Received:** October 05, 2023; **Revised:** November 02, 2023; **Accepted:** January 12, 2024; **Available Online:** April 15, 2026

**Corresponding author:** Yuan Xue; Department of Infectious Diseases, Changzhou Third People's Hospital, Changzhou Medical Center, Nanjing Medical University;  
**E-mail:** xueyuan80908@163.com



This work is licensed under a Creative Commons Attribution-NonCommercial 4.0 International License.

## Introduction

Drug-induced liver injury (DILI), which is an adverse drug reaction (ADR), has become a challenging problem worldwide. The annual incidence of DILI is estimated to be 23.8/100,000 in the general population from the mainland of China, and the leading causes of DILI include traditional Chinese medicine, herbal, and dietary supplements.<sup>[1]</sup>

*Swietenia macrophylla*, commonly known as sky fruit, is widely distributed in South America, Malaysia, southern China, and west India.<sup>[2,3]</sup> As a traditional medicine, *Swietenia macrophylla* seeds (SMS) are widely used for the treatment of diabetes, hypertension, malaria, and even wounds.<sup>[4–10]</sup> Mi et al.<sup>[2]</sup> reported that polyacetylenes extracted from the roots of *Swietenia macrophylla* demonstrated cytotoxicity against human hepatocellular carcinoma cell line, myeloid leukemia cell line, and gastric carcinoma cell line. SMS showed no acute toxicity in Sprague-Dawley rats.<sup>[4,11]</sup> Tan et al.<sup>[12]</sup> reported three cases of DILI caused by SMS, all of whom were elderly men aged from 72 to 80 years old. In addition, Shao et al.<sup>[13]</sup> reported a case of herb-induced autoimmune-like hepatitis associated with SMS. Histological features of autoimmune hepatitis (AIH), including interfacial inflammation, “rosette”-like changes in the hepatocytes, and focal necrosis, were demonstrated in the case of SMS-related liver injury.<sup>[13]</sup> Thus, immune-mediated DILI and AIH could not be classified clearly by histology. For patients with obvious histologic characteristics of AIH, immunosuppressive therapy can be recommended, and DILI can be established if there is no sign of recurrence after withdrawal of immunosuppressive therapy.<sup>[14]</sup> To date, the effect and safety of immunosuppressive therapy in patients with SMS-related autoimmune-like hepatitis remain limited.

We herein reported two cases of DILI caused by SMS. Both patients were followed up for four years, and methylprednisolone was administered for three years in one patient.

## Case Report

Two patients were admitted to the Third People’s Hospital of Changzhou on October 17, 2018, at the same time. Patient 1 was a 57-year-old Chinese woman who presented with a 6-day history of fatigue and

loss of appetite. She had jaundice on the skin and sclera. Liver function parameters were abnormal at the time of admission. She had alanine transaminase (ALT) levels nearly 35 times the upper limit of the normal range (1,402 U/L), whereas aspartate aminotransferase (AST), gamma-glutamyl transpeptidase (GGT), and alkaline phosphatase (ALP) were also high (337 U/L, 420 U/L, and 158 U/L, respectively). Total bilirubin (TBIL) was more than 4 times the upper limit of the normal range (92  $\mu\text{mol/L}$ ), with the majority being conjugated bilirubin (62.3  $\mu\text{mol/L}$ ). She had positive antinuclear antibodies (ANA, 1:100 titers, cytoplasmic granule type) and anti-Ro-52.

Patient 2 was the daughter of the aforementioned woman. She was 35 years old, with an asymptomatic rise in her liver enzymes. Laboratory tests showed elevated ALT (417 U/L), AST (117 U/L), and TBIL (36.5  $\mu\text{mol/L}$ ), with normal ALP (64 U/L) and GGT (39 U/L) levels. She had a high ANA titer (1:1000, centromere type) and positive anti-centromere antibody.

Both patients had no history of liver diseases or alcohol abuse, and they had taken SMS as a traditional dietary supplement for two months. Serological markers of HAV, HBV, HCV, HDV, and HEV were all negative. Moreover, both patients had normal immunoglobulin profiles. Informed consent was obtained from the two patients, and the clinical data were collected during the four-year follow-up period.

The two patients were diagnosed with SMS-induced DILI according to the Roussel Uclaf Causality Assessment Method (RUCAM), and the clinical type was classified based on the R value.<sup>[1]</sup> According to RUCAM, the two patients were given scores of 8 and 7, and thus DILI was diagnosed by the diagnostic tool (<http://www.hepatox.org/rucam>). Both patients had ALT levels  $\geq 3\times$  the upper limit of normal, and R values of  $\geq 5$  (29.95 and 21.99, respectively). Based on this, the hepatocellular type of DILI was classified. SMS was withdrawn instantly at admission, and then glycyrrhizin was administered intravenously every day at a dose of 150 mg. Liver biochemistry improved markedly during the first two weeks after admission (Fig. 1).

The liver functions of Patient 1 appeared to be normal in the 1<sup>st</sup> month after admission, and she had a liver tissue biopsy. Histological features, including focal necrosis, interfacial inflammation, “rosette”-like changes in the hepatocytes, and milder fibrosis, were found. Then, AIH was considered, and methylprednisolone

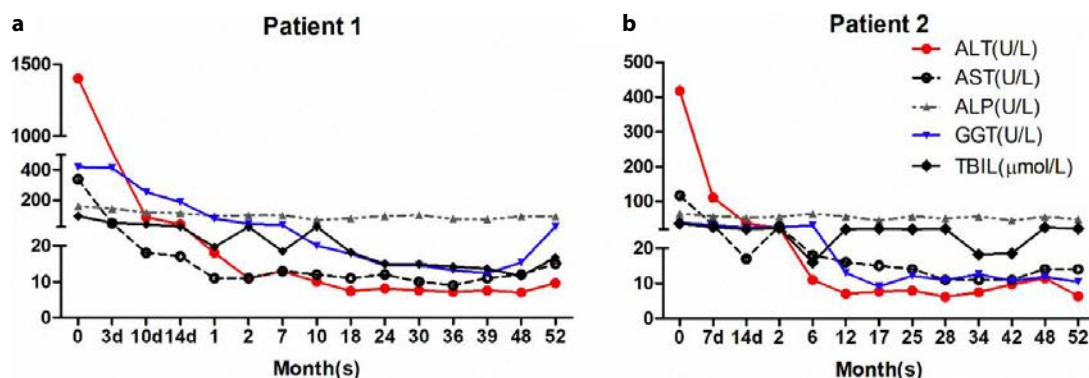


**Figure 1.** Clinical characteristics of patients with *Swietenia macrophylla* seeds induced liver injury.

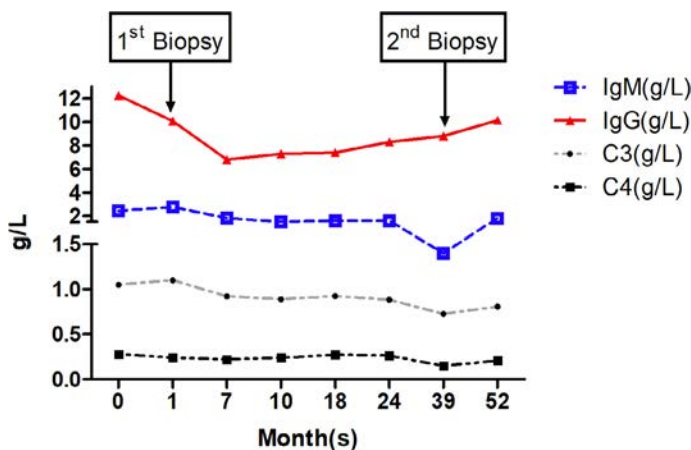


**Figure 2.** Dynamic changes of immunoglobulins and complements in a patient with *Swietenia macrophylla* seeds related liver injury.

was administered at a dose of 24 mg per day. During the 3-year treatment with methylprednisolone, indices of liver function, immunoglobulins, and complements remained at normal levels, and methylprednisolone was reduced gradually. The 2<sup>nd</sup> biopsy in the 3<sup>rd</sup> year of treatment showed no significant abnormality in liver tissue, and then methylprednisolone was withdrawn. No recurrence occurred during the one-year follow-up after withdrawal of methylprednisolone (Fig. 2).

## Discussion

In the present study, two cases of DILI caused by SMS have been reported. Hepatotoxicity of SMS is characterized by elevated ALT and AIH-like inflammation, and these histologic changes could be improved by methylprednisolone.

The clinical presentation of DILI varies widely, ranging from an asymptomatic rise in liver enzymes to liver failure. The severity of DILI is graded as mild, moderate, moderate to severe, severe, and fatal according to liver enzymes, TBIL, international normalized ratio, and complications. This can result from the use of drugs or dietary supplements, especially in patients with multiple drug consumption. However, it remains an exclusive diagnosis. Widespread use of RUCAM is highly recommended to evaluate the causality of suspected drugs. A liver biopsy may help to diagnose DILI when the RUCAM scale is less than 6, or when there is a possibility of autoimmune hepatitis. In cases with hepatocellular DILI, the peak ALT level decreases by >50% at 30–60 days after stopping the suspected offending drug, and then maintains normal levels during the follow-up. This is different from autoimmune hepatitis. However, consistent with Shao et al.,<sup>[13]</sup> our case report suggested that SMS-induced DILI was difficult to distinguish from AIH by liver biopsy.

According to the positive ANA in the two patients, it is possible that AIH may be a comorbidity with SMS-induced DILI. Although urgent administration of an immunosuppressive agent remains controversial for SMS-induced DILI, histological changes in Patient 1 demonstrated that the patient can benefit from methylprednisolone. On the other

hand, SMS should not be recommended to people with positive ANA. Collectively, these data suggest that SMS may increase the risk of liver damage for patients with potential immune disorders.

The mechanisms underlying SMS-induced DILI remain elusive, and new biomarkers for distinguishing SMS-related autoimmune-like hepatitis and AIH need to be further studied in the future.

## Conclusion

In conclusion, SMS may increase the risk of liver damage for patients with potential immune disorders, and patients with SMS-related DILI may benefit from methylprednisolone.

**Ethics Committee Approval:** This is a case report, and therefore ethics committee approval was not required in accordance with institutional policies.

**Informed Consent:** Informed consent was obtained from the two patients, and the clinical data were collected during the four-year follow-up period.

**Conflicts of Interest:** The authors declare no conflict of interest.

**Financial Disclosure:** This work was supported by the Leading Talent of Changzhou “The 14<sup>th</sup> Five-Year Plan” High-Level Health Talents Training Project (2022CZLJ021), Changzhou Key Medical Discipline, the Science and Technology Project of Changzhou (CE20225040).

**Use of AI for Writing Assistance:** Artificial intelligence was not used in the preparation of the article.

**Author Contributions:** Concept: YX; Design: YX; Supervision: YX; Funding: YX; Materials: Z-YH, X-ZJ, X-CT, YX; Analysis and/or Interpretation: Z-YH; Literature Search: Z-YH, X-ZJ, X-CT, YX; Writing: Z-YH, X-ZJ; Critical Reviews: YX.

**Peer-review:** Externally peer-reviewed.




## References

- Shen T, Liu Y, Shang J, Xie Q, Li J, Yan M, et al. Incidence and etiology of drug-induced liver injury in Mainland China. *Gastroenterology* 2019;156(8):2230-2241.e1 [CrossRef]
- Mi CN, Wang H, Chen HQ, Cai CH, Li SP, Mei WL, et al. Polyacetylenes from the Roots of *Swietenia macrophylla* King. *Molecules*. 2019;24(7):12913. [CrossRef]
- Murnigsih T, Subeki, Matsuura H, Takahashi K, Yamasaki M, Yamato O, et al. Evaluation of the inhibitory activities of the extracts of Indonesian traditional medicinal plants against *Plasmodium falciparum* and *Babesia gibsoni*. *J Vet Med Sci* 2005;67(8):829-831. [CrossRef]
- Balijepalli MK, Suppaiah V, Chin AM, Buru AS, Sagineedu SR, Pichika MR. Acute oral toxicity studies of *Swietenia macrophylla* seeds in Sprague Dawley rats. *Pharmacognosy Res* 2015;7(1):38-44. [CrossRef]
- Arias SP, de Jesús Rodríguez B, Lobo-Echeverri T, Ramos RS, Hyslop S, Rangel V. Effects of two fractions of *Swietenia macrophylla* and catechin on muscle damage induced by bothrospivenom and PLA<sub>2</sub>. *Toxins (Basel)* 2019;11(1):40. [CrossRef]

6. Sun YP, Zhu LL, Liu JS, Yu Y, Zhou ZY, Wang G, et al. Limonoids and triterpenoid from fruit of *Swietenia macrophylla*. *Fitoterapia* 2018;125:141-146. [\[CrossRef\]](#)
7. Chen LC, Liao HR, Chen PY, Kuo WL, Chang TH, Sung PJ, et al. Limonoids from the Seeds of *Swietenia macrophylla* and their anti-inflammatory activities. *Molecules* 2015;20(10):18551-18564. [\[CrossRef\]](#)
8. Moghadamtousi SZ, Goh BH, Chan CK, Shabab T, Kadir HA. Biological activities and phytochemicals of *Swietenia macrophylla* King. *Molecules* 2013;18(9):10465-10483. [\[CrossRef\]](#)
9. Ch'ng YS, Loh YC, Tan CS, Ahmad M, Asmawi MZ, Wan Omar WM, et al. Vasodilation and antihypertensive activities of *Swietenia macrophylla* (Mahogany) seed extract. *J Med Food* 2018;21(3):289-301. [\[CrossRef\]](#)
10. Pamplona S, Sá P, Lopes D, Costa E, Yamada E, e Silva C, et al. In vitro cytoprotective effects and antioxidant capacity of phenolic compounds from the leaves of *Swietenia macrophylla*. *Molecules* 2015;20(10):18777-18788. [\[CrossRef\]](#)
11. Sayyad M, Tiang N, Kumari Y, Goh BH, Jaiswal Y, Rosli R, Williams L, Shaikh MF. Acute toxicity profiling of the ethyl acetate fraction of *Swietenia macrophylla* seeds and in-vitro neuroprotection studies. *Saudi Pharm J* 2017;25(2):196-205. [\[CrossRef\]](#)
12. Tan Y, Chen H, Zhou X, Sun L. RUCAM-based assessment of liver injury by xiang-tian-guo (*Swietenia macrophylla*) seeds, a plant used for treatment of hypertension and diabetes. *Ann Hepatol* 2019;18(2):406-407. [\[CrossRef\]](#)
13. Shao YM, Zhang Y, Yin X, Qin TT, Jin QL, Wen XY. Herb-induced autoimmune-like hepatitis associated with Xiang-tian-guo (*Swietenia macrophylla* seeds): A case report and literature review. *Medicine (Baltimore)* 2021;100(2):e24045. [\[CrossRef\]](#)
14. European Association for the Study of the Liver. EASL Clinical Practice Guidelines: Drug-induced liver injury. *J Hepatol* 2019;70(6):1222-1261. [\[CrossRef\]](#)

## CASE REPORT

# Peritonitis due to brucellosis in a patient newly diagnosed with liver cirrhosis complicated by ascites: A case report and literature review

 Remzi Ekici<sup>1</sup>,  Mine Filiz<sup>3</sup>,  Sefa Onus<sup>2</sup>,  Ali Gokhan Akcay<sup>3</sup>,  Tolga Bakir<sup>1</sup>,  Galip Buyukturan<sup>1</sup>,  
 Emine Gul Aydin<sup>1</sup>,  Mustafa Ekici<sup>4</sup>,  Musa Aydinli<sup>1</sup>,  Cemal Nuri Ercin<sup>1</sup>

1: Department of Gastroenterology, University of Health Sciences, Gulhane Training and Research Hospital, Ankara, Turkiye

2: Department of Internal Medicine, University of Health Sciences, Gulhane Training and Research Hospital, Ankara, Turkiye

3: Department of Infectious Diseases and Clinical Microbiology, University of Health Sciences, Gulhane Training and Research Hospital, Ankara, Turkiye

4: Division of Rheumatology, Department of Internal Medicine, School of Medicine, Hacettepe University, Ankara, Turkiye

## Clinical Pearls

- **Unique Features of the Case:** *Brucella*-related SBP revealed previously undiagnosed cirrhosis with ascites. Diagnosis was challenging because serum *Brucella* tests were negative, yet peritoneal fluid cultures were positive after raw-milk cheese exposure.
- **Primary Lesson for Clinicians:** In endemic areas, consider *Brucella* in cirrhotic patients with new-onset ascites or atypical/nonresponding SBP, even when serology is negative; culture-based diagnosis can enable timely targeted treatment.

## ABSTRACT

*Brucellosis* is a common zoonotic disease with a wide variety of clinical manifestations. Spontaneous bacterial peritonitis (SBP) is a rare form among them. Here, we present the case of a 63-year-old woman with newly diagnosed liver cirrhosis complicated with ascites and diagnosed as spontaneous bacterial peritonitis with *Brucella* spp. growth in culture, and the literature is reviewed.

**Keywords:** Brucellosis, cirrhosis, peritonitis.

**How to cite this article:** Ekici R, Filiz M, Onus S, Akcay AG, Bakir T, Buyukturan G, et al. Peritonitis due to brucellosis in a patient newly diagnosed with liver cirrhosis complicated by ascites: A case report and literature review. *Hepatology Forum* 2026; 7(2):167–170.

**Received:** August 13, 2024; **Revised:** January 20, 2025; **Accepted:** March 08, 2025; **Available Online:** April 28, 2026

**Corresponding author:** Remzi Ekici; Department of Gastroenterology, University of Health Sciences, Gulhane Training and Research Hospital, Ankara, Turkiye;  
**E-mail:** dr.remziekici@yahoo.com



This work is licensed under a Creative Commons Attribution-NonCommercial 4.0 International License.

## Introduction

Brucellosis is a zoonotic infection transmitted from infected animals to humans by ingesting food products or contacting tissues and fluids.<sup>[1]</sup> Its endemic regions include the Mediterranean basin countries, the Middle East, and Central Asian countries.<sup>[2]</sup> In particular, Eastern Mediterranean countries such as Syria, Turkiye, and Iraq show the highest prevalence rates, ranging from 0.029 to 200.41 cases per 100,000 people.<sup>[3]</sup> Brucellosis typically manifests with insidious onset of fever, fatigue, night sweats, and joint pain. Brucellosis can affect any organ system and present a wide range of symptoms. Intra-abdominal manifestations are rare, including cholecystitis, hepatic or splenic abscess, pancreatitis, ileitis, colitis, and peritonitis.<sup>[4]</sup>

SBP related to brucellosis is particularly difficult to recognize. It can be fatal if misdiagnosed and left untreated. A review of the literature shows that most of the cases reported with *Brucella* peritonitis had a previous diagnosis of chronic liver or kidney disease. Detection of *Brucella* spp. as the causative agent of SBP in immunocompetent individuals is rare.<sup>[5–7]</sup>

To further emphasize the importance of brucellosis in the differential diagnosis in regions where the disease is endemic, such as the Mediterranean basin, we present the case of newly diagnosed liver cirrhosis in a patient who developed SBP due to brucellosis. In addition, we provide a comprehensive review of the clinical manifestations, diagnostic methods, and therapeutic interventions of this rare condition.

## Case Report

A 63-year-old woman presented with abdominal distension that started two months ago and gradually increased, weakness, and low blood pressure for the last week. She had no complaints of abdominal pain, high fever, nausea, or vomiting at presentation. She had a history of type 2 diabetes mellitus (DM) for 20 years, total colectomy for liposarcoma in the colonic mesentery five years ago, and cholecystectomy for cholelithiasis two months ago. On physical examination: fever: 36°C, pulse: 92/min, blood pressure: 82/43 mmHg, SpO<sub>2</sub>: 92% (room air). On physical examination, the abdomen was found to be severely distended. There was diffuse tenderness on palpation. There was no defense or rebound. On percussion, a mat with an upward-pointing opening was detected. Biochemical test results are given in Table 1.

On abdominal ultrasonography, the contours of the liver were micro-lobulated, and the left lobe corner section was blunted. The spleen was normal, and 11 cm of free fluid was observed in the deepest perihepatic area in each quadrant. Esophageal varices were detected in esophagogastroduodenoscopy. Viral hepatitis serology results are given in Table 2.

Autoimmune test results are given in Table 3. Because she had type 2 DM with a BMI of 30 kg/m<sup>2</sup>, metabolic dysfunction-associated fatty liver disease (MAFLD) was considered as the cause of liver cirrhosis. Diagnostic paracentesis results are given in Table 4. Ascitic fluid cultures were taken. On the second day of follow-up, abdominal pain and high fever (maximum 38°C) developed. Blood cultures were taken. Gram-negative

**Table 1.** Biochemical test results

	Patient value	Reference range
Hemoglobin (g/dL)	12.7	13.0–17.5
Leukocyte count (per mm <sup>3</sup> )	9240	4000–11000
Platelet count (per mm <sup>3</sup> )	190,000	150,000–450,000
International normalized ratio (INR)	1.1	0.4–1.2
Creatinine (mg/dL)	0.89	0.7–1.1
Sodium (mEq/Liter)	131	135–145
Aspartate aminotransferase (U/L)	126	0–32
Alanine aminotransferase (U/L)	83	0–33
γ-glutamyl transferase (U/L)	140	0–42
Alkaline phosphatase (U/L)	166	35–104
Total bilirubin (mg/dL)	0.32	0.3–1.2
Direct bilirubin (mg/dL)	0.05	0.1–0.3
Albumin (g/dL)	2.7	3.5–5.2
Total protein (g/dL)	4.9	6.6–8.7
C-reactive protein (mg/L)	4.4	0–5

**Table 2.** Viral hepatitis serology

HBsAg	Negative
Anti-HBc total	Negative
Anti-HBs	Positive (98 mIU/mL)
Anti-HAV IgG	Positive
Anti-HCV	Negative
HCV-RNA	Negative

HBsAg: Hepatitis B surface antigen; HBc: Hepatitis B core; HBs: Hepatitis B surface; HAV: Hepatitis A virus; IgG: Immunoglobulin G; HCV: Hepatitis C virus; RNA: Ribonucleic acid.

**Table 3.** Autoimmune hepatitis tests

Smooth muscle antigen (SMA)	Negative
Liver-kidney microsomal antigen (LKM)	Negative
Antimitochondrial antigen (AMA)	Negative

**Table 4.** Diagnostic paracentesis

Albumin concentration	0.71 g/dL
Total protein	1.28 g/dL
Total leukocyte count	1867/mm <sup>3</sup>
Neutrophils	443/mm <sup>3</sup>
Serum-ascitic albumin gradient	1.99

coccobacilli were detected on direct Gram staining of peritoneal fluid. The patient was diagnosed as having spontaneous bacterial peritonitis and was put on piperacillin-tazobactam therapy. *Brucella* species growth was detected on the 5<sup>th</sup> day in the peritoneal fluid culture taken

from two different samples. However, the serum *Brucella* agglutination test (*Brucella* standard tube agglutination test and *Brucella* ELISA test) was negative. We diagnosed the patient with seronegative *Brucella* peritonitis due to a negative serum serology titer for *Brucella*. Empirical piperacillin-tazobactam treatment was stopped, and rifampicin (600 mg/dose, once daily, PO) and doxycycline (100 mg/dose, twice daily, PO) were administered. When her anamnesis was detailed, we learned that she had been consuming cheese made from raw milk until about two weeks ago. On the 7<sup>th</sup> day of treatment, the patient's fever returned to normal, abdominal pain decreased, and in control paracentesis, neutrophils were 84 in the peritoneal fluid cell count.

## Discussion

Brucellosis is a multisystemic disease with diverse clinical manifestations, often characterized by non-specific symptoms or multisystemic involvement.<sup>[8]</sup> Peritonitis, although a rare complication of brucellosis, is more commonly observed in peritoneal dialysis patients and those with liver cirrhosis due to an increased risk of bacterial translocation.<sup>[7,9]</sup> Spontaneous bacterial peritonitis (SBP) is a frequent decompensation event in patients with cirrhosis, with an incidence of 15–20% and short-term mortality ranging from 10–33%. While Gram-negative enteric bacteria are the predominant causative agents of SBP (90%), *Brucella* spp. are an extremely rare etiological agent.

In our patient, *Brucella* spp. were isolated from the peritoneal fluid, confirming *brucella*-associated SBP. This diagnosis is rare and typically reported in patients with cirrhosis, chronic liver disease, or peritoneal dialysis. Although our patient lacked a prior diagnosis of cirrhosis or chronic liver disease, imaging findings (microlobulated liver contours, blunting of the left lobe corner, and hepatomegaly), endoscopic findings (grade-2 esophageal varices and portal hypertensive gastropathy), and elevated liver function tests strongly suggested underlying cirrhosis. The potential role of intestinal bacterial translocation in the decompensation process and its association with SBP has been highlighted in this case. Additionally, the patient's two-month clinical history aligns with the typical incubation period of brucellosis, further supporting the suspicion of *Brucella*-related SBP.

The negative *Brucella* serology in our patient presents a diagnostic challenge. Seronegative brucellosis has been described in immunocompromised individuals or those with localized infections, emphasizing the importance of microbiological culture results for definitive diagnosis in such scenarios. This highlights the need for heightened clinical suspicion, particularly in endemic regions.

The decision to initiate piperacillin-tazobactam as the first-line treatment was guided by local antibiotic resistance patterns, empirical treatment guidelines, and the patient's clinical presentation. Although this therapy initially led to clinical improvement, the absence of a follow-up diagnostic paracentesis at 48 hours is a limitation in this case. Standard SBP management protocols recommend repeat paracentesis to assess treatment response, mainly by monitoring changes in ascitic fluid white blood cell counts. The lack of such data limits our ability to confirm the efficacy of the empirical treatment

and to delineate the contribution of subsequent specific brucellosis therapy to the patient's overall recovery.

Differentiating *brucella*-related SBP from cirrhosis-associated SBP is crucial yet challenging. Features such as the rarity of *Brucella* as an SBP agent, the absence of a known source of infection in most cases, and the patient's consumption of unpasteurized dairy products in endemic areas provide valuable diagnostic clues. Literature supports considering brucellosis in the differential diagnosis of new-onset ascites in patients with cirrhosis or those presenting with atypical features of SBP.

*Brucella* peritonitis lacks a standardized treatment protocol. Current guidelines for brucellosis recommend a six-week course of doxycycline combined with rifampicin or streptomycin.<sup>[10,11]</sup> Of the 13 reported cases of *brucella*-associated SBP unrelated to peritoneal catheterization, most patients presented with abdominal pain, and fever was reported in a minority (Appendix 1). In our case, the patient exhibited both fever and abdominal pain, typical symptoms in brucellosis-related SBP. Notably, systemic brucellosis was absent in most reported cases (10/13), including ours.

## Conclusion

In conclusion, *brucella*-associated SBP is a rare yet crucial diagnostic consideration, particularly in endemic regions. Patients with cirrhosis and new-onset ascites who fail to respond to standard SBP treatment should be evaluated for *Brucella* infection, especially if there is a history of exposure to unpasteurized dairy products or contact with infected animals. Enhanced awareness and early identification can facilitate timely and appropriate therapy, potentially improving outcomes in atypical cases.

**Online Appendix Link:** <https://hepatologyforum.org/storage/upload/files/1778482826-appendix-en.pdf>

**Informed Consent:** Written informed consent was obtained to publish potentially identifiable images or data in this article.

**Conflict of Interest:** The author(s) declared no potential conflicts of interest with respect to the research, authorship, and/or publication of this article.

**Financial Disclosure:** The author(s) received no financial support for the research, authorship, and/or publication of this article.

**Use of AI for Writing Assistance:** The study did not use AI-enabled technology.

**Author Contributions:** Concept: RE, TB, GB; Design: RE, MF, SO, AGA; Supervision: RE, MA, CNE; Materials – RE, EGA, ME; Data Collection and/or Processing: RE, ME, MA; Analysis and/or Interpretation: RE, TB, ME; Literature Search: RE, MF, SO, AGA, TB; Writing: RE, TB, EGA; Critical Reviews: ME, MA, CNE.

**Acknowledgements:** The authors would like to thank the patient for providing consent to share clinical details and images for educational and scientific purposes.

**Peer-review:** Externally peer-reviewed.

## References

1. Pappas G, Akritidis N, Bosilkovski M, Tsianos E. Brucellosis. *N Engl J Med* 2005;352(22):2325-2336. [\[CrossRef\]](#)
2. Pappas G, Papadimitriou P, Akritidis N, Christou L, Tsianos EV. The new global map of human brucellosis. *Lancet Infect Dis* 2006;6(2):91-99. [\[CrossRef\]](#)
3. Liu Z, Gao L, Wang M, Yuan M, Li Z. Long ignored but making a comeback: a worldwide epidemiological evolution of human brucellosis. *Emerg Microbes Infect* 2024;13(1):2290839. [\[CrossRef\]](#)
4. Mantur BG, Amarnath SK, Shinde RS. Review of clinical and laboratory features of human brucellosis. *Indian J Med Microbiol* 2007;25(3):188-202. [\[CrossRef\]](#)
5. Akritidis N, Pappas G. Ascites caused by brucellosis: a report of two cases. *Scand J Gastroenterol* 2001;36(1):110-112. [\[CrossRef\]](#)
6. Gencer S, Ozer S. Spontaneous bacterial peritonitis caused by *Brucella melitensis*. *Scand J Infect Dis* 2003;35(5):341-343. [\[CrossRef\]](#)
7. Makaritsis KP, Liaskos C, Papadamou G, Dalekos GN. Spontaneous bacterial peritonitis: an unusual manifestation of brucellosis in a previous healthy male patient. *BMJ Case Rep* 2015;2015:bcr2015209387. [\[CrossRef\]](#)
8. Buzgan T, Karahocagil MK, Irmak H, Baran AI, Karsen H, Evirgen O, et al. Clinical manifestations and complications in 1028 cases of brucellosis: a retrospective evaluation and review of the literature. *Int J Infect Dis* 2010;14:e469-e478. [\[CrossRef\]](#)
9. Lewis S, Holmes C. Host defense mechanisms in the peritoneal cavity of continuous ambulatory peritoneal dialysis patients. *Perit Dial Int* 1991;11(1):14-21. [\[CrossRef\]](#)
10. Demirkan F, Akalin HE, Simşek H, Ozyilkan E, Telatar H. Spontaneous peritonitis due to *Brucella melitensis* in a patient with cirrhosis. *Eur J Clin Microbiol Infect Dis* 1993;12(1):66-67. [\[CrossRef\]](#)
11. Huang Y, Zhu X, Shen W, Wang Y, Han M. Brucellosis-induced peritonitis and abdominal aortitis in a non-endemic area patient on peritoneal dialysis: a case report and literature review. *Front Med (Lausanne)* 2024;11:1393548. [\[CrossRef\]](#)
12. Ferreira AO, Martins LN, Marinho RT, Velosa J. Spontaneous bacterial peritonitis by *Brucella* in a cirrhotic patient. *BMJ Case Rep* 2013;2013:bcr2013008629. [\[CrossRef\]](#)
13. Dizbay M, Hizel K, Kilic S, Mutluay R, Ozkan Y, Karakan T. *Brucella* peritonitis and leucocytoclastic vasculitis due to *Brucella melitensis*. *Braz J Infect Dis* 2007;11(4):443-444. [\[CrossRef\]](#)
14. Kantarçeken B, Harputluoğlu MM, Bayindir Y, Bayraktar MR, Aladağ M, Hilmioğlu F. Spontaneous bacterial peritonitis due to *Brucella melitensis* in a cirrhotic patient. *Turk J Gastroenterol* 2005;16(1):38-40.
15. GURSOY S, BASKOL M, OZBAKIR O, GÜVEN K, PATIROĞLU T, YÜCESOY M. Spontaneous bacterial peritonitis due to *Brucella* infection. *Turk J Gastroenterol* 2003;14(2):145-147.
16. Erbay A, Bodur H, Akinci E, Colpan A, Cevik MA. Spontaneous bacterial peritonitis due to *Brucella melitensis*. *Scand J Infect Dis* 2003;35(3):196-197. [\[CrossRef\]](#)
17. Ozakyol AH, Sariçam T, Zubaroglu I. Spontaneous bacterial peritonitis due to *Brucella melitensis* in a cirrhotic patient. *Am J Gastroenterol* 1999;94(9):2572-2573. [\[CrossRef\]](#)
18. Alcalá L, Muñoz P, Rodríguez-Crèixems M, Bañares R, Bouza E. *Brucella* spp. peritonitis. *Am J Med* 1999;107(3):300.
19. Halim MA, Ayub A, Abdulkareem A, Ellis ME, al-Gazlan S. *Brucella* peritonitis. *J Infect* 1993;27(2):169-172. [\[CrossRef\]](#)

## CASE REPORT

# Chanarin-Dorfman Syndrome: Two siblings with steatohepatitis, cirrhosis, and a novel mutation

 Nermin Mutlu Bilgic<sup>1</sup>,  Gupse Adali<sup>1</sup>,  Burak Ozturkeri<sup>2</sup>,  Sezin Canbek<sup>3</sup>,  Reyhan Surmeli<sup>4</sup>

1: Department of Gastroenterology and Hepatology, Istanbul Umraniye Training and Research Hospital, Istanbul, Turkiye

2: Department of Cardiology, Istanbul Umraniye Training and Research Hospital, Istanbul, Turkiye

3: Department of Medical Genetics, Istanbul Umraniye Training and Research Hospital, Istanbul, Turkiye

4: Department of Neurology, Istanbul Umraniye Training and Research Hospital, Istanbul, Turkiye

## Clinical Pearls

### • Unique Features of the Case:

Two adult siblings with Chanarin-Dorfman syndrome presented with advanced steatohepatitis and cirrhosis, despite normal lipid profiles. A novel homozygous *ABHD5* frameshift mutation was identified. Multisystem involvement and phenotypic variability were evident within the same family.

### • Primary Lesson for Clinicians:

Consider CDS in unexplained steatotic liver disease with ichthyosis. Early recognition, peripheral smear evaluation, and genetic testing are essential, particularly in consanguineous populations, to enable timely management and prevent progression.

## ABSTRACT

Chanarin-Dorfman Syndrome (CDS) is a rare autosomal recessive lipid storage disorder characterized by systemic triglyceride accumulation in various tissues, including the muscle, skin, central nervous system, liver, and white blood cells. Lipid accumulation results from mutations in the *abhydrolase domain-containing 5 (ABHD5)* gene, located on the p arm of chromosome 3. This report describes two adult Turkish siblings diagnosed with CDS who exhibited clinical features such as ichthyosis and cirrhosis secondary to steatotic liver disease. Genetic analysis revealed a novel homozygous frameshift mutation in the *ABHD5* gene, c.29\_30del (p.Ser10CysfsTer26), a variant previously documented in only one pediatric case. This report underscores the necessity of considering CDS in the differential diagnosis of steatotic liver disease, particularly when associated with ichthyosis, and highlights its relevance in populations from the Mediterranean region where such cases may be underdiagnosed.

**Keywords:** Chanarin-Dorfman syndrome, cirrhosis, ichthyosis, steatohepatitis, steatotic liver disease.

**How to cite this article:** Mutlu Bilgic N, Adali G, Ozturkeri B, Canbek S, Surmeli R. Chanarin-Dorfman Syndrome: Two siblings with steatohepatitis, cirrhosis, and a novel mutation. *Hepatology Forum* 2026; 7(2):171–175.

**Received:** September 17, 2024; **Revised:** February 13, 2025; **Accepted:** April 14, 2025; **Available Online:** April 28, 2026

**Corresponding author:** Nermin Mutlu Bilgic; Department of Gastroenterology and Hepatology, Istanbul Umraniye Training and Research Hospital, Istanbul, Turkiye;

**E-mail:** drnerminbilgic@gmail.com



This work is licensed under a Creative Commons Attribution-NonCommercial 4.0 International License.

## Introduction

Chanarin-Dorfman Syndrome (CDS) is a rare non-lysosomal lipid storage disorder caused by mutations in the *abhydrolase domain-containing 5 (ABHD5)* gene, leading to impaired intracellular lipolysis and accumulation of triglycerides in multiple tissues, such as skin fibroblasts, intestinal mucosa, myocytes, hepatocytes, bone marrow, central nervous system cells, and leukocytes. Common manifestations include ichthyosis, liver involvement, and myopathy, and the diagnosis is based on the presence of ichthyosis and identification of lipid droplets in granulocytes (Jordan's anomaly) in a peripheral blood smear.<sup>[1–3]</sup>

Liver involvement, which manifests as macrovesicular steatosis, steatohepatitis, and cirrhosis, is a significant cause of morbidity and mortality in patients with CDS, making early diagnosis and management crucial. Currently, no targeted treatment is available for individuals diagnosed with this syndrome. For those exhibiting hepatic steatosis, a diet low in fat and enriched with medium-chain fatty acids is recommended.<sup>[4–6]</sup> This report presents two siblings with CDS, emphasizing the liver-related aspects of the disease and discusses a novel mutation that may provide further insight into the genetic variability of the disease.

## Case Report

### Sibling 1

A 41-year-old male, followed up in dermatology and internal medicine clinics since the age of 15 for elevated liver enzymes and ichthyosis vulgaris, was admitted to our clinic with a request to investigate the etiology of decompensated cirrhosis and ascites. He was referred to our outpatient clinic for the evaluation of elevated alanine aminotransferase (ALT), aspartate aminotransferase (AST), gamma-glutamyl transferase (GGT), and ascites. The patient was initially assessed at another clinic, where an abdominal ultrasound performed five months prior indicated grade 2 hepatic steatosis, gallbladder wall thickening, pericholecystic fluid, and a 12.5 mm gallstone, suggestive of acute calculous cholecystitis.

The patient presented with fatigue and ichthyosis upon admission to our outpatient clinic. On physical examination, his height was 1.7 m, weight was 79 kg, and body mass index (BMI) was 26.99 kg/m<sup>2</sup>. Hepatomegaly, hyperpigmentation, and hyperkeratosis were observed throughout his body, which was diagnosed as ichthyosis. Ascites was also noted, and other system examinations were normal. He was a non-smoker and had no alcohol intake. At the age of 15 years, he was diagnosed with ichthyosis, and at the age of 20 years, he was diagnosed with steatotic liver disease, and ursodeoxycholic acid 250 mg three times daily was started. The patient was diagnosed with gallstones at the age of 25 years. The patient's parents were third-degree relatives (cousins), indicating a consanguineous marriage. The patient's father, who was diagnosed with ichthyosis, underwent liver transplantation for steatotic liver disease at the age of 43 years. Additionally, several

other family members, such as cousins, experienced premature mortality before the age of 40 years, and the specific causes of death remain unreported.

The patient underwent cholecystectomy for cholecystitis, during which cirrhotic nodules in the liver and minimal ascites in the abdominal cavity were observed. Two months post-surgery, paracentesis revealed a serum-ascites albumin gradient (SAAG) of 1.2 g/dL and a leukocyte count of 1300/μL. No bacterial growth was observed in the peritoneal culture, leading to a diagnosis of spontaneous bacterial peritonitis, which was treated with ceftriaxone. Follow-up imaging confirmed hepatomegaly, steatosis, splenomegaly, and ascites. The patient also underwent esophagogastroscopy, which revealed gastritis and no varices. Subsequently, he underwent a liver biopsy, in which macrovesicular steatosis, steatohepatitis, and nodules consistent with cirrhosis were observed.

Laboratory tests revealed leukocyte 4.95 × 10<sup>3</sup>/μL, neutrophil 2.11 × 10<sup>3</sup>/μL, lymphocyte 2.38 × 10<sup>3</sup>/μL, hemoglobin 15.6 g/dL, MCV 83.8 fL, and platelet 206 × 10<sup>3</sup>/μL. A peripheral blood smear revealed leukocytic vacuolation. Albumin 4.9 g/dL, creatinine 0.89 mg/dL, international normalized ratio (INR) 1.14, alpha-fetoprotein 3.87 μg/L, ALT 44 U/L (normal <41 U/L), AST 46 U/L (normal <40 U/L), alkaline phosphatase (ALP) 57 U/L, GGT 115 U/L (normal <71 U/L), direct bilirubin 0.29 mg/dL, total bilirubin 0.48 mg/dL, and creatine phosphokinase (CPK) 678 U/L (normal <220 U/L). No proteinuria or microalbuminuria was detected in the patient's urine tests. His lipid profile was normal. No viral infections (hepatitis A, B, and C; CMV; EBV), celiac disease, thyroid dysfunction, hemochromatosis, or Wilson's disease were found in the evaluations. In addition, abdominal Doppler ultrasonography showed normal flow in all arteries and veins in the abdomen and portal system.

The transient elastography assessment revealed a controlled attenuation parameter (CAP) of 332 dB/m, indicative of severe steatosis (greater than 30% of hepatocytes affected). The liver stiffness measurement (LSM) was 70.3 kPa, consistent with F4 fibrosis, indicating cirrhosis.<sup>[7]</sup>

The patient, who presented with elevated CPK levels, was referred to the neurology department for further evaluation. Needle electromyography (EMG) was performed because of mild diffuse muscle pain. EMG findings were indicative of significant myopathy affecting both the upper and lower extremities (Fig. 1). Echocardiography revealed an ejection fraction of 58%, with evidence of diastolic dysfunction and delayed relaxation of the left ventricle. Pericardial thickness was normal. Ophthalmological examination revealed the presence of cataracts.

### Sibling 2

A 39-year-old male, the younger brother of Sibling 1, had a known diagnosis of ichthyosis and had been under follow-up for steatotic liver disease over the past three years. Physical examination revealed that his height was 1.85 m, weight 75 kg, and BMI was 21.9 kg/m<sup>2</sup>. He had hepatomegaly, hyperpigmentation, and hyperkeratosis throughout his body, consistent with his diagnosis of ichthyosis.

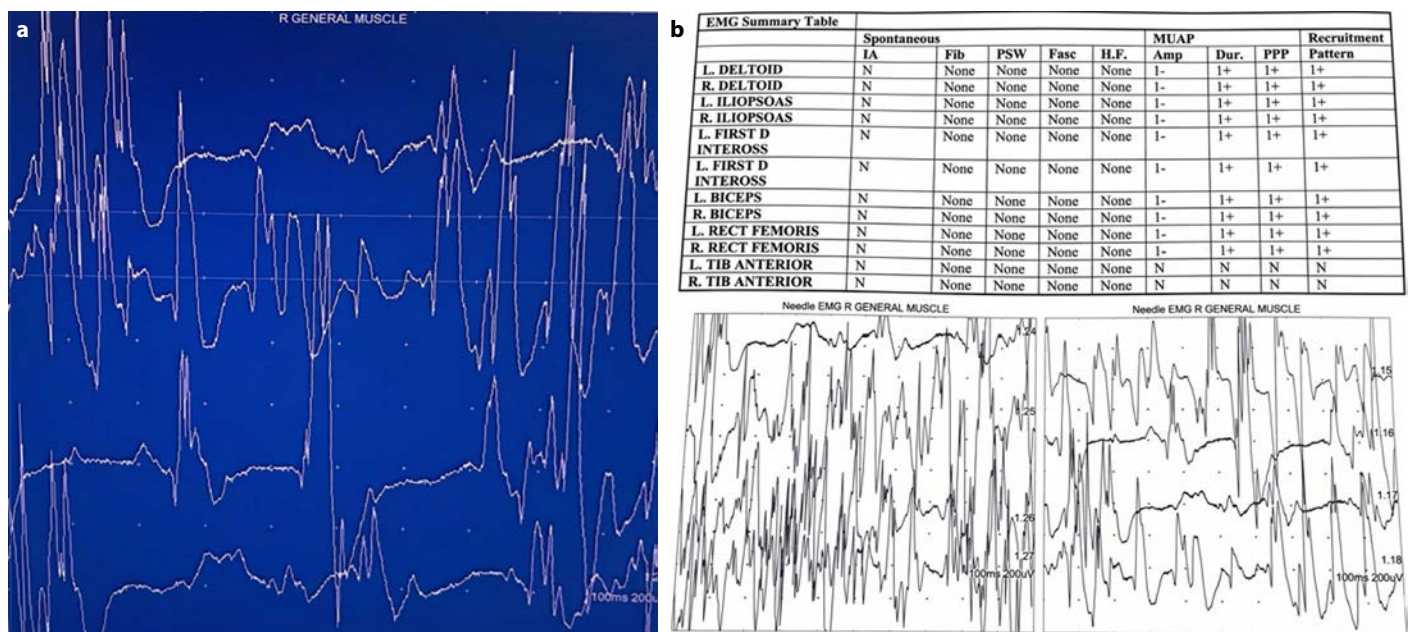


**Figure 1.** Needle EMG results of Sibling 1 showing myopathic changes. (a) Electrical activity of general muscles. (b) Summary table of EMG results.

**Table 1.** Clinical characteristics of the siblings

Clinical feature	Sibling 1	Sibling 2
Ichthyosis	+	+
Leukocyte vacuoles	+	+
Creatine phosphokinase (U/L)	678	218
Electromyographic examination	Myopathy	NA
Echocardiography	Left ventricular diastolic dysfunction, ejection fraction 58%	
Lipid levels	Normal	Normal
Cataracts	+	-
AST (U/L) (Normal <40)	46	68
ALT (U/L) (Normal <40)	44	128
GGT (U/L) (Normal <71)	115	129
Hepatomegaly	+	+
Hepatosteatorsis	+	+
Steatohepatitis	+	NA
Cirrhosis	+	+
Transient elastography	Severe steatorsis and F4 fibrosis	Severe steatorsis and F4 fibrosis

AST: Aspartate transaminase; ALT: Alanine aminotransferase; GGT: Gamma-glutamyl transferase; NA: Not available.

Laboratory evaluation revealed the following results: albumin 4.3 g/dL, creatinine 0.74 mg/dL, INR 1.07, alpha-fetoprotein 2.72 µg/L, ALT 128 U/L, AST 68 U/L, ALP 111 U/L, GGT 129 U/L, direct bilirubin 0.19 mg/dL, total bilirubin 0.41 mg/dL, CPK 218 U/L, leukocyte count  $5.95 \times 10^3/\mu\text{L}$ , neutrophils  $2.11 \times 10^3/\mu\text{L}$ , lymphocytes  $2.38 \times 10^3/\mu\text{L}$ , hemoglobin 15.6 g/dL, MCV 83.8 fL, and platelet count  $206 \times 10^3/\mu\text{L}$ . Leukocytic vacuolations were noted on the peripheral blood smear. The patient's lipid profile was within normal limits.

Abdominal ultrasonography performed upon admission revealed an enlarged liver (191 mm) with smooth contours and grade 2 hepatic steatorsis. Transient elastography reported a CAP of 328 dB/m, indicating S3 severe steatorsis, and an LSM of 20.0 kPa, consistent with F4 fibrosis/cirrhosis.<sup>[7]</sup> Ophthalmological and cardiological evaluations showed no abnormalities. A summary of the clinical characteristics and laboratory findings of the siblings is presented in Table 1.

The siblings were born to consanguineous parents, a factor commonly associated with autosomal recessive disorders, including Chanarin-Dorfman Syndrome (CDS). A comprehensive family history revealed several relatives with early mortality potentially attributable to undiagnosed CDS or related complications. The diagnosis of CDS in both patients was established based on their distinctive clinical features, including ichthyosis, Jordan's anomaly, and early-onset steatosis and cirrhosis, which occurred without known common etiological factors.<sup>[1,2]</sup>

Genetic analysis of both siblings identified a homozygous frameshift variant in the *ABHD5* gene, c.29\_30del (p.Ser10CysfsTer26). This variant has not been previously documented in ClinVar; however, it has recently been reported in one pediatric CDS case.<sup>[8]</sup> According to the guidelines of the American College of Medical Genetics and Genomics (ACMG), this variant is classified as likely pathogenic.<sup>[9]</sup>

## Discussion

CDS is characterized by multiorgan involvement, with liver disease being a prominent feature. In this case, both siblings showed severe liver involvement, including steatosis and cirrhosis, which aligns with previous reports highlighting liver pathology as a major clinical manifestation of CDS.<sup>[3]</sup> The genetic basis, involving a novel mutation in the *ABHD5* gene, leads to impaired activation of adipose triglyceride lipase (ATGL) and subsequent lipid accumulation, particularly in triglyceride-rich organs such as the liver.

Cutaneous, hepatic, and neurological involvement are typical findings in CDS. Mild or moderate nonbulbar ichthyosis may be seen alone or with multi-organ involvement. Diffuse erythematous ichthyosis with mild white scales on the body folds, scalp, and face is a common presentation.<sup>[1,3]</sup> Since adolescence, our patients had complaints of ichthyosis. Therefore, CDS should be considered in the differential diagnosis in patients with systemic findings accompanying ichthyosis from a young age.

Both siblings presented with hepatic steatosis and elevated AST and ALT levels at an early age, and both had severe steatosis and cirrhosis in transient elastography evaluation. Liver biopsy of Sibling 1 demonstrated steatohepatitis, macrovesicular steatosis, and cirrhosis. Liver involvement in CDS can range from steatosis to cirrhosis, with elevated liver enzyme levels being a common laboratory finding. A recent review reported liver involvement in 86% of CDS patients, with 90% showing steatohepatitis, 74% exhibiting macrovesicular steatosis, and 10% presenting with cirrhosis.<sup>[3]</sup> Sibling 1 presented with a cataract, a feature observed in 22% of Chanarin-Dorfman Syndrome (CDS) cases, and myopathy, which has been reported in 59% of patients according to a recent review.<sup>[3]</sup>

The mutation identified, c.29\_30del (p.Ser10CysfsTer26), is novel and has been previously documented in a single pediatric case with CDS who presented with similar clinical symptoms, including significant liver involvement and skin lesions.<sup>[10]</sup> The discovery of this mutation in multiple unrelated cases may suggest a wider prevalence than previously thought and highlight the genetic diversity of CDS.

Although there is no definitive treatment for CDS, reduction in liver size and improvement in liver enzyme levels have been reported in some cases with low-fat diets containing medium-chain triglycerides.<sup>[2,4]</sup> In our case, liver enzymes improved and liver size decreased after dietary modification. Moreover, liver transplantation is an important treatment option in patients with decompensated cirrhosis.<sup>[3]</sup>

## Conclusion

This case report of two siblings with CDS underscores the critical role of liver involvement in the clinical course of the disease and highlights a novel mutation in the *ABHD5* gene. This emphasizes the need for early diagnosis through genetic testing and the importance of considering CDS in patients with unexplained steatotic liver disease, particularly in populations with high rates of consanguinity.

**Informed Consent:** Written informed consent was obtained from participants.

**Conflict of Interest:** The authors have no conflict of interest to declare.

**Financial Disclosure:** The authors declared that this study has received no financial support.

**Use of AI for Writing Assistance:** Artificial intelligence was not used in the preparation of the article.

**Author Contributions:** Concept – GA, NMB; Design – SC, BO; Supervision – GA; Materials – SC, BO; Data Collection and/or Processing – NMB, RS; Analysis and/or Interpretation – GA, NMB; Literature Search – NMB; Writing – NMB; Critical Reviews – GA.

**Peer-review:** Externally peer-reviewed.

## References

1. Bruno C, Bertini E, Di Rocco M, Cassandrini D, Ruffa G, De Toni T, et al. Clinical and genetic characterization of Chanarin-Dorfman syndrome. *Biochem Biophys Res Commun* 2008;369(4):1125-1128. [\[CrossRef\]](#)
2. Peña-Penabad C, Almagro M, Martínez W, García-Silva J, Del Pozo J, Yebra MT, et al. Dorfman--Chanarin syndrome (neutral lipid storage disease): new clinical features. *Br J Dermatol* 2001;144(2):430-432. [\[CrossRef\]](#)
3. Cakmak E, Bagci G. Chanarin-Dorfman Syndrome: A comprehensive review. *Liver Int* 2021;41(5):905-914. [\[CrossRef\]](#)
4. Ujihara M, Nakajima K, Yamamoto M, Teraishi M, Uchida Y, Akiyama M, et al. Epidermal triglyceride levels are correlated with severity of ichthyosis in Dorfman-Chanarin syndrome. *J Dermatol Sci* 2010;57(2):102-107. [\[CrossRef\]](#)
5. Emre S, Unver N, Evans SE, Yüzbaşıoğlu A, Gürakan F, Gümrük F, et al. Molecular analysis of Chanarin-Dorfman syndrome (CDS) patients: Identification of novel mutations in the *ABHD5* gene. *Eur J Med Genet* 2010;53(3):141-144. [\[CrossRef\]](#)
6. Cakir M, Bruno C, Cansu A, Cobanoglu U, Erduran E. Liver cirrhosis in an infant with Chanarin-Dorfman syndrome caused by a novel splice-site mutation in *ABHD5*. *Acta Paediatr* 2010;99(10):1592-1594. [\[CrossRef\]](#)

7. European Association for the Study of the Liver (EASL). Electronic address: easloffice@easloffice.eu; European Association for the Study of Diabetes (EASD); European Association for the Study of Obesity (EASO); European Association for the Study of the Liver (EASL). EASL-EASD-EASO Clinical Practice Guidelines on the management of metabolic dysfunction-associated steatotic liver disease (MASLD). *J Hepatol* 2024;81(3):492-542.
8. ClinVar. RCV000012345. National Center for Biotechnology Information (NCBI). Available at: <https://www.ncbi.nlm.nih.gov/clinvar/RCV000012345/?redir=rcv&variant=RCV000012345> Accessed Apr 27, 2026.
9. Richards S, Aziz N, Bale S, Bick D, Das S, Gastier-Foster J, et al; ACMG Laboratory Quality Assurance Committee. Standards and guidelines for the interpretation of sequence variants: a joint consensus recommendation of the American College of Medical Genetics and Genomics and the Association for Molecular Pathology. *Genet Med* 2015;17(5):405-424. [\[CrossRef\]](#)
10. Çetinarslan T, Yazıcı H, Erdoğan KM, Kalkan Uçar S, Dalgıç G, Kaya G, et al. Four cases of Chanarin-Dorfman syndrome presenting with different types of erythrokeratoderma. *Pediatr Dermatol* 2024;41(6):1174-1178. [\[CrossRef\]](#)